Dissertation zur Erlangung des Doktorgrades
der Fakultät für Chemie und Pharmazie
der Ludwig-Maximilians-Universität München

Structure-Reactivity Relationships in Unsaturated Organosilanes and Ynamides

Hans Arnold Laub
aus
München

2013

Erklärung

Diese Dissertation wurde im Sinne von § 7 der Promotionsordnung vom 28. November 2011 von Herrn Prof. Dr. Herbert Mayr betreut.

Eidesstattliche Versicherung

Diese Dissertation wurde eigenständig und ohne unerlaubte Hilfe erarbeitet.

München, den 17.12.2013

……..

Hans Laub

Dissertation eingereicht am	17.12.2013
1. Gutachter	Prof. Dr. Herbert Mayr
2. Gutachter	Prof. Dr. Anja Hoffmann-Röder
Mündliche Prüfung am	12.02.2014

Für meine Frau Nikola und

meine Kinder Valerie und David

„Nothing shocks me. I'm a scientist"

(Prof. Dr. Henry Jones Jr.)

Danksagung

Großer Dank gebührt Prof. Dr. Herbert Mayr für die Möglichkeit mich diesen interessanten Themengebieten zu widmen. Die von ihm bereitgestellten, hervorragenden Arbeitsbedingungen und seine unerlässliche Hilfs- und Diskussionsbereitschaft haben maßgeblich zum Gelingen dieser Arbeit beigetragen. Darüber hinaus danke ich ihm dafür, dass er mir dabei die nötige Zeit zur Betreuung meiner Kinder einräumte.

Den weiteren Mitgliedern des Prüfungsausschusses sei für ihre Teilnahmebereitschaft gedankt. Für die Zweitbegutachtung meiner Arbeit danke ich insbesondere Prof. Dr. Anja Hoffmann-Röder.

Enorme Freude bereiteten mir die Kooperationen mit anderen Arbeitsgruppen aus der Organischen Chemie. Für die professionelle und erfolgreiche Zusammenarbeit möchte ich mich daher bei Prof. Dr. Hisashi Yamamoto, Daniel Gladow, Prof. Dr. Hans-Ulrich Reissig und Prof. Dr. Gwilherm Evano bedanken.

Für seine Diskussionsbereitschaft und die kritische Durchsicht meiner Publikationen bin ich PD Dr. Armin Ofial zu großem Dank verpflichtet. Gerne denke ich auch an den gemeinsamen Besuch der ESOC 2011 auf Kreta mit ihm und Dr. Dominik Allgäuer (meinem sehr geschätzten Bürokollegen) zurück. Dies trifft ebenso auf die gemeinsame Teilnahme mit Francisco Corral an der EuCheMS 2012 in Prag zu.

Brigitte Janker und Hildegard Lipfert danke ich für die Übernahme vieler organisatorischer Angelegenheiten. Für die Bereitstellung der Referenzelektrophile in herausragender Qualität und der Aufreinigung mancher Produktstudien möchte ich mich außerdem bei Nathalie Hampel bedanken.

Weiterer Dank gebührt den Mitarbeitern der Analytik für die stets zügigen und verlässlichen Untersuchungen meiner Proben. Für die tatkräftige Unterstützung bei Heterokern-NMR und die hilfreichen Diskussionen möchte ich mich besonders bei Dr. David Stephenson und Prof. Dr. Konstantin Karaghiosoff bedanken.

Meinen gegenwärtigen und ehemaligen Kollegen des Paul-von-Ragué-Schleyer-Labors Dr. Saloua Chelli, Maximilian Heininger, Dr. Markus Horn, Brigitte Janker, Dr. Ángel R. Puente Garcia, Dr. Heike Schaller, Elija Wiedemann, Dr. Ivo Zenz und insbesondere meinen

beiden Banknachbarn Dr. Oliver Kaumanns und Anna Antipova danke ich für eine sehr vergnügliche und kollegiale Atmosphäre. Für die schöne gemeinsame Zeit im Arbeitskreis möchte ich mich außerdem bei Dr. Tanja Kanzian, Dr. Sami Lakhdar, Dr. Tobias A. Nigst, Dr. Nicolas Streidl und Dr. Konstantin Troshin bedanken.

Dr. Johannes Ammer, Francisco Corral, Dr. Ángel R. Puente Garcia, Alexander Wagner und Elija Wiedemann danke ich für die zügige und kritische Durchsicht meiner Arbeit. Für ihre Unterstützung bei Laserblitzphotolyse-Experimenten möchte ich Dr. Johannes Ammer und Dr. Jörg Bartl danken. Den restlichen ehemaligen und aktuellen Mitgliedern des Arbeitskreises danke ich für die gute Zusammenarbeit und die hilfreichen Diskussionen.

Meiner Mutter und meinen Schwiegereltern gilt ein ganz besonderer Dank, da sie durch ihre Hilfe bei der Betreuung unserer Kinder einen wesentlichen Beitrag zum Gelingen dieser Arbeit geleistet haben. Ihnen und meiner restlichen Familie danke ich außerdem für die Unterstützung die mir nicht nur während meiner Ausbildung sondern jederzeit zuteilwurde. Meinen Kindern Valerie und David danke ich dafür, dass sie mir täglich zeigen, welche Dinge wirklich wichtig sind.

Am meisten danke ich meiner Frau Nikola. Ihr ist es gelungen mir nicht nur so viel Zeit wie möglich für das Anfertigen dieser Arbeit zu verschaffen, sondern mir auch noch eine große moralische Stütze zu sein. Ohne ihren Beistand wäre diese Arbeit nicht möglich gewesen.

Copyrights

The following articles have been or will be published in peer-reviewed journals. They are reproduced in this work with the permission of the respective publisher and according to the format of this thesis.

Effect of the "Supersilyl" Group on the Reactivities of Allylsilanes and Silyl Enol Ethers (Chapter 2)

H. A. Laub, H. Yamamoto, H. Mayr, *Org. Lett.* **2010**, *12*, 5206–5209.

http://dx.doi.org/10.1021/ol102220e

The Influence of Perfluorinated Substituents on the Nucleophilic Reactivities of Silyl Enol Ethers (Chapter 3)

H. A. Laub, D. Gladow, H.-U. Reissig, H. Mayr, *Org. Lett.* **2012**, *14*, 3990–3993.

http://dx.doi.org/10.1021/ol301766w

Electrophilic Alkylations of Vinylsilanes – A Comparison of α- and β-Silyl Effects (Chapter 4 without appendix)

H. A. Laub, H. Mayr, *Chem. Eur. J.* **2014**, *20*, 1103–1110.

http://dx.doi.org/10.1002/chem.201303215

Hydrocarbation of CC-Triple Bonds: Quantification of the Nucleophilic Reactivity of Ynamides (Chapter 5)

H. A. Laub, G. Evano, H. Mayr, *Angew. Chem.*; *Angew. Chem. Int. Ed.* in press.

http://dx.doi.org/10.1002/ange.201402055 and http://dx.doi.org/10.1002/anie.201402055

Contributions to Conferences

Parts of this work were presented as posters at the following scientific meetings:

Effect of the "Supersilyl" Group on the Nucleophilicities of Organosilanes

H. A. Laub, H. Yamamoto, H. Mayr, *17th European Symposium on Organic Chemistry,* Crete (Greece) **July 2011**.

The Influence of Perfluorinated Substituents on the Nucleophilic Reactivities of Silyl Enol Ethers

H. A. Laub, D. Gladow, H.-U. Reissig, H. Mayr, *4th EuCheMS Chemistry Conference,* Prague (Czech Republic) **August 2012**.

Table of Contents

Chapter 0

Summary

0.1 General

It has been shown previously that second-order rate constants k of polar reactions of π-nucleophiles with electrophiles at 20 °C follow the linear free energy relationship given in Equation (0.1), where nucleophilic reactivity is expressed by the solvent-dependent parameters N (nucleophilicity) and s_N (sensitivity) and electrophiles are characterized by the solvent-independent parameter E (electrophilicity).

$$\lg k\,(20\ °C) = s_N(N + E) \qquad (0.1)$$

The focus of this work was to examine the applicability of this relationship to reactions of benzhydrylium ions with organosilanes and ynamides. This allowed the inclusion of these nucleophiles in the most comprehensive reactivity scale presently available, which currently covers a range of over 30 orders of magnitude. In consequence, it was possible to compare the nucleophilic reactivities found for different organosilanes and ynamides with those of previously studied structurally related compounds and to gain insight in the respective structure-reactivity relationships.

0.2 Effect of the "Supersilyl" Group on the Reactivities of Allylsilanes and Silyl Enol Ethers[*]

Kinetics of the reactions of allylsilanes and silyl enol ethers possessing a tris(trimethylsilyl)silyl (supersilyl) moiety with benzhydrylium ions have been measured photometrically in dichloromethane under pseudo-first order conditions. The obtained first-order rate constants correlated linearly with the concentrations of the nucleophiles used in excess and the corresponding second-order rate constants k_2 were obtained as the slopes of these correlations. Plots of lg k_2 against the empirical electrophilicities E of the electrophiles were

[*] Reproduced with permission from H. A. Laub, H. Yamamoto, H. Mayr, *Org. Lett.* **2010**, *12*, 5206–5209. Copyright © 2010 American Chemical Society

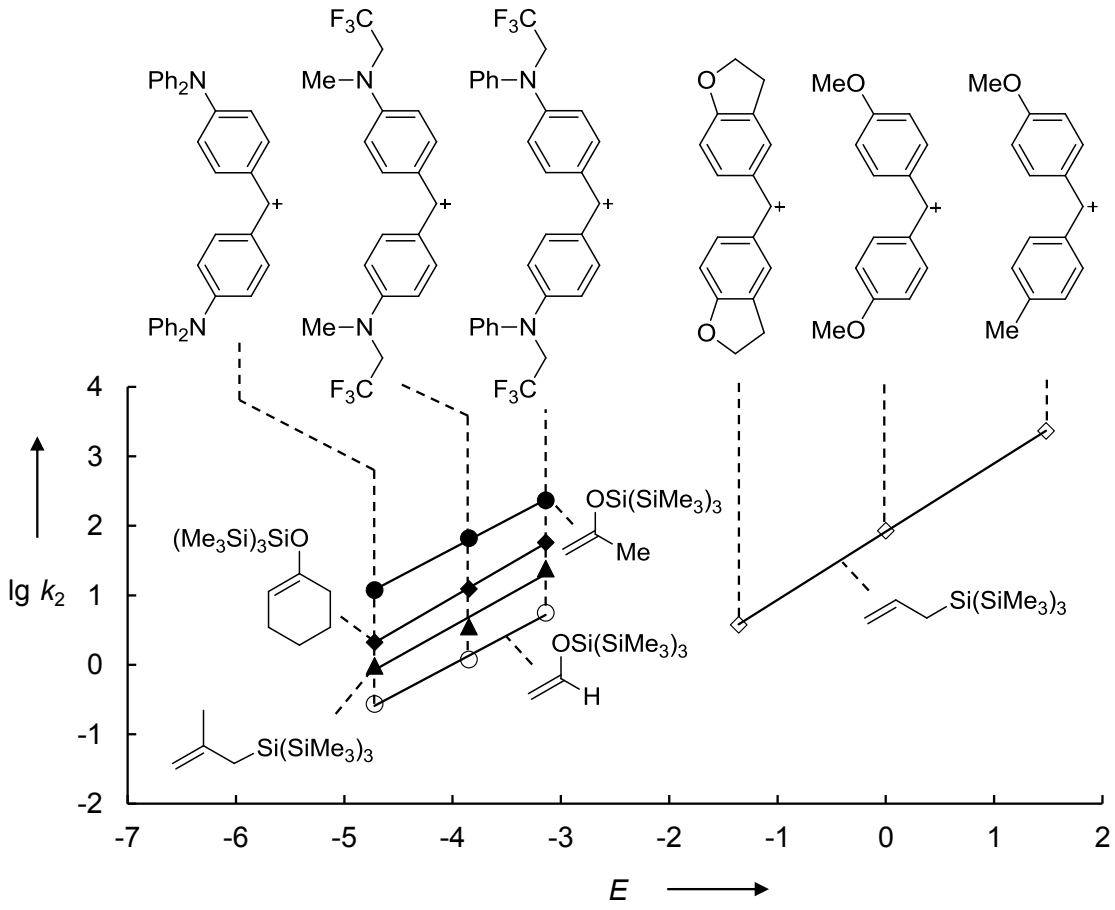

Figure 0.1. Plots of lg k_2 for the reactions of supersilyl substituted allylsilanes and silyl enol ethers with benzhydrylium ions in CH_2Cl_2 at 20 °C against the corresponding electrophilicity parameters E of the reference electrophiles.

linear, thus showing that Equation (0.1) is applicable (Figure 0.1). In consequence, the nucleophile-specific parameters N and s_N could be derived for supersilyl substituted allylsilanes and silyl enol ethers. This allows the comparison of the nucleophilicities of these compounds with those of the corresponding trialkylsilyl substituted analogs (Figure 0.2).

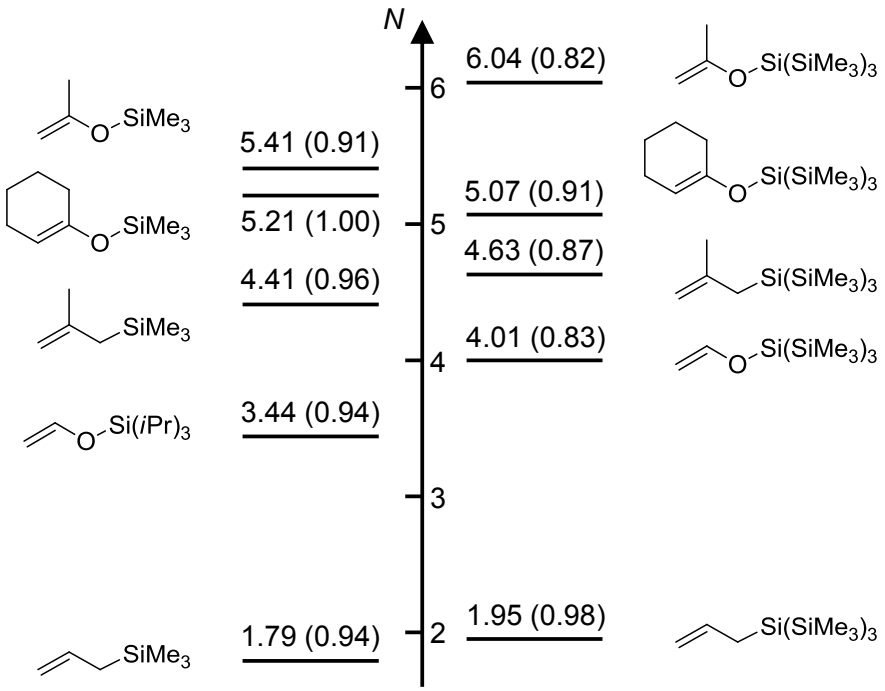

Figure 0.2. Comparison of the nucleophilicities of supersilyl substituted allylsilanes and silyl enol ethers (right) with those of the corresponding allyltrimethylsilanes and trialkylsilyl enol ethers (left; s_N values given in parentheses).

According to Figure 0.2, the exchange of $SiMe_3$ by $Si(SiMe_3)_3$ in allylsilanes and silylated enol ethers has little effect on the rates of the reactions of these electron-rich π-nucleophiles. The significantly lower first vertical ionization energies of tris(trimethylsilyl)silyl substituted benzenes compared to the trimethylsilyl analogues, which indicates a stronger α-effect of the $Si(SiMe_3)_3$ group compared with $SiMe_3$, obviously does not have a consequence for the reactivities of allylsilanes and silylated enol ethers bearing the supersilyl group. One can, therefore, conclude that the high selectivities observed for [2+2] cycloadditions and aldol reactions with supersilyl-substituted enol ethers cannot be attributed to electronic effects but are due to the steric bulk and the umbrella like structure created by the $Si(SiMe_3)_3$ group.

0.3 The Influence of Perfluorinated Substituents on the Nucleophilic Reactivities of Silyl Enol Ethers†

Kinetics of the reactions of benzhydrylium ions with silyl enol ethers possessing perfluorinated alkyl and aryl substituents at the developing carbenium center were studied by UV-Vis spectroscopy in dichloromethane solution under pseudo-first order conditions. Fast reactions at 20 °C ($\tau_{1/2}$ < 10 s) and those involving highly reactive benzhydrylium ions ($E \geq 3.63$) were investigated between –70 and –10 °C to furnish the corresponding Eyring activation parameters $\Delta H^{\ddagger}$ and $\Delta S^{\ddagger}$. This allowed the calculation of the second-order rate constants k_2 at 20 °C for these reactions. For slower reactions involving less reactive benzhydrylium ions ($E \leq 0.61$) the second-order rate constants k_2 at 20 °C were obtained from the linear correlation of the first-order rate constants determined at 20 °C versus the respective

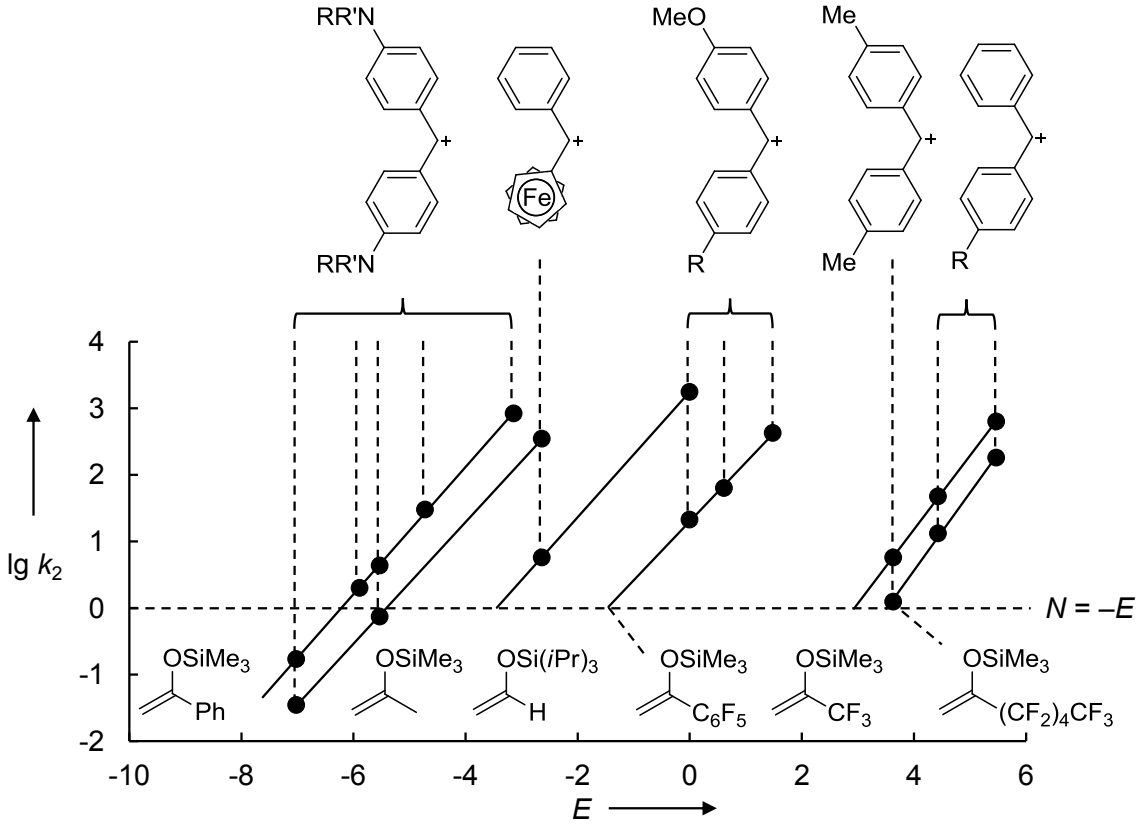

Figure 0.3. Plots of lg k_2 for the reactions of silyl enol ethers with benzhydrylium ions in CH_2Cl_2 at 20 °C versus the electrophilicity parameters E of the reference electrophiles.

† Reproduced with permission from H. A. Laub, D. Gladow, H.-U. Reissig, H. Mayr, *Org. Lett.* **2012**, *14*, 3990–3993. Copyright © 2012 American Chemical Society

concentrations of the nucleophiles used in excess.

It was shown that Equation (0.1) can be used for describing the rates of the reactions of the studied fluorinated silyl enol ethers with benzhydrylium ions, as linear correlations were obtained from the plots of lg k_2 at 20 °C against the electrophilicities E of the electrophiles (Figure 0.3). Thus, it was possible to integrate silyl enol ethers with perfluorinated substituents in the nucleophilicity scale and compare them with structurally related compounds.

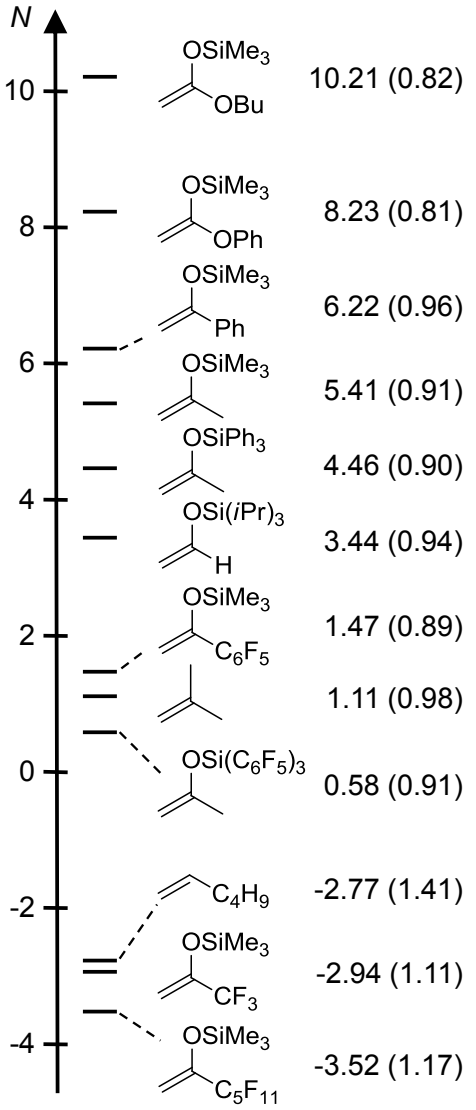

Figure 0.4. Nucleophilicities N of fluorinated silyl enol ethers compared to those of other π-Nucleophiles (s_N values given in parentheses).

Figure 0.4 shows that through replacement of the other substituent attached to the developing carbenium center during electrophilic attack, terminal trimethylsilyl enol ethers cover a reactivity range of more than 13 orders of magnitude. Thereby, the replacement of CH_3 by CF_3 reduces the nucleophilicity by a factor of 10^8, while the exchange of C_6H_5 by C_6F_5 retards the reactions by 4.5 orders of magnitude. Thus, the studied fluorinated silyl enol ethers show nucleophilicities comparable to those of alkyl substituted ethylenes (e.g., isobutylene or hex-1-ene). With N-parameters around –3, the perfluoroalkyl substituted silyl enol ethers can be expected only to react with electrophiles having electrophilic reactivities of $E > -2$. According to the reactivity database built on Equation (0.1) this includes Mukaiyama-type aldol reactions with carbonyl Lewis acid complexes, but not iminium activated reactions.

0.4 Electrophilic Alkylations of Vinylsilanes – A Comparison of α- and β-Silyl Effects[‡]

Kinetics of the reactions of benzhydrylium ions with propene- and styrene-derived vinylsilanes have been measured photometrically in dichloromethane solution. All reactions follow second-order kinetics, and the second-order rate constants at 20 °C correlate linearly with the electrophilicity parameters *E* of the benzhydrylium ions (Figure 0.5 and Figure 0.6).

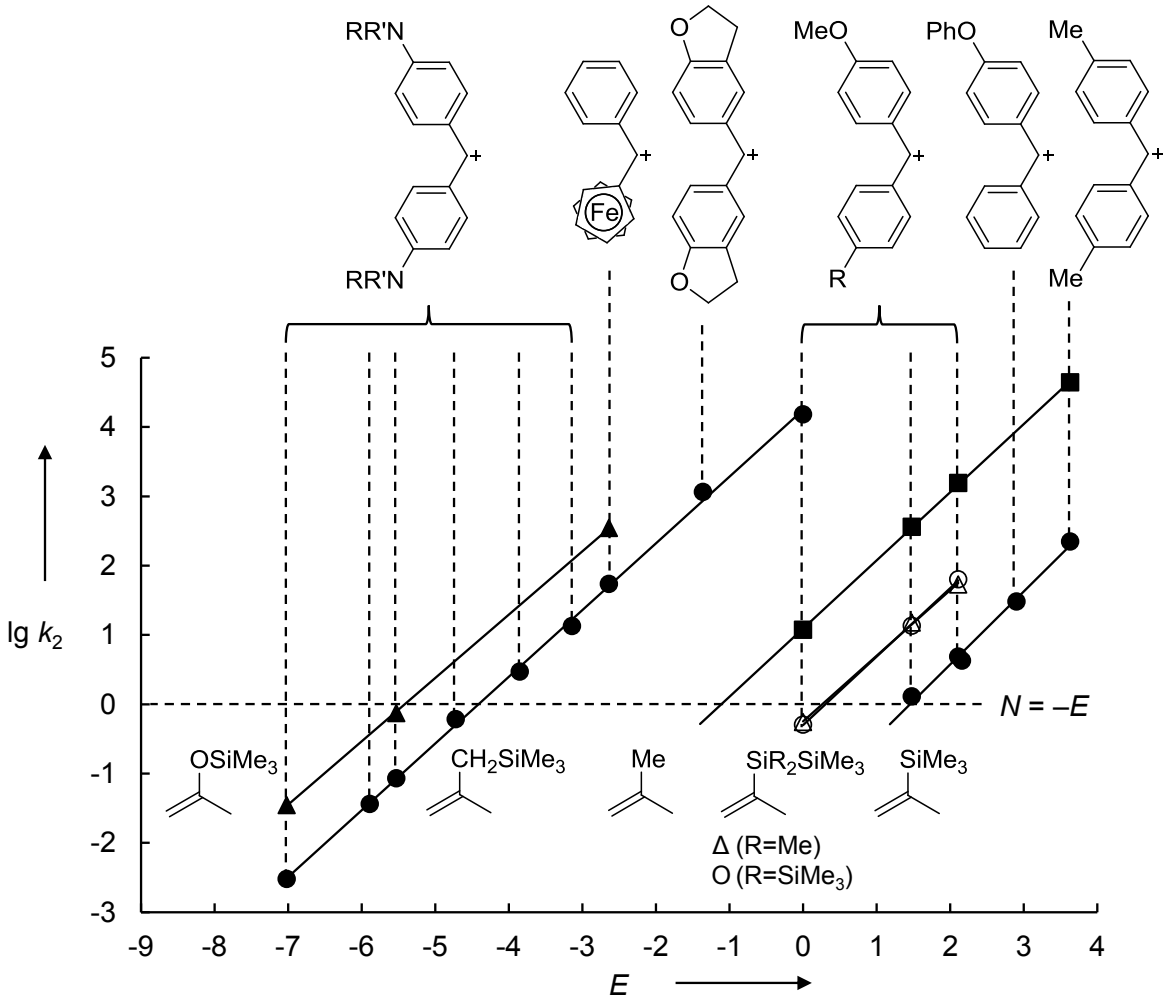

Figure 0.5. Plots of lg k_2 for the reactions of benzhydrylium ions with propene derivatives in CH_2Cl_2 at 20 °C versus the electrophilicity parameters *E* of the benzhydrylium ions.

[‡] Reproduced with permission from H. A. Laub, H. Mayr, *Chem. Eur. J.* **2014**, *20*, 1103–1110. Copyright © 2014 Wiley-VCH Verlag GmbH & Co. KGaA, Weinheim

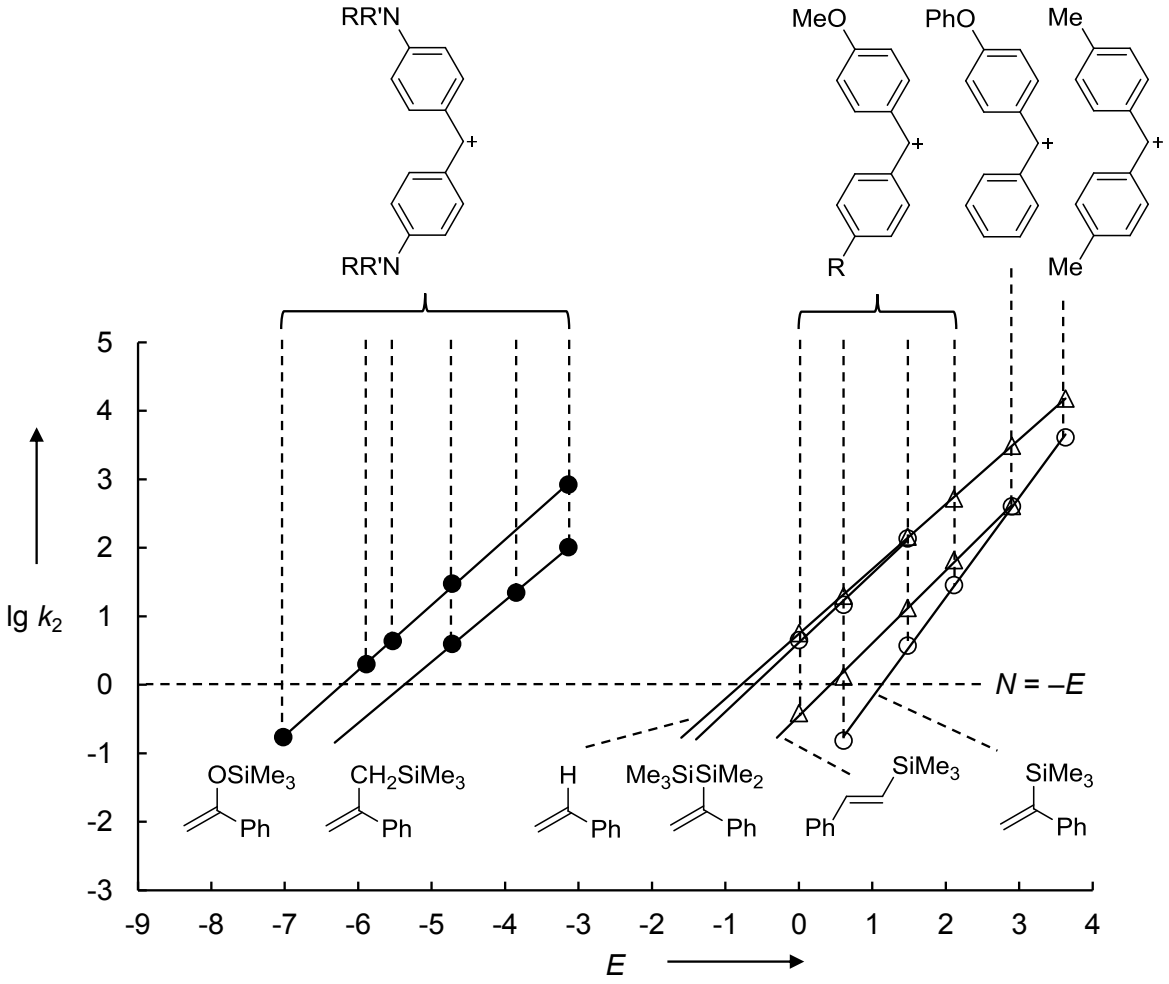

Figure 0.6. Plots of lg k_2 for the reactions of benzhydrylium ions with styrene derivatives in CH_2Cl_2 at 20 °C versus the electrophilicity parameters E of the benzhydrylium ions.

This allowed the inclusion of these vinylsilanes in the benzhydrylium-based nucleophilicity scale (Figure 0.7), which showed that vinylsilanes are significantly less reactive than structurally related allylsilanes. From the reactivity order for propene derivatives given in Figure 0.7 the following series of carbenium-stabilizing effects was derived: H < Si-C < Si-Si < C-C ≈ C-H << C-Si. It was shown that the magnitudes of these effects relative to hydrogen are each diminished by approximately a factor of 10^2 in the analogous styrene series when comparing their reactivities towards the *p*-methoxy substituted benzhydrylium ion. This decrease in the relative nucleophilic reactivities was attributed to perturbations of π-conjugation in α-substituted styrenes as indicated by the UV spectra of these compounds. Quantum chemical calculations concerning the corresponding torsion barriers and the vinylic bond lengths confirmed that π-conjugation is significantly disturbed in the ground states of the studied α-substituted styrenes.

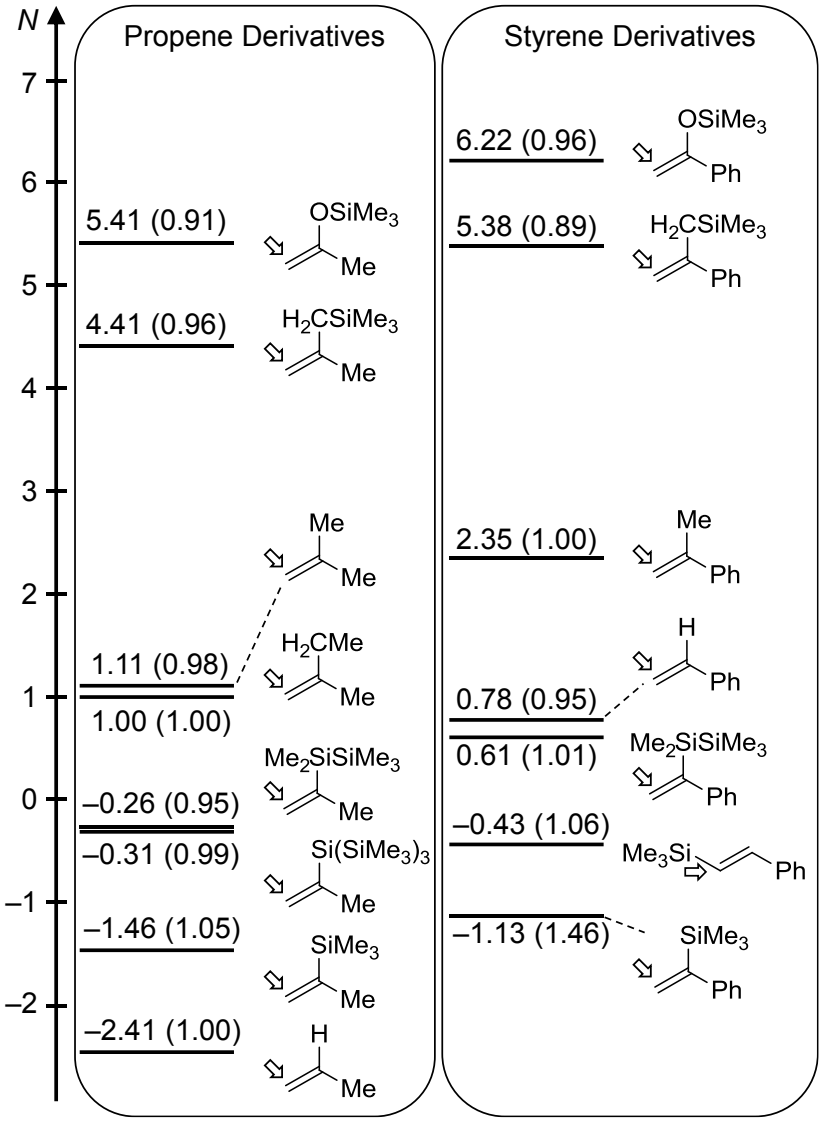

Figure 0.7. Nucleophilicities of propene (left) and styrene derivatives (right) compared to those of other π-nucleophiles (s_N values given in parentheses).

In contrast to the negligible activating effects found when introducing the $Si(SiMe_3)_3$ (supersilyl) group in allylsilanes and silyl enol ethers, the supersilyl substituted vinylsilane is one order of magnitude more reactive than its trimethylsilyl analog (Figure 0.7). This strengthened the assumption that the electron-donating effect of the tris(trimethylsilyl)silyl group operates mainly in the α-position and led to the consideration of vinylsilanes incorporating the supersilyl (or the $SiMe_2SiMe_3$) group as sila-allylsilanes.

The strong activating effects observed for β-silyl substituents when replacing an allylic hydrogen in isobutylene against a trimethylsilyl group were not found when exchanging a β-vinylic hydrogen in styrene giving *trans*-β-(trimethylsilyl)styrene (Figure 0.7). In fact, this

substitution led to a decrease of the nucleophilic reactivity of styrene which indicated that the steric retardation overcompensates the weak electronic activation, because the perpendicular orientation between the developing carbenium center and the C-Si σ-bond inhibits significant hyperconjugative stabilization of the transition state of electrophilic attack.

As a result, vinylsilanes are generally only slightly activated or deactivated compared to the corresponding alkenes, independent of the position of the silyl group in α- or β-position of the intermediate carbocation.

0.5 Hydrocarbation of CC-Triple Bonds: Quantification of the Nucleophilic Reactivity of Ynamides[§]

During the kinetic experiments regarding the reactions of benzhydrylium ions with ynamides in dichloromethane at 20 °C, the formation of colored products with bathochromic shifts of the

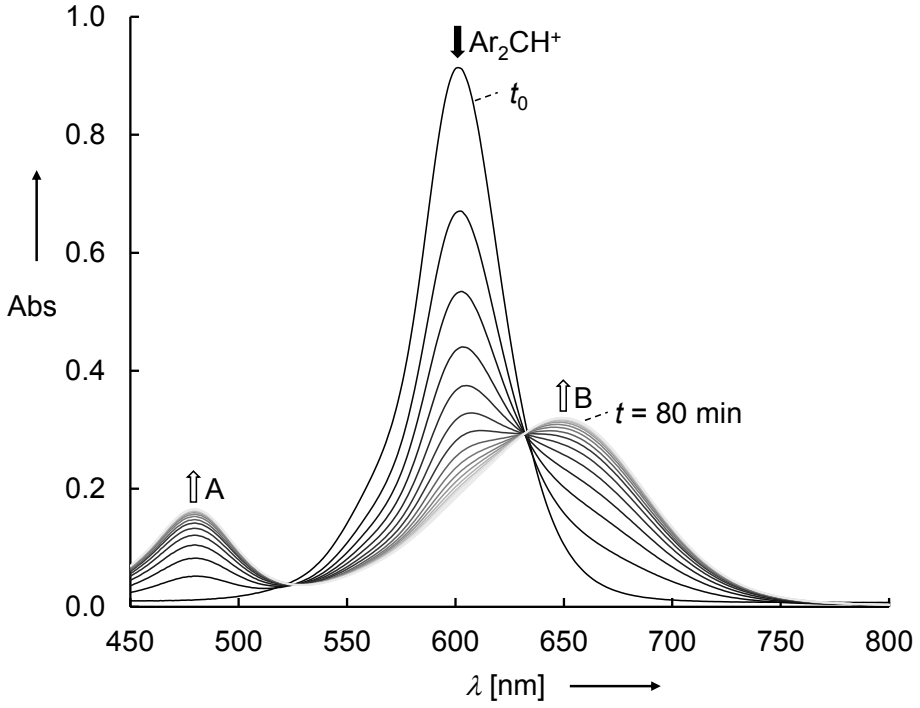

Figure 0.8. Time-dependent UV-Vis spectra during the reaction of an ynamide with a benzhydrylium ion Ar_2CH^+ in CH_2Cl_2 at 20 °C.

[§] Reproduced with permission from H. A. Laub, G. Evano, H. Mayr, *Angew. Chem.*; *Angew. Chem. Int. Ed.* in press. Unpublished work copyright © 2014 Wiley-VCH Verlag GmbH & Co. KGaA, Weinheim

absorption maxima relative to the absorption maxima of the benzhydrylium ions was observed. UV-Vis spectroscopic monitoring of this reaction showed that the new species was formed with the same rate as the benzhydrylium ion was consumed (Figure 0.8).

The isolation of an allylsulfonamide (Figure 0.9, right), when the reaction product was treated with DIBAL-H before aqueous workup, confirmed the assumption that the new species is the result of a hydrocarbation reaction.

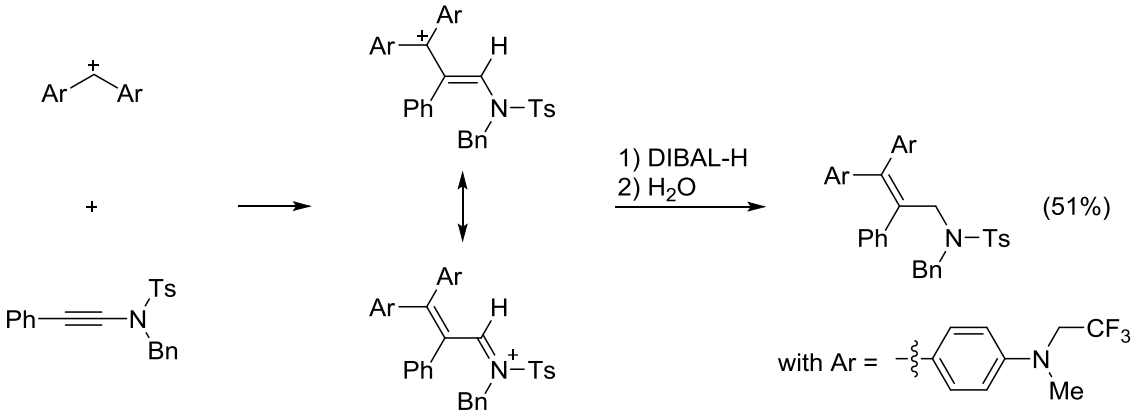

Figure 0.9. An allylsulfonamide was obtained by treating the colored unsaturated iminium ions with DIBAL-H.

The kinetics of the reactions of ynamides with benzhydrylium ions were studied under pseudo-first order conditions. Mono-exponential decays of the absorbances of the benzhydrylium ions and mono-exponential increases of both absorbances of the unsaturated iminium ions were observed. The second-order rate constants k_2 for the consumption of the benzhydrylium ions and for the formation of both bands of the iminium ions were derived as the slopes of the linear correlations of the respective first-order rate constants against the concentrations of the nucleophiles used in excess.

It was shown that a C-1-deuterated benzhydrylium ion reacts slightly faster than its ^{1}H-isotopomer, which excludes breaking of the C-H bond in the rate-determining step. From this inverse α-secondary kinetic isotope effect it was concluded, that the obtained rate constants reflect the attack of the benzhydrylium ions at the ynamides with irreversible formation of the keteniminium ions. These type of reactions can be described with Equation (0.1) and therefore, linear correlations were found when plotting the second-order rate constants (derived from the consumption of the benzhydrylium ions) against the electrophilicity parameters E of the reference electrophiles (Figure 0.10).

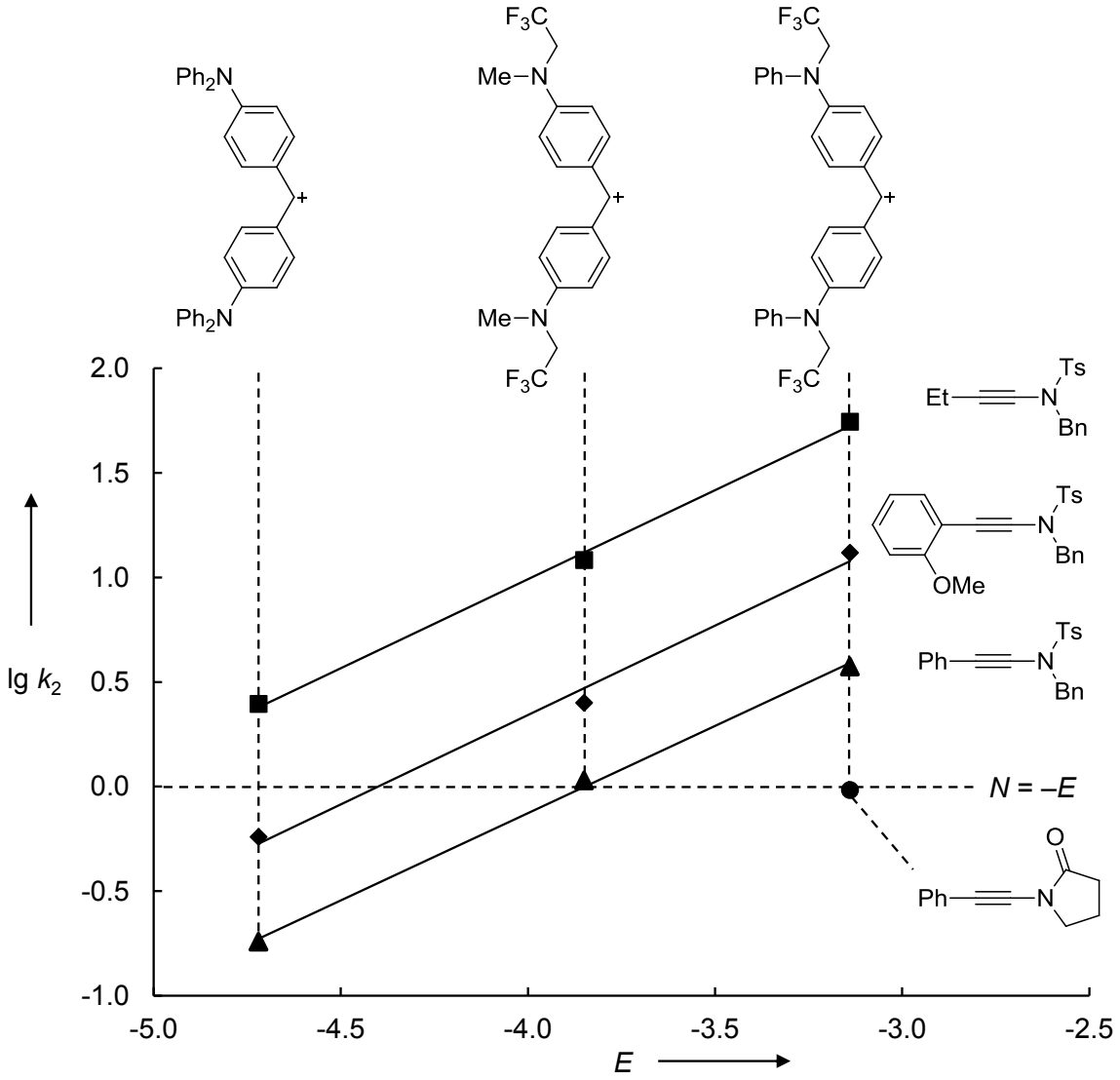

Figure 0.10. Plots of lg k_2 (derived from the consumption of the benzhydrylium ions) for the reactions of benzhydrylium ions with ynamides in CH_2Cl_2 at 20 °C versus the electrophilicity parameters E of the reference electrophiles.

From these plots the nucleophile-specific parameters N and s_N for ynamides were obtained. This allowed integrating these compounds in the comprehensive nucleophilicity scale and comparing them to structurally related nucleophiles. According to Figure 0.11, ynamides possess nucleophilic reactivities which are comparable to those of (2-methylallyl)trimethylsilane and butyl vinyl ether. While enamides are just slightly more reactive than ynamides, the nucleophilicity of structurally related enamines is significantly increased.

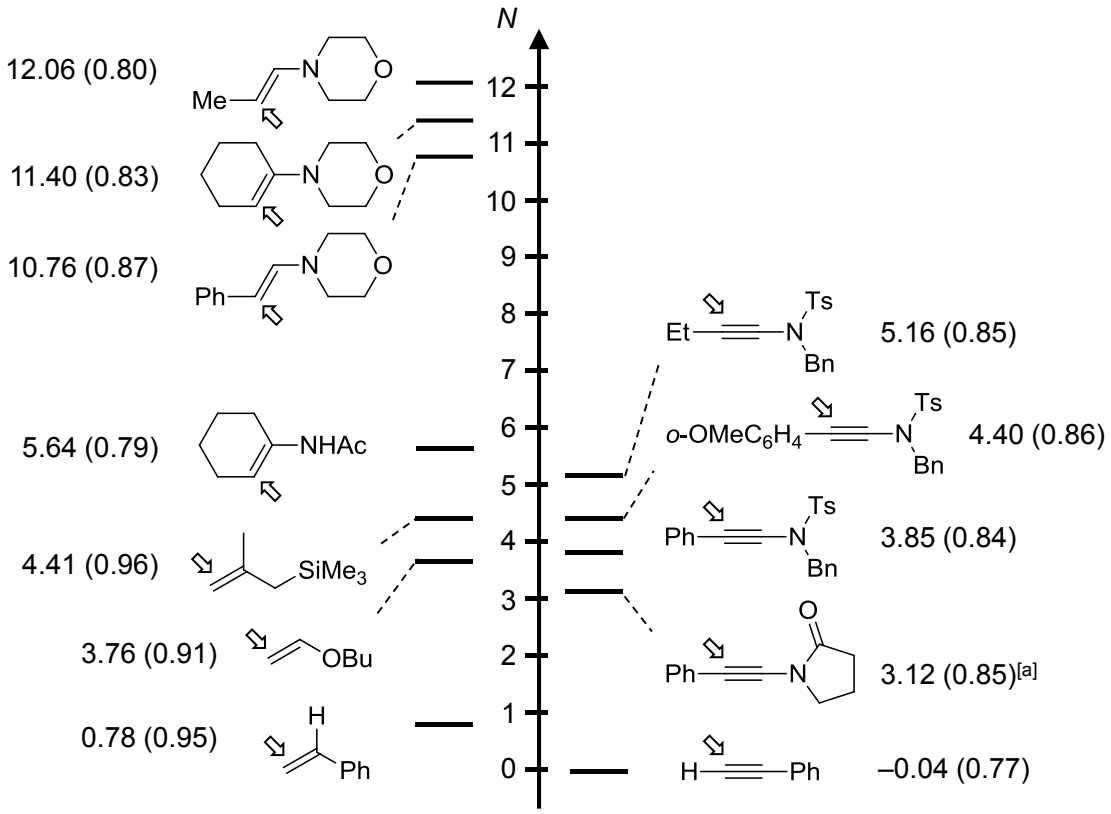

Figure 0.11. Comparison of the nucleophilicity of ynamides with those of other π-nucleophiles in CH_2Cl_2 (CH_3CN for enamides; [a] estimated value of s_N).

Chapter 1

Introduction

"Since it is proposed to regard chemical reactions as electrical transactions in which reagents act by reason of a constitutional affinity either for electrons or for atomic nuclei, it is important to be able to recognize which type of reactivity any given reagent exhibits."

Christopher K. Ingold (1934)[1]

With his classification of organic molecules into "nucleophiles" (affinity for atomic nuclei) and "electrophiles" (affinity for electrons) Ingold awoke the interest of many chemists in finding general concepts for quantifying these affinities, termed nucleophilicity and electrophilicity, respectively.[1,2] The first concept was developed by Swain and Scott[3] in 1953 on the basis of 47 reactions of a set of nucleophiles and electrophiles in water. They described the linear free energy relationship given in Equation (1.1) where k_0 is the rate constant for the reaction of an electrophile with water and k gives the rate constant for the reaction of the same electrophile with any given nucleophile. These nucleophiles are characterized by their nucleophilicities n (defined as 0.00 for water) and the sensitivity of the reaction to the variation of the nucleophile is given by the electrophile-dependent parameter s (defined as 1.00 for methyl bromide).

$$\lg (k/k_0) = s\, n \qquad (1.1)$$

In 1972, Ritchie[4] showed that the rates of the reactions of carbocations and diazonium ions with various nucleophiles follow Equation (1.2). Thereby, the nucleophilicity is given by the solvent specific, electrophile-independent parameter N_+, and the reactivities of the electrophiles are quantified by the rates k_0 of their reactions with water. From these two parameters, the rate constant k for the reaction of the corresponding reactants in a specific solvent can be obtained.

$$\lg (k/k_0) = N_+ \qquad (1.2)$$

The resulting reactivity scale covered a broad range of reactivity. However, Ritchie's later observation that the relative reactivities of nucleophiles can strongly differ when different classes of electrophiles are considered, is not in line with the constant selectivity relationship described in Equation (1.2).[5]

During their studies concerning the reactions of benzhydrylium ions with alkenes, Mayr *et al.*[6] found that even when considering the same class of electrophiles deviations from constant selectivity relationships can be observed. For considering these changes in selectivity, Mayr and Patz[7] introduced the nucleophile-specific sensitivity parameter s_N in Equation (1.3).

$$\lg k\ (20\ °C) = s_N(N + E) \qquad (1.3)$$

While the electrophilic reactivity is expressed in the solvent-independent electrophilicity parameter E, the nucleophile-specific parameters N (nucleophilicity) and s_N refer to a specific solvent. The second-order rate constants k at 20 °C for the reaction of a nucleophile with an electrophile is thus obtained from these three parameters. In 1994,[7] this linear free energy relationship was based on the rates of the reactions of n-, π-, and σ-nucleophiles with carbocations, aryldiazonium ions and metal-π-complexes. With the expansion of the reactivity range covered by variably *p*- and *m*-substituted benzhydrylium ions, it was later possible to base the relationship solely on reference electrophiles, where the steric shielding of the reaction center is kept constant.[8] On this basis it was possible to construct the most comprehensive reactivity scale presently available, covering a reactivity range of over 30 orders of magnitude.[9]

Two important classes of nucleophiles which are part of this nucleophilicity scale are allylsilanes and silyl enol ethers. They are frequently used reagents in organic synthesis, especially when combined with Lewis acid activated carbonyl compounds. The corresponding reactions are known as Hosomi-Sakurai[10] (allylsilanes) and Mukaiyama aldol[11] (silyl enol ethers) reactions.

It has been shown by Yamamoto and co-workers[12] that the implementation of the tris(trimethylsilyl)silyl (supersilyl) group in silyl enol ethers led to high diastereoselectivities and yields in Lewis acid catalyzed [2+2]-cycloaddition and Mukaiyama aldol reactions when compared to commonly used silyl enol ethers. As Bock[13] previously described the $Si(SiMe_3)_3$ group as a strong electron-donor, this property together with its steric bulk was proposed as a possible reason for these findings. In order to evaluate if electronic effects account for the unique properties and whether similar effects can be found for related allylsilanes, one focus of this work was to study the nucleophilic reactivities of supersilyl substituted allylsilanes and silyl enol ethers and compare them to those of the previously investigated trimethylsilyl substituted analogs.

The introduction of fluorine in organic molecules is attractive as many fluorinated compounds are known to possess biological activity.[14] Due to the already mentioned importance of silyl enol ethers in organic synthesis, perfluorinated variants of these nucleophiles could be interesting building blocks. However, the introduction of fluorine with its high electronegativity could considerably influence the nucleophilicity of these compounds. In order to quantify these effects and thus assessing the scope of these substrates in organic synthesis, a part of this work investigated the structure-reactivity relationships in fluorinated silyl enol ethers.

Apart from allylsilanes and silyl enol ethers, vinylsilanes represent organosilicon compounds which are widely used for chemical transformations. They can be combined with a great variety of electrophiles and commonly undergo electrophilic substitution reactions.[10b,c,15] In analogy to the previously mentioned allylsilanes, the attack of an electrophile leads in most cases to the formation of β-silyl substituted carbocations. In spite of their close relation to vinylsilanes, allylsilanes are known to undergo reactions with weaker electrophiles and under milder conditions.[15j] In addition, it has been reported that the introduction of electron-donating substituents in α-position to the silyl group, directs the electrophilic attack to the β-position with respect to the silicon moiety.[16] In consequence, α-silyl substituted carbocations are formed as intermediates. These different pathways for electrophilic attack at vinylsilanes provided the opportunity to study structure-reactivity relationships for these compounds with respect to α- and β-silyl effects.

While organosilanes are well established building blocks in organic synthesis, broader interest of synthetic chemists in ynamides was stimulated just in recent years due to novel and more convenient procedures for their preparation.[17] It has already been shown that these compounds can be used for many transformations, including cycloadditions, oxidations and reductions providing the possibility of preparing a great manifold of nitrogen-containing compounds.[18] Owing to the strong polarization of the triple bond by the amido group, ynamides can act as nucleophiles as well as electrophiles. While the use Lewis or Brønsted acids is commonly needed for nucleophilic additions to ynamides, no activation is generally required for electrophilic attack. For this reason, a part of this work is concerned with understanding the different effects that can influence the nucleophilic reactivity of ynamides by employing the benzhydrylium method. The inclusion of these compounds in the comprehensive

nucleophilicity scale provides the opportunity of comparing them with previously investigated enamines[8,19] and enamides.[20]

References

[1] C. K. Ingold, *Chem. Rev.* **1934**, *15*, 225–274.

[2] a) C. K. Ingold, *Recl. Trav. Chim. Pays-Bas* **1929**, *42*, 797–812; b) C. K. Ingold, *J. Chem. Soc.* **1933**, 1120–1127.

[3] C. G. Swain, C. B. Scott, *J. Am. Chem. Soc.* **1953**, *75*, 141–147.

[4] C. D. Ritchie, *Acc. Chem. Res.* **1972**, *5*, 348–354.

[5] C. D. Ritchie, *Can. J. Chem.* **1986**, *64*, 2239–2250.

[6] H. Mayr, R. Schneider, B. Irrgang, C. Schade, *J. Am. Chem. Soc.* **1990**, *112*, 4454–4459.

[7] H. Mayr, M. Patz, *Angew. Chem.* **1994**, *106*, 990–1010; *Angew. Chem. Int. Ed. Engl.* **1994**, *33*, 938–957.

[8] H. Mayr, T. Bug, M. F. Gotta, N. Hering, B. Irrgang, B. Janker, B. Kempf, R. Loos, A. R. Ofial, G. Remennikov, H. Schimmel, *J. Am. Chem. Soc.* **2001**, *123*, 9500–9512.

[9] a) R. Lucius, R. Loos, H. Mayr, *Angew. Chem.* **2002**, *114*, 97–102; *Angew. Chem., Int. Ed.* **2002**, *41*, 91–95; b) H. Mayr, B. Kempf, A. R. Ofial, *Acc. Chem. Res.* **2003**, *36*, 66–77; c) H. Mayr, A. R. Ofial in *Carbocation Chemistry* (Eds.: G. A. Olah, G. K. S. Prakash), Wiley, Hoboken, NJ, **2004**, pp. 331–358; d) H. Mayr, A. R. Ofial, *Pure Appl. Chem.* **2005**, *77*, 1807–1821; e) H. Mayr, A. R. Ofial, *J. Phys. Org. Chem.* **2008**, *21*, 584–595; f) D. Richter, N. Hampel, T. Singer, A. R. Ofial, H. Mayr, *Eur. J. Org. Chem.* **2009**, 3203–3211; g) J. Ammer, C. Nolte, H. Mayr, *J. Am. Chem. Soc.* **2012**, *134*, 13902–13911, h) Reactivity database can be accessed at: http://www.cup.uni-muenchen.de/oc/mayr/DBintro.html.

[10] (a) A. Hosomi, H. Sakurai, *J. Am. Chem. Soc.* **1977**, *99*, 1673–1675; b) T. K. Sarkar in *Science of Synthesis, Vol. 4* (Ed.: I. Fleming), Thieme Verlag, Stuttgart, **2002**, pp. 837–925; c) L. Chabaud, P. James, Y. Landais, *Eur. J. Org. Chem.* **2004**, 3173–3199.

[11] a) T. Mukaiyama, K. Narasaka, K. Banno, *Chem. Lett.* **1973**, 1011–1014; b) T. Mukaiyama, *Org. React.* **1982**, *28*, 203–331; c) P. Brownbridge, *Synthesis* **1983**, 1–28; d) T. Bach, *Angew. Chem.* **1994**, *106*, 433–435; *Angew. Chem., Int. Ed. Engl.* **1994**, *33*, 417–419; e) S. G. Nelson, *Tetrahedron: Asymmetry* **1998**, *9*, 357–389; f) E. M. Carreira in *Comprehensive Asymmetric Catalysis*; *Vol. 3* (Eds.: E. N. Jacobsen, A. Pfalz, H. Yamamoto), Springer: Berlin, **1999**, pp 997–1065; g) R. Mahrwald, *Chem. Rev.* **1999**, *99*, 1095–1120.

[12] a) M. B. Boxer, H. Yamamoto, *Org. Lett.* **2005**, *7*, 3127–3129; b) M. B. Boxer, H. Yamamoto, *J. Am. Chem. Soc.* **2006**, *128*, 48–49; c) M. B. Boxer, H. Yamamoto, *Nat. Protoc.* **2006**, *1*, 2434–2438; d) M. B. Boxer, H. Yamamoto, *J. Am. Chem. Soc.* **2007**, *129*, 2762–2763; e) M. B. Boxer, H. Yamamoto, *Org. Lett.* **2008**, *10*, 453–455; f) M. B. Boxer, M. Akakura, H. Yamamoto, *J. Am. Chem. Soc.* **2008**, *130*, 1580–1582; g) M. B. Boxer, B. J. Albert, H. Yamamoto, *Aldrichimica Acta* **2009**, *42*, 3–15; h) Y. Yamaoka, H. Yamamoto, *J. Am. Chem. Soc.* **2010**, *132*, 5354–5356; i) B. J. Albert, H. Yamamoto, *Angew. Chem., Int. Ed.* **2010**, *49*, 2747–2749.

[13] H. Bock, J. Meuret, R. Baur, K. Ruppert, *J. Organomet. Chem.* **1993**, *446*, 113–122.

[14] a) W. R. Dolbier Jr, *J. Fluorine Chem.* **2005**, *126*, 157–163; b) T. Hiyama in *Organofluorine Compounds: Chemistry and Applications*, (Ed.: H. Yamamoto), Springer, Berlin, **2000**; c) K. Müller, C. Faeh, F. Diederich, *Science* **2007**, *317*, 1881–1886; d) D. O'Hagan, *Chem. Soc. Rev.* **2008**, *37*, 308–319; e) T. Yamazaki, T. Taguchi, I. Ojima in *Fluorine in Medicinal Chemistry and Chemical Biology*, (Ed.: I. Ojima), Wiley, Chichester, **2009**, pp. 1–46; f) *Fluorine and Health*, (Eds.: A. Tressaud, G. Haufe), Elsevier, Amsterdam, **2008**.

[15] a) C. Eaborn, *Organosilicon Compounds*, Butterworth, London, **1960**; b) E. W. Colvin, *Chem. Soc. Rev.* **1978**, *7*, 15–64; c) T. H. Chan, I. Fleming, *Synthesis* **1979**, 761–786; d) E. W. Colvin, *Silicon in Organic Synthesis*, Butterworth, London, **1981**; e) I. Fleming, *Chem. Soc. Rev.* **1981**, *10*, 83–111; f) L. A. Paquette, *Science* **1982**, *217*, 793–800; g) S. Pawlenko, *Organosilicon Chemistry*, de Gruyter, Berlin, **1986**; h) E. W. Colvin, *Silicon Reagents in Organic Synthesis*, Academic Press, London, **1988**; i) I. Fleming, J. Dunoguès, R. Smithers in *Organic Reactions*, *Vol. 37*, Wiley, Hoboken, NJ, **1989**, pp. 57–575; j) J. S. Panek in *Comprehensive Organic Synthesis, Vol. 1* (Eds.: B. M. Trost, I. Fleming, S. L. Schreiber), Pergamon, Oxford, **1991**, pp. 579–627; k) I. Fleming, A. Barbero, D. Walter, *Chem. Rev.* **1997**, *97*, 2063–2192; l) M. A. Brook, *Silicon in Organic, Organometallic, and Polymer Chemistry*, Wiley, New York, **2000**; m) K. Oshima in *Science of Synthesis*, *Vol. 4* (Eds.: I. Fleming), Thieme Verlag, Stuttgart, **2002**, pp. 713–756; n) M. J. Curtis-Long, Y. Aye, *Chem. Eur. J.* **2009**, *15*, 5402–5416.

[16] a) L. H. Sommer, F. J. Evans, *J. Am. Chem. Soc.* **1954**, *76*, 1186–1187; b) L. H. Sommer, D. L. Bailey, G. M. Goldberg, C. E. Buck, T. S. Bye, F. J. Evans, F. C. Whitmore, *J. Am. Chem. Soc.* **1954**, *76*, 1613–1618.

[17] a) K. S. Feldman, M. M. Bruendl, K. Schildknegt, A. C. Bohnstedt, *J. Org. Chem.* **1996**, *61*, 5440–5452; b) X. Zhang, Y. Zhang, J. Huang, R. P. Hsung, K. C. M. Kurtz, J. Oppenheimer, M. E. Petersen, I. K. Sagamanova, L. Shen, M. R. Tracey, *J. Org. Chem.* **2006**, *71*, 4170–4177; c) T. Hamada, X. Ye, S. S. Stahl, *J. Am. Chem. Soc.* **2008**, *130*, 833–835; d) A. Coste, G. Karthikeyan, F. Couty, G. Evano, *Angew. Chem. Int. Ed.* **2009**, *48*, 4381–4385.

[18] a) C. A. Zificsak, J. A. Mulder, R. P. Hsung, C. Rameshkumar, L.-L. Wei, *Tetrahedron* **2001**, *57*, 7575–7606; b) K. A. DeKorver, H. Li, A. G. Lohse, R. Hayashi, Z. Lu, Y. Zhang, R. P. Hsung, *Chem. Rev.* **2010**, *110*, 5064–5106; c) G. Evano, A. Coste, K. Jouvin, *Angew. Chem.* **2010**, *122*, 2902–2921; *Angew. Chem. Int. Ed.* **2010**, *49*, 2840–2859; d) X.-N. Wang, H.-S. Yeom, L.-C. Fang, S. He, Z.-X. Ma, B. L. Kedrowski, R. P. Hsung, *Acc. Chem. Res.* **2014**, *47*, 560-578.

[19] B. Kempf, N. Hampel, A. R. Ofial, H. Mayr, *Chem. Eur. J.* **2003**, *9*, 2209–2218.

[20] B. Maji, S. Lakhdar, H. Mayr, *Chem. Eur. J.* **2012**, *18*, 5732–5740.

Chapter 2

Effect of the "Supersilyl" Group on the Reactivities of Allylsilanes and Silyl Enol Ethers

Reproduced with permission from

H. A. Laub, H. Yamamoto, H. Mayr, *Org. Lett.* **2010**, *12*, 5206–5209.

2.1 Introduction

Allylsilanes and silyl enol ethers represent two important classes of organosilanes. While allylsilanes are widely used as allylating reagents for Lewis acid activated carbonyl compounds (Hosomi-Sakurai reaction),[1] silylated enol ethers are key substrates for the Mukaiyama variant of aldol reactions.[2]

Cyclobutane rings can be formed via Lewis acid catalyzed [2+2]-cycloaddition reactions of silyl enol ethers with α,β-unsaturated esters.[3] In these reactions, higher yields and *trans*-selectivity were found, when the $SiMe_3$ group was replaced by the bulkier $SiMe_2tBu$ group.[3d] Utilization of the tris(trimethylsilyl)silyl group led to the first [2+2] cycloaddition of an acetaldehyde derived silyl enol ether with an acrylic ester (Scheme 2.1).[4]

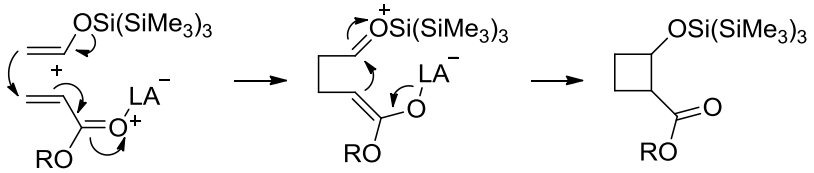

Scheme 2.1. Stepwise [2+2] cycloaddition of a silyl enol ether with an acrylic ester.

Intrigued by the high yields and selectivities obtained by application of the so-called "supersilyl" group for cycloaddition reactions, the corresponding tris(trimethylsilyl)silyl enol ethers were used for Mukaiyama aldol reactions.[5] High diastereoselectivities and yields were even obtained with acetaldehyde-derived substrates. Moreover, sequential reactions with diverse reagents opened the pathway to the facile synthesis of molecules with substructures known for their biological activity.[5c-f]

The observed reactivities have been explained by the steric demand and the electronic properties of the tris(trimethylsilyl)silyl group. Bock and co-workers reported that the first vertical ionization energies (IE_1^v) for supersilyl-substituted benzenes are much smaller than those of the corresponding trimethylsilyl derivatives (Table 2.1); the supersilyl group has, therefore, been considered as a very strong electron donor.[6] As demonstrated by the last entry of Table 2.1, the hyperconjugative effect of the trimethylsilylmethyl substituent causes a slightly weaker decrease of the ionization energy. In contrast, hydride abstractions from trialkylsilanes and tris(trimethylsilyl)silane have been reported to proceed with comparable rates.[7]

Table 2.1. First Vertical Ionization Energies for Silyl Substituted Benzenes Reported by Bock and Co-Workers.[6]

	IE_1^v (eV)	
X	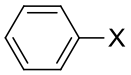	
$SiMe_3$	9.05	8.70
$Si(SiMe_3)_3$	8.04	7.37
CH_2SiMe_3	8.35	7.86

Kinetic investigations of the nucleophilicities of allylsilanes and silyl enol ethers with $Si(SiMe_3)_3$ substitution have so far not been performed. We now report on the application of the benzhydrylium method[8] for characterizing the nucleophilic reactivities of the tris(trimethylsilyl)silyl-substituted allyl compounds **1** and enol ethers **2** (Scheme 2.2) and the comparison with the corresponding allyltrimethylsilanes[8a,9] and trimethylsilyl enol ethers.[8a,10]

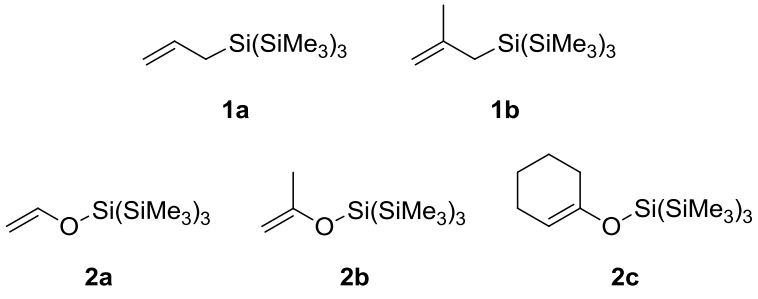

Scheme 2.2. Organosilanes studied for the quantification of the effect of the supersilyl group on the nucleophilic reactivities of allylsilanes and silyl enol ethers.

Benzhydrylium ions with variable *p*- and *m*-substituents, which cover a broad range of reactivity while the steric shielding of the reaction center is kept constant, have been used as reference electrophiles for the construction of a comprehensive nucleophilicity scale based on Equation (2.1), in which electrophiles are characterized by one parameter (E) and nucleophiles are characterized by the solvent-dependent parameters s_N (sensitivity) and N (nucleophilicity).[8a]

$$\lg k\ (20\ °C) = s_N(N + E) \qquad (2.1)$$

In this investigation, benzhydrylium ions **3a-f** (Table 2.2) with electrophilicity parameters E ranging from –5 to +1.5 were used because they reacted with the organosilanes **1** and **2** with conveniently measurable rates.

Table 2.2. Reference Electrophiles Utilized for Quantifying the Nucleophilicities of **1** and **2**.

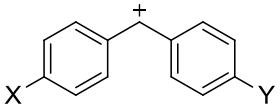

ArAr'CH$^+$ [a]	X	Y	E[b]
(tol)(ani)CH$^+$ (**3a**)	CH_3	OMe	1.48
(ani)$_2$CH$^+$ (**3b**)	OMe	OMe	0.00
(fur)$_2$CH$^+$ (**3c**)	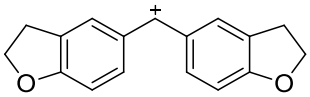		–1.36
(pfa)$_2$CH$^+$ (**3d**)	N(Ph)CH_2CF_3	N(Ph)CH_2CF_3	–3.14
(mfa)$_2$CH$^+$ (**3e**)	N(Me)CH_2CF_3	N(Me)CH_2CF_3	–3.85
(dpa)$_2$CH$^+$ (**3f**)	NPh_2	NPh_2	–4.72

[a] tol = *p*-*tol*yl; ani = *p*-*ani*syl; fur = 2,3-dihydrobenzo*fur*an-5-yl; pfa = 4-(*p*henyl(tri*f*luoro-ethyl)*a*mino)phenyl; mfa = 4-(*m*ethyl(tri*f*luoroethyl)*a*mino)phenyl; dpa = 4-(*dip*henyl*a*mino)-phenyl. [b] Empirical electrophilicities E from ref [8a].

2.2 Results and Discussion

Compounds **1b** and **2b** reacted with the colored benzhydrylium salt **3f-BF$_4$** in CH_2Cl_2 to give the desilylated products **5** (Scheme 2.3), as previously reported for the corresponding trimethylsilyl compounds.[8a,9,10] As the intermediates **4** and the products **5** are colorless, the nucleophilic attack at the electrophilic center was followed spectrophotometrically.

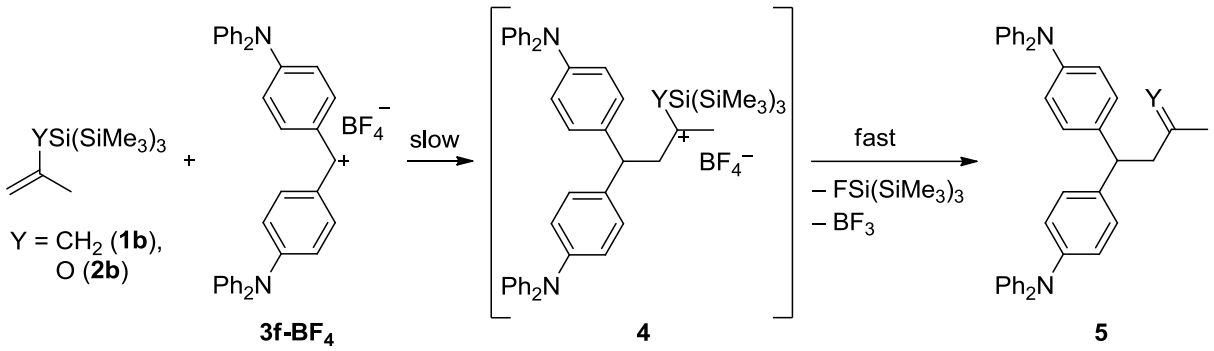

Scheme 2.3. Reactions of **1b** and **2b** with the benzhydrylium salt **3f-BF$_4$**.

Addition of at least 7 equiv of the supersilanes **1** and **2** to solutions of the benzhydrylium tetrahaloborates, tetrachlorogallates, or pentachlorostannates **3-MX$_{n+1}$** in CH_2Cl_2 led to mono-exponential decays of the electrophiles' absorbances (Figure 2.1a).

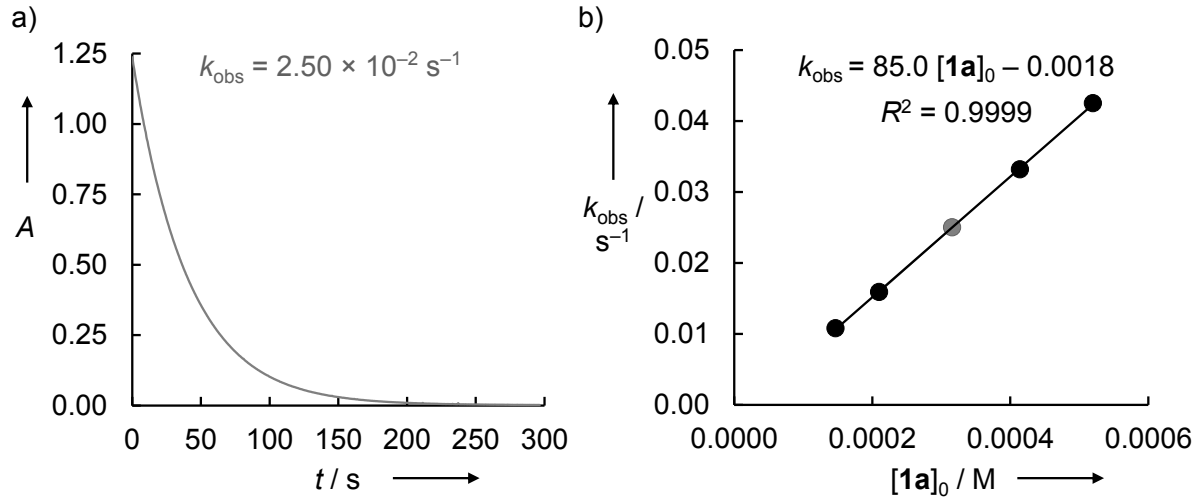

Figure 2.1. a) Exponential decay of the absorbance at 513 nm during the reaction of **1a** ($c = 3.16 \times 10^{-4}$ M) with **3b-SnCl$_5$** ($c = 2.09 \times 10^{-5}$ M) at 20 °C in CH_2Cl_2. b) Determination of the second-order rate constant $k_2 = 85.0$ M^{-1} s^{-1} as the slope of the correlation between the first-order rate constant k_{obs} and the concentration of **1a**.

The resulting first-order rate constants k_{obs} correlated linearly (with R^2 values ranging from 0.935 to 0.9999) with the concentrations of the nucleophiles **1** and **2** as depicted in Figure 2.1b. The second-order rate constants k_2 given in Tables 2.3 and 2.5 were derived from the slopes of such correlations.

Table 2.3. Second-Order Rate Constants for the Reactions of **1a** (1.4×10^{-4} to 5.2×10^{-4} M) with Different Benzhydrylium Salts **3b-MX$_{n+1}$** (1.6×10^{-5} to 2.3×10^{-5} M).

MX_{n+1}^-	k_2 / M^{-1} s^{-1}
BCl_4^-	84.9
BF_4^-	74.8
$GaCl_4^-$	77.5
$SnCl_5^-$	85.0

Table 2.3 shows that the rates of the reactions of allyltris(trimethylsilyl)silane (**1a**) with the benzhydryl cation **3b** are only slightly affected by the counterion, indicating the rate-determining formation of intermediate **4** (Scheme 2.3) as previously observed for the corresponding trimethylsilyl compounds.[9,10] The rate-determining formation of the C-C bond is furthermore supported by the independence of the rate constants of the concentration of $Bu_4N^+BCl_4^-$ (Table 2.4).

Table 2.4. First-Order Rate Constants for the Reactions of **1a** with **3b-BCl$_4$** (1.9×10^{-5} M) in the Presence of Various Amounts of $Bu_4N^+BCl_4^-$.

[**1a**]$_0$ / M	$[Bu_4N^+BCl_4^-]_0$ / [**1a**]$_0$	k_{obs} / s^{-1}
1.87×10^{-4}	0	1.76×10^{-2}
1.85×10^{-4}	1	1.73×10^{-2}
1.84×10^{-4}	5	1.77×10^{-2}
1.84×10^{-4}	100	1.77×10^{-2}

Table 2.5 compares the second-order rate constants for the attack of the nucleophiles **1** and **2** at the reference electrophiles with the previously reported values for the corresponding trimethylsilanes **6** and **7**.[9,10]

Table 2.5. Second-Order Rate Constants k_2 for the Reactions of the Silanes **1**, **2**, **6**, and **7** with the Benzhydrylium Ions **3**.

Nucleophiles	**3**	k_2 / $M^{-1}s^{-1}$	Nucleophiles	**3**	k_2[a] / $M^{-1}s^{-1}$	$k_2(Si(SiMe_3)_3)$ / $k_2(Si(alkyl)_3)$
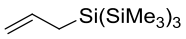 **1a**	**3a**	2.30×10^3 [b]	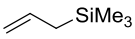 **6a**	**3a**	1.41×10^3	1.63
	3b	8.49×10^1		**3b**	4.69×10^1	1.81
	3c	3.75		**3c**	2.14	1.75
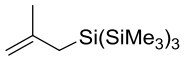 **1b**	**3d**	2.40×10^1	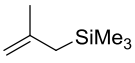 **6b**	**3d**	1.35×10^1	1.78
	3e	3.54		**3e**	2.97	1.19
	3f	9.65×10^{-1}		**3f**	6.13×10^{-1}	1.57
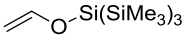 **2a**	**3d**	5.59	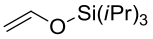 **7a**	**3d**	1.91[c]	2.93
	3e	1.19		**3e**	4.12×10^{-1} [c]	2.89
	3f	2.72×10^{-1}		**3f**	6.26×10^{-2} [c]	4.35
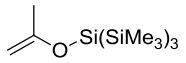 **2b**	**3d**	2.32×10^2	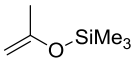 **7b**	**3d**	1.16×10^2 [c]	2.00
	3e	6.58×10^1		**3e**	2.63×10^1 [c]	2.50
	3f	1.18×10^1		**3f**	4.25[c]	2.78
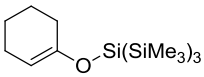 **2c**	**3d**	5.70×10^1	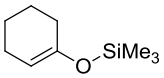 **7c**	**3d**	1.17×10^2 [c]	0.487
	3e	1.23×10^1		**3e**	2.17×10^1	0.567
	3f	2.10		**3f**	2.05	1.02

[a] Data from ref [8a] if not stated otherwise. [b] Calculated by using the Eyring equation with k_2 values for temperatures varying from –71 to –22 °C (for details see Experimental Part). [c] Calculated by using Equation (2.1) from N and s_N in ref [8a] and E from Table 2.2.

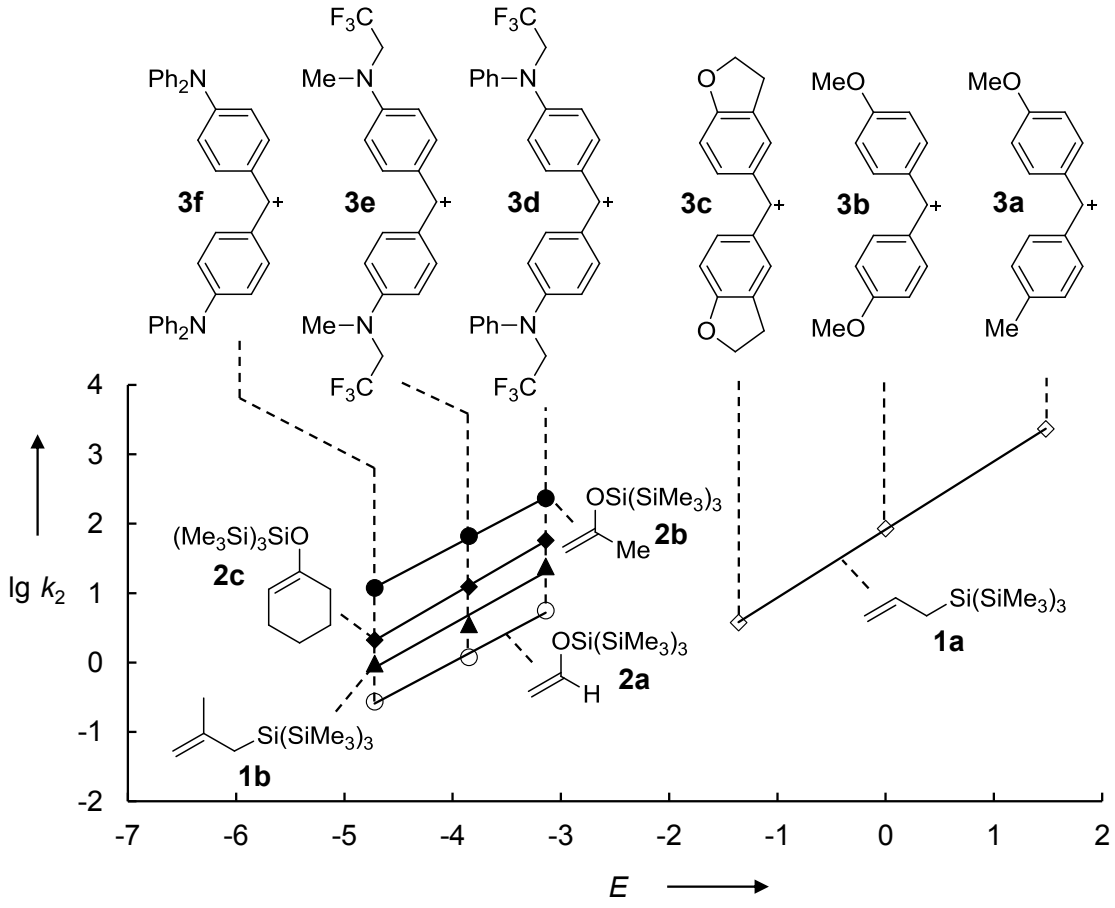

Figure 2.2. Plots of lg k_2 for the reactions of **1** and **2** with benzhydrylium ions **3** in CH_2Cl_2 at 20 °C versus the corresponding electrophilicity parameters *E*.

Plots of lg k_2 for the reactions of the supersilylated nucleophiles **1** and **2** with the reference electrophiles **3** versus the empirical electrophilicity parameters *E* are linear (Figure 2.2), indicating that Equation (2.1) is applicable, thus providing the *N* and s_N parameters for the supersilyl derivatives **1** and **2** (Scheme 2.4).

Table 2.5 and Scheme 2.4 show that the allylsilanes **1** which carry supersilyl groups are less than 2-times more nucleophilic than the structurally analogous allyltrimethylsilanes **6**. Exchange of $SiMe_3$ by $Si(SiMe_3)_3$ has also a marginal effect on the reactivities of enol ethers. While the acetone-derived enol ether **2b** is 2-3 times more reactive than **7b**, the cyclohexanone-derived enol ether **2c** is even slightly less reactive than **7c**. The somewhat reduced reactivity of **2c** might be explained by the shielding of the reaction center by the tris(trimethylsilyl)silyl group in the preferred conformation of the cyclohexenyl ether. The slightly higher ratios for the acetaldehyde-derived enol ethers **2a**/**7a** may be due to the fact that **7a** bears the $Si(iPr)_3$ group instead of the $SiMe_3$ group.

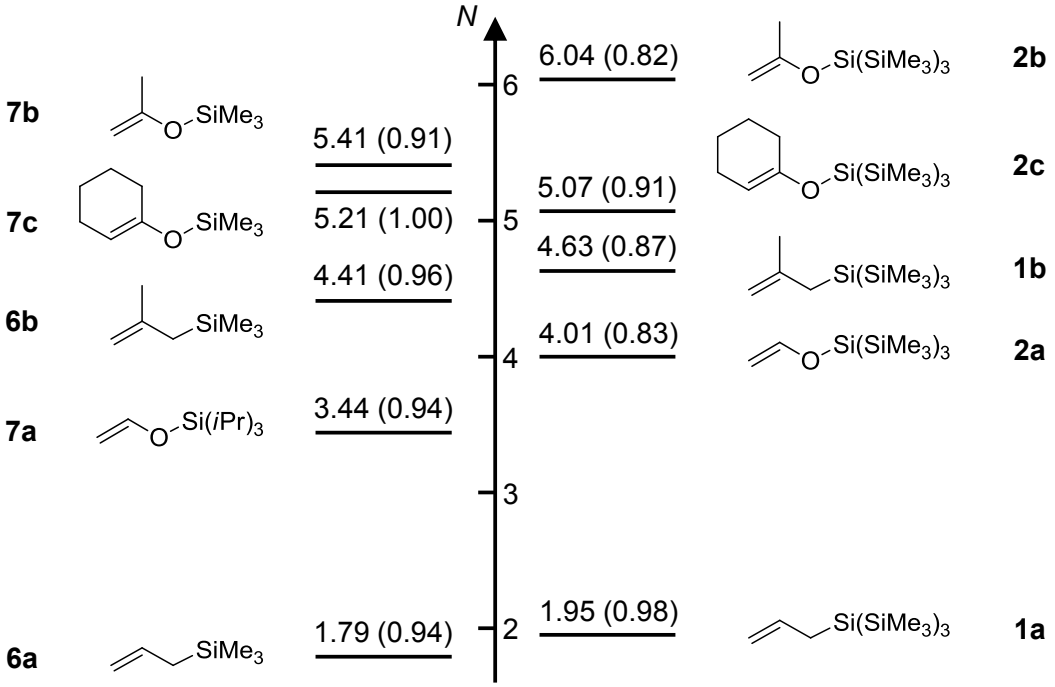

Scheme 2.4. Nucleophilicities of **1** and **2** compared to the corresponding allyltrimethylsilanes **6** and trialkylsilyl enol ethers **7** (s_N values given in parentheses).

Scheme 2.4 shows that with the exception of **1a**/**6a** the supersilyl derivatives **1b** and **2a**–**c** generally have smaller s_N values than the corresponding trimethylsilyl derivatives **6b** and **7a**–**c**. As a consequence, the $Si(SiMe_3)_3/SiMe_3$ ratio can be expected to decrease slightly, when the electrophilicity of the reaction partner is increased.

2.3 Conclusion

The kinetic data in Table 2.5 and Scheme 2.4 show that the exchange of $SiMe_3$ by $Si(SiMe_3)_3$ in allylsilanes and silylated enol ethers has little effect on the rates of reactions of these electron-rich π-nucleophiles. The significantly lower first vertical ionization energies of tris(trimethylsilyl)silyl substituted benzenes compared to the trimethylsilyl analogues, which indicates a stronger α-effect of the $Si(SiMe_3)_3$ group compared with $SiMe_3$, obviously does not have a consequence for the reactivities of allylsilanes and silylated enol ethers bearing the supersilyl group. One can, therefore, conclude that the high selectivities observed for [2+2] cycloadditions and aldol reactions with supersilyl-substituted enol ethers cannot be attributed to electronic effects but are due to the steric bulk and the umbrella like structure created by the $Si(SiMe_3)_3$ group.

2.4 Experimental Section

2.4.1 General Methods

All reactions were performed in carefully dried Schlenk glassware in an atmosphere of dry nitrogen. The reactions were not optimized for high yields.

Solvents. For the kinetic experiments, *p.a.* grade dichloromethane (Merck) was successively treated with concentrated sulfuric acid, water, 10% $NaHCO_3$ solution, and water. After drying with $CaCl_2$, it was freshly distilled over CaH_2 under exclusion of moisture (N_2 atmosphere).

Chemicals. Tris(trimethylsilyl)silane was purchased (ABCR) or prepared by the reported methods.[11] Chlorotris(trimethylsilyl)silane was either purchased (Aldrich) or prepared by stirring tris(trimethylsilyl)silane in tetrachloromethane.[12]

Nucleophiles. Allylsilanes **1** were synthesized by applying a procedure for the synthesis of cyclic allylsilanes reported by Salomon and co-workers.[13] Supersilyl-substituted enol ethers **2** were prepared according to procedures described in the literature.[5a,b]

Reference Electrophiles. Procedures for the syntheses of benzhydryl chlorides[14] and benzhydrylium tetrafluoroborates **3d–f** were reported previously.[8a]

2.4.2 Products from the Reactions of 1b and 2b with 3f-BF_4

Reaction of $(dpa)_2CH^+BF_4^-$ (**3f-BF_4**) with (2-methylallyl)tris(trimethylsilyl)silane (**1b**)

A solution of **3f-BF_4** (87 mg, 0.15 mmol) in dichloromethane (20 mL) was prepared. Then, a solution of **1b** (0.18 g, 0.60 mmol) in dichloromethane (10 mL) was added at ambient temperature. After 10 min the reaction mixture was filtered through basic Al_2O_3 (Brockmann activity III, CH_2Cl_2). After the solvent was evaporated, the crude product was recrystallized (Et_2O/pentane) to yield 4,4-bis(4-(diphenylamino)phenyl)-2-methyl-1-butene as a colorless powder (55 mg, 66%); mp 79–81°C. The spectral data were in accordance with the literature.[8a]

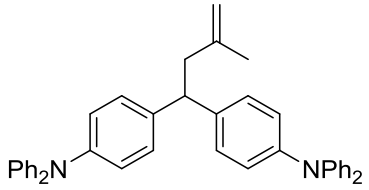

^{1}H NMR (300 MHz, $CDCl_3$) δ = 7.30–6.98 (m, 28 H, Ar-H), 4.76 (s, 1 H, 1-H_2), 4.65 (s, 1 H, 1-H_2), 4.10 (t, ^3J = 7.8 Hz, 1 H, 4-H), 2.76 (d, ^3J = 7.8 Hz, 2 H, 3-H), 1.74 (s, 3 H, 2-Me).

^{13}C NMR (75.5 MHz, $CDCl_3$) δ = 148.1 (s, Ar-C), 145.8 (s, Ar-C), 143.7 (s, C-2), 139.4 (s, Ar-C), 129.3 (d, Ar-C), 128.8 (d, Ar-C), 124.2 (d, Ar-C), 124.1 (d, Ar-C), 122.6 (d, Ar-C), 112.7 (t, C-1), 48.5 (d, C-4), 44.5 (t, C-3), 22.8 (q, 2-Me).

Reaction of $(dpa)_2CH^+BF_4^-$ (**3f-BF$_4$**) with acetone tris(trimethylsilyl)silyl enol ether (**2b**)

A solution of **3f-BF$_4$** (87 mg, 0.15 mmol) in dichloromethane (20 mL) was prepared. Then a solution of **2b** (0.18 g, 0.59 mmol) in dichloromethane (10 mL) was added at ambient temperature. After 10 min the reaction mixture was filtered through basic Al_2O_3 (Brockmann activity III, CH_2Cl_2). After the solvent was evaporated, the crude product was purified by silica gel column chromatography (pentane:Et_2O = 4:1) to furnish 4,4-bis(4-(diphenylamino)phenyl)-butan-2-one as a greenish oil (47 mg, 56%). Signal assignments are based on additional DEPT, gDQCOSY and HSQCAD experiments.

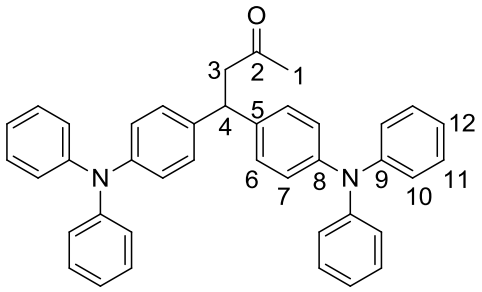

^{1}H NMR (400 MHz, CD_2Cl_2) δ = 7.27–7.21 (m, 8 H, 11-H), 7.13 (d, ^3J = 8.3 Hz, 4 H, Ar-H), 7.07–6.96 (m, 16 H, Ar-H), 4.46 (t, ^3J = 7.5 Hz, 1 H, 4-H), 3.15 (d, ^3J = 7.5 Hz, 2 H, 3-H), 2.09 (s, 3 H, 1-H).

^{13}C NMR (101 MHz, CD_2Cl_2) δ = 207.1 (s, C-2), 148.4 (s, Ar-C), 146.7 (s, Ar-C), 139.2 (s, Ar-C), 129.8 (d, C-11), 128.9 (d, Ar-C), 124.7 (d, Ar-C), 124.5 (d, Ar-C), 123.3 (d, Ar-C), 50.3 (t, C-3), 45.5 (d, C-4), 30.9 (q, C-1).

IR (ATR) ν_{max} = 3031, 1719, 1587, 1503, 1488, 1326, 1315, 1275, 752, 695 cm^{-1}.

HR-MS (ESI) *m*/*z* calcd. for $C_{40}H_{35}N_2O$ $[M+H]^+$ 559.2749, found 559.2743.

2.4.3 Kinetic Experiments

The rates of the slow reactions ($\tau_{1/2} > 10$ s) were determined by using a J&M TIDAS diode array spectrophotometer controlled by Labcontrol Spectacle Software and connected to a Hellma 661.502-QX quartz Suprasil immersion probe (5 mm light path) via fibre optic cables and standard SMA connectors.

Stock solutions of the nucleophiles and the stable electrophiles were prepared by dissolving the compounds in dichloromethane. Less stable electrophiles were generated from stock solutions of the corresponding benzhydryl chlorides in dichloromethane by addition of Lewis acids in dichloromethane solution. Tetrachloroborates were generated quantitatively by injection of borontrichloride gas into the solution of the benzhydryl chlorides. The flame-dried Schlenk flasks with nitrogen atmosphere were filled with approximately 24 mL of solvent. The exact quantity was determined by weighing. Then, this flask was submerged into a circulating water bath with a constant temperature of 20 °C, followed by the equipment with the Hellma probe. After addition of defined volumes of the stock solutions by using Hamilton syringes, the decay of the absorbance in dependence of the recording time was monitored.

For the determined of fast kinetics ($\tau_{1/2} < 10$ s) the first-order rate constants were determined at lower temperatures and the second-order rate constant at 20 °C evaluated using the Eyring equation.

Kinetics of the Reactions of **1a** with **3a–c**

Rate constants for the reactions of allyltris(trimethylsilyl)silane (**1a**) with $(fur)_2CH^+GaCl_4^-$ (**3c-GaCl4**) in CH_2Cl_2 (diode array spectrophotometer, 20 °C, λ = 535 nm).

[**1a**]$_0$ / M	[**3c-Cl**]$_0$ / M	[$GaCl_3$]$_0$ / M	[**1a**]$_0$/[**3c-GaCl4**]$_0$	k_{obs} / s^{-1}
5.59×10^{-4}	1.88×10^{-5}	1.30×10^{-4}	30	2.43×10^{-3}
6.54×10^{-4}	1.87×10^{-5}	8.67×10^{-5}	35	2.93×10^{-3}
7.63×10^{-4}	1.90×10^{-5}	9.78×10^{-5}	40	3.21×10^{-3}
8.55×10^{-4}	1.89×10^{-5}	1.17×10^{-4}	45	3.58×10^{-3}
9.41×10^{-4}	1.86×10^{-5}	1.15×10^{-4}	51	3.92×10^{-3}

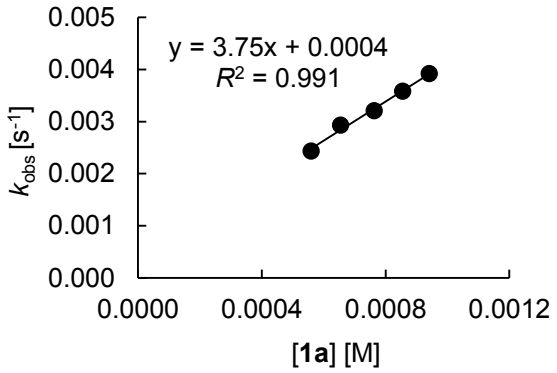

k_2 **(20 °C) = 3.75 M^{-1} s^{-1}**

Rate constants reported for the reactions of allyltris(trimethylsilyl)silane (**1a**) with $(ani)_2CH^+BCl_4^-$ (**3b-BCl$_4$**) in CH_2Cl_2 (diode array spectrophotometer, 20 °C, λ = 513 nm).[15]

[**1a**]$_0$ / M	[**3b-BCl$_4$**]$_0$ / M	[**1a**]$_0$/[**3b-BCl$_4$**]$_0$	k_{obs} / s^{-1}
1.35×10^{-4}	1.93×10^{-5}	7.0	1.50×10^{-2}
1.59×10^{-4}	1.58×10^{-5}	10	1.46×10^{-2}
2.60×10^{-4}	1.71×10^{-5}	15	2.58×10^{-2}
3.30×10^{-4}	1.66×10^{-5}	20	3.17×10^{-2}
3.93×10^{-4}	1.57×10^{-5}	25	3.51×10^{-2}

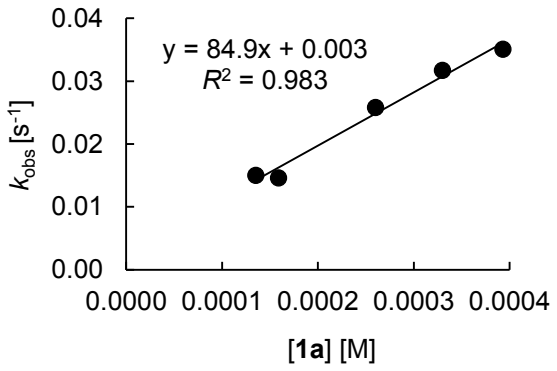

k_2 **(20 °C) = 84.9 M^{-1} s^{-1}**

Rate constants reported for the reactions of allyltris(trimethylsilyl)silane (**1a**) with $(ani)_2CH^+BCl_4^-$ (**3b-BCl$_4$**) in CH_2Cl_2 in the presence of different amounts of $Bu_4N^+BCl_4^-$ (diode array spectrophotometer, 20 °C, λ = 513 nm).[15]

[**1a**]$_0$ / M	[**3b-BCl$_4$**]$_0$/ M	[$Bu_4N^+BCl_4^-$]$_0$/ M	[$Bu_4N^+BCl_4^-$]$_0$/[**1a**]$_0$	k_{obs} / s^{-1}
1.87×10^{-4}	1.88×10^{-5}	0.00	0	1.76×10^{-2}
1.85×10^{-4}	1.86×10^{-5}	1.85×10^{-4}	1	1.73×10^{-2}
1.84×10^{-4}	1.85×10^{-5}	9.21×10^{-4}	5	1.77×10^{-2}
1.84×10^{-4}	1.85×10^{-5}	1.84×10^{-2}	100	1.77×10^{-2}

Rate constants for the reactions of allyltris(trimethylsilyl)silane (**1a**) with $(ani)_2CH^+BF_4^-$ (**3b-BF$_4$**; prepared from the corresponding benzhydrol and HBF_4 in Et_2O and used for kinetics on the same day) in CH_2Cl_2 (diode array spectrophotometer, 20 °C, λ = 513 nm).

[**1a**]$_0$ / M	[**3b-BF$_4$**]$_0$ / M	[**1a**]$_0$/[**3b-BF$_4$**]$_0$	k_{obs} / s^{-1}
1.77×10^{-4}	2.25×10^{-5}	8	1.34×10^{-2}
2.41×10^{-4}	2.21×10^{-5}	11	1.87×10^{-2}
3.12×10^{-4}	2.24×10^{-5}	14	2.45×10^{-2}
3.82×10^{-4}	2.25×10^{-5}	17	2.86×10^{-2}

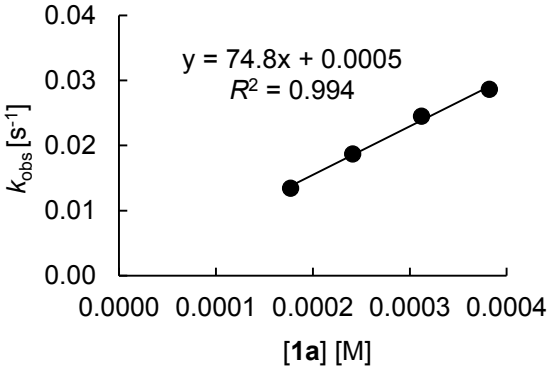

k_2 (20 °C) = 74.8 M^{-1} s^{-1}

Rate constants for the reactions of allyltris(trimethylsilyl)silane (**1a**) with $(ani)_2CH^+GaCl_4^-$ (**3b-GaCl$_4$**) in CH_2Cl_2 (diode array spectrophotometer, 20 °C, λ = 513 nm).

[**1a**]$_0$ / M	[**3b-Cl**]$_0$ / M	[$GaCl_3$]$_0$ / M	[**1a**]$_0$/[**3b-GaCl$_4$**]$_0$	k_{obs} / s^{-1}
2.01×10^{-4}	2.00×10^{-5}	8.28×10^{-5}	10	1.75×10^{-2}
2.95×10^{-4}	2.01×10^{-5}	8.80×10^{-5}	15	2.58×10^{-2}
3.44×10^{-4}	2.01×10^{-5}	7.33×10^{-5}	17	3.30×10^{-2}
4.00×10^{-4}	1.98×10^{-5}	8.67×10^{-5}	20	3.15×10^{-2}
4.97×10^{-4}	1.98×10^{-5}	1.06×10^{-4}	25	4.14×10^{-2}

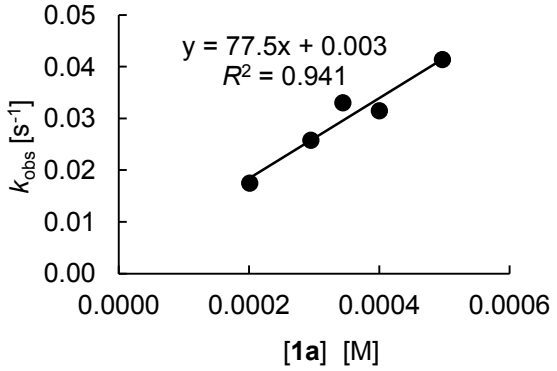

k_2 (20 °C) = 77.5 M^{-1} s^{-1}

Rate constants for the reactions of allyltris(trimethylsilyl)silane (**1a**) with $(ani)_2CH^+SnCl_5^-$ (**3b-SnCl$_5$**) in CH_2Cl_2 (diode array spectrophotometer, 20 °C, λ = 513 nm).

[**1a**]$_0$ / M	[**3b-Cl**]$_0$ / M	[$SnCl_4$]$_0$ / M	[**1a**]$_0$/[**3b-SnCl$_5$**]$_0$	k_{obs} / s^{-1}
1.47×10^{-4}	2.11×10^{-5}	1.21×10^{-4}	7	1.08×10^{-2}
2.10×10^{-4}	2.10×10^{-5}	1.14×10^{-4}	10	1.59×10^{-2}
3.16×10^{-4}	2.09×10^{-5}	1.07×10^{-4}	15	2.50×10^{-2}
4.14×10^{-4}	2.10×10^{-5}	1.20×10^{-4}	20	3.32×10^{-2}
5.20×10^{-4}	2.08×10^{-5}	1.32×10^{-4}	25	4.25×10^{-2}

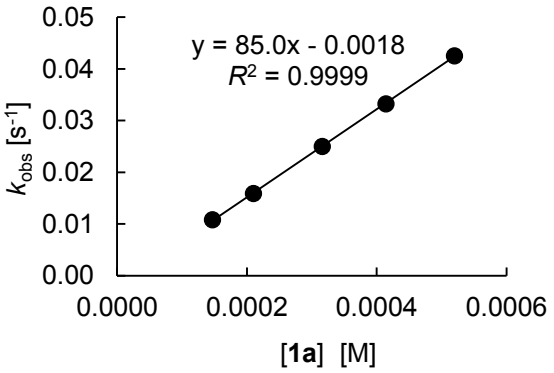

k_2 (20 °C) = 85.0 M^{-1} s^{-1}

Rate constants reported for the reactions of allyltris(trimethylsilyl)silane (**1a**) with (ani)(tol)$CH^+BCl_4^-$ (**3a-BCl$_4$**) in CH_2Cl_2 (diode array spectrophotometer, –71 °C to –22 °C, λ = 486 nm).[15]

T / °C	[**1a**]$_0$ / M	[**3a-BCl$_4$**]$_0$ / M	[**1a**]$_0$/[**3a-BCl$_4$**]$_0$	k_{obs} / s^{-1}	k_2 / M^{-1} s^{-1} [a]
–22.2	3.47×10^{-4}	2.34×10^{-5}	14.8	1.74×10^{-1}	519
–32.1	3.48×10^{-4}	2.34×10^{-5}	14.8	1.13×10^{-1}	336
–42.2	4.75×10^{-4}	2.38×10^{-5}	20.0	1.04×10^{-1}	225
–51.8	3.47×10^{-4}	2.34×10^{-5}	14.8	4.32×10^{-2}	129
–61.3	3.45×10^{-4}	2.32×10^{-5}	14.8	2.66×10^{-2}	79.8
–71.0	3.44×10^{-4}	2.32×10^{-5}	14.8	1.50×10^{-2}	45.1

[a] Calculated from $k_2 = k_{obs}/([\mathbf{1a}] - 0.5[\mathbf{3a\text{-}BCl_4}]_0)$.

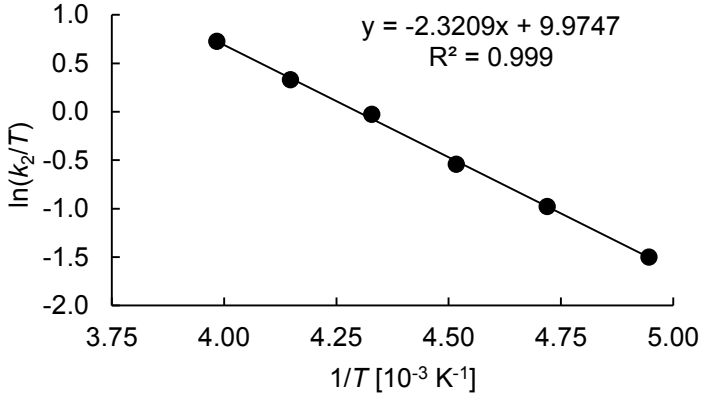

Eyring correlation for the reaction of **3a**–**GaCl$_4$** with **1a**.

Eyring-parameter:

$\Delta H^{\ddagger}$ = (19.3 ± 0.3) kJ mol^{-1}

$\Delta S^{\ddagger}$ = (–114.6 ± 1.4) J mol^{-1} K^{-1}

Coefficient of correlation: 0.9990

Arrhenius-parameter:

E_A = (21.2 ± 0.3) kJ mol^{-1}

ln A = 16.4 ± 0.2

Coefficient of correlation: 0.9992

k_2 (20 °C) = 2.30×10^3 M^{-1} s^{-1}

Kinetics of the Reactions of **1b** with **3d–f**

Rate constants reported for the reactions of (2-methylallyl)tris(trimethylsilyl)silane (**1b**) with $(dpa)_2CH^+BF_4^-$ (**3f-BF4**) in CH_2Cl_2 (diode array spectrophotometer, 20 °C, λ = 672 nm).[15]

$[\mathbf{1b}]_0$ / M	$[\mathbf{3f\text{-}BF_4}]_0$ / M	$[\mathbf{1b}]_0/[\mathbf{3f\text{-}BF_4}]_0$	k_{obs} / s^{-1}
2.01×10^{-3}	2.02×10^{-5}	100	1.86×10^{-3}
3.24×10^{-3}	2.14×10^{-5}	151	3.04×10^{-3}
4.25×10^{-3}	2.14×10^{-5}	199	4.15×10^{-3}
4.99×10^{-3}	1.99×10^{-5}	251	4.84×10^{-3}
6.15×10^{-3}	2.03×10^{-5}	303	5.80×10^{-3}

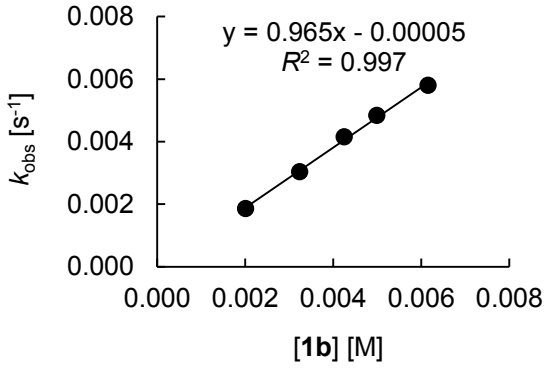

k_2 (20 °C) = 0.965 M^{-1} s^{-1}

Rate constants reported for the reactions of (2-methylallyl)tris(trimethylsilyl)silane (**1b**) with $(mfa)_2CH^+BF_4^-$ (**3e-BF4**) in CH_2Cl_2 (diode array spectrophotometer, 20 °C, λ = 593 nm).[15]

$[\mathbf{1b}]_0$ / M	$[\mathbf{3e\text{-}BF_4}]_0$ / M	$[\mathbf{1b}]_0/[\mathbf{3e\text{-}BF_4}]_0$	k_{obs} / s^{-1}
2.02×10^{-4}	1.01×10^{-5}	20	6.70×10^{-4}
5.10×10^{-4}	8.94×10^{-6}	57	1.65×10^{-3}
7.35×10^{-4}	9.19×10^{-6}	80	2.57×10^{-3}
9.41×10^{-4}	9.36×10^{-6}	101	3.25×10^{-3}

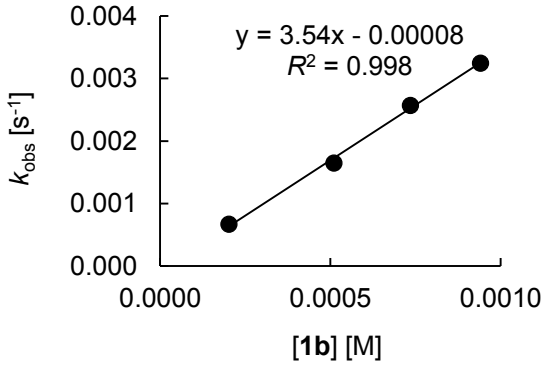

k_2 **(20 °C) = 3.54 M^{-1} s^{-1}**

Rate constants reported for the reactions of (2-methylallyl)tris(trimethylsilyl)silane (**1b**) with $(pfa)_2CH^+BF_4^-$ (**3d-BF$_4$**) in CH_2Cl_2 (diode array spectrophotometer, 20 °C, λ = 601 nm).[15]

[**1b**]$_0$ / M	[**3d-BF$_4$**]$_0$ / M	[**1b**]$_0$/[**3d-BF$_4$**]$_0$	k_{obs} / s^{-1}
1.17×10^{-4}	1.17×10^{-5}	10	2.58×10^{-3}
2.33×10^{-4}	1.24×10^{-5}	19	5.80×10^{-3}
3.57×10^{-4}	1.19×10^{-5}	30	8.67×10^{-3}
4.70×10^{-4}	1.19×10^{-5}	40	1.13×10^{-2}
5.64×10^{-4}	1.20×10^{-5}	47	1.34×10^{-2}

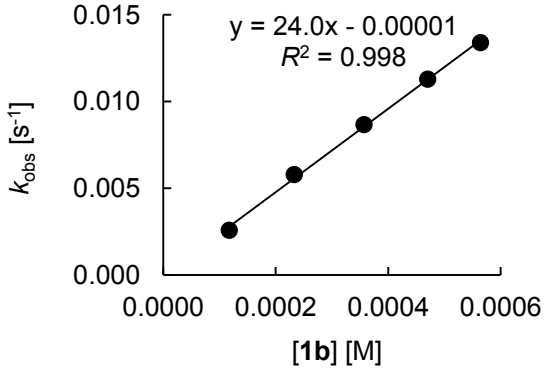

k_2 **(20 °C) = 24.0 M^{-1} s^{-1}**

Kinetics of the Reactions of **2a** with **3d–f**

Rate constants for the reactions of tris(trimethylsilyl)vinyloxysilane (**2a**) with $(dpa)_2CH^+BF_4^-$ (**3f-BF$_4$**) in CH_2Cl_2 (diode array spectrophotometer, 20 °C, λ = 672 nm).

[**2a**]$_0$ / M	[**3f-BF$_4$**]$_0$ / M	[**2a**]$_0$/[**3f-BF$_4$**]$_0$	k_{obs} / s^{-1}
9.78×10^{-4}	1.78×10^{-5}	55	2.76×10^{-4}
1.92×10^{-3}	1.66×10^{-5}	116	4.81×10^{-4}
3.05×10^{-3}	1.65×10^{-5}	185	7.93×10^{-4}
4.13×10^{-3}	1.65×10^{-5}	250	1.13×10^{-3}

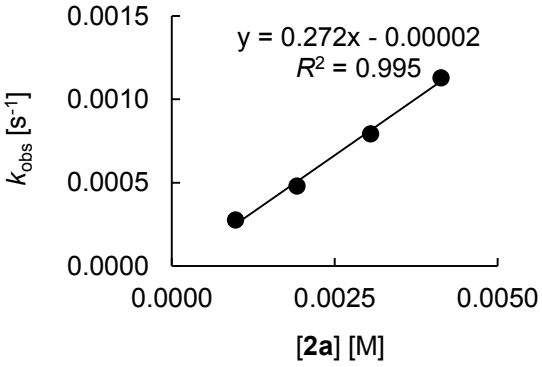

k_2 (20 °C) = 0.272 M^{-1} s^{-1}

Rate constants for the reactions of tris(trimethylsilyl)vinyloxysilane (**2a**) with $(mfa)_2CH^+BF_4^-$ (**3e-BF$_4$**) in CH_2Cl_2 (diode array spectrophotometer, 20 °C, λ = 593 nm).

[**2a**]$_0$ / M	[**3e-BF$_4$**]$_0$ / M	[**2a**]$_0$/[**3e-BF$_4$**]$_0$	k_{obs} / s^{-1}
8.95×10^{-4}	9.90×10^{-6}	90	1.22×10^{-3}
9.93×10^{-4}	9.93×10^{-6}	100	1.30×10^{-3}
1.09×10^{-3}	9.97×10^{-6}	109	1.45×10^{-3}
1.19×10^{-3}	9.95×10^{-6}	119	1.56×10^{-3}

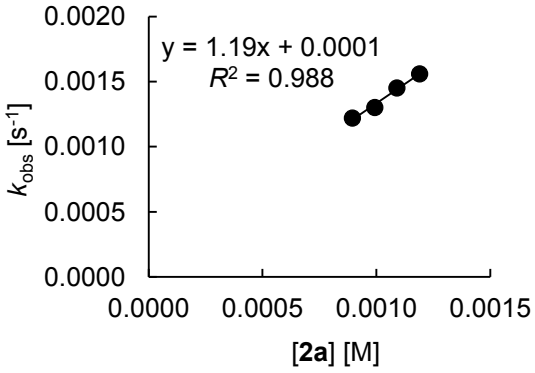

k_2 **(20 °C) = 1.19 M^{-1} s^{-1}**

Rate constants for the reactions of tris(trimethylsilyl)vinyloxysilane (**2a**) with $(pfa)_2CH^+BF_4^-$ (**3d-BF$_4$**) in CH_2Cl_2 (diode array spectrophotometer, 20 °C, λ = 601 nm).

[**2a**]$_0$ / M	[**3d-BF$_4$**]$_0$ / M	[**2a**]$_0$/[**3d-BF$_4$**]$_0$	k_{obs} / s^{-1}
1.20×10^{-4}	1.23×10^{-5}	10	8.34×10^{-4}
1.80×10^{-4}	1.24×10^{-5}	15	1.31×10^{-3}
2.49×10^{-4}	1.24×10^{-5}	20	1.55×10^{-3}
3.06×10^{-4}	1.23×10^{-5}	25	1.79×10^{-3}
3.73×10^{-4}	1.23×10^{-5}	30	2.36×10^{-3}

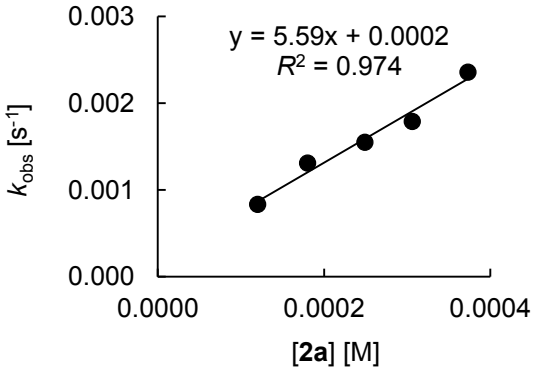

k_2 **(20 °C) = 5.59 M^{-1} s^{-1}**

Kinetics of the Reactions of **2b** with **3d–f**

Rate constants reported for the reactions of acetone tris(trimethylsilyl)silyl enol ether (**2b**) with $(dpa)_2CH^+BF_4^-$ (**3f-BF$_4$**) in CH_2Cl_2 (diode array spectrophotometer, 20 °C, λ = 672 nm).[15]

[**2b**]$_0$ / M	[**3f-BF$_4$**]$_0$ / M	[**2b**]$_0$/[**3f-BF$_4$**]$_0$	k_{obs} / s^{-1}
3.28×10^{-4}	1.61×10^{-5}	20	3.75×10^{-3}
6.64×10^{-4}	1.63×10^{-5}	41	7.99×10^{-3}
9.52×10^{-4}	1.59×10^{-5}	60	1.17×10^{-2}
1.24×10^{-3}	1.55×10^{-5}	80	1.41×10^{-2}
1.53×10^{-3}	1.52×10^{-5}	101	1.83×10^{-2}

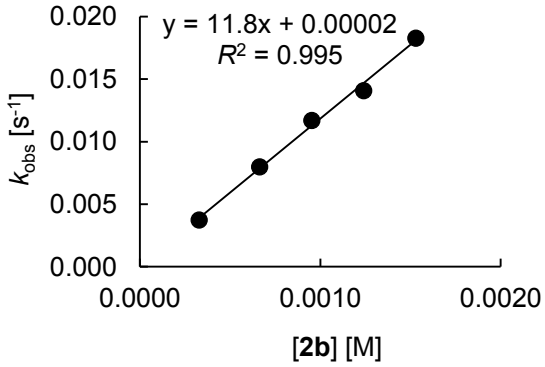

k_2 **(20 °C) = 11.8 M^{-1} s^{-1}**

Rate constants reported for the reactions of acetone tris(trimethylsilyl)silyl enol ether (**2b**) with $(mfa)_2CH^+BF_4^-$ (**3e-BF$_4$**) in CH_2Cl_2 (diode array spectrophotometer, 20 °C, λ = 593 nm).[15]

[**2b**]$_0$ / M	[**3e-BF$_4$**]$_0$ / M	[**2b**]$_0$/[**3e-BF$_4$**]$_0$	k_{obs} / s^{-1}
1.78×10^{-4}	8.84×10^{-6}	20	9.43×10^{-3}
3.73×10^{-4}	9.32×10^{-6}	40	1.75×10^{-2}
6.16×10^{-4}	1.02×10^{-5}	60	3.34×10^{-2}
7.02×10^{-4}	8.78×10^{-6}	80	4.43×10^{-2}
7.39×10^{-4}	9.24×10^{-6}	80	4.49×10^{-2}

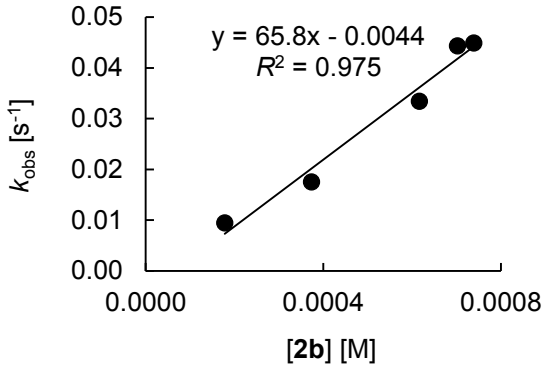

k_2 **(20 °C) = 65.8 M^{-1} s^{-1}**

Rate constants reported for the reactions of acetone tris(trimethylsilyl)silyl enol ether (**2b**) with $(pfa)_2CH^+BF_4^-$ (**3d-BF$_4$**) in CH_2Cl_2 (diode array spectrophotometer, 20 °C, λ = 601 nm).[15]

[**2b**]$_0$ / M	[**3d-BF$_4$**]$_0$ / M	[**2b**]$_0$/[**3d-BF$_4$**]$_0$	k_{obs} / s^{-1}
2.29×10^{-4}	1.21×10^{-5}	19	4.90×10^{-2}
4.86×10^{-4}	1.22×10^{-5}	40	1.04×10^{-1}
8.40×10^{-4}	1.39×10^{-5}	60	1.75×10^{-1}
1.07×10^{-3}	1.35×10^{-5}	79	2.42×10^{-1}
1.07×10^{-3}	1.13×10^{-5}	95	2.47×10^{-1}

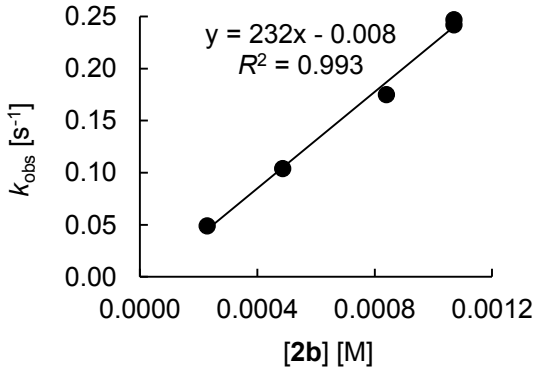

k_2 **(20 °C) = 232 M^{-1} s^{-1}**

Kinetics of the Reactions of **2c** with **3d–f**

Rate constants for the reactions of (cyclohex-1-enyloxy)tris(trimethylsilyl)silane (**2c**) with $(dpa)_2CH^+BF_4^-$ (**3f-BF4**) in CH_2Cl_2 (diode array spectrophotometer, 20 °C, λ = 672 nm).

$[\mathbf{2c}]_0$ / M	$[\mathbf{3f\text{-}BF_4}]_0$ / M	$[\mathbf{2c}]_0/[\mathbf{3f\text{-}BF_4}]_0$	k_{obs} / s^{-1}
3.42×10^{-4}	2.27×10^{-5}	15	1.11×10^{-3}
5.64×10^{-4}	2.28×10^{-5}	25	1.50×10^{-3}
6.87×10^{-4}	2.29×10^{-5}	30	1.77×10^{-3}
8.08×10^{-4}	2.28×10^{-5}	35	2.04×10^{-3}
9.00×10^{-4}	2.26×10^{-5}	40	2.29×10^{-3}

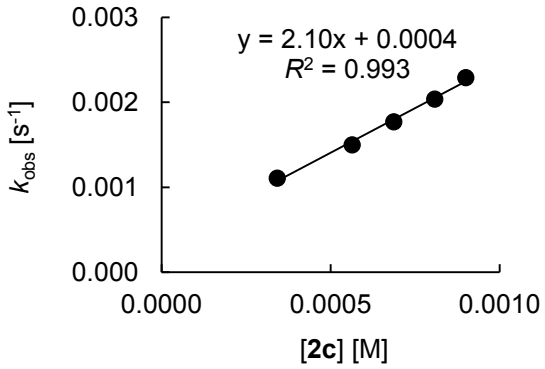

k_2 **(20 °C) = 2.10 M^{-1} s^{-1}**

Rate constants for the reactions of (cyclohex-1-enyloxy)tris(trimethylsilyl)silane (**2c**) with $(mfa)_2CH^+BF_4^-$ (**3e-BF4**) in CH_2Cl_2 (diode array spectrophotometer, 20 °C, λ = 593 nm).

$[\mathbf{2c}]_0$ / M	$[\mathbf{3e\text{-}BF_4}]_0$ / M	$[\mathbf{2c}]_0/[\mathbf{3e\text{-}BF_4}]_0$	k_{obs} / s^{-1}
1.52×10^{-4}	1.04×10^{-5}	15	2.07×10^{-3}
2.06×10^{-4}	1.04×10^{-5}	20	2.71×10^{-3}
2.60×10^{-4}	1.04×10^{-5}	25	3.34×10^{-3}
3.13×10^{-4}	1.04×10^{-5}	30	3.96×10^{-3}
3.65×10^{-4}	1.04×10^{-5}	35	4.72×10^{-3}

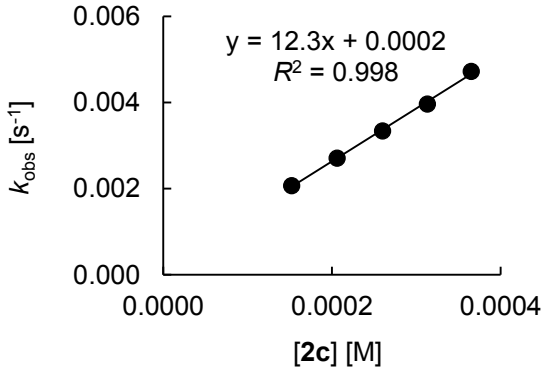

k_2 **(20 °C) = 12.3 M^{-1} s^{-1}**

Rate constants for the reactions of (cyclohex-1-enyloxy)tris(trimethylsilyl)silane (**2c**) with $(pfa)_2CH^+BF_4^-$ (**3d-BF$_4$**) in CH_2Cl_2 (diode array spectrophotometer, 20 °C, λ = 601 nm).

[**2c**]$_0$ / M	[**3d-BF$_4$**]$_0$ / M	[**2c**]$_0$/[**3d-BF$_4$**]$_0$	k_{obs} / s^{-1}
1.62×10^{-4}	1.61×10^{-5}	10	9.42×10^{-3}
2.38×10^{-4}	1.60×10^{-5}	15	1.32×10^{-2}
3.20×10^{-4}	1.61×10^{-5}	20	1.82×10^{-2}
3.94×10^{-4}	1.59×10^{-5}	25	2.23×10^{-2}
4.74×10^{-4}	1.59×10^{-5}	30	2.71×10^{-2}

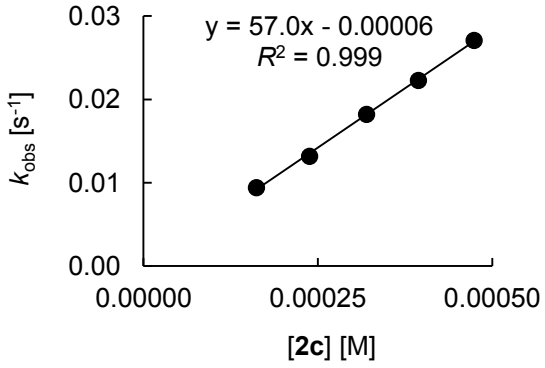

k_2 **(20 °C) = 57.0 M^{-1} s^{-1}**

2.5 References

[1] (a) A. Hosomi, H. Sakurai, *J. Am. Chem. Soc.* **1977**, *99*, 1673–1675; b) L. Chabaud, P. James, Y. Landais, *Eur. J. Org. Chem.* **2004**, 3173–3199; c) T. K. Sarkar in *Science of Synthesis, Vol. 4* (Ed.: I. Fleming), Thieme Verlag, Stuttgart, **2002**, pp. 837–925.

[2] a) T. Mukaiyama, K. Narasaka, K. Banno, *Chem. Lett.* **1973**, 1011–1014; b) T. Mukaiyama, *Org. React.* **1982**, *28*, 203–331; c) P. Brownbridge, *Synthesis* **1983**, 1–28; d) T. Bach, *Angew. Chem.* **1994**, *106*, 433–435; *Angew. Chem., Int. Ed. Engl.* **1994**, *33*, 417–419; e) S. G. Nelson, *Tetrahedron: Asymmetry* **1998**, *9*, 357–389; f) E. M. Carreira in *Comprehensive Asymmetric Catalysis*; *Vol. 3* (Eds.: E. N. Jacobsen, A. Pfalz, H. Yamamoto), Springer: Berlin, **1999**, pp 997–1065; g) R. Mahrwald, *Chem. Rev.* **1999**, *99*, 1095–1120.

[3] a) R.D. Clark, K. G. Untch, *J. Org. Chem.* **1979**, *44*, 253–255; b) K. Takasu, M. Ueno, M. Ihara, *Tetrahedron Lett.* **2000**, *41*, 2145–2148; c) K. Takasu, M. Ueno, M. Ihara, *J. Org. Chem.* **2001**, *66*, 4667–4672; d) K. Takasu, M. Ueno, K. Inanaga, M. Ihara, *J. Org. Chem.* **2004**, *69*, 517–521; e) K. Takasu, S. Nagao, M. Ueno, M. Ihara, *Tetrahedron* **2004**, *60*, 2071–2078; f) K. Inanaga, K. Takasu, M. Ihara, *J. Am. Chem. Soc.* **2005**, *127*, 3668–3669; g) K. Takasu, T. Ishii, K. Inanaga, M. Ihara, *Org. Synth.* **2006**, *83*, 193–199; h) E. Canales, E. J. Corey, *J. Am. Chem. Soc.* **2007**, *129*, 12686–12687.

[4] M. B. Boxer, H. Yamamoto, *Org. Lett.* **2005**, *7*, 3127–3129.

[5] a) M. B. Boxer, H. Yamamoto, *J. Am. Chem. Soc.* **2006**, *128*, 48–49; b) M. B. Boxer, H. Yamamoto, *Nat. Protoc.* **2006**, *1*, 2434–2438; c) M. B. Boxer, H. Yamamoto, *J. Am. Chem. Soc.* **2007**, *129*, 2762–2763; d) M. B. Boxer, H. Yamamoto, *Org. Lett.* **2008**, *10*, 453–455; e) M. B. Boxer, M. Akakura, H. Yamamoto, *J. Am. Chem. Soc.* **2008**, *130*, 1580–1582; f) M. B. Boxer, B. J. Albert, H. Yamamoto, *Aldrichimica Acta* **2009**, *42*, 3–15; g) Y. Yamaoka, H. Yamamoto, *J. Am. Chem. Soc.* **2010**, *132*, 5354–5356; h) B. J. Albert, H. Yamamoto, *Angew. Chem., Int. Ed.* **2010**, *49*, 2747–2749.

[6] H. Bock, J. Meuret, R. Baur, K. Ruppert, *J. Organomet. Chem.* **1993**, *446*, 113–122.

[7] H. Mayr, N. Basso, G. Hagen, *J. Am. Chem. Soc.* **1992**, *114*, 3060–3066.

[8] a) H. Mayr, T. Bug, M. F. Gotta, N. Hering, B. Irrgang, B. Janker, B. Kempf, R. Loos, A. R. Ofial, G. Remennikov, H. Schimmel, *J. Am. Chem. Soc.* **2001**, *123*, 9500–9512; b) R. Lucius, R. Loos, H. Mayr, *Angew. Chem.* **2002**, *114*, 97–102; *Angew. Chem., Int. Ed.* **2002**, *41*, 91–95; (c) H. Mayr, B. Kempf, A. R. Ofial, *Acc. Chem. Res.* **2003**, *36*, 66–77; d) H. Mayr, A. R. Ofial in *Carbocation Chemistry* (Eds.: G. A. Olah, G. K. S. Prakash), Wiley, Hoboken, NJ, **2004**, pp. 331–358; e) H. Mayr, A. R. Ofial, *Pure Appl. Chem.* **2005**, *77*,

1807–1821; f) H. Mayr, A. R. Ofial, *J. Phys. Org. Chem.* **2008**, *21*, 584–595; g) D. Richter, N. Hampel, T. Singer, A. R. Ofial, H. Mayr, *Eur. J. Org. Chem.* **2009**, 3203–3211.

[9] Nucleophilicities of allylsilanes were determined by using the benzhydrylium method: G. Hagen, H. Mayr, *J. Am. Chem. Soc.* **1991**, *113*, 4954–4961.

[10] Nucleophilicity parameters for silyl enol ethers determined by using the benzhydrylium method: J. Burfeindt, M. Patz, M. Müller, H. Mayr, *J. Am. Chem. Soc.* **1998**, *120*, 3629–3634.

[11] a) H. Bürger, W. Kilian, *J. Organomet. Chem.* **1969**, *18*, 299–306; b) C. Marschner, *Eur. J. Inorg. Chem.* **1998**, 221–226.

[12] H. Gilman, R. L. Harrell, *J. Organomet. Chem.* **1966**, *5*, 199–200.

[13] J. M. Reuter, A. Sinha, R. G. Salomon, *J. Org. Chem.* **1978**, *43*, 2438–2442.

[14] B. Denegri, A. Streiter, S. Juric, A. R. Ofial, O. Kronja, H. Mayr, *Chem. Eur. J.* **2006**, *12*, 1648–1656; *Chem. Eur. J.* **2006**, *12*, 5415.

[15] H. A. Laub, Master Thesis, Ludwig-Maximilians-Universität München (Germany), **2008**.

Chapter 3

The Influence of Perfluorinated Substituents on the Nucleophilic Reactivities of Silyl Enol Ethers

Reproduced with permission from

H. A. Laub, D. Gladow, H.-U. Reissig, H. Mayr, *Org. Lett.* **2012**, *14*, 3990–3993.

The results obtained by D. Gladow are not listed in the Experimental Section.

3.1 Introduction

Owing to its high electronegativity and lipophilicity, the introduction of fluorine into organic molecules significantly changes chemical, physical, and biological properties.[1] Approximately 20% of all presently used pharmaceuticals and 30% of agrochemicals contain one or more fluorine atoms. Due to this importance we started an investigation of silyl enol ethers bearing perfluoroalkyl substituents that should be interesting building blocks for the synthesis of many fluorinated products, including donor-acceptor-substituted cyclopropanes.[2]

Although silyl enol ethers are widely used in synthetic chemistry,[3] studies on the preparation and reactivity of fluoroalkyl substituted silyl enol ethers are very limited.[4,5] In order to investigate the effect of fluorine substitution on the nucleophilic reactivity of CC-double bonds, we prepared three different silyl enol ethers: **3a** with a trifluoromethyl group, **3b** bearing the longer perfluoropentyl substituent, and the pentafluorophenyl substituted compound **3c** (Scheme 3.1).

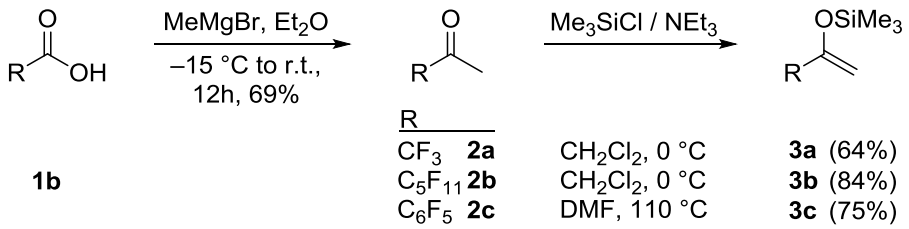

Scheme 3.1. Synthesis of fluorinated silyl enol ethers **3**.

Trifluoroacetone (**2a**) and pentafluoroacetophenone (**2c**) were obtained from commercial sources, and **2b**[6] was prepared in analogy to other methyl perfluoroalkyl ketones by treatment of the corresponding carboxylic acid **1b** with MeMgBr.[7] The moderate yield of **2b** (64%) results from the formation of a tertiary alcohol by addition of MeMgBr to the ketone. The enol ethers **3a–c** where synthesized by treatment of the methyl ketones **2a–c** with triethylamine and trimethylsilyl chloride. Due to the strong electron-withdrawing effect of the perfluoroalkyl groups, the conversions of **2a** and **2b** into **3a** and **3b**, respectively, proceeded already at 0 °C, while elevated temperatures were necessary for the preparation of the perfluorophenyl substituted product **3c**.[8] Enol ethers **3b** and **3c** were isolated in yields of 87% and 75%, respectively. We attribute the lower yield of 66% for **3a** to its higher volatility.

In order to quantify the influence of the electron-withdrawing substituents on the nucleophilic reactivities of the corresponding trimethylsilyl enol ethers **3a–c**, the benzhydrylium method[9] was employed, which allowed us to compare the data with those of previously investigated silyl enol ethers.[9a,b,10] Benzhydrylium ions with variable *p*- and *m*-substituents, which cover a broad range of reactivity while the steric shielding of the reaction center is kept constant, have been used as reference electrophiles for the construction of a comprehensive nucleophilicity scale based on Equation (3.1), where electrophiles are characterized by one parameter (E) and nucleophiles are characterized by the solvent-dependent parameters s_N (slope) and N (nucleophilicity).[9a]

$$\lg k\ (20\ °C) = s_N(N + E) \qquad (3.1)$$

The benzhydrylium ions **4a–f** (Table 3.1) with electrophilicity parameters E ranging from 0 to +5.47 reacted with the silyl enol ethers **3a–c** with conveniently measurable rates.

Table 3.1. Reference Electrophiles Utilized for Quantifying the Nucleophilicities of **3a–c**.

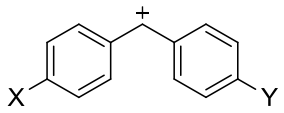

ArAr'CH$^+$ [a]	X	Y	E[b]
$(Ph)_2CH^+$ (**4a**)	H	H	5.47[c]
(Ph)(tol)CH^+ (**4b**)	H	CH_3	4.43[c]
$(tol)_2CH^+$ (**4c**)	CH_3	CH_3	3.63
(tol)(ani)CH^+ (**4d**)	CH_3	OMe	1.48
(ani)(pop)CH^+ (**4e**)	OMe	OPh	0.61
$(ani)_2CH^+$ (**4f**)	OMe	OMe	0.00

[a] tol = *p-tol*yl; ani = *p-ani*syl; pop = *p-p*hen*oxyp*henyl. [b] Empirical electrophilicities E from ref [9a]. [c] The electrophilicities of **4a** and **4b** in ref [9a] have been revised in ref [11].

3.2 Results and Discussion

The fluorinated enol ethers **3a–c** gave analogous reaction products as previously investigated silylated enol ethers,[10] as demonstrated by the formation of **6a** and **6b** from **4a-GaCl$_4$** and **3a** or **3b**, respectively, and of **6c** from **4f-GaCl$_4$** and **3c** (Scheme 3.2).

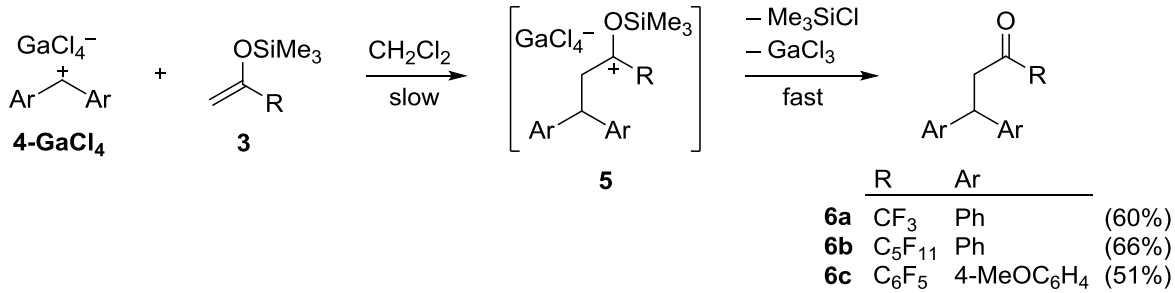

Scheme 3.2. Reactions of **3** with the benzhydrylium salts **4-GaCl$_4$**.

As the intermediates **5** and the products **6** are colorless, the nucleophilic attack at the electrophilic center was followed spectrophotometrically. Addition of at least 8 equiv of the trimethylsilyl enol ethers **3** to solutions of the colored benzhydrylium tetrachlorogallates **4-GaCl$_4$** in CH_2Cl_2 led to mono-exponential decays of the absorbances of the benzhydrylium

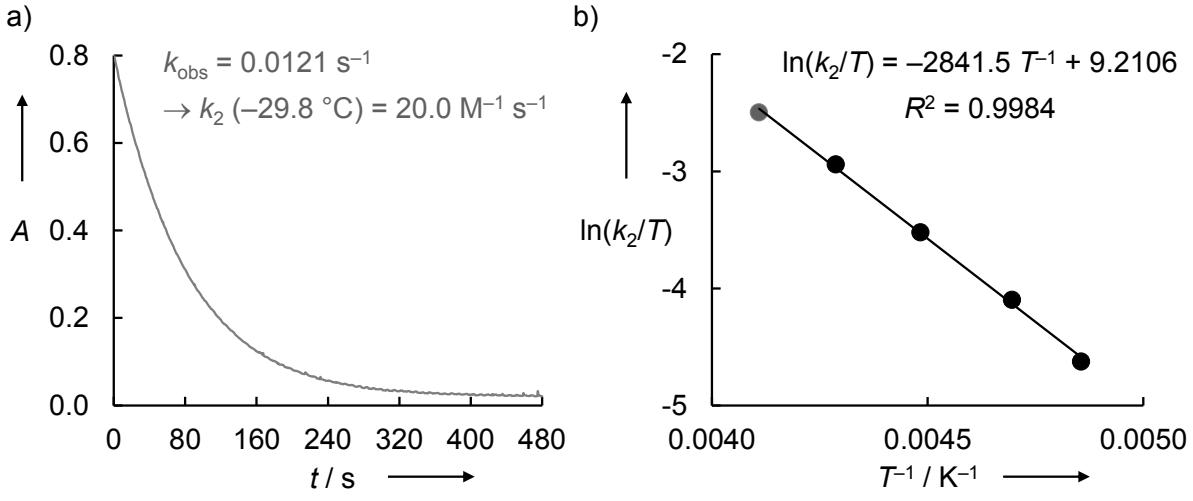

Figure 3.1. a) Exponential decay of the absorbance at 452 nm during the reaction of **3b** ($c = 6.27 \times 10^{-4}$ M) with **4a-GaCl$_4$** ($c = 4.69 \times 10^{-5}$ M) at –29.8 °C in CH_2Cl_2. b) Correlation of ln(k_2/T) vs. 1/T allows the computation of the second-order rate constant k_2 (20 °C) = 181 M^{-1} s^{-1} by using the Eyring equation.

ions (Figure 3.1a). As previous studies have shown that the rates of the reactions are only slightly affected by the counterion and the desilylations to products **6** are fast,[10] the measured reaction rates correspond to the formation of the C–C bonds.

The reactions with the highly electrophilic benzhydrylium ions **4a–d** were studied between –70 and –10 °C. For electrophiles **4a,b** a shift of the absorption maximum (–14 nm for **4a** and 5 nm for **4b**) was observed at conversions above 80%. As the origin of this shift is not clear, the corresponding measurements were evaluated until this shift occurred (when evaluating over the whole time period, k_{obs} changes by up to 10%). The resulting first-order rate constants k_{obs} were divided by the corresponding mean nucleophile concentrations $[\mathbf{3}]_{av} = [\mathbf{3}]_0 - 0.5[\mathbf{4\text{-}GaCl_4}]_0$ to give the second-order rate constants k_2 at the specific temperature. The values of k_2 at 20 °C (given in Table 3.2) were calculated from the linear Eyring plot of ln(k_2/T) versus 1/T (Figure 3.1b).

The reactions of the benzhydrylium ions **4e** and **4f** with **3c** were studied at 20 °C. As the resulting first-order rate constants k_{obs} correlated linearly with the concentrations of **3c** (see Experimental Section), the second-order rate constants given in Table 3.2 could be derived from the slopes of these linear correlations. Plots of lg k_2 for the reactions of the fluorinated silyl enol ethers **3** with the reference electrophiles **4** versus their empirical electrophilicity parameters E gave linear correlations (Figure 3.2) and allowed us to calculate the N and s_N parameters for compounds **3** according to Equation (3.1).

Table 3.2. Second-Order Rate Constants k_2 and Eyring Activation Parameters for the Reactions of the Enol Ethers **3** with the Benzhydrylium Ions **4**.

Nucleophiles **3**	**4**	k_2 (20 °C) / M^{-1} s^{-1}	$\Delta H^{\ddagger}$ / kJ mol^{-1}	$\Delta S^{\ddagger}$ / J mol^{-1} K^{-1}
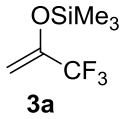 **3a**	**4a**	634	27.5	–97.2
	4b	47.6	30.6	–108.5
	4c	5.73	36.9	–104.3
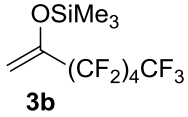 **3b**	**4a**	181	23.6	–121.0
	4b	13.2	29.3	–123.5
	4c	1.25	33.4	–128.9
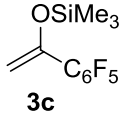 **3c**	**4d**	427	21.9	–119.6
	4e	63.1	–	–
	4f	21.2	–	–

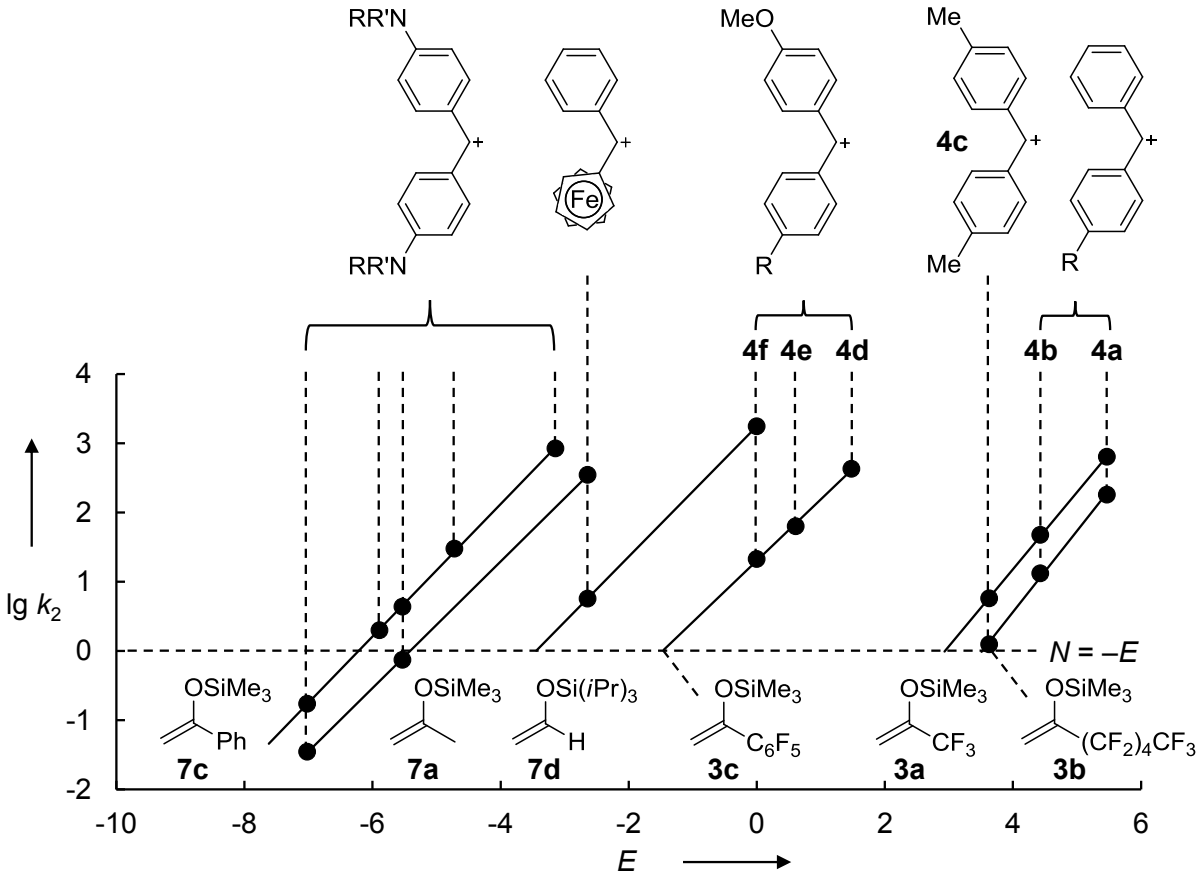

Figure 3.2. Plots of lg k_2 for the reactions of the silyl enol ethers **3** and **7a,c,d** (from ref [9a]) with benzhydrylium ions in CH_2Cl_2 at 20 °C versus the electrophilicity parameters E of the benzhydrylium ions used as reference electrophiles.

Scheme 3.3 compares the reactivities of **3a–c** with those of other π-systems[9f] and shows that substitution of the methyl group of **7a** attached to the developing carbenium center by a trifluoromethyl group (compound **3a**) reduces the nucleophilic reactivity by more than 8 orders of magnitude.

As the activating effects of triisopropylsiloxy and trimethylsiloxy have been shown to be comparable,[10a] the comparison of **3a** with triisopropylsiloxyethylene (**7d**) demonstrates a deactivation of more than 6 orders of magnitude by the trifluoromethyl group relative to hydrogen. Elongation of the perfluorinated alkyl chain to undecafluoropentyl (compound **3b**) results in a further decrease in nucleophilicity by a factor of 3–4 (Table 3.2 and Scheme 3.3).

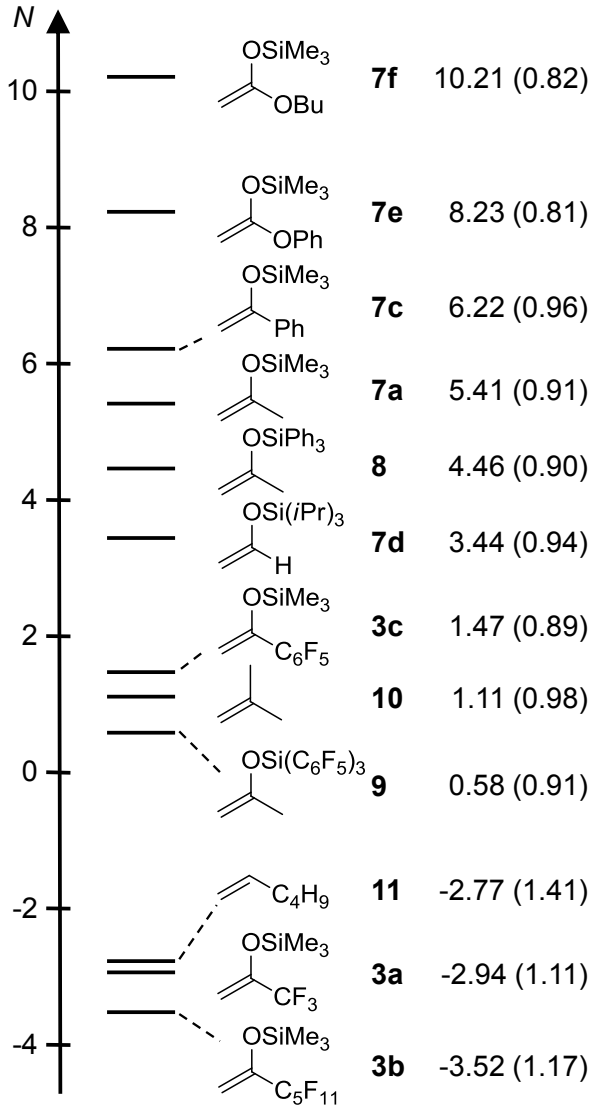

Scheme 3.3. Nucleophilicities *N* of fluorinated silyl enol ethers **3** compared to those of other π-nucleophiles[9f] (s_N values given in parentheses).

Comparison of compounds **7c** and **3c** demonstrates that replacement of the phenyl group by a pentafluorophenyl substituent reduces the reactivity by approximately 4.5 orders of magnitude, showing that perfluorination of the phenyl group has a slightly smaller deactivating effect than perfluorination of an alkyl group. A comparable deactivation was observed when the three phenyl groups in **8** were perfluorinated (→**9**, Scheme 3.3).[10c]

3.3 Conclusion

In summary, Scheme 3.3 demonstrates that the nucleophilic reactivities of silyl enol ethers are so strongly reduced by the introduction of perfluorinated alkyl and phenyl groups that compounds **3a–c** show nucleophilicities comparable to those of alkyl substituted ethylenes (e.g., isobutylene (**10**)[9a] or hex-1-ene (**11**)[9a,11]). With *N*-parameters around –3, the perfluoroalkyl substituted enol ethers **3a,b** can be expected only to react with electrophiles of $E > -2$; i.e., they should be accessible to Mukaiyama-type aldol reactions (for *E*-parameters for carbonyl Lewis acid complexes, see ref [12]) but not to iminium activated reactions (for *E*-parameters for iminium ions, see ref [13]).

3.4 Experimental Section

3.4.1 General Methods

All reactions were performed in carefully dried Schlenk glassware in an atmosphere of dry nitrogen. The reactions were not optimized for high yields.

NMR spectra were recorded on Varian NMR instruments (300, 400 and 600 MHz). Chemical shifts are expressed in ppm and refer to $CDCl_3$ (δ_H: 7.26, δ_C: 77.16) as internal standard. Infrared spectra were recorded on a PerkinElmer FT-IR-BX spectrometer with ATR probe. MS and HRMS have been performed on a Finnigan MAT 95 instrument (EI). Melting points were determined on a Büchi B-540 and are not corrected.

Solvents. For the kinetic experiments, dichloromethane (Merck *p.a.* grade) was subsequently treated with concentrated sulfuric acid, water, 10% $NaHCO_3$ solution, and water. After drying with $CaCl_2$, it was freshly distilled over CaH_2 under exclusion of moisture (N_2 atmosphere).

Chemicals. $GaCl_3$ was purchased (Aldrich) and used as obtained.

Nucleophiles. The perfluorinated silyl enol ethers **3** were synthesized by D. Gladow. Details are given in the Supporting Information of the reproduced article.

Reference electrophiles. Procedures for the syntheses of benzhydryl chlorides[14] were reported previously.

3.4.2 Products from the Reactions of 3 with 4-$GaCl_4$

1,1,1-Trifluoro-4,4-diphenylbutan-2-one (**6a**)

A solution of benzhydryl chloride **4a–Cl** (0.17 g, 0.84 mmol) in dichloromethane (10 mL) was cooled to –78 °C and subsequently treated with a solution of $GaCl_3$ (0.11 g, 0.62 mmol) in dichloromethane (8.0 mL). Then, a solution of **3a** (0.40 g, 2.2 mmol) in dichloromethane (4.0 mL) was added. After 5 min the reaction mixture was warmed to room temperature with a water bath, followed by filtration through basic Al_2O_3 (Brockmann activity III, CH_2Cl_2). After the solvent was evaporated, the crude product was purified by column chromatography (silica gel, pentane:Et_2O = 40:1) to furnish **6a**[15] as a colorless oil (0.14 g, 60%).

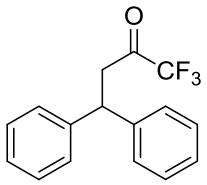

6a

^{1}H NMR (300 MHz, $CDCl_3$): δ = 3.53 (d, ^3J = 7.5 Hz, 2 H, 3-H), 4.71 (t, ^3J = 7.5 Hz, 1 H, 4-H), 7.20–7.40 (m, 10 H, Ph) ppm.

^{13}C NMR (75.5 MHz, $CDCl_3$): δ = 42.6 (t, C-3), 44.8 (d, C-4), 115.6 (q, $^1J_{CF}$ = 292 Hz, C-1), 127.1 (d, Ph), 127.7 (d, Ph), 128.9 (d, Ph), 142.6 (s, Ph),189.4 (q, $^2J_{CF}$ = 35.5 Hz, C-2) ppm.

^{19}F NMR (282 MHz, $CDCl_3$): δ = -79.4 (s, 1-F) ppm.

IR (ATR): ν = 3100–3000 (C_{Ar}-H), 1764 (C=O), 1205 (C-F), 1138 (C-F), 696 (C_{Ar}-H) cm^{-1}.

HR-MS (EI, pos.) *m*/*z* calcd. for $C_{16}H_{13}F_3O$ $[M]^+$ 278.0913, found 278.0918.

4,4,5,5,6,6,7,7,8,8,8-Undecafluoro-1,1-diphenyloctan-3-one (**6b**)

A solution of benzhydryl chloride **4a–Cl** (0.18 g, 0.89 mmol) in dichloromethane (10 mL) was cooled to –78 °C and subsequently treated with a solution of $GaCl_3$ (0.10 g, 0.57 mmol) in dichloromethane (8.0 mL). Then, a solution of **3b** (0.55 g, 1.4 mmol) in dichloromethane (4.0 mL) was added. After 10 min the reaction mixture was warmed to room temperature with a water bath, followed by filtration through basic Al_2O_3 (Brockmann activity III, CH_2Cl_2). After the solvent was evaporated, the crude product was purified by column chromatography (silica gel, pentane:Et_2O = 40:1) to furnish **6b** as a pale yellow oil (0.28 g, 66%). Signal assignments are based on additional ^{19}F decoupled ^{13}C NMR spectra, gDQCOSY (^1H and ^{19}F), HSQCAD ($^1H/^{13}C$), gHSQC ($^{19}F/^{13}C$) and gHMBCAD ($^1H/^{13}C$) experiments.

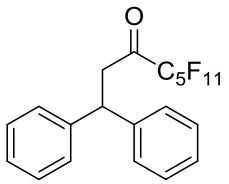

6b

^{1}H NMR (300 MHz, $CDCl_3$): δ = 3.52 (d, ^3J = 7.4 Hz, 2 H, 2-H), 4.66 (t, ^3J = 7.4 Hz, 1 H, 1-H), 7.15–7.37 (m, 10 H, Ph) ppm.

^{13}C NMR (101 MHz, $CDCl_3$): δ = 44.2 (t, C-2), 44.9 (d, C-1), 108.5 (m_C, CF_2), 109.2 (m_C, CF_2), 110.3 (m_C, CF_2), 110.9 (m_C, CF_2), 117.3 (m_C, CF_3), 127.1 (d, Ph), 127.7 (d, Ph), 128.9 (d, Ph), 142.6 (s, Ph),191.9 (t, $^2J_{CF}$ = 26.4 Hz, C-3) ppm.

^{19}F NMR (376 MHz, $CDCl_3$): δ = -126.4 to -126.2 (m, 2 F), -122.5 to -122.2 (m, 4 F), -120.4 to -120.2 (m, 2 F),-81.1 to -80.8 (m, 3 F) ppm.

IR (ATR): ν = 3100–3000 (C_{Ar}-H), 1753 (C=O), 1234 (C-F), 1191 (C-F), 1140 (C-F), 698 (C_{Ar}-H) cm^{-1}.

HR-MS (EI, pos.) *m/z* calcd. for $C_{20}H_{13}F_{11}O$ $[M]^+$ 478.0785, found 478.0787.

3,3-Bis(4-methoxyphenyl)-1-(pentafluorophenyl)propan-1-one (**6c**)

A solution of bis(4-methoxyphenyl)methyl chloride **4f–Cl** (0.15 g, 0.57 mmol) in dichloromethane (3.5 mL) was treated with a solution of $GaCl_3$ (0.10 g, 0.57 mmol) in dichloromethane (7.5 mL) at ambient temperature. Then, a solution of **3c** (0.14 g, 0.50 mmol) in dichloromethane (4.0 mL) was added. After 10 min the reaction mixture was filtered through basic Al_2O_3 (Brockmann activity III, CH_2Cl_2). After the solvent was evaporated, the crude product was purified by column chromatography (silica gel, pentane:Et_2O = 9:1) to furnish **6c** as a colorless solid (0.11 g, 51%); mp 88.7–89.1°C. Signal assignments are based on additional gDQCOSY (^{1}H and ^{19}F), HSQCAD (^{1}H/^{13}C), gHSQC (^{19}F/^{13}C), gHMBCAD (^{1}H/^{13}C) and gHMBC (^{19}F/^{13}C) experiments.

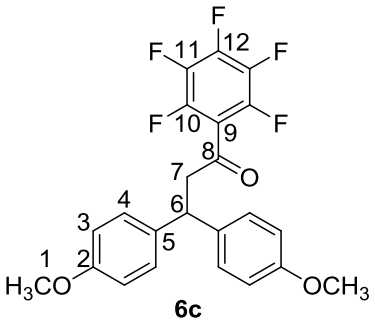

6c

^{1}H NMR (400 MHz, $CDCl_3$): δ = 3.57 (d, ^3J = 7.7 Hz, 2 H, 7-H), 3.76 (s, 6 H, 1-H), 4.56 (t, ^3J = 7.7 Hz, 1 H, 6-H), 6.77–6.85 (m, 4 H, 3-H), 7.08–7.14 (m, 4 H, 4-H) ppm.

{^{19}F}^{13}C NMR (101 MHz, $CDCl_3$): δ = 44.8 (d, $^1J_{CH}$ = 130 Hz, C-6), 51.6 (td, $^1J_{CH}$ = 129.2 Hz, $^2J_{CH}$ = 5.6 Hz, C-7), 55.4 (q, $^1J_{CH}$ = 143.7 Hz, C-1), 114.2 (d, $^1J_{CH}$ = 158.8 Hz, C-3), 115.2 (s, C-9), 128.6 (d, $^1J_{CH}$ = 156.2 Hz, C-4), 135.2–135.6 (m, C-5), 137.6 (s, C-11), 142.8 (s, C-12), 144.2 (s, C-10), 158.2–158.6 (m, C-2), 192.7 (td, $^2J_{CH}$ = 6.0 Hz, $^3J_{CH}$ = 3.1 Hz, C-8) ppm.

^{19}F NMR (376 MHz, $CDCl_3$): δ = -160.2 to -160.0 (m, 2 F, 11-F), -149.6 to -149.4 (m, 1 F, 12-F),-140.9 to -140.8 (m, 2 F, 10-F) ppm.

IR (ATR): ν = 3050–2920 (C_{Ar}-H), 1702 (C=O), 1509 (C=C), 1495 (C=C), 1251 (C-F) cm^{-1}.

HR-MS (EI, pos.) *m*/*z* calcd. for $C_{23}H_{17}F_5O_3$ $[M]^+$ 436.1092, found 436.1093.

3.4.3 Kinetic Experiments

The kinetics of the reactions of nucleophiles **3** with reference electrophiles **4a–d** were determined via the method described previously.[16] The rates of the reactions of **3c** with **4e,f** were determined by using a J&M TIDAS diode array spectrophotometer controlled by Labcontrol Spectacle Software and connected to a Hellma 661.502-QX quartz Suprasil immersion probe (5 mm light path) via fibre optic cables and standard SMA connectors.

Stock solutions of the nucleophiles, benzhydryl chlorides **4-Cl** and $GaCl_3$ were prepared by dissolving the compounds in dichloromethane. The flame-dried Schlenk flasks with nitrogen atmosphere were filled with approximately 25 mL of solvent. The exact solvent quantity was determined by weighing. Then, this flask was submerged into a circulating ethanol bath with a constant temperature, followed by the equipment with the Hellma probe or the quartz rods and a digital thermometer (for temperatures < 20°C). When a constant temperature was reached a well-defined amount of the benzhydryl chloride stock solution was added via a gas-tight syringe, followed by the addition of an excess of the $GaCl_3$ stock solution, leading to the generation of the corresponding benzhydrylium tetrachlorogallates **4-GaCl$_4$**. After addition of a well-defined amount of the nucleophile stock solution, the decay of the absorbance in dependence of the recording time was monitored. All the concentrations given are those at the actual operating temperatures, calculated via the polynomial expansion equation given in ref [17].

Kinetics for the Reactions of **3a** with **4a–c**

Rate constants for the reactions of **3a** with $(Ph)_2CH^+GaCl_4^-$ (**4a-GaCl₄**) in CH_2Cl_2 (λ = 452 nm).

T / °C	[**3a**]$_0$ / M	[**4a-Cl**]$_0$ / M	[$GaCl_3$]$_0$ / M	[**3a**]$_0$/[**4a**]$_0$	k_{obs} / s^{-1}	k_2 / M^{-1} s^{-1} [a]
–66.8	1.64×10^{-3}	5.63×10^{-5}	2.14×10^{-3}	29	5.81×10^{-3}	3.60
–60.3	1.40×10^{-3}	5.62×10^{-5}	1.65×10^{-3}	25	9.67×10^{-3}	7.05
–49.1	1.15×10^{-3}	5.51×10^{-5}	1.94×10^{-3}	21	1.77×10^{-2}	15.8
–40.9	9.25×10^{-4}	5.49×10^{-5}	2.12×10^{-3}	17	2.10×10^{-2}	23.4
–30.2	6.87×10^{-4}	5.37×10^{-5}	2.39×10^{-3}	13	3.42×10^{-2}	51.8
–20.4	4.59×10^{-4}	5.26×10^{-5}	3.22×10^{-3}	8.7	3.92×10^{-2}	90.6

[a] Calculated from $k_2 = k_{obs}/([\mathbf{3a}]_0 - 0.5[\mathbf{4a}]_0)$.

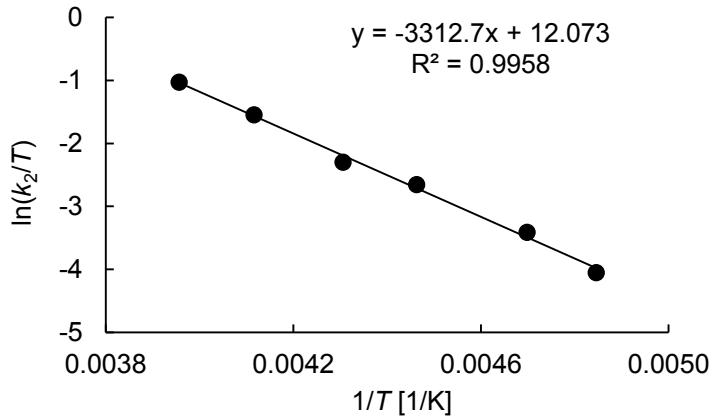

Eyring correlation for the reaction of **4a**–**GaCl₄** with **3a**.

Eyring-parameter:

$\Delta H^{\ddagger}$ = (27.5 ± 0.9) kJ mol^{-1}

$\Delta S^{\ddagger}$ = (–97.2 ± 3.9) J mol^{-1} K^{-1}

Coefficient of correlation: 0.996

Arrhenius-parameter:

E_A = (29.4 ± 0.9) kJ mol^{-1}

lg A = 18.5 ± 0.5

Coefficient of correlation: 0.996

k_2 (20 °C) = 6.34 × 10^2 M^{-1} s^{-1}

Rate constants for the reactions of **3a** with (tol)(Ph)$CH^+GaCl_4^-$ (**4b-GaCl$_4$**) in CH_2Cl_2 (λ = 463 nm).

T / °C	[**3a**]$_0$ / M	[**4b-Cl**]$_0$ / M	[$GaCl_3$]$_0$ / M	[**3a**]$_0$/[**4b**]$_0$	k_{obs} / s^{-1}	k_2 / M^{-1} s^{-1} [a]
–66.2	2.46×10^{-3}	4.89×10^{-5}	2.03×10^{-3}	50	4.10×10^{-4}	1.68×10^{-1}
–58.5	4.79×10^{-3}	4.76×10^{-5}	1.70×10^{-3}	101	1.85×10^{-3}	3.88×10^{-1}
–48.4	6.25×10^{-3}	4.72×10^{-5}	1.52×10^{-3}	132	5.04×10^{-3}	8.09×10^{-1}
–40.0	6.16×10^{-3}	4.66×10^{-5}	1.50×10^{-3}	132	9.42×10^{-3}	1.54
–29.0	6.07×10^{-3}	4.59×10^{-5}	1.47×10^{-3}	132	1.87×10^{-2}	3.09
–19.4	4.59×10^{-3}	4.56×10^{-5}	1.79×10^{-3}	101	2.67×10^{-2}	5.85

[a] Calculated from $k_2 = k_{obs}/([\mathbf{3a}]_0 - 0.5[\mathbf{4b}]_0)$.

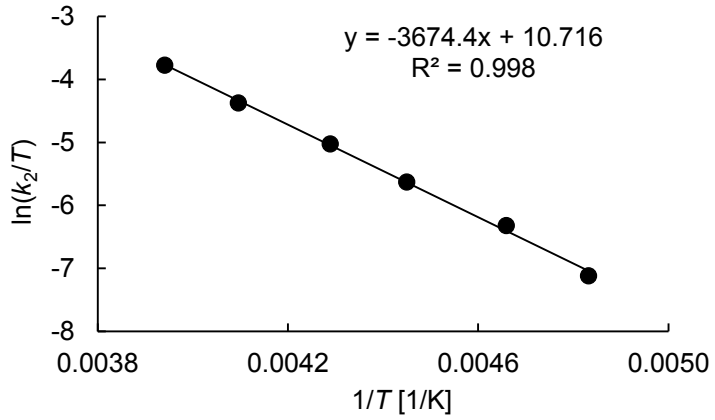

Eyring correlation for the reaction of **4b**–**GaCl$_4$** with **3a**.

Eyring-parameter:

$\Delta H^{\ddagger}$ = (30.6 ± 0.7) kJ mol^{-1}

$\Delta S^{\ddagger}$ = (–108.5 ± 3.0) J mol^{-1} K^{-1}

Coefficient of correlation: 0.998

Arrhenius-parameter:

E_A = (32.5 ± 0.7) kJ mol^{-1}

lg A = 17.2 ± 0.4

Coefficient of correlation: 0.998

k_2 (20 °C) = 4.76×10^1 M^{-1} s^{-1}

Rate constants for the reactions of **3a** with $(tol)_2CH^+GaCl_4^-$ (**4c-GaCl$_4$**) in CH_2Cl_2 (λ = 477 nm).

T / °C	[**3a**]$_0$ / M	[**4c-Cl**]$_0$ / M	[$GaCl_3$]$_0$ / M	[**3a**]$_0$/[**4c**]$_0$	k_{obs} / s^{-1}	k_2 / M^{-1} s^{-1} [a]
–49.3	1.43×10^{-2}	2.68×10^{-5}	1.39×10^{-3}	534	5.83×10^{-4}	4.08×10^{-2}
–40.6	1.33×10^{-2}	2.65×10^{-5}	1.49×10^{-3}	502	1.15×10^{-3}	8.66×10^{-2}
–29.9	1.24×10^{-2}	2.63×10^{-5}	1.33×10^{-3}	471	2.64×10^{-3}	2.13×10^{-1}
–20.1	1.15×10^{-2}	2.61×10^{-5}	1.21×10^{-3}	441	5.03×10^{-3}	4.38×10^{-1}
–10.2	1.06×10^{-2}	2.57×10^{-5}	1.22×10^{-3}	412	9.75×10^{-3}	9.21×10^{-1}

[a] Calculated from $k_2 = k_{obs}/([\mathbf{3a}]_0 - 0.5[\mathbf{4c}]_0)$.

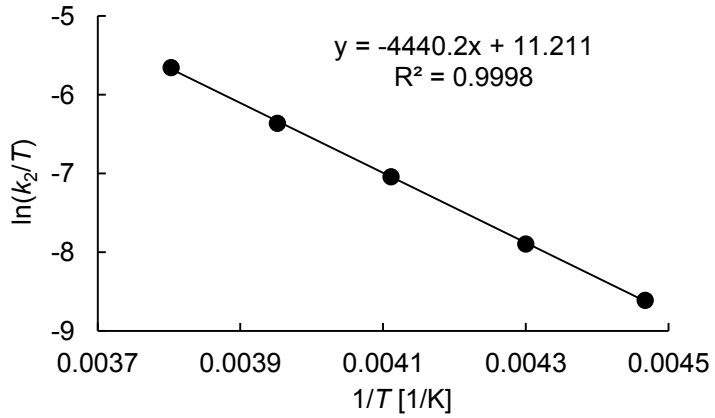

Eyring correlation for the reaction of **4c**–**GaCl$_4$** with **3a**.

Eyring-parameter:

$\Delta H^{\ddagger}$ = (36.9 ± 0.3) kJ mol^{-1}

$\Delta S^{\ddagger}$ = (–104.3 ± 1.4) J mol^{-1} K^{-1}

Coefficient of correlation: 0.999

Arrhenius-parameter:

E_A = (38.9 ± 0.4) kJ mol^{-1}

lg A = 17.7 ± 0.2

Coefficient of correlation: 0.999

k_2 (20 °C) = 5.73 M^{-1} s^{-1}

Kinetics for the Reactions of **3b** with **4a–c**

Rate constants for the reactions of **3b** with $(Ph)_2CH^+GaCl_4^-$ (**4a-GaCl₄**) in CH_2Cl_2 ($\lambda = 452$ nm).

T / °C	[**3b**]$_0$ / M	[**4a-Cl**]$_0$ / M	[$GaCl_3$]$_0$ / M	[**3b**]$_0$/[**4a**]$_0$	k_{obs} / s^{-1}	k_2 / M^{-1} s^{-1} [a]
–67.2	1.11×10^{-3}	5.97×10^{-5}	2.70×10^{-3}	19	2.18×10^{-3}	2.02
–60.2	9.79×10^{-4}	4.88×10^{-5}	3.26×10^{-3}	20	3.38×10^{-3}	3.54
–50.1	8.61×10^{-4}	5.80×10^{-5}	3.08×10^{-3}	15	5.48×10^{-3}	6.59
–39.9	7.40×10^{-4}	4.75×10^{-5}	3.99×10^{-3}	16	8.78×10^{-3}	12.3
–29.8	6.27×10^{-4}	4.69×10^{-5}	3.62×10^{-3}	13	1.21×10^{-2}	20.0

[a] Calculated from $k_2 = k_{obs}/([\mathbf{3b}]_0 - 0.5[\mathbf{4a}]_0)$.

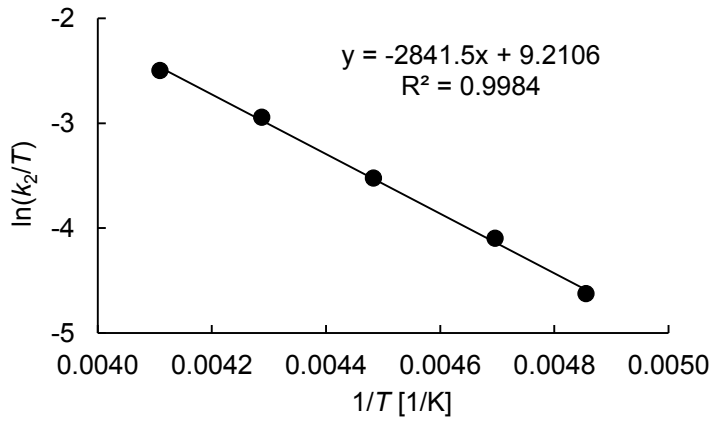

Eyring correlation for the reaction of **4a**–**GaCl₄** with **3b**.

Eyring-parameter:

$\Delta H^{\ddagger} = (23.6 \pm 0.5)$ kJ mol^{-1}

$\Delta S^{\ddagger} = (-121.0 \pm 2.5)$ J mol^{-1} K^{-1}

Coefficient of correlation: 0.998

Arrhenius-parameter:

$E_A = (25.5 \pm 0.5)$ kJ mol^{-1}

$\lg A = 15.6 \pm 0.3$

Coefficient of correlation: 0.999

k_2 (20 °C) = 1.81×10^2 M^{-1} s^{-1}

Rate constants for the reactions of **3b** with (tol)(Ph)$CH^+GaCl_4^-$ (**4b-GaCl$_4$**) in CH_2Cl_2 (λ = 463 nm).

T / °C	[**3b**]$_0$ / M	[**4b-Cl**]$_0$ / M	[$GaCl_3$]$_0$ / M	[**3b**]$_0$/[**4b**]$_0$	k_{obs} / s^{-1}	k_2 / M^{-1} s^{-1} [a]
–69.3	8.15×10^{-3}	3.68×10^{-5}	1.11×10^{-3}	221	3.58×10^{-4}	4.40×10^{-2}
–60.6	7.36×10^{-3}	3.68×10^{-5}	2.33×10^{-3}	200	7.95×10^{-4}	1.08×10^{-1}
–50.3	6.77×10^{-3}	3.63×10^{-5}	2.11×10^{-3}	187	1.62×10^{-3}	2.40×10^{-1}
–40.8	6.22×10^{-3}	3.59×10^{-5}	2.30×10^{-3}	173	2.86×10^{-3}	4.61×10^{-1}
–30.4	5.74×10^{-3}	3.59×10^{-5}	2.06×10^{-3}	160	4.87×10^{-3}	8.51×10^{-1}

[a] Calculated from $k_2 = k_{obs}/([\mathbf{3b}]_0 - 0.5[\mathbf{4b}]_0)$.

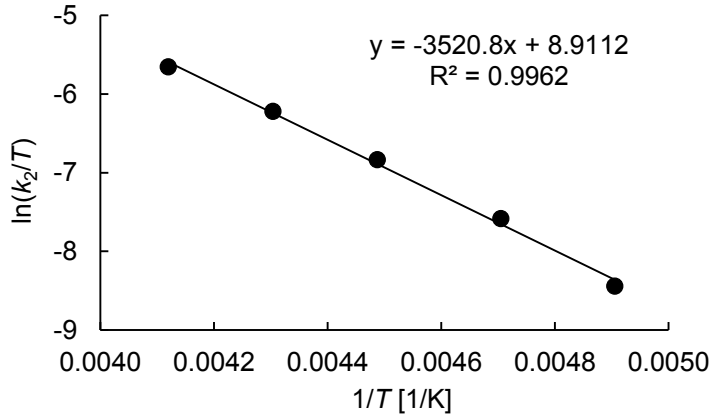

Eyring correlation for the reaction of **4b**–**GaCl$_4$** with **3b**

Eyring-parameter:

$\Delta H^{\ddagger}$ = (29.3 ± 1.0) kJ mol^{-1}

$\Delta S^{\ddagger}$ = (–123.5 ± 4.7) J mol^{-1} K^{-1}

Coefficient of correlation: 0.996

Arrhenius-parameter:

E_A = (31.1 ± 1.0) kJ mol^{-1}

lg A = 15.3 ± 0.5

Coefficient of correlation: 0.997

k_2 (20 °C) = 1.32 × 10^1 M^{-1} s^{-1}

Rate constants for the reactions of **3b** with $(tol)_2CH^+GaCl_4^-$ (**4c-GaCl$_4$**) in CH_2Cl_2 (λ = 477 nm).

T / °C	[**3b**]$_0$ / M	[**4c-Cl**]$_0$ / M	[$GaCl_3$]$_0$ / M	[**3b**]$_0$/[**4c**]$_0$	k_{obs} / s^{-1}	k_2 / M^{-1} s^{-1} [a]
–58.6	1.78×10^{-2}	2.54×10^{-5}	8.99×10^{-4}	701	1.09×10^{-4}	6.13×10^{-3}
–50.3	9.48×10^{-3}	2.64×10^{-5}	1.20×10^{-3}	359	1.02×10^{-4}	1.08×10^{-2}
–41.1	1.55×10^{-2}	2.59×10^{-5}	1.13×10^{-3}	598	4.98×10^{-4}	3.22×10^{-2}
–30.4	1.37×10^{-2}	2.55×10^{-5}	1.20×10^{-3}	537	8.50×10^{-4}	6.21×10^{-2}
–20.6	1.20×10^{-2}	2.51×10^{-5}	1.32×10^{-3}	478	1.30×10^{-3}	1.08×10^{-1}
–10.3	1.05×10^{-2}	2.49×10^{-5}	1.10×10^{-3}	422	2.45×10^{-3}	2.34×10^{-1}

[a] Calculated from $k_2 = k_{obs}/([\mathbf{3b}]_0 - 0.5[\mathbf{4c}]_0)$.

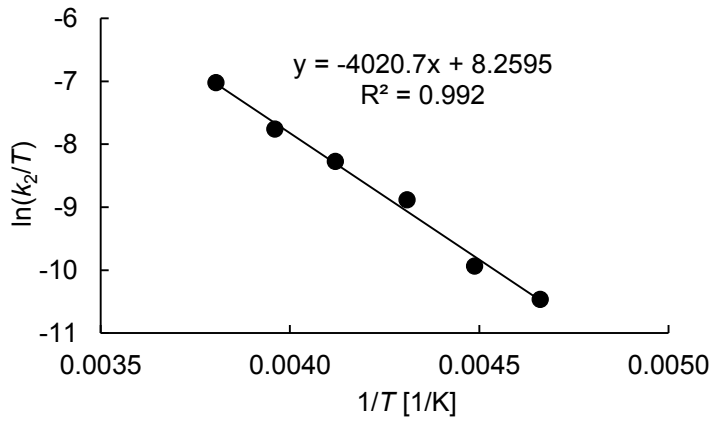

Eyring correlation for the reaction of **4c**–**GaCl$_4$** with **3b**.

Eyring-parameter:

$\Delta H^{\ddagger}$ = (33.4 ± 1.5) kJ mol^{-1}

$\Delta S^{\ddagger}$ = (–128.9 ± 6.3) J mol^{-1} K^{-1}

Coefficient of correlation: 0.992

Arrhenius-parameter:

E_A = (35.4 ± 1.5) kJ mol^{-1}

lg A = 14.7 ± 0.8

Coefficient of correlation: 0.993

k_2 (20 °C) = 1.25 M^{-1} s^{-1}

Kinetics for the Reactions of **3c** with **4d–f**

Rate constants for the reactions of **3c** with (ani)(tol)$CH^+GaCl_4^-$ (**4d-GaCl₄**) in CH_2Cl_2 (λ = 490 nm).

T / °C	[**3c**]$_0$ / M	[**4d-Cl**]$_0$ / M	[$GaCl_3$]$_0$ / M	[**3c**]$_0$/[**4d**]$_0$	k_{obs} / s^{-1}	k_2 / M^{-1} s^{-1} [a]
–70.8	1.55×10^{-3}	2.69×10^{-5}	6.26×10^{-4}	58	7.97×10^{-3}	5.19
–60.8	1.39×10^{-3}	2.64×10^{-5}	5.32×10^{-4}	53	1.39×10^{-2}	10.1
–49.8	1.20×10^{-3}	2.55×10^{-5}	4.65×10^{-4}	47	2.31×10^{-2}	19.5
–40.0	1.07×10^{-3}	2.55×10^{-5}	4.65×10^{-4}	42	3.57×10^{-2}	33.8
–30.5	9.16×10^{-4}	2.49×10^{-5}	3.35×10^{-4}	37	4.88×10^{-2}	54.0

[a] Calculated from $k_2 = k_{obs}/([\mathbf{3c}]_0 - 0.5[\mathbf{4d}]_0)$.

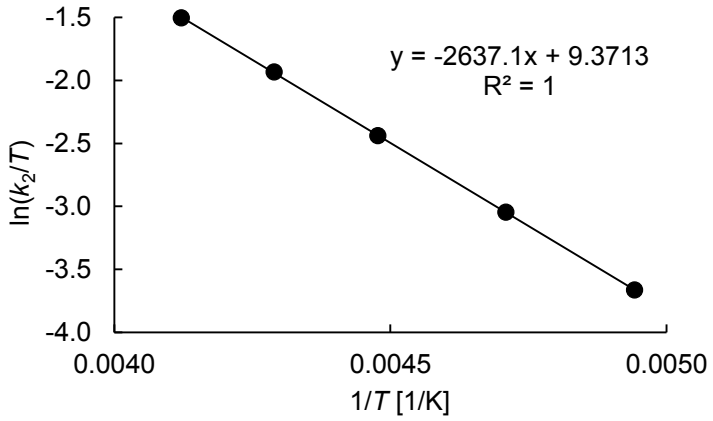

Eyring correlation for the reaction of **4d**–**GaCl₄** with **3c**.

Eyring-parameter:

$\Delta H^{\ddagger}$ = (21.9 ± 0.08) kJ mol^{-1}

$\Delta S^{\ddagger}$ = (–119.6 ± 0.4) J mol^{-1} K^{-1}

Coefficient of correlation: 0.999

Arrhenius-parameter:

E_A = (23.8 ± 0.07) kJ mol^{-1}

lg A = 15.8 ± 0.04

Coefficient of correlation: 0.999

k_2 (20 °C) = 4.27×10^2 M^{-1} s^{-1}

Rate constants for the reactions of **3c** with (ani)(OPh)$CH^+GaCl_4^-$ (**4e-GaCl$_4$**) in CH_2Cl_2 (20 °C, λ = 516 nm).

[**3c**]$_0$ / M	[**4e-Cl**]$_0$ / M	[$GaCl_3$]$_0$ / M	[**3c**]$_0$/[**4e**]$_0$	k_{obs} / s^{-1}
3.76×10^{-4}	1.84×10^{-5}	2.45×10^{-4}	20	2.08×10^{-2}
5.94×10^{-4}	1.85×10^{-5}	1.73×10^{-4}	32	3.43×10^{-2}
8.13×10^{-4}	1.86×10^{-5}	1.98×10^{-4}	44	4.77×10^{-2}
1.04×10^{-3}	1.87×10^{-5}	1.50×10^{-4}	56	6.30×10^{-2}
1.24×10^{-3}	1.84×10^{-5}	1.48×10^{-4}	67	7.50×10^{-2}

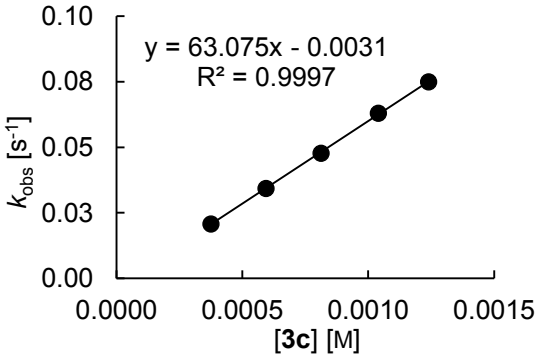

k_2 (20 °C) = 6.31×10^1 M^{-1} s^{-1}

Rate constants for the reactions of **3c** with $(ani)_2CH^+GaCl_4^-$ (**4f-GaCl$_4$**) in CH_2Cl_2 (20 °C, λ = 513 nm).

[**3c**]$_0$ / M	[**4f-Cl**]$_0$ / M	[$GaCl_3$]$_0$ / M	[**3c**]$_0$/[**4f$^+$**]$_0$	k_{obs} / s^{-1}
4.88×10^{-4}	1.56×10^{-5}	1.49×10^{-4}	31	9.23×10^{-3}
8.08×10^{-4}	1.55×10^{-5}	7.38×10^{-5}	52	1.61×10^{-2}
1.07×10^{-3}	1.55×10^{-5}	9.81×10^{-5}	69	2.17×10^{-2}
1.35×10^{-3}	1.56×10^{-5}	1.24×10^{-4}	87	2.71×10^{-2}
1.62×10^{-3}	1.56×10^{-5}	7.41×10^{-5}	104	3.35×10^{-2}

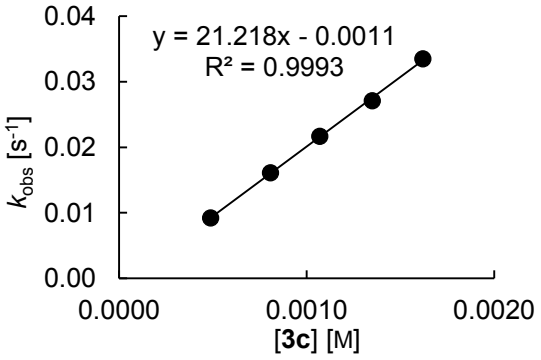

k_2 (20 °C) = 2.12 × 10^1 M^{-1} s^{-1}

3.5 References

[1] a) W. R. Dolbier Jr, *J. Fluorine Chem.* **2005**, *126*, 157–163; b) T. Hiyama in *Organofluorine Compounds: Chemistry and Applications*, (Ed.: H. Yamamoto), Springer, Berlin, **2000**; c) K. Müller, C. Faeh, F. Diederich, *Science* **2007**, *317*, 1881–1886; d) D. O'Hagan, *Chem. Soc. Rev.* **2008**, *37*, 308–319; e) T. Yamazaki, T. Taguchi, I. Ojima in *Fluorine in Medicinal Chemistry and Chemical Biology*, (Ed.: I. Ojima), Wiley, Chichester, **2009**, pp. 1–46; f) *Fluorine and Health*, (Eds.: A. Tressaud, G. Haufe), Elsevier, Amsterdam, **2008**.

[2] H.-U. Reissig, R. Zimmer, *Chem. Rev.* **2003**, *103*, 1151–1196.

[3] S. Kobayashi, K. Manabe, H. Ishitani, J. I. Matsuo in *Science of Synthesis*, *Vol. 4* (Ed.: I. Fleming), Thieme Verlag, Stuttgart, **2002**,pp. 317–369.

[4] a) D. Hass, H. Holfter, U. Schröder, *J. Fluorine Chem.* **1994**, *69*, 89–95; b) O. Provot, J.-F. Berrien, H. Moskowitz, J. Mayrargue, *J. Fluorine Chem.* **1997**, *86*, 185–187.

[5] For examples with special substitution patterns (in particular with additional electron-withdrawing groups) see: a) J. Jullien, J. M. Pechine, F. Perez, J. J. Piade, *Tetrahedron* **1982**, *38*, 1413–1416; b) F. U. Seifert, G.-V. Röschenthaler, *J. Fluorine Chem.* **1994**, *68*, 169–174; c) D. A. Neumayer, J. A. Belot, R. L. Feezel, C. Reedy, C. L. Stern, T. J. Marks, L. M. Liable-Sands, A. L. Rheingold, *Inorg. Chem.* **1998**, *37*, 5625–5633; d) I. S. Kruchok, I. I. Gerus, V. P. Kukhar, *Tetrahedron* **2000**, *56*, 6533–6539; e) A. D. Dilman, P. A. Belyakov, A. A. Korlyukov, V. A. Tartakovsky, *Tetrahedron Lett.* **2004**, *45*, 3741–3744; f) W. J. Chung, S. C. Ngo, S. Higashiya, J. T. Welch, *Tetrahedron Lett.* **2004**, *45*, 5403–5406; g) Vitalij V. Levin, Alexander D. Dilman, Pavel A. Belyakov, Alexander A. Korlyukov, Marina I. Struchkova, Vladimir A. Tartakovsky, *Eur. J. Org. Chem.* **2004**, 5141–5148; h) D. L. Chizhov, G.-V. Röschenthaler, *J. Fluorine Chem.* **2006**, *127*, 235–239; i) S. Büttner, A. Riahi, I. Hussain, M. A. Yawer, M. Lubbe, A. Villinger, H. Reinke, C. Fischer, P. Langer, *Tetrahedron* **2009**, *65*, 2124–2135; j) S. Metz, C. Burschka, R. Tacke, *Organometallics* **2009**, *28*, 2311–2317; k) S. Büttner, F. Bendrath, P. Langer, *Tetrahedron Lett.* **2010**, *51*, 5106–5108.

[6] Compound **2b** was previously described, but its synthesis was not specified: N. Nakazawa, M. Kawamura, A. Sekiya, K. Ootake, R. Tamai, Y. Kurokawa, J. Murata, *Nippon Reito Kucho Gakkai Ronbunshu (Trans. of the JSRAE)* **2001**, *18*, 427–434.

[7] a) A. Kondo, S. Iwatsuki, *J. Fluorine Chem.* **1984**, *26*, 59–67; b) B. Croxtall, J. Fawcett, E. G. Hope, A. M. Stuart, *J. Fluorine Chem.* **2003**, *119*, 65–73.

[8] B. A. Gostevskii, O. A. Vyazankina, N. S. Vyazankin, *Zh. Obshch. Khim.* **1984**, *54*, 2613–2617; *J. Gen. Chem. USSR* **1985**, *54*, 2334–2337.

[9] a) H. Mayr, T. Bug, M. F. Gotta, N. Hering, B. Irrgang, B. Janker, B. Kempf, R. Loos, A. R. Ofial, G. Remennikov, H. Schimmel, *J. Am. Chem. Soc.* **2001**, *123*, 9500–9512; b) H. Mayr, B. Kempf, A. R. Ofial, *Acc. Chem. Res.* **2003**, *36*, 66–77; c) H. Mayr, A. R. Ofial in *Carbocation Chemistry* (Eds.: G. A. Olah, G. K. S. Prakash), Wiley, Hoboken, NJ, **2004**, pp. 331–358; d) H. Mayr, A. R. Ofial, *Pure Appl. Chem.* **2005**, *77*, 1807–1821; e) H. Mayr, A. R. Ofial, *J. Phys. Org. Chem.* **2008**, *21*, 584–595; f) For a comprehensive database of reactivity parameters, see http://www.cup.uni-muenchen.de/oc/mayr/DBintro.html.

[10] a) J. Burfeindt, M. Patz, M. Müller, H. Mayr, *J. Am. Chem. Soc.* **1998**, *120*, 3629–3634; b) T. Tokuyasu, H. Mayr, *Eur. J. Org. Chem.* **2004**, 2791–2796; c) A. D. Dilman, H. Mayr, *Eur. J. Org. Chem.* **2005**, 1760–1764; d) H. A. Laub, H. Yamamoto, H. Mayr, *Org. Lett.* **2010**, *12*, 5206–5209.

[11] J. Ammer, C. Nolte, H. Mayr, *J. Am. Chem. Soc.* **2012**, *134*, 13902–13911.

[12] H. Mayr, G. Gorath, *J. Am. Chem. Soc.* **1995**, *117*, 7862–7868.

[13] S. Lakhdar, J. Ammer, H. Mayr, *Angew. Chem., Int. Ed.* **2011**, *50*, 9953–9956.

[14] B. Denegri, A. Streiter, S. Juric, A. R. Ofial, O. Kronja, H. Mayr, *Chem. Eur. J.* **2006**, *12*, 1648–1656; *Chem. Eur. J.* **2006**, *12*, 5415.

[15] R. J. Andrew, J. M. Mellor, *Tetrahedron* **2000**, *56*, 7261–7266.

[16] H. Mayr, R. Schneider, C. Schade, J. Bartl, R. Bederke, *J. Am. Chem. Soc.* **1990,** *112*, 4446–4454.

[17] M. Frenkel, X. Hong, Q. Dong, X. Yan, R. D. Chirico in *Landolt-Börnstein, New Series*, *Vol. IV/8J* (Eds.: M. Frenkel, K. N. Marsh), Springer, Berlin, **2003**, p 113.

Chapter 4

Electrophilic Alkylations of Vinylsilanes – A Comparison of α- and β-Silyl Effects

Reproduced with permission from

H. A. Laub, H. Mayr, *Chem. Eur. J.* **2014**, *20*, 1103–1110.

4.1 Introduction

Vinylsilanes represent important reagents in organic synthesis, which commonly undergo electrophilic substitution reactions with replacement of the silyl group.[1] It has been shown that they can be combined with a large variety of electrophiles, including carbonyl compounds, Michael acceptors, acyl derivatives, halogens, and stabilized carbocations.[1] Reactions involving reagents of low electrophilicity, like carbonyl compounds, commonly need activation of either the electrophile by Lewis acids or the vinylsilanes by nucleophiles, *e.g.*, fluoride ions. The vinylsilane functionality has also been utilized as internal nucleophile for trapping intermediate carbocations.[2] Carbenes and peracids have been applied for the vinylsilane-based synthesis of silylated cyclopropanes[3] and epoxysilanes,[1c,i,4] respectively.

Electrophilic attack at vinylsilanes commonly occurs at the olefinic carbon α to the silicon moiety eventually leading to the direct displacement of the silyl group (*ipso*-substitution, Scheme 4.1a). Electrophilic substitutions of allylsilanes usually follow an S_E2' mechanism, where the electrophilic attack occurs in γ-position to the silyl substituent, giving the product with allyl rearrangement (Scheme 4.1b).[1i]

Although the reactions in Scheme 4.1a and 4.1b proceed via intermediates with a carbocationic center in the β-position to the silyl group, allylsilanes are known to react under milder conditions and with weaker electrophiles than the corresponding vinylsilanes,[1i] indicating that allylsilanes are more nucleophilic than vinylsilanes. The lower efficiency of the organosilicon moiety to enhance the nucleophilic reactivity of vinylsilanes can also be deduced from the fact that the introduction of electron-donating substituents *e.g.*, alkoxy, alkyl, or aryl

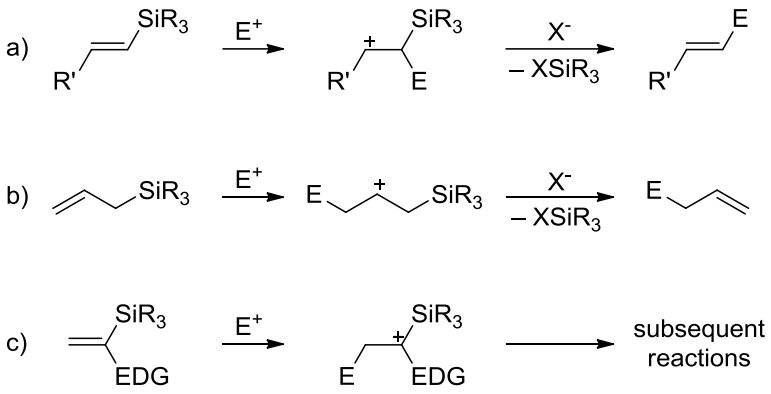

Scheme 4.1. Electrophilic substitution of vinyl- (a+c) and allylsilanes (b); E = electrophile, EDG = electron-donating group.

groups, in α-position to the silyl group of vinylsilanes directs the electrophilic attack to the β-position of the vinylsilanes, thus giving rise to the formation α-silyl stabilized carbocations (Scheme 4.1c).[5]

Soderquist and Hassner[6] studied the rates of formation of such α-silyl stabilized carbocations through the deuterolyses of α-silylated methyl vinyl ethers. We now report on the magnitude of α- and β-silyl effects on the electrophilic alkylations of vinylsilanes by studying the kinetics of the reactions of the propene- (**1a–c**) and styrene-derived organosilanes (**1d–h**, Scheme 4.2) with carbenium ions.

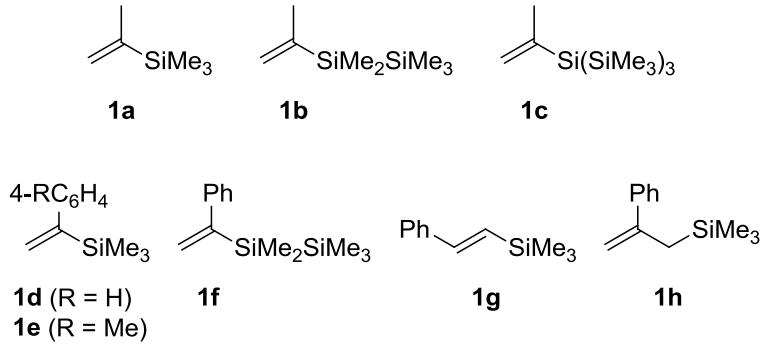

Scheme 4.2. Organosilanes studied for the quantification of the α- and β-silyl effects in vinylsilanes.

By utilizing the benzhydrylium method[7] for the quantification of the nucleophilic reactivities of **1a–h**, it will be possible to compare their nucleophilicities with those of previously investigated compounds, including allylsilanes,[7a,f,8] silyl enol ethers,[7a,8b,9] and

ordinary alkenes.[7a,b,f,g] All of these compounds are part of a comprehensive nucleophilicity scale, which has been derived by the method of overlapping correlation lines using benzhydrylium ions with variable *p*- and *m*-substituents as reference electrophiles.[7a] The correlations are based on Equation (4.1), where electrophiles are characterized by the electrophilicity parameter E and nucleophiles by the solvent-dependent parameters s_N (sensitivity) and N (nucleophilicity).

$$\lg k\ (20\ °C) = s_N(N + E) \qquad (4.1)$$

For this study, benzhydrylium ions **2a–j** with electrophilicity parameters E from –4.72 to +3.63 (Table 4.1) were used as reaction partners for the organosilanes **1a–h**.

Table 4.1. Reference Electrophiles ArAr'CH^+ Used for Quantifying the Nucleophilicities of **1a–h**.

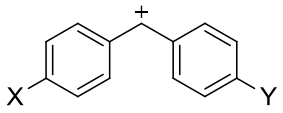

ArAr'CH^+ [a]	X	Y	E[b]
$(tol)_2CH^+$ (**2a**)	CH_3	CH_3	3.63
(Ph)(pop)CH^+ (**2b**)	H	OPh	2.90
(tol)(pop)CH^+ (**2c**)	CH_3	OPh	2.16
(Ph)(ani)CH^+ (**2d**)	H	OMe	2.11
(tol)(ani)CH^+ (**2e**)	CH_3	OMe	1.48
(ani)(pop)CH^+ (**2f**)	OMe	OPh	0.61
$(ani)_2CH^+$ (**2g**)	OMe	OMe	0.00
$(pfa)_2CH^+$ (**2h**)	$N(Ph)CH_2CF_3$	$N(Ph)CH_2CF_3$	–3.14
$(mfa)_2CH^+$ (**2i**)	$N(Me)CH_2CF_3$	$N(Me)CH_2CF_3$	–3.85
$(dpa)_2CH^+$ (**2j**)	NPh_2	NPh_2	–4.72

[a] tol = *p*-*tol*yl; pop = *p*-*p*heno*xyp*henyl; ani = *p*-*ani*syl; pfa = 4-(*p*henyl(tri*f*luoroethyl)-*a*mino)phenyl; mfa = 4-(*m*ethyl(tri*f*luoroethyl)*a*mino)phenyl; dpa = 4-(*dip*henyl*a*mino)phenyl. [b] Empirical electrophilicities E from ref [7a].

4.2 Results and Discussion

Product Analysis. For the attack of electrophiles at vinylsilanes two sites of attack are conceivable – in position α or β to silicon (Scheme 4.1a+c). As shown in Scheme 4.3, the vinylsilanes **1a–f** with a terminal double bond are attacked at β-position with formation of the α-silyl stabilized carbocations, which undergo different subsequent reactions.

While the formation of **4a** can be explained by a 1,2-hydride shift in **3a**, followed by a chloride-induced desilylation,[10a] carbocations **3b** and **3f** are probably intercepted by chloride ions to give α-chlorosilanes, which hydrolyze with formation of the alcohols **4b** and **4f** during workup. The formation of **4f'** as a side-product is probably due to the oxidation of **4f** by atmospheric oxygen; an analogous conversion of α-silyl substituted benzyl alcohols by *t*BuONO into arylalkylketones has previously been reported.[11] 1,2-Silyl migration in **3c** followed by fluoride trapping of the resulting silylium ion can explain the formation of the fluorosilane **4c**. In analogy to previously reported reactions of benzhydrylium ions with ordinary alkenes[12] the α-silyl substituted carbocation **3d** cyclizes with formation of the indane **4d** with high diastereoselectivity (dr 98:2, main diastereoisomer shown in Scheme 4.3).

In contrast to the vinylsilanes with terminal double bonds, *trans*-β-(trimethylsilyl)styrene **1g** was attacked at the silyl-substituted vinylic carbon yielding the phenyl-stabilized carbocation **3g**, which gives **4g** by desilylation.[10b] For comparison, also the allylsilane **1h** was investigated and found to give the common S_E2' substitution product **4h**.

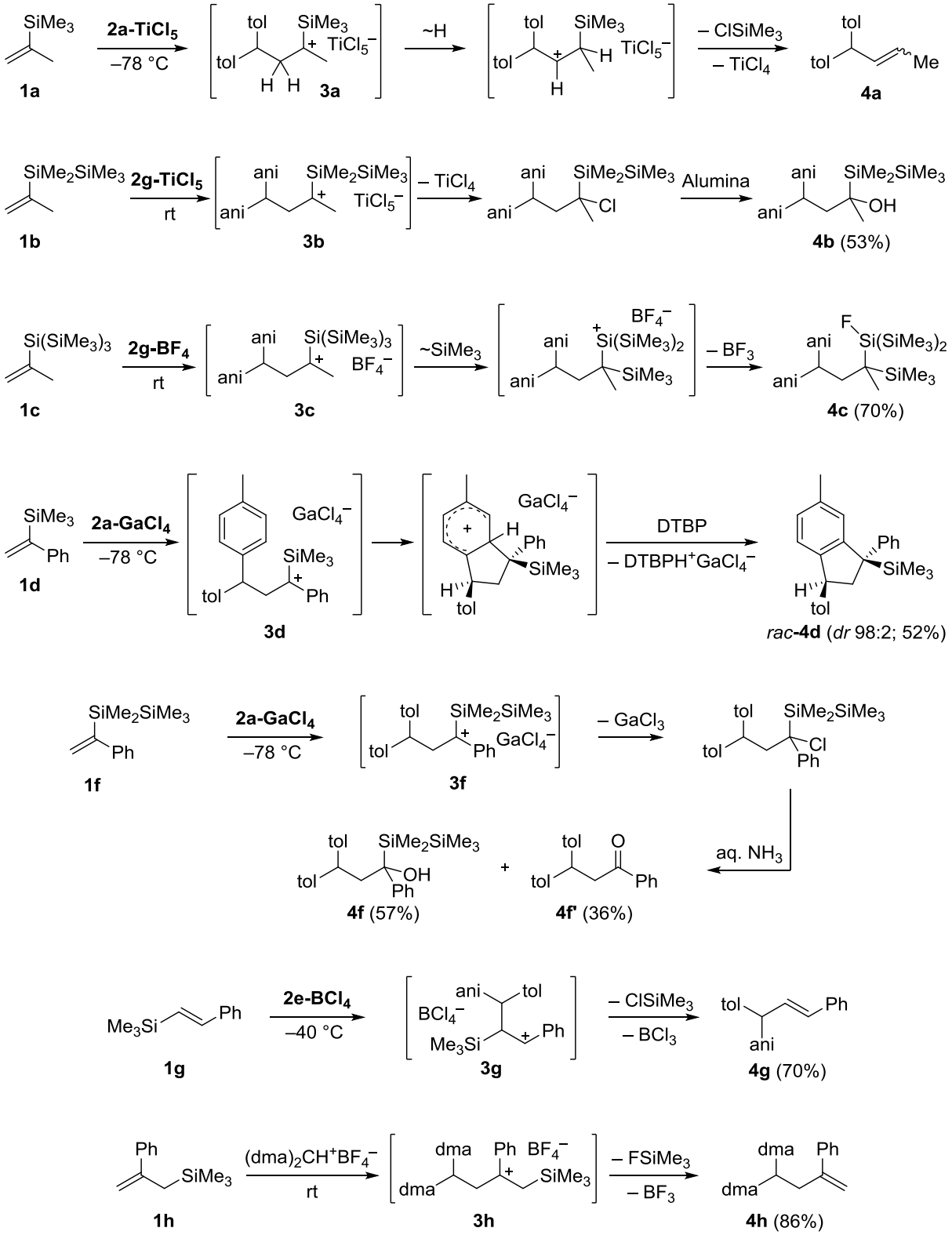

Scheme 4.3. Reactions of silyl substituted propenes (**1a–c**) and styrenes **1d,f–h** with benzhydrylium salts (DTBP = 2,6-di-*tert*-butylpyridine; dma = 4-(*dim*ethyl*a*mino)phenyl).

Kinetic Measurements. Since the benzhydrylium ions **2a–j** possess absorption maxima in the visible spectrum, while the products arising from the nucleophilic attack are colorless, we were able to study the kinetics of these bimolecular reactions in CH_2Cl_2 spectrophotometrically. First-order conditions were obtained by employing at least 9 equivalents of the unsaturated organosilanes **1a–h** with respect to the benzhydrylium ions **2a–j**. From the resulting mono-exponential decays of the absorbances of the benzhydrylium ions, the corresponding first-order rate constants k_{obs} were derived (Figure 4.1a). The second-order rate constants k_2 given in Table 4.2 and Table 4.3 were derived as the slopes of the linear correlations of the k_{obs} values against the corresponding nucleophile concentrations $[Nu]_0$ (Figure 4.1b).

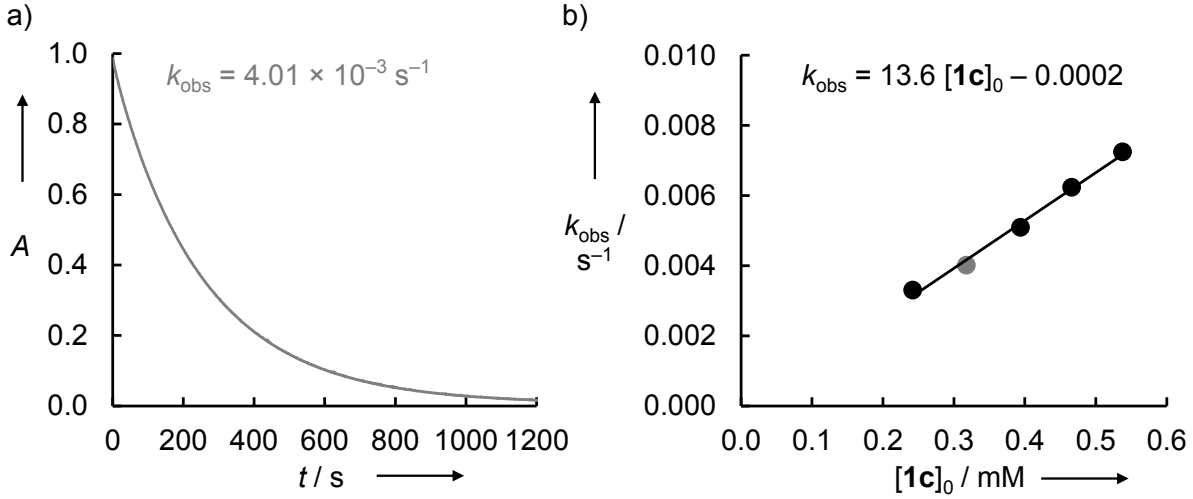

Figure 4.1. a) Exponential decay of the absorbance at 488 nm during the reaction of **1c** (c = 3.18 × 10^{-4} M) with **2e–GaCl$_4$** (c = 2.43 × 10^{-5} M) at 20 °C in CH_2Cl_2. b) k_2 = 13.6 M^{-1} s^{-1} is obtained as the slope of the linear correlation of the first-order rate constants k_{obs} against $[\mathbf{1c}]_0$.

The reactions with the highly reactive benzhydrylium ions **2a,b** and the reaction of **1e** with **2d-GaCl$_4$** were studied in the temperature range between –70 °C and –20 °C. In these cases, the second-order rate constants k_2 were calculated by dividing the corresponding first-order rate constants k_{obs} by the corresponding mean nucleophile concentrations $[Nu]_{av} = [Nu]_0 - 0.5[\mathbf{2}–\mathbf{MX}_{n+1}]_0$. Figure 4.2 shows exemplarily the linear Eyring plot for the reaction of **1d** with **2b–GaCl$_4$** between –69 °C and –30 °C. From analogous correlations, the activation parameters $\Delta H^{\ddagger}$ and $\Delta S^{\ddagger}$ and the second-order rate constants k_2 at 20 °C given in Table 4.2 were calculated.

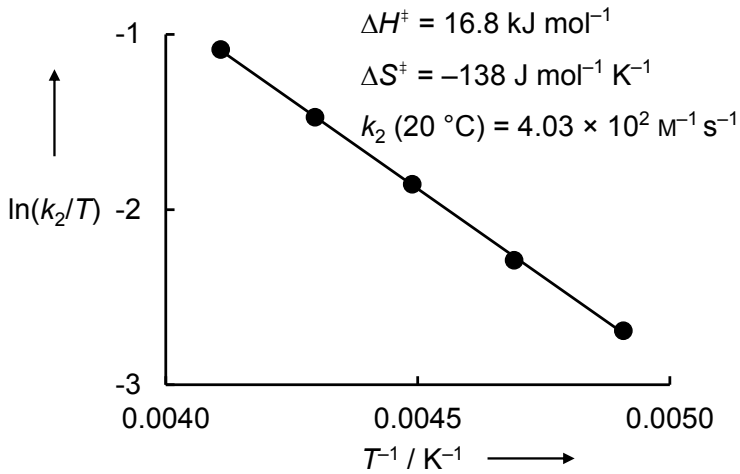

Figure 4.2. Eyring plot for the reaction of **1d** with **2b–GaCl₄** in CH_2Cl_2 between –69 °C and –30 °C.

Table 4.2. Second-Order Rate Constants k_2 for the Reactions of Organosilanes **1a–h** with Benzhydrylium Ions **2** (Counterion $GaCl_4^-$) in Dichloromethane and the Nucleophilicity Parameters for **1a–h** Derived Thereof.

Nucleophile (N, s_N)[a]	**2**	k_2 (20 °C) / M^{-1} s^{-1}	$\Delta H^{\ddagger}$ / kJ mol^{-1}	$\Delta S^{\ddagger}$ / J mol^{-1} K^{-1}
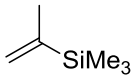 **1a** (–1.46, 1.05)	**2a**	223[b]	25.9	–112
	2b	30.6[b]	27.1	–124
	2c	4.28	–	–
	2d	4.89	–	–
	2e	1.30	–	–
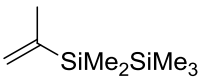 **1b** (–0.26, 0.95)	**2d**	53.7	–	–
	2e	15.2	–	–
	2g	0.557	–	–
 **1c** (–0.31, 0.99)	**2d**	63.6	–	–
	2e	13.6	–	–
	2g	0.507	–	–

Table 4.2. continued.

Nucleophile (N, s_N)[a]	**2**	k_2 (20 °C) / M^{-1} s^{-1}	$\Delta H^{\ddagger}$ / kJ mol^{-1}	$\Delta S^{\ddagger}$ / J mol^{-1} K^{-1}
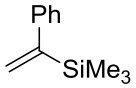 **1d** (–1.13, 1.46)	**2a**	4.10×10^3 [b]	16.1	–121
	2b	403[b]	16.8	–138
	2d	28.7	–	–
	2e	3.75	–	–
	2f	0.153	–	–
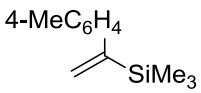 **1e** (–0.65, 1.59)	**2d**	177[b]	13.3	–156
	2e	28.3	–	–
	2f	0.777	–	–
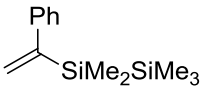 **1f** (0.61, 1.01)	**2e**	137	–	–
	2f	14.8	–	–
	2g	4.49	–	–
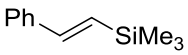 **1g** (–0.43, 1.06)	**2b**	407[b]	18.1	–133
	2d	66.1	–	–
	2e	13.3	–	–
	2f	1.32	–	–
	2g	0.387	–	–
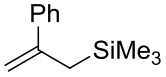 **1h** (5.38, 0.89)	**2h**	102	–	–
	2i	22.1	–	–
	2j	3.94	–	–

[a] Determination see next section. [b] Calculated by using the Eyring activation parameters $\Delta H^{\ddagger}$ and $\Delta S^{\ddagger}$ which were determined between –70 °C and –20 °C, see Experimental Section for details.

Table 4.2 shows that most reactions studied at variable temperature possess activation entropies between –112 and –138 J mol^{-1} K^{-1}, similar to those previously reported for the reactions of benzhydrylium ions with terminal alkenes[12b,13] and allylsilanes.[8a,13b] It is not clear, why the reaction of **1e** with **2d** proceeds with significantly more negative activation entropy.

As depicted in Table 4.3 the second-order rate constants for the reactions of the organosilanes **1b,f,g** with the benzhydrylium ions **2d**, **2e**, and **2g** are only slightly affected by the counterions. Therefore, the second-order rate constants given in Table 4.2 can be assigned to the formation of the initial C-C bond while the subsequent reactions of the intermediates **3b,f,g** with the halometallates MX_{n+1}^- have no or only little influence on the overall rate. As counterion independence of the rate constants has already been shown in previous studies of allylsilanes, we assume that the measured rate constants for the reactions of allylsilane **1h** with benzhydrylium ions also refer to the C-C bond-forming step.[8-9]

Table 4.3. Counterion Effects on the Second-Order Rate Constants for the Reactions of Vinylsilanes **1b,f,g** with Benzhydrylium Salts **2–MX$_{n+1}$** in Dichloromethane.

MX_{n+1}	k_2 (20 °C) / M^{-1} s^{-1}				
	1b + **2d**	**1f** + **2e**	**1g** + **2d**	**1g** + **2e**	**1g** + **2g**[a]
$GaCl_4^-$	53.7	137	66.1	13.3	0.387
$SnCl_5^-$	45.9	–	–	–	0.468
$FeCl_4^-$	57.2	141	–	–	0.402
BCl_4^-	–	–	73.4[b]	15.0[c]	–

[a] With triflate as counterion the kinetics do not follow a first-order rate law. [b,c] Calculated by using the following Eyring activation parameters (for determination see Experimental Section): [b] $\Delta H^{\ddagger}$ = 23.2 kJ mol^{-1} and $\Delta S^{\ddagger}$ = –130 J mol^{-1} K^{-1}; [c] $\Delta H^{\ddagger}$ = 26.7 kJ mol^{-1} and $\Delta S^{\ddagger}$ = –131 J mol^{-1} K^{-1}.

Linear Free Energy Relationships. Plots of lg k_2 for the reactions of the benzhydrylium ions **2** with the propene derivatives **1a–c** (Figure 4.3) and styrene derivatives **1d–h** (Figure 4.4) against the electrophilicity parameters E of the reference electrophiles show linear correlations. Equation (4.1) allowed us to calculate the N and s_N parameters for the organosilanes **1a–h**,

which are given in Table 4.2. These correlations do not only confirm the consistency of the rate constants determined in this work but also allow to extrapolate rate constants for reactions that cannot be directly measured. Such rate constants are needed for the structure-reactivity correlations in Table 4.4. Since the s_N parameters differ slightly for the various π-systems, the relative reactivities depend somewhat on the nature of the attacking electrophile. For that reason, small reactivity differences should only be discussed when systems with equal s_N are compared. In order to avoid ambiguity, the following discussion will focus on the reactivities toward the *p*-methoxy substituted benzhydrylium ion **2d**, for which most directly measured rate constants are available.

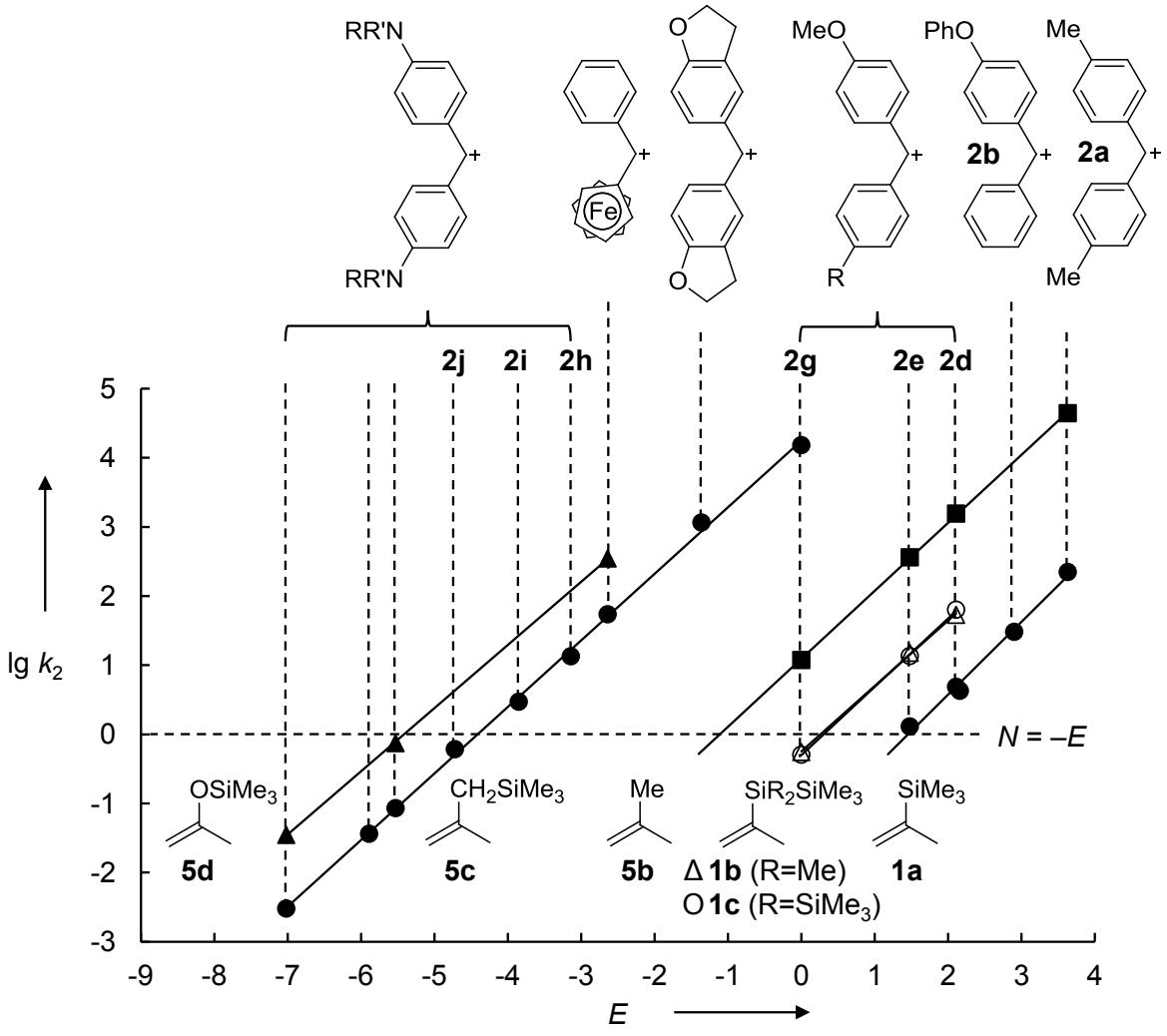

Figure 4.3. Plots of lg k_2 for the reactions of the propene derivatives **1a–c** and **5b–d** (from ref [7a]) with benzhydrylium ions in CH_2Cl_2 at 20 °C versus the electrophilicity parameters E of the benzhydrylium ions.

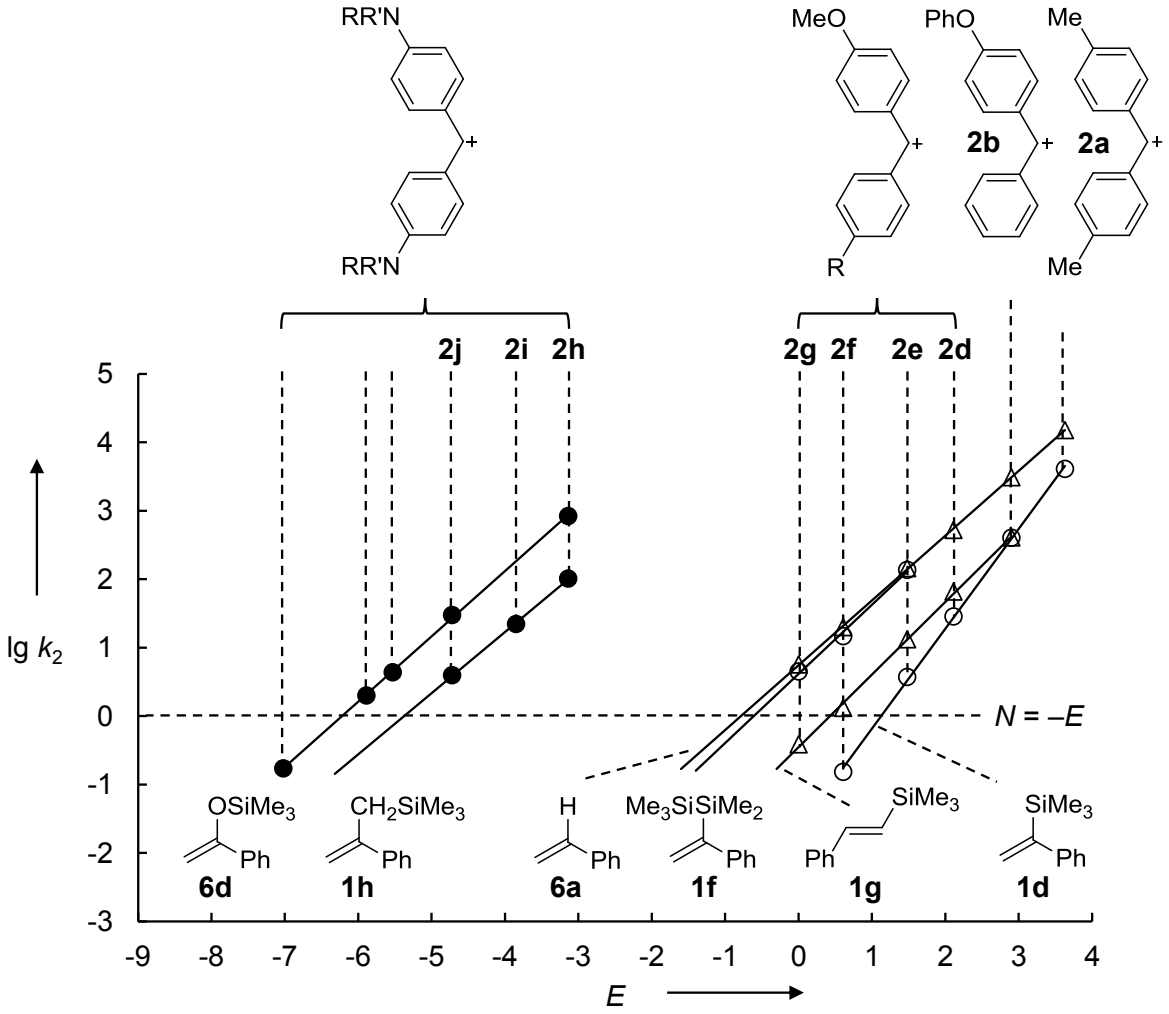

Figure 4.4. Plots of lg k_2 for the reactions of styrene derivatives **1d,f–h** and **6a,d** (from ref [7a,b]) with benzhydrylium ions in CH_2Cl_2 at 20 °C versus the electrophilicity parameters E of the benzhydrylium ions.

Table 4.4 shows that all vinylsilanes (**1a–f**) investigated are significantly less nucleophilic than the allylsilanes **5c** and **1h** due to the fact that the stabilization of the intermediate carbocation is much more effective by a β- than an α-silyl substituent. Comparison of propene (**5a**) with **1a** and of styrene (**6a**) with **1d** shows different silyl effects in both reaction series: While the trimethylsilyl group in α-position of the new carbenium center activates propene by a factor of 10 (**1a**/**5a**), it deactivates styrene by a factor of 18 (**1d**/**6a**). These opposing effects can be assigned to the perturbation of conjugation in α-substituted styrenes, in line with the observation that introduction of an α-methyl group activates propene by a factor of 3100 (**5b**/**5a**) and styrene by only 55 (**6b**/**6a**). Analogously, an α-CH_2SiMe_3 group activates propene

by 3.5×10^6 (**5c**/**5a**) and styrene by only 8.7×10^3 (**1h**/**6a**); for the same reason, $OSiMe_3$ also activates propene 10^2 times more (**5d**/**5a** = 1.4×10^7) than styrene (**6d**/**6a** = 1.9×10^5).

Table 4.4. Comparison of Absolute (in M^{-1} s^{-1}) and Relative Rate Constants for the Reactions of Silyl Substituted Propenes (Number Columns 1–3) and Styrenes (Number Columns 4–6) with the *p*-Methoxy Substituted Benzhydrylium Ion **2d** in CH_2Cl_2 at 20 °C.

Nucleophiles	Propene Derivatives (R = Me)			Styrene Derivatives (R = Ph)		
		k_2 (**2d**)	k_{rel}		k_2 (**2d**)	k_{rel}
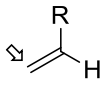	**5a**	0.51[a]	1	**6a**	5.3×10^2 [a]	1
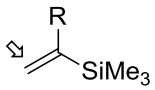	**1a**	4.9	9.6	**1d**	2.9×10^1	5.5×10^{-2}
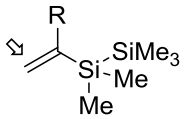	**1b**	5.4×10^1	1.1×10^2	**1f**	5.6×10^2 [b]	1.1
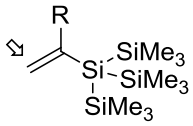	**1c**	6.4×10^1	1.3×10^2	–	–	–
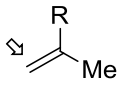	**5b**	1.6×10^3 [a]	3.1×10^3	**6b**	2.9×10^4 [c]	5.5×10^1
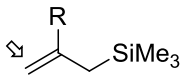	**5c**	1.8×10^6 [d]	3.5×10^6	**1h**	4.6×10^6 [b]	8.7×10^3
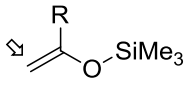	**5d**	7.0×10^6 [d]	1.4×10^7	**6d**	9.9×10^7 [d]	1.9×10^5

[a] Taken from ref [12b]. [b,d] Calculated by using Equation (4.1), E(**2d**) = 2.11 and the corresponding nucleophilicity parameters reported in: [b] Table 2; [d] ref [7a]. [c] Calculated by using the Eyring equation, k_2 (–70 °C) = 1.45×10^3 M^{-1} s^{-1} reported in ref [12b], and a value of $\Delta S^{\ddagger} = -110$ J mol^{-1} K^{-1} (estimated by taking activation parameters of structurally related compounds into account[7a,b]).

Perturbation of π-conjugation in α-substituted styrenes also explains why $SiMe_2SiMe_3$ activates by a factor of 10^2 in the propene series (**1b**/**5a**), but has no effect in the styrene series (**1f**/**6a**). The perturbation of the conjugation between vinyl and phenyl group by $SiMe_3$, CH_3, CH_2SiMe_3, and $OSiMe_3$ in α-position is also reflected by the UV spectra of the styrenes[14] listed in Table 4.6 of the Experimental Section.

In the propene as in the styrene series, the $SiMe_2SiMe_3$ group activates one order of magnitude more than the $SiMe_3$ group (**1b**/**1a** and **1f**/**1d**), while the supersilyl group[15] ($Si(SiMe_3)_3$) activates by the same extent as $SiMe_2SiMe_3$ (**1c**/**1b**), because only one Si-Si σ-bond of the $Si(SiMe_3)_3$ group can be aligned coplanar with the empty p-orbital of the developing carbenium center. The vinyl silanes **1b**, **1c**, and **1f** may thus be considered as sila-allylsilanes as illustrated in Figure 4.5.

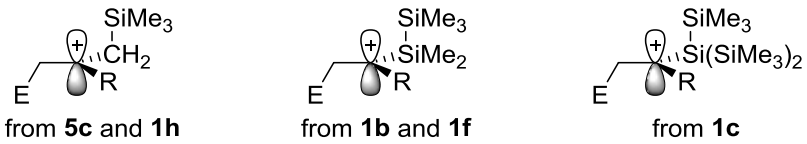

Figure 4.5. Comparison of β-silyl stabilization of the intermediate carbocations obtained by electrophilic attack at allylsilanes (left) and $SiMe_2SiMe_3$ (middle) as well as supersilyl (right) substituted vinylsilanes.

While an allylic $SiMe_3$ group activates isobutylene by 3 orders of magnitude (**5c**/**5b**), the introduction of an analogously positioned $SiMe_3$ group in **1a** accelerates only by one order of magnitude (**1b**/**1a**). Therefore, the hyperconjugative stabilization of a carbocation by a C-Si bond (Figure 4.5, left) is significantly larger than the hyperconjugative stabilization of a carbocation by a Si-Si bond (Figure 4.5, middle).

Nevertheless, replacement of the $SiMe_3$ group by the supersilyl group has an effect in the vinylsilane series, as **1c** is one order of magnitude more reactive than **1a**. In contrast, earlier work has shown that replacement of the $SiMe_3$ group by the supersilyl group $Si(SiMe_3)_3$ has almost no effect in allylsilanes and silylated enol ethers (Table 4.5) due to the fact that in these species the Si-Si bond is not in a suitable position for hyperconjugative interaction with the new carbenium center.[8b]

Table 4.5. Supersilyl Effects in Allylsilanes and Silyl Enol Ethers (Absolute and Relative Rate Constants Toward **2i** in CH_2Cl_2, 20 °C).[8b]

Nucleophiles	k_2 (R = $SiMe_3$) / M^{-1} s^{-1}	k_2 (R = Me) / M^{-1} s^{-1}	$\frac{k_2(Si(SiMe_3)_3)}{k_2(SiMe_3)}$
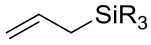	84.9[a]	46.9[a]	1.81[a]
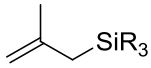	3.54	2.97	1.19
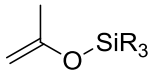	65.8	26.3[b]	2.50

[a] Toward **2g**. [b] Calculated by using Equation (4.1), N and s_N from ref [7a] and E(**2i**) = –3.85.

Soderquist and Hassner[6] reported that the silylated vinyl ether **7b** is deuterated only 1.8 times faster than the vinyl ether **7a**, while we found an activation by a factor of 9.6 when comparing the electrophilic alkylations of the analogous propene derivatives **1a** and **5a** with the benzhydrylium ion **2d** (Scheme 4.4). The diminished α-silyl effect observed for the vinyl ether **7b** may not only be due to the different electrophile considered but could also result from the smaller electron-demand of the alkoxy-substituted carbenium ion which is generated from vinyl ethers in the rate-determining step.

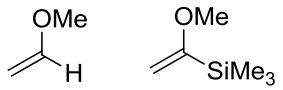

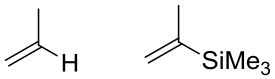

	7a	**7b**		**5a**	**1a**
k_{rel} (D^+)	1	1.8	k_{rel} (**2d**)	1	9.6

Scheme 4.4. Comparison of the relative rates for the deuterolyses of vinyl ethers **7a,b**[6] with the relative rates for the alkylation of the propene derivatives **5a** and **1a** with the benzhydrylium ion **2d**.

In contrast, Scheme 4.5 shows that the introduction of a 4-methyl substituent activates styrene for the reaction with benzhydrylium ion **2e** by a factor of 17 (**8**/**6a**), while a 4-methyl group activates the less reactive α-(trimethylsilyl)styrene by only 7.4 (**1e**/**1d**). This reduction of the electron-releasing effect of the 4-methyl substituent can again be rationalized by the perturbation of conjugation in α-substituted styrenes.

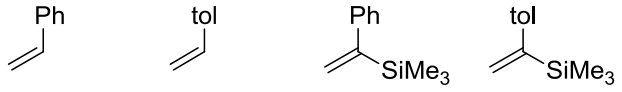

	6a	**8**	**1d**	**1e**
k_2 (**2e**)	1.5×10^2	2.6×10^3	3.8	28
k_{rel}	1	17	1	7.4

Scheme 4.5. Comparison of absolute (in M^{-1} s^{-1}) and relative rate constants for the reactions of 4-methyl substituted styrenes with the benzhydrylium ion **2e** in CH_2Cl_2 at 20 °C (tol = *p-tol*yl).[7a]

Vinylsilanes without electron donating substituents at C_α or with electron donors at C_β are usually attacked at C_α by electrophiles to give β-silyl stabilized carbenium ions. Despite this stabilization, **1g** reacts almost one order of magnitude more slowly with the benzhydrylium ion **2d** than styrene (Scheme 4.6). This retardation of the electrophilic attack can be explained by the steric shielding of the *ipso*-position and the fact that the hyperconjugative stabilization of the intermediate carbocation requires rotation around the former C=C bond and is obviously not yet effective in the transition state of electrophilic attack.

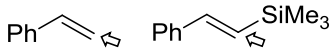

	6a	**1g**
k_2 (**2d**)	5.3×10^2	6.6×10^1
k_{rel}	1	0.12

Scheme 4.6. Absolute (in M^{-1} s^{-1}) and relative rate constants for the reactions of styrene (**6a**) and *trans*-β-(trimethylsilyl)styrene (**1g**) toward the *p*-methoxy substituted benzhydrylium ion **2d** in CH_2Cl_2 at 20 °C.[7a]

As shown in Scheme 4.7 the situation in vinylsilanes differs from that in allylsilanes, where the hyperconjugative β-silyl stabilization can already become effective in the transition state.

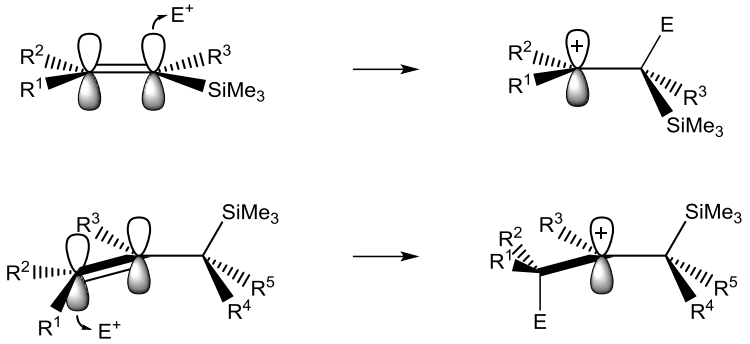

Scheme 4.7. Differences of the stereoelectronic effects in reactions of electrophiles with vinylsilanes (top) and allylsilanes (bottom).

Related silyl effects have previously been observed in the furan and thiophene series (Scheme 4.8).[16] Comparison of the first and third number column of Scheme 4.8 shows that a methyl group in 2-position increases the nucleophilicity by three orders of magnitude, similar to the isobutylene/propene (**5b**/**5a**) ratio (Table 4.4). From the almost equal reactivities of non-silylated and silylated compounds in columns 3 and 4 of Scheme 4.8, one can derive that in the heteroarene series the weak electronic activation of the silyl-substituted position is fully compensated by the steric retardation. The stereoelectronic arguments (Scheme 4.7, top) which explain the (even retarding) silyl effect in the comparison **1g**/**6a** (Scheme 4.6) apply analogously.

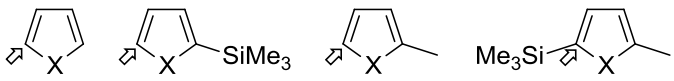

k_{rel} (X = O)[a]	1[b]	3.2×10^1	1.5×10^3	1.1×10^3
k_{rel} (X = S)[c]	1[b]	4.1	5.6×10^2	4.3×10^2

Scheme 4.8. Relative rate constants k_2 for the reactions of furan and thiophene derivatives toward benzhydrylium ions in CH_2Cl_2 at 20 °C ([a] towards the ferrocenylphenylcarbenium ion, [b] partial rate constant, [c] towards the bis(*p*-anisyl)carbenium ion **2g**).[16]

The weak activation of the 5-position in furan and thiophene by a 2-trimethylsilyl group (compare columns 1 and 2 in Scheme 4.8) is in the same order of magnitude as in the comparison **1a**/**5a** (Table 4.4), which also measures the effect of $SiMe_3$ in α-position of the resulting carbenium ion. As this activation is stronger than the *ipso*-activation, 2-(trimethylsilyl)furan and 2-(trimethylsilyl)thiophene react with electrophiles in 5- not in 2-

position, as indicated by the arrows in Scheme 4.8.[16] The substituent effects found in the vinylsilane series are, therefore, fully consistent with those previously observed in the furan and thiophene series.

4.3 Conclusion

The kinetic measurements reported in this article allow us to include vinylsilanes in our comprehensive nucleophilicity scale (Figure 4.6), which shows that vinylsilanes are significantly less reactive than structurally related allylsilanes.

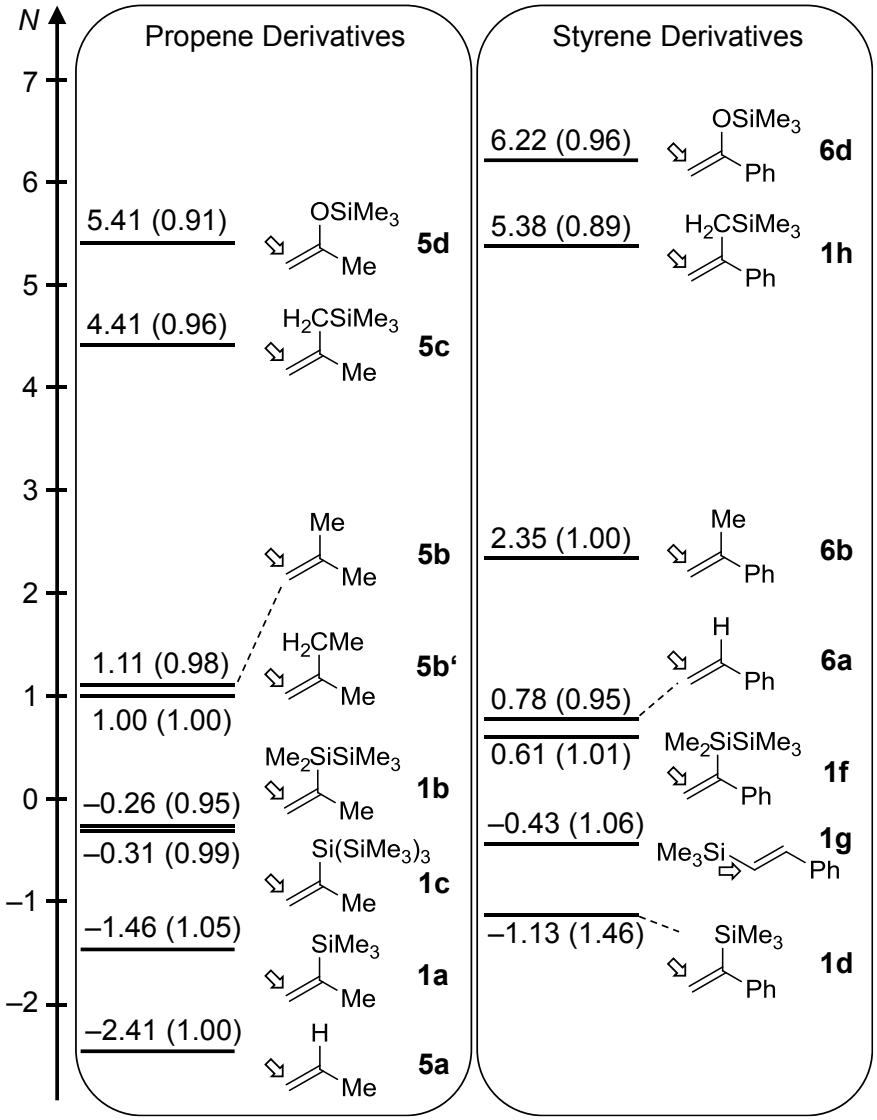

Figure 4.6. Nucleophilicities of propene (left) and styrene derivatives (right) compared to those of other π-nucleophiles[7b] (s_N values given in parentheses).

Scheme 4.9 compares the effects on nucleophilicity when allylic and vinylic hydrogens (marked by shaded circles) are replaced by different groups. Replacement of the marked allylic hydrogen in isobutylene by the trimethylsilyl or the supersilyl group activates the π-bond for electrophilic attack by a factor of 10^3 (Scheme 4.9A), which is explained by the well-known hyperconjugative stabilization of the intermediate carbenium ion by the C-Si σ-bond.[1,8a] The equal effects of $SiMe_3$ and $Si(SiMe_3)_3$ can be explained by the large separation of the developing carbenium center from the Si-Si bond. Replacement of the allylic hydrogen by an alkyl group has little effect on nucleophilicity due to the similar magnitude of C-H and C-C hyperconjugation.[12b]

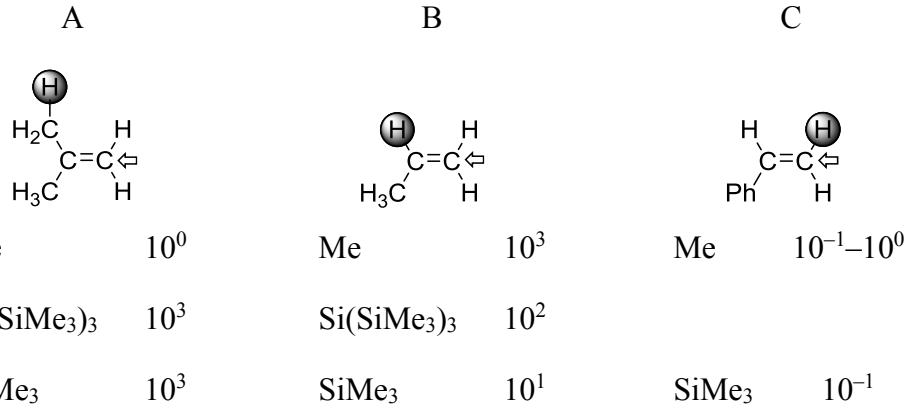

Scheme 4.9. Approximate changes of nucleophilicity due to replacement of the marked hydrogens by different groups.

Replacement of the marked vinylic hydrogen in propene by $SiMe_3$ activates by one order of magnitude showing that the stabilizing effect of silicon in α-position of the developing carbocation is significantly smaller than the effect of a methyl group (10^3, Scheme 4.9B). The larger effect of a supersilyl group at the developing carbenium center (10^2) can be explained by stabilization of the intermediate carbenium ion by Si-Si hyperconjugation, which prompted us to consider vinylsilanes incorporating the supersilyl group (or the $SiMe_2SiMe_3$ group) as sila-allylsilanes.

From the comparison of **5a** < **1a** < **1b** < **5b'** ≈ **5b** << **5c** in Figure 4.6 we can derive the following series of carbenium-stabilizing effects H < Si-C < Si-Si < C-C ≈ C-H << C-Si. At first glance, it may be surprising that the hyperconjugative stabilization of a carbenium center through a Si-C bond is so much weaker than that through a C-Si bond. One reason is the smaller overlap between the empty p-orbital with the Si-C bond than with the C-Si bond because of the

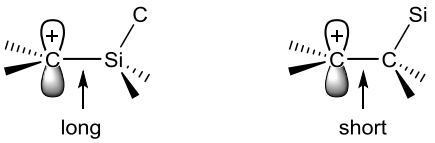

Scheme 4.10. Comparison between hyperconjugative stabilization of a carbenium center by a Si-C (left) and a C-Si (right) bond.

longer C^+-Si bond compared with the C^+-C bond (Scheme 4.10).[17] A second reason is the polarization of the carbon-silicon bond which is reflected by the larger AO coefficient at the carbon in a $\sigma_{C\text{-}Si}$ bond.

Whereas methyl groups in β-position of styrene have a weak activating or deactivating effect on the reactivity towards electrophiles,[13b] β-trimethylsilyl groups deactivate slightly (Scheme 4.9C) indicating that the steric retardation overcompensates the weak electronic activation, because the perpendicular orientation between developing carbenium center and the C-Si σ-bond inhibits significant hyperconjugative stabilization of the transition state of electrophilic attack. As a result, vinylsilanes are generally only slightly activated or deactivated compared to the corresponding alkenes, independent of the position of the silyl group in α- or β-position of the intermediate carbocation.

4.4 Experimental Section

4.4.1 General Methods

All reactions were performed in carefully dried Schlenk glassware in an atmosphere of dry nitrogen. The reactions were not optimized for high yields.

NMR spectra were recorded on Varian NMR instruments (300, 400 and 600 MHz). Chemical shifts are expressed in ppm and refer to $CDCl_3$ (δ_H: 7.26, δ_C: 77.16) and TMS (δ_H: 0.00, δ_C: 0.00) as internal standard. UV spectra for the data given in Table 4.6 were recorded at ambient temperature on a JASCO v630 spectrophotometer with 10 mm cuvette length. MS and HRMS were performed on a Finnigan MAT 95 instrument (EI). Melting points were determined on a Büchi B-540 and are not corrected.

Solvents. CH_2Cl_2 (*p.a.* grade) used for kinetic experiments was purchased from Merck and successively treated with concentrated sulfuric acid, water, 10% $NaHCO_3$ solution, and water. After drying with $CaCl_2$, it was freshly distilled over CaH_2 under exclusion of moisture (N_2 atmosphere).

Chemicals. $GaCl_3$, $TiCl_4$, $FeCl_3$ and BCl_3 were purchased and used as obtained. $SnCl_4$ was purchased and distilled prior to use. Ethereal $HBF_4 \cdot Et_2O$ was purchased from Aldrich. Tris(trimethylsilyl)silane was purchased (ABCR) or prepared by the reported methods.[18] Chlorotris(trimethylsilyl)silane was either purchased (Aldrich) or prepared by stirring tris(trimethylsilyl)silane in tetrachloromethane.[19]

Nucleophiles. The following compounds were prepared by following literature procedures: isopropenyltrimethylsilane (**1a**)[20], isopropenylpentamethyldisilane (**1b**)[21], trimethyl(1-phenylvinyl)silane (**1d**)[22], pentamethyl(1-phenylvinyl)disilane (**1f**)[23], (*E*)-(2-phenylvinyl)trimethylsilane (**1g**)[24], and (2-phenylallyl)trimethylsilane (**1h**)[25].

Reference Electrophiles. Procedures for the syntheses of benzhydryl chlorides[26] and benzhydrylium tetrafluoroborates **2h–j**[7a] were reported previously.

4.4.2 Synthesis of Vinylsilanes 1c and 1e

Isopropenyltris(trimethylsilyl)silane (**1c**)

In analogy to ref [21], dry THF (10 mL) was added to Mg turnings (0.46 g, 19 mmol) in a dried three-necked flask under nitrogen equipped with stirring bar and reflux condenser. A solution of 2-bromopropene (1.4 mL, 16 mmol) in dry THF (3 mL) was added dropwise and the resulting mixture was heated to reflux for 2h. The solution with the Grignard reagent was then transferred to a solution of chlorotris(trimethylsilyl)silane (3.0 g, 11 mmol) in dry THF (10 mL) in another dried three-necked flask under nitrogen equipped with stirring bar and reflux condenser. The resulting mixture was heated to reflux for 30 h before it was cooled to room temperature. After the addition of water (25 mL) and saturated aqueous NH_4Cl solution (10 mL) the layers were separated and the aqueous layer extracted with Et_2O (3 × 30 mL). The combined organic layers were dried over $MgSO_4$ before the solvent was removed. Recrystallization from MeCN furnished **1c** (2.8 g, 88%) as a colorless solid (mp 175.1–176.1 °C).

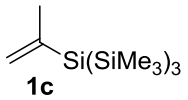

1c

^{1}H NMR (400 MHz, $CDCl_3$): δ = 0.20 (s, 27 H, $SiMe_3$), 1.90 (dd, ^4J = 1.7 Hz, ^4J = 1.2 Hz, 3 H, CH_3), 5.21 (dq, ^2J = 3.1 Hz, ^4J = 1.2 Hz, 1 H), 5.57 (dq, ^2J = 3.1 Hz, ^4J = 1.7 Hz, 1 H) ppm.

^{13}C NMR (101 MHz, $CDCl_3$): δ = 1.4 (q, $SiMe_3$), 28.6 (q, CH_3), 127.2 (t, CH_2), 143.0 (s, $\underline{C}$=CH_2) ppm.

^{29}Si NMR (79 MHz, $CDCl_3$) δ = –77.1 (s, $\underline{Si}(SiMe_3)_3$), –13.3 (s, $Si(\underline{Si}Me_3)_3$) ppm.

HR-MS (EI, pos.) *m*/*z* calcd. for $C_{12}H_{32}Si_4$ $[M]^+$ 288.1576, found 288.1573.

Trimethyl(1-(*p*-tolyl)vinyl)silane (**1e**) was prepared in analogy to ref [22b]. The analytical data matches the literature.[27]

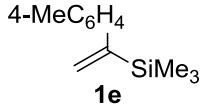

1e

^{1}H NMR (300 MHz, $CDCl_3$): δ = 0.18–0.20 (m, 9 H, $SiMe_3$), 2.36 (s, 3 H, CH_3), 5.59 (d, ^2J = 3.0 Hz, 1 H), 5.83 (d, ^2J = 3.0 Hz, 1 H), 7.07–7.16 (m, 4H) ppm.

^{13}C NMR (75 MHz, $CDCl_3$): δ = –0.7 (q, $SiMe_3$), 21.2 (q, CH_3), 126.7 (d, Ar), 126.8 (t, CH_2) 129.0 (d, Ar), 136.0 (s, $\underline{C}CH_3$), 141.9 (s, Ar), 153.3 (s, $\underline{C}SiMe_3$) ppm.

^{29}Si NMR (79 MHz, $CDCl_3$) δ = –4.5 ppm.

HR-MS (EI, pos.) *m*/*z* calcd. for $C_{12}H_{18}Si$ $[M]^+$ 190.1172, found 190.1174.

4.4.3 Products from the Reactions of Silanes 1a–h with Benzhydrylium Ions 2

Reaction of isopropenyltrimethylsilane (**1a**) with $(tol)_2CH^+TiCl_5^-$ (**2a-TiCl$_5$**)[10a]

This protocol is taken from the Ph.D. thesis of Gisela Hagen[10a]:

Under stirring, a solution of **2a-Cl** in dry dichloromethane was cooled to –78 °C and treated with $TiCl_4$. To the colored solution **1a** was added. After fading of the color, the same volume of concentrated aqueous ammonia was added and the layers were separated. The organic layer was dried over $CaCl_2$ before the solvent was removed.

The following NMR data was given for the mixture of the *E* and *Z* isomer (ratio not determined) and is in good agreement with related compounds found in the literature[28]:

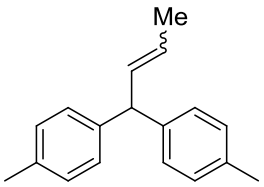

4a

^{1}H NMR (200 MHz, $CDCl_3$): δ = 1.73 (br d, J = 6.8 Hz, 3 H, 4-H), 2.32 (s, 6 H, $ArCH_3$), 4.61 and 4.97 (2 d, J = 8.2, J = 9.8, 1 H, 1-H), 5.46–5.93 (m, 2 H, 2-H and 3-H), 7.10–7.14 (m, 8 H, ArH) ppm.

Reaction of isopropenylpentamethyldisilane (**1b**) with $(ani)_2CH^+TiCl_5^-$ (**2g-TiCl$_5$**)

$TiCl_4$ (0.15 mL, 1.4 mmol) was added to a solution of benzhydryl chloride **2g-Cl** (0.27 g, 1.0 mmol) in dichloromethane (20 mL) at room temperature. After the addition of a solution of isopropenylpentamethyldisilane (**1b**, 0.30 g, 1.7 mmol) in dichloromethane (4 mL) the resulting mixture was stirred for 15 min and subsequently filtered through basic Al_2O_3 (Brockmann activity III, CH_2Cl_2). After removal of the solvent the crude product was purified by column chromatography (silica gel, pentane:Et_2O = 7:3) and gave **4b** (0.22 g, 53%) as a colorless oil. Signal assignments are based on additional gDQCOSY (^{1}H), gHSQCAD (^{1}H/^{13}C) and gHMBCAD (^{1}H/^{13}C) experiments.

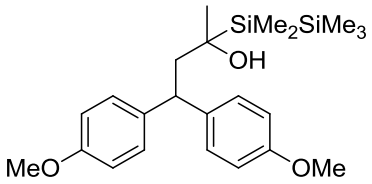

4b

^{1}H NMR (400 MHz, $CDCl_3$): δ = 0.08 (s, 9 H, $SiMe_3$), 0.16 (s, 3 H, Si<u>Me</u>Me$SiMe_3$), 0.19 (s, 3 H, SiMe<u>Me</u>$SiMe_3$), 0.83 (s, 3 H, CH_3), 1.46 (s, 1 H, OH), 2.34 (d, ^3J = 6.4 Hz, 2 H, CH_2), 3.75 (s, 3 H, OMe), 3.76 (s, 3 H, OMe), 4.15 (t, ^3J = 6.4 Hz, 1 H, CH), 6.79–6.84 (m, 4 H, Ar), 7.19–7.25 (m, 4 H) ppm.

^{13}C NMR (101 MHz, $CDCl_3$): δ = –1.3 (q, $SiMe_3$), 0.36, 0.38 (2q, $SiMe_2$), 15.4 (s, COH), 16.2 (q, CH_3), 39.2 (t, CH_2), 48.8 (d, CH), 55.3 (q, OMe), 114.00, 114.02 (2d, Ar), 128.3 (d, Ar), 128.4 (d, Ar), 139.4 (s, Ar), 139.8 (s, Ar), 157.77, 157.80 (2s, <u>C</u>OMe) ppm.

HR-MS (EI, pos.) *m*/*z* calcd. for $C_{23}H_{36}O_3Si_2$ $[M]^+$ 416.2197, found 416.2215.

Reaction of isopropenyltris(trimethylsilyl)silane (**1c**) with $(ani)_2CH^+BF_4^-$ (**2g-BF$_4$**)

Under argon atmosphere a solution of **1c** (0.18 g, 0.62 mmol) in dichloromethane (4 mL) was added to a solution of benzhydryl tetrafluoroborate **2g-BF$_4$** (0.15 g, 0.48 mmol) in dichloromethane (20 mL) at room temperature. The resulting mixture was stirred for 2 h before concentrated aqueous ammonia (24 mL) and water (10 mL) were added. The layers were separated and the aqueous layer was extracted with dichloromethane (3 × 30 mL). The combined organic layers were washed with brine (50 mL) and dried over $MgSO_4$. After removal of the solvent the crude product was purified by column chromatography (silica gel, pentane:Et_2O = 20:1) to give 0.21 g of a 6:1 mixture of **4c** (0.18 g, 70%) together with an unidentified isomer (30 mg, 12%; *m*/*z* = 534 $[M]^+$ for byproduct from GC-MS analysis of mixture). **4c** was obtained as a colorless solid after recrystallization from Et_2O/pentane; mp 96.5–97.1 °C. Signal assignments are based on additional gCOSY (^{1}H), gHSQC (^{1}H/^{13}C), gHMBCAD (^{1}H/^{13}C), gHMBC (^{19}F/^{13}C) and HMBC (^{1}H/^{29}Si) experiments.

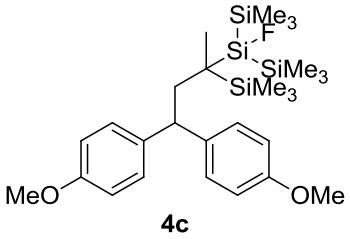

4c

^{1}H NMR (300 MHz, $CDCl_3$): δ = 0.09–0.13 (m, 9 H, CSi<u>Me</u>$_3$), 0.18–0.23 (m, 18 H, Si(Si<u>Me</u>$_3$)$_2$F), 0.98 (s, 3H, CCH_3), 2.41–2.59 (m, 2 H, CH_2), 3.74, 3.75 (2s, 2×3 H, OMe), 3.96–4.05 (m, 1 H, CH), 6.75–6.82 (m, 4 H, Ar), 7.14–7.23 (m, 4 H, Ar) ppm.

^{13}C NMR (75 MHz, $CDCl_3$): δ = –0.8 (dq, $^4J_{C\text{-}F}$ = 1.7 Hz, CSi<u>Me</u>$_3$), 0.5 (2dq, Si(Si<u>Me</u>$_3$)$_2$F), 18.6 (dq, $^3J_{C\text{-}F}$ = 1.7 Hz, CH_3), 21.3 (d, $^2J_{C\text{-}F}$ = 9.3 Hz, <u>C</u>SiMe$_3$), 39.6 (dt, $^3J_{C,F}$ = 2.6 Hz, CH_2), 49.6 (dd, $^4J_{C,F}$ = 2.0 Hz CH), 55.29, 55.31 (2q, OMe), 114.0 (2d, Ar), 128.1 (d, Ar), 128.2 (d, Ar), 139.8 (s, Ar), 140.1 (s, Ar), 157.7, 157.8 (2s, <u>C</u>OMe) ppm.

^{19}F NMR (282 MHz, $CDCl_3$): δ = –202.8 ppm.

^{29}Si NMR (79 MHz, $CDCl_3$) δ = –18.3 (d, $^2J_{Si\text{-}F}$ = 12.1 Hz, Si(<u>Si</u>Me$_3$)(SiMe$_3$)F), –18.0 (d, $^2J_{Si\text{-}F}$ = 12.3 Hz, Si(SiMe$_3$)(<u>Si</u>Me$_3$)F), 5.6 (d, $^3J_{Si\text{-}F}$ = 5.6 Hz, CSiMe$_3$), 43.8 (d, $^1J_{Si\text{-}F}$ = 333 Hz, <u>Si</u>(SiMe$_3$)$_2$F) ppm.

HR-MS (EI, pos.) *m*/*z* calcd. for $C_{27}H_{47}FO_2Si_4$ $[M]^+$ 534.2632, found 534.2623.

Reaction of trimethyl(1-phenylvinyl)silane (**1d**) with $(tol)_2CH^+GaCl_4^-$ (**2a-GaCl$_4$**) in the presence of 2,6-di-*tert*-butylpyridine

A mixture of benzhydryl chloride **2a-Cl** (0.15 g, 0.65 mmol) and 2,6-di-*tert*-butylpyridine (0.25 g, 1.3 mmol) in dichloromethane (20 mL) was cooled to –78 °C. Subsequent treatment with a solution of $GaCl_3$ (0.10 g, 0.57 mmol) in dichloromethane (2.0 mL) led to a yellow color of the mixture. When adding a solution of trimethyl(1-phenylvinyl)silane (**1d**, 0.17 g, 0.96 mmol) in dichloromethane (3 mL) the mixture turned immediately red, with the color fading after a few seconds. After 5 min the reaction mixture was warmed to room temperature with a water bath, followed by addition of aqueous ammonia (20 mL). The layers were separated and the aqueous layer was extracted with dichloromethane (3 × 25 mL). The combined organic layers were dried over $MgSO_4$ before the solvent was evaporated. The crude product was purified by column chromatography (silica gel, pentane) and gave a colorless oil from which **4d** was crystallized with ethanol as a colorless solid (0.11 g, 52%); mp 117.7–118.7 °C. Signal assignments are based on additional gCOSY (^{1}H), gHSQCAD (^{1}H/^{13}C), gHMBCAD (^{1}H/^{13}C) and NOESY (^{1}H) experiments.

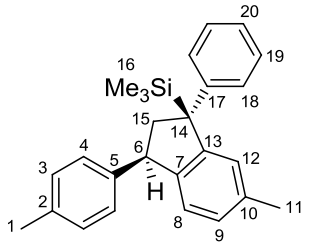

rac-**4d**

^{1}H NMR (400 MHz, $CDCl_3$): δ = 0.06–0.10 (m, 9 H, $SiMe_3$), 2.39 (s, 3 H, 1-H), 2.43 (m_C, 1 H, 15-H), 2.47 (s, 3 H, 11-H), 2.99 (dd, ^2J = 12.7 Hz, ^3J = 6.8 Hz, 1 H, 15-H), 4.14 (dd, ^3J = 11.0 Hz, ^3J = 6.8 Hz, 1 H, 6-H), 6.81 (d, ^3J = 7.7 Hz, 1 H, 8-H), 7.02 (d, ^3J = 7.7 Hz, 1 H, 9-H), 7.10–7.20 (m, 5 H, Ar), 7.24–7.32 (m, 5 H, Ar) ppm.

^{13}C NMR (101 MHz, $CDCl_3$): δ = -2.2 (q, $SiMe_3$), 21.2 (q, C-1), 21.8 (q, C-11), 47.1 (s, C-14), 48.9 (t, C-15), 49.0 (d, C-6), 124.8 (d, Ar), 125.1 (d, C-8), 126.9 (d, Ar), 127.3 (d, C-12), 127.4 (d, C-9), 128.1 (d, Ar), 128.4 (d, Ar), 129.3 (d, Ar), 135.5 (s, C-10), 136.1 (s, C-2), 142.0 (s, Ar), 144.86 (s, Ar), 144.92 (s, Ar), 148.2 (s, Ar) ppm.

HR-MS (EI, pos.) *m*/*z* calcd. for $C_{26}H_{30}Si$ $[M]^+$ 370.2111, found 370.2105.

Reaction of pentamethyl(1-phenylvinyl)disilane (**1f**) with $(tol)_2CH^+GaCl_4^-$ (**2a-GaCl$_4$**)

A solution of the benzhydryl chloride **2a-Cl** (0.12 g, 0.52 mmol) in dichloromethane (20 mL) was cooled to –78 °C. Subsequent treatment with a solution of $GaCl_3$ (90 mg, 0.51 mmol) in dichloromethane (3 mL) led to a yellow color of the mixture. A solution of pentamethyl(1-phenylvinyl)disilane (**1f**, 0.18 g, 0.77 mmol) in dichloromethane (4 mL) was added and the mixture stirred at –78 °C for 5 min before warming it to room temperature with a water bath. Aqueous ammonia (25 mL) was added and the aqueous layer was extracted with dichloromethane (3 × 30 mL). The combined organic layers were dried over $MgSO_4$ before the solvent was evaporated. The products were separated by column chromatography (silica gel, pentane:Et_2O = 10:1) to give 3,3-di-*p*-tolylpropiophenone[29] (**4f'**) as a colorless solid (58 mg, 36%, R_f = 0.31) and **4f** as a colorless oil (0.13 g, 57 %, R_f = 0.18). Signal assignments for **4f** are based on additional gCOSY (^{1}H), gHSQCAD (^{1}H/^{13}C) and gHMBCAD (^{1}H/^{13}C) experiments.

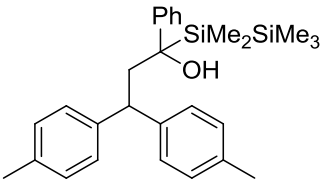

4f

^{1}H NMR (300 MHz, $CDCl_3$): δ = 0.03 (s, 9 H, $SiMe_3$), 0.08 (s, 3 H, SiMe<u>Me</u>$SiMe_3$), 0.27 (s, 3 H, Si<u>Me</u>$MeSiMe_3$), 1.30 (s, 1 H, OH), 2.26 (s, 3 H, CCH_3), 2.28 (s, 3 H, CCH_3), 2.96–3.12 (m, 2 H, CH_2, diastereotopic), 3.87–3.93 (m, 1 H, CH), 6.92–7.27 (m, 13 H, Ar) ppm.

^{13}C NMR (75 MHz, $CDCl_3$): δ = -0.7 (q, $SiMe_3$), 2.6, 3.4 (2q, $SiMe_2$), 21.1 (q, C<u>C</u>H_3), 33.9 (s, COH), 36.6 (t, CH_2), 49.5 (d, CH), 123.6 (d, Ar), 127.2 (d, Ar), 127.5 (d, Ar), 127.8 (d, Ar), 129.3 (d, Ar), 129.4 (d, Ar), 129.7 (d, Ar), 135.2 (s, <u>C</u>CH_3), 135.9 (s, <u>C</u>CH_3), 142.3 (s, Ar), 144.4 (s, Ar), 146.4 (s, Ar) ppm.

HR-MS (EI, pos.) *m*/*z* calcd. for $C_{28}H_{38}OSi_2$ $[M]^+$ 446.2456, found 446.2465.

Reaction of (*E*)-(2-phenylvinyl)trimethylsilane (**1g**) with (tol)(ani)$CH^+BCl_4^-$ (**2e-BCl_4**)[10b]

This protocol is taken from the Ph.D. thesis of Mirjam Herrlich[10b]:

A solution of the benzhydryl chloride **2e-Cl** (0.30 g, 1.2 mmol) in dry dichloromethane (20 mL) was cooled to 0 °C, before ionizing with gaseous BCl_3 (40 mL). After cooling to –40 °C, the colored reaction mixture was treated with 1.5 equivalents of **1g**. After fading of the color, the mixture was warmed to room temperature and treated with half-concentrated aqueous ammonia (20 mL). The layers were separated and the aqueous layer was extracted with dichloromethane (3 × 30 mL). The combined organic layers were dried over $MgSO_4$ before the solvent was removed. The crude product was purified by column chromatography (silica gel, pentane:Et_2O = 3:1) and gave **4g** as a yellow-orange oil (70%) with minor impurities. The NMR spectroscopic data is in good agreement with related compounds found in the literature[30]:

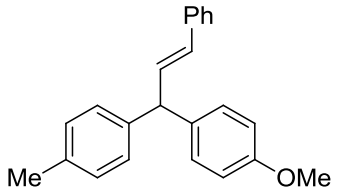

4g

^{1}H NMR (300 MHz, $CDCl_3$): δ = 2.32 (s, 3 H, CH_3), 3.77 (s, 3 H, OCH_3), 4.80 (d, ^3J = 7.4 Hz, 1 H, C<u>H</u>ArAr'), 6.31 (d, ^3J = 15.8 Hz, 1 H, RHC=C<u>H</u>Ph), 6.63 (dd, ^3J = 15.8 Hz, ^3J = 7.4 Hz, 1 H, R<u>H</u>C=CHPh), 6.79 – 6.87 (m, 2 H, ArH), 7.05–7.38 (m, 11 H, superimposed by solvent) ppm.

^{13}C NMR (75 MHz, $CDCl_3$): δ = 21.2 (q, CH_3), 53.1, 55.4 (d and q, <u>C</u>HArAr' and OCH_3), 114.0 (d, Ar), 126.4 (d, Ar), 127.3 (d, Ar), 128.6 (d, Ar), 128.8 (d, Ar), 129.3 (d, Ar), 129.7 (d, Ar), 131.1 (d, Ar), 133.3 (d, Ar), 136.0 (2s, Ar), 137.6 (s, Ar), 141.0 (s, Ar), 158.3 (s, <u>C</u>OCH_3) ppm.

HR-MS (EI, pos.) *m*/*z* calcd. for $C_{23}H_{22}O$ $[M]^+$ 314.1665, found 314.1656.

Reaction of (2-phenylallyl)trimethylsilane (**1h**) with $(dma)_2CH^+BF_4^-$

A solution of (2-phenylallyl)trimethylsilane (**1h**, 0.11 mg, 0.58 mmol) in dichloromethane (1 mL) was added to a solution of $(dma)_2CH^+BF_4^-$ (0.17 g, 0.50 mmol) in dichloromethane (20 mL) at room temperature. The resulting mixture was stirred for 4 h and subsequently filtered through basic Al_2O_3 (Brockmann activity III, CH_2Cl_2). Removal of the solvent gave a oil from which **4h** was crystallized with Et_2O/pentane to give a colorless solid (0.16 mg, 86%); mp 79.7–80.7 °C. Signal assignments are based on additional gCOSY (^1H), gHSQC ($^1H/^{13}C$) and gHMBCAD ($^1H/^{13}C$) experiments.

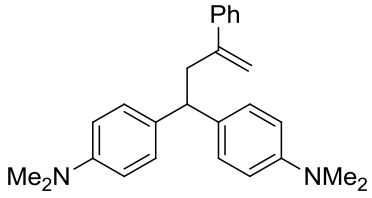

4h

^{1}H NMR (300 MHz, $CDCl_3$): δ = 2.88 (s, 12 H, NMe_2), 3.17 (d, ^3J = 7.6 Hz, 2 H, $CHCH_2$), 3.92 (t, ^3J = 7.6 Hz, 1 H, CH), 4.85 (s, 1 H, C=CHH), 5.14 (s, 1 H, C=CHH), 6.64 (d, ^3J = 8.7 Hz, 4 H, Ar), 7.03 (d, ^3J = 8.7 Hz, 4 H, Ar), 7.21 – 7.38 (m, 5 H, Ph) ppm.

^{13}C NMR (75 MHz, $CDCl_3$): δ = 40.9 (q, NMe_2), 42.2 (t, $CHCH_2$), 47.3 (d, CH), 112.9 (d, Ar), 114.7 (t, $C=CH_2$), 126.6 (d, Ph), 127.3 (d, Ph), 128.3 (d, Ph), 128.6 (d, Ar), 133.8 (s, Ar), 141.6 (s, $C=CH_2$), 146.9 (s, Ph), 149.0 (s, $CNMe_2$).

HR-MS (EI, pos.) *m*/*z* calcd. for $C_{26}H_{30}N_2$ $[M]^+$ 370.2404, found 370.2410.

4.4.4 UV Data

Experimental evidence for the non-planar structures of α-substituted styrenes has been found in their UV absorption spectra in hexane solutions.[14c] Table 4.6 gives the absorption maxima and the corresponding molar absorption coefficients determined in dichloromethane and ethanol. It has already been shown by Suzuki[14a,b] that the introduction of alkyl substituents in *p*- and *trans*-β-positions led to batho- and hyperchromic effects in the absorption spectra, as can also be seen in Table 4.6 by comparing styrene (**6a**) to *p*-methylstyrene (**8**). The opposite trends (*i.e.* hypso- and hypochromic effects) were reported for the absorption spectra when *o*-, α- and/or *cis*-β-hydrogens of styrene were exchanged for alkyl groups (comparison **6a**/**6b** in Table 4.6).[14a,b]

Similar to alkylations, batho- and hyperchromic effects were observed[31] when silyl groups were introduced in positions that do not disturb the coplanarity of the conjugated π-system (comparison **6a**/**1g**). Thus, the hypso- and hypochromic effects found for the silyl substituted styrene derivatives **1d,f,h** when compared to parental styrene (**6a**) and for silylated compound **1e** compared to *p*-methylstyrene (**8**) indicate twists between the phenyl and vinyl planes in the ground states of these silylated derivatives.

Table 4.6. UV-Absorption Maxima and Corresponding Molar Absorption Coefficients for Styrene Derivatives in Dichloromethane and Ethanol.

	λ_{max} [nm] in CH_2Cl_2 ($\log \varepsilon_{max}$)	λ_{max} [nm] in ethanol ($\log \varepsilon_{max}$)
 **6a**	249.4 (4.25)	247.8 (4.23)
 **8**	253.6 (4.31)	251.6 (4.32)
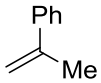 **6b**	245.4 (4.07)	243.0 (4.08)
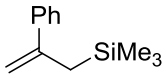 **1h**	248.4 (3.92)	245.0 (3.93)
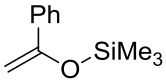 **6d**	255.8 (3.99)	252.8 (4.00)
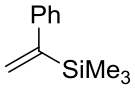 **1d**	240.2 (3.95)	238.0 (3.86)
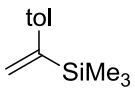 **1e**	247.6 (3.96)	245.4 (3.94)
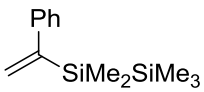 **1f**	no distinct maximum, due to overlap	238.2 (3.92)
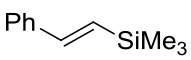 **1g**	259.4 (4.34)	257.8 (4.35)

4.4.5 Kinetic Experiments

The kinetics of the reactions with highly reactive electrophiles **2a,b** and the combination of **1e** with **2d-GaCl$_4$** were determined via the method described previously.[13a] The rates of the reactions studied at 20 °C were determined by using a J&M TIDAS diode array spectrophotometer controlled by Labcontrol Spectacle Software and connected to a Hellma 661.502-QX quartz Suprasil immersion probe (5 mm light path) via fibre optic cables and standard SMA connectors.

Stock solutions of the nucleophiles, benzhydryl chlorides **2(a–g)–Cl**, benzhydryl tetrafluoroborates **2(g–j)–BF$_4$** and Lewis acids were prepared by dissolving the compounds in dichloromethane. The flame-dried Schlenk flasks with nitrogen atmosphere were filled with approximately 25 mL of solvent. The exact solvent quantity was determined by weighing. Then, this flask was submerged into a circulating ethanol bath with a constant temperature, followed by the equipment with the Hellma probe or the quartz rods and a digital thermometer (for temperatures below 20 °C). When a constant temperature was reached a well-defined amount of the benzhydryl chloride or tetrafluoroborate stock solution was added via a gas-tight syringe. Benzhydryl chlorides were ionized to the corresponding benzhydrylium ions by the subsequent addition of an excess of a Lewis acid stock solution ($GaCl_3$ in most cases). After addition of a well-defined amount of the nucleophile stock solution, the decay of the absorbance in dependence of the recording time was monitored. All the concentrations given are those at the actual operating temperatures, calculated via the polynomial expansion equation given in ref [32].

Kinetics for the Reactions of Isopropenyltrimethylsilane (**1a**) with **2a–e**

Rate constants for the reactions of **1a** with $(tol)_2CH^+GaCl_4^-$ (**2a–GaCl4**) in CH_2Cl_2 (λ = 477 nm).

T / °C	[**1a**]$_0$ / M	[**2a–Cl**]$_0$ / M	[$GaCl_3$]$_0$ / M	[**1a**]$_0$/[**2a**]$_0$	k_{obs} / s^{-1}	k_2 / M^{-1} s^{-1} [a]
–70.5	1.00×10^{-3}	2.18×10^{-5}	1.96×10^{-3}	46	1.33×10^{-3}	1.34
–61.0	8.67×10^{-4}	2.14×10^{-5}	1.93×10^{-3}	41	2.42×10^{-3}	2.83
–50.7	7.48×10^{-4}	2.14×10^{-5}	1.93×10^{-3}	35	4.33×10^{-3}	5.87
–40.5	6.12×10^{-4}	2.08×10^{-5}	2.36×10^{-3}	29	6.68×10^{-3}	11.1
–30.1	4.91×10^{-4}	2.05×10^{-5}	2.17×10^{-3}	24	1.00×10^{-2}	20.8

[a] Calculated from $k_2 = k_{obs}/([\mathbf{1a}]_0 - 0.5[\mathbf{2a}]_0)$.

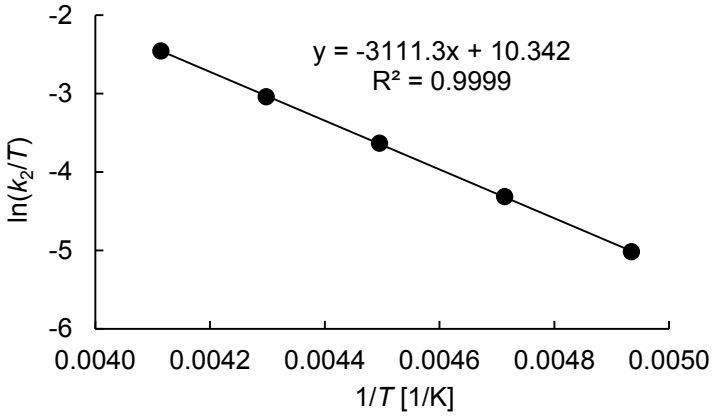

Eyring correlation for the reaction of **2a–GaCl4** with **1a**.

Eyring-parameter:

$\Delta H^{\ddagger}$ = (25.9 ± 0.1) kJ mol^{-1}

$\Delta S^{\ddagger}$ = (–111.6 ± 0.6) J mol^{-1} K^{-1}

Coefficient of correlation: 0.9999

Arrhenius-parameter:

E_A = (27.7 ± 0.1) kJ mol^{-1}

ln A = 16.7 ± 0.1

Coefficient of correlation: 0.9999

k_2 (20 °C) = 2.23×10^2 M^{-1} s^{-1}

Rate constants for the reactions of **1a** with (Ph)(pop)$CH^+GaCl_4^-$ (**2b–GaCl$_4$**) in CH_2Cl_2 (λ = 478 nm).

T / °C	[**1a**]$_0$ / M	[**2b–Cl**]$_0$ / M	[$GaCl_3$]$_0$ / M	[**1a**]$_0$/[**2b**]$_0$	k_{obs} / s^{-1}	k_2 / M^{-1} s^{-1} [a]
–70.6	6.27×10^{-3}	3.63×10^{-5}	1.12×10^{-3}	173	8.13×10^{-4}	1.30×10^{-1}
–60.5	6.73×10^{-3}	3.54×10^{-5}	1.08×10^{-3}	190	2.66×10^{-3}	3.96×10^{-1}
–50.8	5.51×10^{-3}	3.54×10^{-5}	1.14×10^{-3}	156	3.57×10^{-3}	6.50×10^{-1}
–40.3	4.20×10^{-3}	3.47×10^{-5}	1.38×10^{-3}	121	5.97×10^{-3}	1.43
–29.8	4.11×10^{-3}	3.39×10^{-5}	1.27×10^{-3}	121	1.04×10^{-2}	2.54
–20.1	3.50×10^{-3}	3.37×10^{-5}	1.17×10^{-3}	104	1.54×10^{-2}	4.42

[a] Calculated from $k_2 = k_{obs}/([\mathbf{1a}]_0 - 0.5[\mathbf{2b}]_0)$.

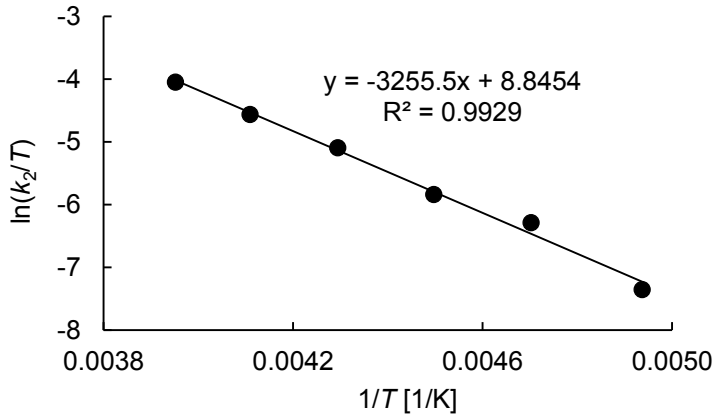

Eyring correlation for the reaction of **2b**–**GaCl$_4$** with **1a**.

Eyring-parameter:

$\Delta H^{\ddagger}$ = (27.1 ± 1.1) kJ mol^{-1}

$\Delta S^{\ddagger}$ = (–124.0 ± 5.1) J mol^{-1} K^{-1}

Coefficient of correlation: 0.9929

Arrhenius-parameter:

E_A = (28.9 ± 1.1) kJ mol^{-1}

ln A = 15.3 ± 0.6

Coefficient of correlation: 0.9939

k_2 (20 °C) = 3.06×10^1 M^{-1} s^{-1}

Rate constants for the reactions of **1a** with (tol)(pop)$CH^+GaCl_4^-$ (**2c–GaCl$_4$**) in CH_2Cl_2 (20 °C, λ = 495 nm).

[**1a**]$_0$ / M	[**2c–Cl**]$_0$ / M	[$GaCl_3$]$_0$ / M	[**1a**]$_0$/[**2c**]$_0$	k_{obs} / s^{-1}
4.61×10^{-4}	2.23×10^{-5}	1.08×10^{-4}	21	1.71×10^{-3}
8.98×10^{-4}	2.23×10^{-5}	9.85×10^{-5}	40	3.42×10^{-3}
1.31×10^{-3}	2.20×10^{-5}	1.07×10^{-4}	60	5.29×10^{-3}
1.75×10^{-3}	2.18×10^{-5}	9.94×10^{-5}	80	6.97×10^{-3}
2.15×10^{-3}	2.16×10^{-5}	9.52×10^{-5}	100	8.99×10^{-3}

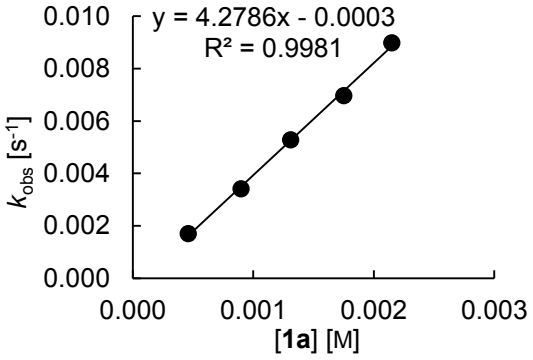

k_2 (20 °C) = 4.28 M^{-1} s^{-1}

Rate constants for the reactions of **1a** with (Ph)(ani)$CH^+GaCl_4^-$ (**2d–GaCl$_4$**) in CH_2Cl_2 (20 °C, λ = 469 nm).

[**1a**]$_0$ / M	[**2d–Cl**]$_0$ / M	[$GaCl_3$]$_0$ / M	[**1a**]$_0$/[**2d**]$_0$	k_{obs} / s^{-1}
5.54×10^{-4}	2.82×10^{-5}	2.49×10^{-4}	20	2.05×10^{-3}
1.11×10^{-3}	2.84×10^{-5}	1.93×10^{-4}	39	4.43×10^{-3}
1.66×10^{-3}	2.81×10^{-5}	2.12×10^{-4}	59	6.78×10^{-3}
2.21×10^{-3}	2.81×10^{-5}	1.95×10^{-4}	79	9.69×10^{-3}
2.74×10^{-3}	2.79×10^{-5}	2.11×10^{-4}	98	1.28×10^{-2}

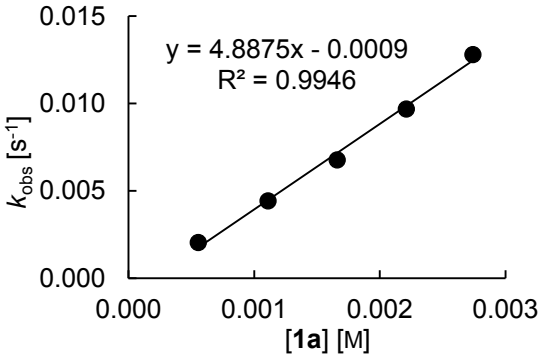

k_2 **(20 °C) = 4.89 M^{-1} s^{-1}**

Rate constants for the reactions of **1a** with (tol)(ani)CH$^+$GaCl$_4^-$ (**2e–GaCl$_4$**) in CH_2Cl_2 (20 °C, λ = 488 nm).

[**1a**]$_0$ / M	[**2e–Cl**]$_0$ / M	[$GaCl_3$]$_0$ / M	[**1a**]$_0$/[**2e**]$_0$	k_{obs} / s^{-1}
2.09×10^{-3}	2.08×10^{-5}	1.07×10^{-4}	100	2.72×10^{-3}
2.50×10^{-3}	2.07×10^{-5}	8.06×10^{-5}	121	3.01×10^{-3}
3.28×10^{-3}	2.06×10^{-5}	6.43×10^{-5}	159	4.13×10^{-3}
3.71×10^{-3}	2.06×10^{-5}	5.79×10^{-5}	180	4.75×10^{-3}
4.08×10^{-3}	2.04×10^{-5}	5.40×10^{-5}	200	5.21×10^{-3}

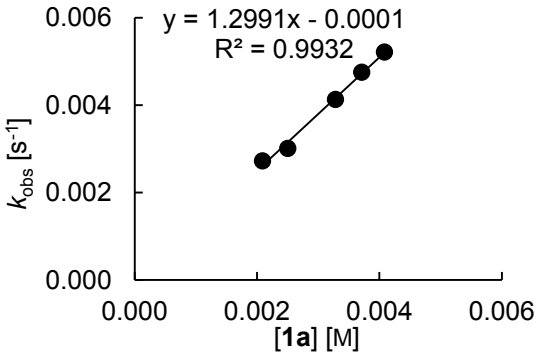

k_2 **(20 °C) = 1.30 M^{-1} s^{-1}**

Kinetics for the Reactions of Isopropenylpentamethyldisilane (**1b**) with **2d,e,g**

Rate constants for the reactions of **1b** with (Ph)(ani)$CH^+GaCl_4^-$ (**2d–GaCl$_4$**) in CH_2Cl_2 (20 °C, λ = 469 nm).

[**1b**]$_0$ / M	[**2d–Cl**]$_0$ / M	[$GaCl_3$]$_0$ / M	[**1b**]$_0$/[**2d**]$_0$	k_{obs} / s^{-1}
3.78×10^{-4}	3.83×10^{-5}	1.93×10^{-4}	9.9	1.36×10^{-2}
4.65×10^{-4}	3.81×10^{-5}	1.88×10^{-4}	12	1.83×10^{-2}
5.48×10^{-4}	3.77×10^{-5}	2.01×10^{-4}	15	2.27×10^{-2}
6.40×10^{-4}	3.79×10^{-5}	2.04×10^{-4}	17	2.90×10^{-2}
7.29×10^{-4}	3.80×10^{-5}	2.19×10^{-4}	19	3.18×10^{-2}

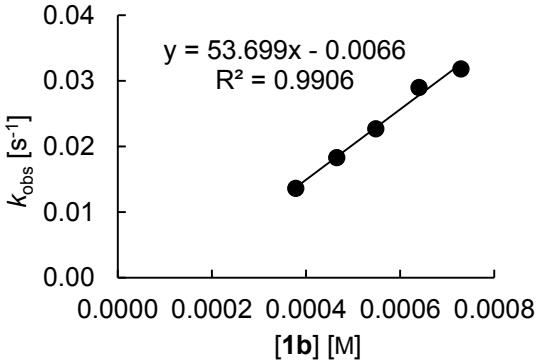

k_2 (20 °C) = 5.37 × 10^1 M^{-1} s^{-1}

Rate constants for the reactions of **1b** with (Ph)(ani)$CH^+SnCl_5^-$ (**2d–SnCl$_5$**) in CH_2Cl_2 (20 °C, λ = 469 nm).

[**1b**]$_0$ / M	[**2d–Cl**]$_0$ / M	[$SnCl_4$]$_0$ / M	[**1b**]$_0$/[**2d**]$_0$	k_{obs} / s^{-1}
3.26×10^{-4}	3.28×10^{-5}	2.02×10^{-2}	9.9	1.26×10^{-2}
4.62×10^{-4}	3.78×10^{-5}	2.85×10^{-2}	12	1.89×10^{-2}
5.53×10^{-4}	3.81×10^{-5}	2.88×10^{-2}	15	2.27×10^{-2}
6.41×10^{-4}	3.82×10^{-5}	2.88×10^{-2}	17	2.65×10^{-2}
7.29×10^{-4}	3.82×10^{-5}	2.88×10^{-2}	19	3.06×10^{-2}
8.18×10^{-4}	3.83×10^{-5}	2.89×10^{-2}	21	3.56×10^{-2}

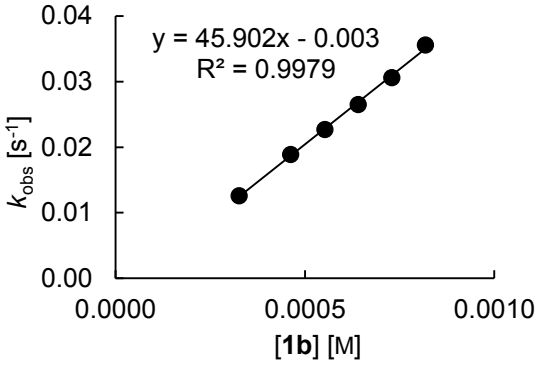

k_2 **(20 °C) = 4.59 × 10^1 M^{-1} s^{-1}**

Rate constants for the reactions of **1b** with (Ph)(ani)CH$^+$FeCl$_4^-$ (**2d–FeCl$_4$**) in CH_2Cl_2 (20 °C, λ = 469 nm). A saturated solution of $FeCl_3$ in CH_2Cl_2 was used for the ionization of **2d–Cl**.

[**1b**]$_0$ / M	[**2d–Cl**]$_0$ / M	[**1b**]$_0$/[**2d**]$_0$	k_{obs} / s^{-1}
4.30×10^{-4}	3.68×10^{-5}	12	2.35×10^{-2}
4.91×10^{-4}	3.61×10^{-5}	14	2.60×10^{-2}
5.61×10^{-4}	3.60×10^{-5}	16	3.05×10^{-2}
6.37×10^{-4}	3.64×10^{-5}	18	3.49×10^{-2}
7.01×10^{-4}	3.61×10^{-5}	19	3.87×10^{-2}

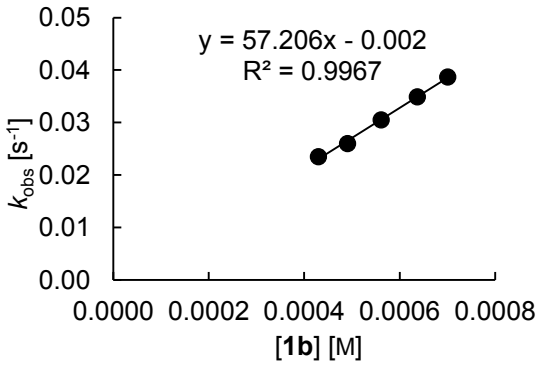

k_2 **(20 °C) = 5.72 × 10^1 M^{-1} s^{-1}**

Rate constants for the reactions of **1b** with (tol)(ani)$CH^+GaCl_4^-$ (**2e–GaCl$_4$**) in CH_2Cl_2 (20 °C, λ = 488 nm).

[**1b**]$_0$ / M	[**2e–Cl**]$_0$ / M	[$GaCl_3$]$_0$ / M	[**1b**]$_0$/[**2e**]$_0$	k_{obs} / s^{-1}
2.69×10^{-4}	2.64×10^{-5}	8.17×10^{-5}	10	3.60×10^{-3}
3.35×10^{-4}	2.63×10^{-5}	8.34×10^{-5}	13	4.67×10^{-3}
4.01×10^{-4}	2.62×10^{-5}	7.32×10^{-5}	15	5.62×10^{-3}
4.66×10^{-4}	2.61×10^{-5}	6.71×10^{-5}	18	6.62×10^{-3}
5.34×10^{-4}	2.62×10^{-5}	6.73×10^{-5}	20	7.66×10^{-3}

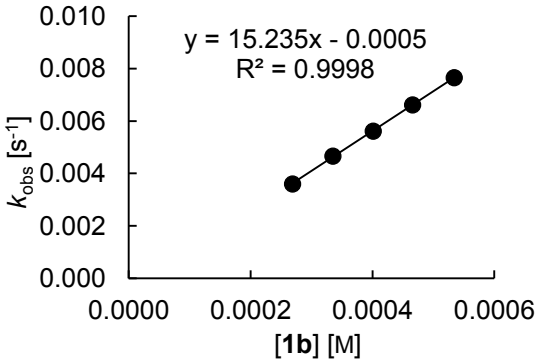

k_2 **(20 °C) = 1.52 × 10^1 M^{-1} s^{-1}**

Rate constants for the reactions of **1b** with $(ani)_2CH^+GaCl_4^-$ (**2g–GaCl$_4$**) in CH_2Cl_2 (20 °C, λ = 513 nm).

[**1b**]$_0$ / M	[**2g–Cl**]$_0$ / M	[$GaCl_3$]$_0$ / M	[**1b**]$_0$/[**2g**]$_0$	k_{obs} / s^{-1}
3.12×10^{-3}	1.83×10^{-5}	3.44×10^{-5}	170	2.00×10^{-3}
3.29×10^{-3}	1.83×10^{-5}	3.65×10^{-5}	180	2.09×10^{-3}
3.44×10^{-3}	1.81×10^{-5}	5.33×10^{-5}	190	2.17×10^{-3}
3.64×10^{-3}	1.82×10^{-5}	3.86×10^{-5}	200	2.29×10^{-3}

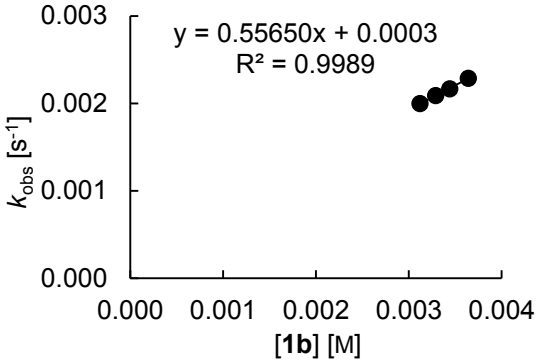

k_2 **(20 °C) = 5.57 × 10^{-1} M^{-1} s^{-1}**

Kinetics for the Reactions of Isopropenyltris(trimethylsilyl)silane (**1c**) with **2d,e,g**

Rate constants for the reactions of **1c** with (Ph)(ani)CH$^+$GaCl$_4^-$ (**2d–GaCl$_4$**) in CH_2Cl_2 (20 °C, λ = 469 nm).

[**1c**]$_0$ / M	[**2d–Cl**]$_0$ / M	[$GaCl_3$]$_0$ / M	[**1c**]$_0$/[**2d**]$_0$	k_{obs} / s^{-1}
4.09 × 10^{-4}	4.04 × 10^{-5}	2.84 × 10^{-4}	10	1.51 × 10^{-2}
4.82 × 10^{-4}	4.00 × 10^{-5}	3.48 × 10^{-4}	12	1.98 × 10^{-2}
5.57 × 10^{-4}	3.97 × 10^{-5}	2.86 × 10^{-4}	14	2.33 × 10^{-2}
6.38 × 10^{-4}	4.00 × 10^{-5}	1.67 × 10^{-4}	16	3.05 × 10^{-2}
7.13 × 10^{-4}	3.98 × 10^{-5}	1.54 × 10^{-4}	18	3.40 × 10^{-2}

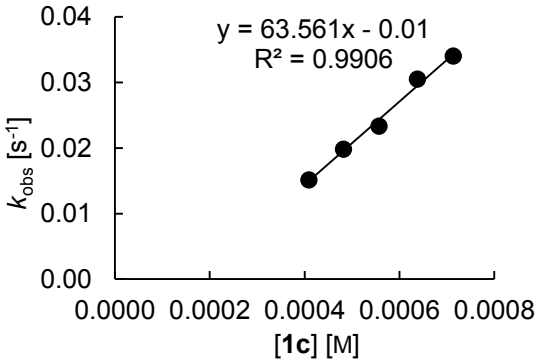

k_2 **(20 °C) = 6.36 × 10^{1} M^{-1} s^{-1}**

Rate constants for the reactions of **1c** with (tol)(ani)$CH^+GaCl_4^-$ (**2e–GaCl$_4$**) in CH_2Cl_2 (20 °C, λ = 488 nm).

[**1c**]$_0$ / M	[**2e–Cl**]$_0$ / M	[$GaCl_3$]$_0$ / M	[**1c**]$_0$/[**2e**]$_0$	k_{obs} / s^{-1}
2.42×10^{-4}	2.43×10^{-5}	1.13×10^{-4}	10	3.30×10^{-3}
3.18×10^{-4}	2.43×10^{-5}	7.83×10^{-5}	13	4.01×10^{-3}
3.94×10^{-4}	2.43×10^{-5}	7.83×10^{-5}	16	5.09×10^{-3}
4.66×10^{-4}	2.42×10^{-5}	5.62×10^{-5}	19	6.23×10^{-3}
5.38×10^{-4}	2.40×10^{-5}	5.59×10^{-5}	22	7.24×10^{-3}

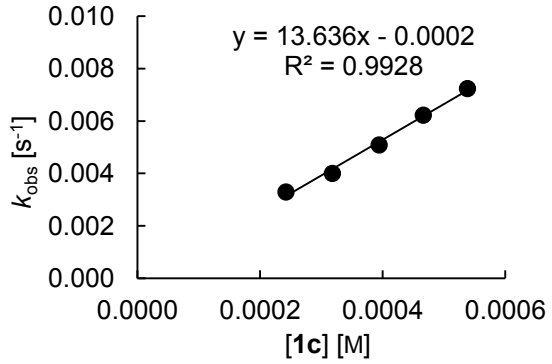

k_2 (20 °C) = 1.36 × 10^1 M^{-1} s^{-1}

Rate constants for the reactions of **1c** with $(ani)_2CH^+GaCl_4^-$ (**2g–GaCl$_4$**) in CH_2Cl_2 (20 °C, λ = 513 nm).

[**1c**]$_0$ / M	[**2g–Cl**]$_0$ / M	[$GaCl_3$]$_0$ / M	[**1c**]$_0$/[**2g**]$_0$	k_{obs} / s^{-1}
2.10×10^{-4}	1.94×10^{-5}	4.72×10^{-5}	11	1.00×10^{-4}
4.36×10^{-4}	1.97×10^{-5}	4.62×10^{-5}	22	2.10×10^{-4}
6.20×10^{-4}	1.88×10^{-5}	6.25×10^{-5}	33	3.14×10^{-4}
8.47×10^{-4}	1.92×10^{-5}	3.74×10^{-5}	44	4.20×10^{-4}

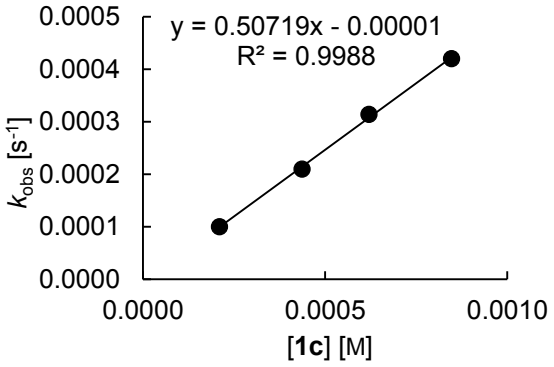

k_2 (20 °C) = 5.07 × 10^{-1} M^{-1} s^{-1}

Kinetics for the Reactions of Trimethyl(1-phenylvinyl)silane (**1d**) with **2a,b,d–f**

Rate constants for the reactions of **1d** with $(tol)_2CH^+GaCl_4^-$ (**2a–GaCl$_4$**) in CH_2Cl_2 (λ = 476 nm).

T / °C	[**1d**]$_0$ / M	[**2a–Cl**]$_0$ / M	[$GaCl_3$]$_0$ / M	[**1d**]$_0$/[**2a**]$_0$	k_{obs} / s^{-1}	k_2 / M^{-1} s^{-1} [a]
–72.3	4.23×10^{-4}	2.10×10^{-5}	1.28×10^{-3}	20	5.48×10^{-2}	133
–67.3	3.75×10^{-4}	2.07×10^{-5}	1.30×10^{-3}	18	6.49×10^{-2}	178
–62.6	3.32×10^{-4}	2.06×10^{-5}	1.28×10^{-3}	16	7.11×10^{-2}	221
–57.5	2.90×10^{-4}	2.06×10^{-5}	1.35×10^{-3}	14	7.86×10^{-2}	281
–52.7	2.48×10^{-4}	2.06×10^{-5}	1.34×10^{-3}	12	8.35×10^{-2}	351
–47.5	2.43×10^{-4}	2.01×10^{-5}	1.48×10^{-3}	12	1.01×10^{-1}	434

[a] Calculated from $k_2 = k_{obs}/([\mathbf{1d}]_0 - 0.5[\mathbf{2a}]_0)$.

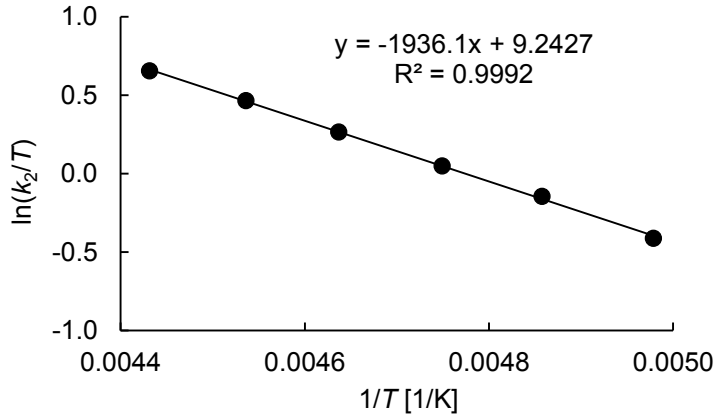

Eyring correlation for the reaction of **2a**–**GaCl$_4$** with **1d**.

Eyring-parameter:

$\Delta H^{\ddagger}$ = (16.1 ± 0.2) kJ mol^{-1}

$\Delta S^{\ddagger}$ = (–120.7 ± 1.1) J mol^{-1} K^{-1}

Coefficient of correlation: 0.9992

Arrhenius-parameter:

E_A = (17.9 ± 0.2) kJ mol^{-1}

ln A = 15.6 ± 0.1

Coefficient of correlation: 0.9994

k_2 (20 °C) = 4.10×10^3 M^{-1} s^{-1}

Rate constants for the reactions of **1d** with (Ph)(pop)$CH^+GaCl_4^-$ (**2b–GaCl$_4$**) in CH_2Cl_2 (λ = 478 nm).

T / °C	[**1d**]$_0$ / M	[**2b–Cl**]$_0$ / M	[$GaCl_3$]$_0$ / M	[**1d**]$_0$/[**2b**]$_0$	k_{obs} / s^{-1}	k_2 / M^{-1} s^{-1} [a]
–69.4	1.93×10^{-3}	3.32×10^{-5}	1.31×10^{-3}	58	2.64×10^{-2}	13.8
–60.0	3.77×10^{-4}	3.23×10^{-5}	1.53×10^{-3}	12	7.79×10^{-3}	21.6
–50.4	5.24×10^{-4}	3.21×10^{-5}	1.59×10^{-3}	16	1.77×10^{-2}	34.8
–40.4	4.42×10^{-4}	3.16×10^{-5}	1.60×10^{-3}	14	2.27×10^{-2}	53.3
–29.8	2.91×10^{-4}	3.12×10^{-5}	1.27×10^{-3}	9.3	2.26×10^{-2}	82.1

[a] Calculated from $k_2 = k_{obs}/([\mathbf{1d}]_0 - 0.5[\mathbf{2b}]_0)$.

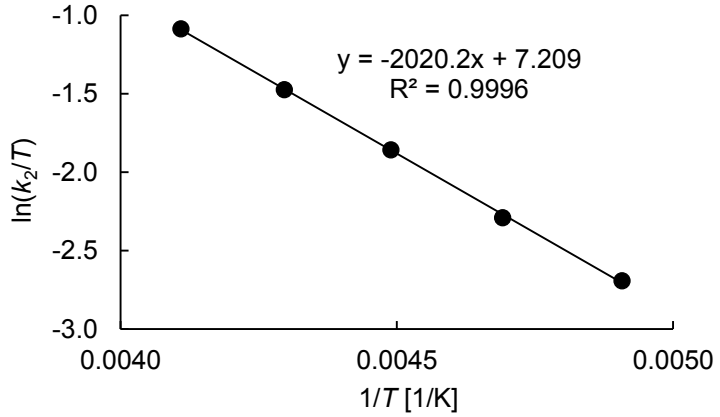

Eyring correlation for the reaction of **2b–GaCl$_4$** with **1d**.

Eyring-parameter:

$\Delta H^{\ddagger} = (16.8 \pm 0.2)$ kJ mol^{-1}

$\Delta S^{\ddagger} = (-137.6 \pm 0.9)$ J mol^{-1} K^{-1}

Coefficient of correlation: 0.9996

Arrhenius-parameter:

$E_A = (18.6 \pm 0.2)$ kJ mol^{-1}

$\ln A = 13.6 \pm 0.1$

Coefficient of correlation: 0.9996

k_2 (20 °C) = 4.03×10^2 M^{-1} s^{-1}

Rate constants for the reactions of **1d** with (Ph)(ani)$CH^+GaCl_4^-$ (**2d–GaCl$_4$**) in CH_2Cl_2 (20 °C, λ = 469 nm).

[**1d**]$_0$ / M	[**2d–Cl**]$_0$ / M	[$GaCl_3$]$_0$ / M	[**1d**]$_0$/[**2d**]$_0$	k_{obs} / s^{-1}
3.82×10^{-4}	3.95×10^{-5}	2.40×10^{-4}	9.7	1.20×10^{-2}
7.59×10^{-4}	3.92×10^{-5}	2.39×10^{-4}	19	2.35×10^{-2}
1.14×10^{-3}	3.92×10^{-5}	4.55×10^{-4}	29	3.43×10^{-2}
1.51×10^{-3}	3.91×10^{-5}	2.38×10^{-4}	39	4.41×10^{-2}
1.89×10^{-3}	3.91×10^{-5}	2.28×10^{-4}	48	5.57×10^{-2}

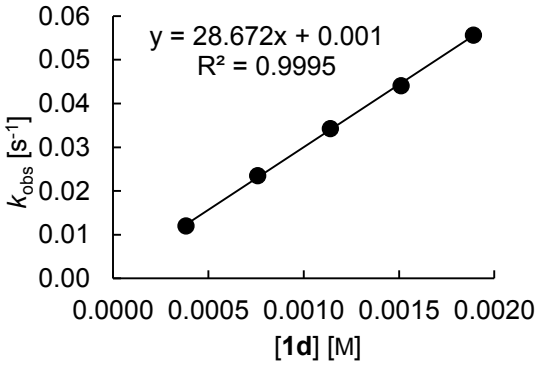

k_2 (20 °C) = 2.87 × 10^1 M^{-1} s^{-1}

Rate constants for the reactions of **1d** with (tol)(ani)$CH^+GaCl_4^-$ (**2e–GaCl$_4$**) in CH_2Cl_2 (20 °C, λ = 488 nm).

[**1d**]$_0$ / M	[**2e–Cl**]$_0$ / M	[$GaCl_3$]$_0$ / M	[**1d**]$_0$/[**2e**]$_0$	k_{obs} / s^{-1}
8.36×10^{-4}	2.55×10^{-5}	1.19×10^{-4}	33	3.49×10^{-3}
1.11×10^{-3}	2.55×10^{-5}	1.36×10^{-4}	44	4.37×10^{-3}
1.39×10^{-3}	2.54×10^{-5}	1.13×10^{-4}	55	5.43×10^{-3}
1.65×10^{-3}	2.51×10^{-5}	1.23×10^{-4}	66	6.57×10^{-3}
1.93×10^{-3}	2.52×10^{-5}	1.57×10^{-4}	77	7.51×10^{-3}

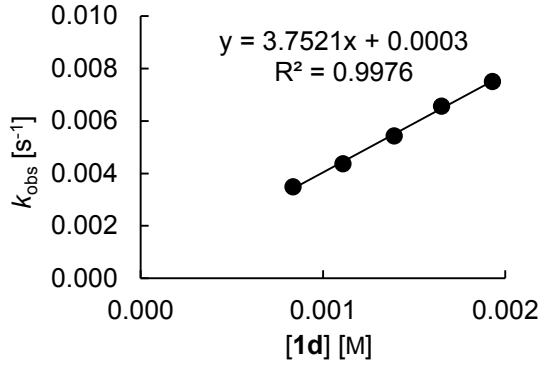

k_2 **(20 °C) = 3.75 M^{-1} s^{-1}**

Rate constants for the reactions of **1d** with (ani)(pop)CH$^+$GaCl$_4^-$ (**2f–GaCl$_4$**) in CH_2Cl_2 (20 °C, λ = 516 nm).

[**1d**]$_0$ / M	[**2f–Cl**]$_0$ / M	[$GaCl_3$]$_0$ / M	[**1d**]$_0$/[**2f**]$_0$	k_{obs} / s^{-1}
2.75×10^{-3}	2.16×10^{-5}	1.23×10^{-4}	127	4.80×10^{-4}
3.27×10^{-3}	2.15×10^{-5}	8.89×10^{-5}	152	5.63×10^{-4}
3.81×10^{-3}	2.14×10^{-5}	8.87×10^{-5}	178	6.20×10^{-4}
4.32×10^{-3}	2.13×10^{-5}	1.10×10^{-4}	203	7.29×10^{-4}

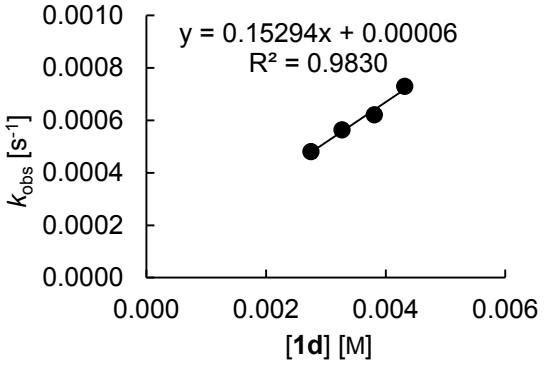

k_2 **(20 °C) = 1.53 × 10^{-1} M^{-1} s^{-1}**

Kinetics for the Reactions of Trimethyl(1-(*p*-tolyl)vinyl)silane (**1e**) with **2d–f**

Rate constants for the reactions of **1e** with (Ph)(ani)$CH^+GaCl_4^-$ (**2d–GaCl$_4$**) in CH_2Cl_2 (λ = 471 nm).

T / °C	[**1e**]$_0$ / M	[**2d–Cl**]$_0$ / M	[$GaCl_3$]$_0$ / M	[**1e**]$_0$/[**2d**]$_0$	k_{obs} / s^{-1}	k_2 / M^{-1} s^{-1} [a]
–69.7	1.04×10^{-3}	3.72×10^{-5}	5.45×10^{-4}	28	1.09×10^{-2}	10.7
–61.6	9.24×10^{-4}	3.67×10^{-5}	5.26×10^{-4}	25	1.43×10^{-2}	15.8
–51.5	8.21×10^{-4}	3.67×10^{-5}	5.26×10^{-4}	22	1.89×10^{-2}	23.5
–40.6	8.04×10^{-4}	3.59×10^{-5}	4.21×10^{-4}	22	2.62×10^{-2}	33.3
–30.2	6.95×10^{-4}	3.55×10^{-5}	4.40×10^{-4}	20	3.17×10^{-2}	46.8
–30.1	9.90×10^{-4}	3.54×10^{-5}	4.04×10^{-4}	28	4.62×10^{-2}	47.5

[a] Calculated from $k_2 = k_{obs}/([\mathbf{1e}]_0 - 0.5[\mathbf{2d}]_0)$.

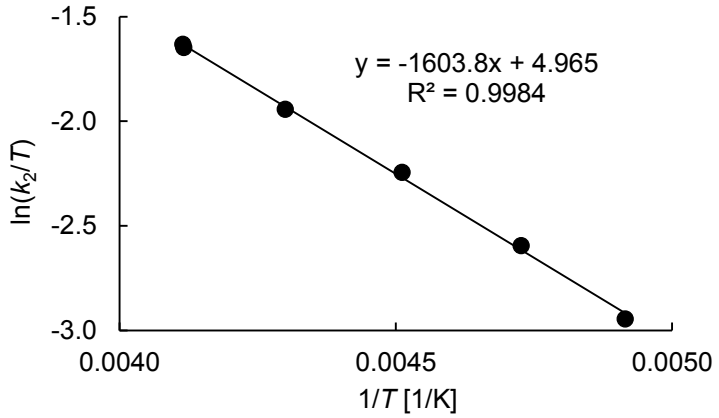

Eyring correlation for the reaction of **2d–GaCl$_4$** with **1e**.

Eyring-parameter:

$\Delta H^{\ddagger}$ = (13.3 ± 0.3) kJ mol^{-1}

$\Delta S^{\ddagger}$ = (–156.3 ± 1.2) J mol^{-1} K^{-1}

Coefficient of correlation: 0.9984

Arrhenius-parameter:

E_A = (15.2 ± 0.2) kJ mol^{-1}

ln A = 11.4 ± 0.1

Coefficient of correlation: 0.9989

k_2 (20 °C) = 1.77×10^2 M^{-1} s^{-1}

Rate constants for the reactions of **1e** with (tol)(ani)$CH^+GaCl_4^-$ (**2e–GaCl$_4$**) in CH_2Cl_2 (20 °C, λ = 488 nm).

[**1e**]$_0$ / M	[**2e–Cl**]$_0$ / M	[$GaCl_3$]$_0$ / M	[**1e**]$_0$/[**2e**]$_0$	k_{obs} / s^{-1}
3.74×10^{-4}	2.44×10^{-5}	1.87×10^{-4}	15	1.06×10^{-2}
4.32×10^{-4}	2.42×10^{-5}	1.62×10^{-4}	18	1.21×10^{-2}
4.97×10^{-4}	2.43×10^{-5}	1.63×10^{-4}	20	1.36×10^{-2}
5.56×10^{-4}	2.42×10^{-5}	1.86×10^{-4}	23	1.57×10^{-2}
6.16×10^{-4}	2.41×10^{-5}	1.62×10^{-4}	26	1.74×10^{-2}

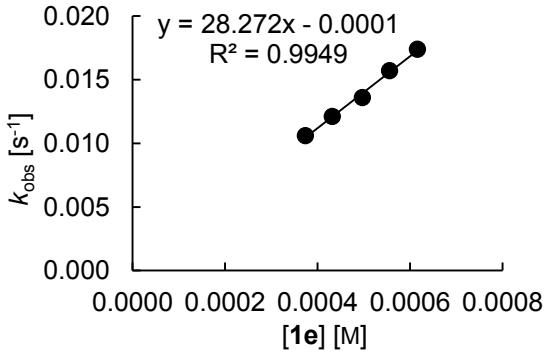

k_2 (20 °C) = 2.83 × 10^1 M^{-1} s^{-1}

Rate constants for the reactions of **1e** with (ani)(pop)$CH^+GaCl_4^-$ (**2f–GaCl$_4$**) in CH_2Cl_2 (20 °C, λ = 516 nm).

[**1e**]$_0$ / M	[**2f–Cl**]$_0$ / M	[$GaCl_3$]$_0$ / M	[**1e**]$_0$/[**2f**]$_0$	k_{obs} / s^{-1}
1.69×10^{-3}	2.13×10^{-5}	1.00×10^{-4}	79	1.46×10^{-3}
2.05×10^{-3}	2.16×10^{-5}	1.01×10^{-4}	95	1.79×10^{-3}
2.37×10^{-3}	2.13×10^{-5}	1.00×10^{-4}	111	2.06×10^{-3}
2.72×10^{-3}	2.15×10^{-5}	9.08×10^{-5}	127	2.28×10^{-3}
3.01×10^{-3}	2.11×10^{-5}	8.92×10^{-5}	143	2.50×10^{-3}

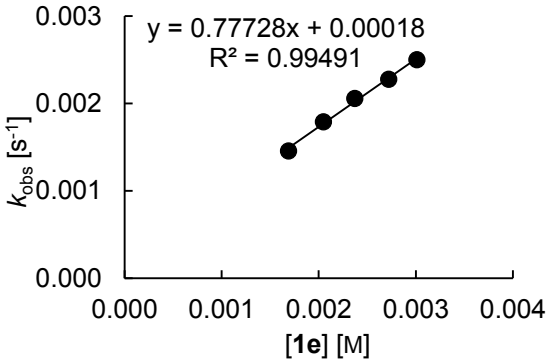

k_2 **(20 °C) = 7.77 × 10^{-1} M^{-1} s^{-1}**

Kinetics for the Reactions of Pentamethyl(1-phenylvinyl)disilane (**1f**) with **2e–g**

Rate constants for the reactions of **1f** with (tol)(ani)CH$^+$GaCl$_4^-$ (**2e–GaCl$_4$**) in CH_2Cl_2 (20 °C, λ = 488 nm).

[**1f**]$_0$ / M	[**2e–Cl**]$_0$ / M	[$GaCl_3$]$_0$ / M	[**1f**]$_0$/[**2e**]$_0$	k_{obs} / s^{-1}
2.48×10^{-4}	2.52×10^{-5}	1.60×10^{-4}	9.8	3.13×10^{-2}
3.08×10^{-4}	2.54×10^{-5}	1.40×10^{-4}	12	3.99×10^{-2}
3.64×10^{-4}	2.53×10^{-5}	1.61×10^{-4}	14	4.73×10^{-2}
4.21×10^{-4}	2.53×10^{-5}	1.29×10^{-4}	17	5.51×10^{-2}
4.77×10^{-4}	2.52×10^{-5}	1.50×10^{-4}	19	6.29×10^{-2}
2.41×10^{-4}	2.44×10^{-5}	[a]	9.9	3.23×10^{-2}

[a] A saturated solution of $FeCl_3$ in CH_2Cl_2 was used for the ionization of **2e–Cl**; data point (open circle) was not used for correlation;

k_2 (**2e–FeCl$_4$**) = $k_{obs}/([\mathbf{1f}]_0 - 0.5[\mathbf{2e}]_0)$ = **1.41×10^2 M^{-1} s^{-1}**.

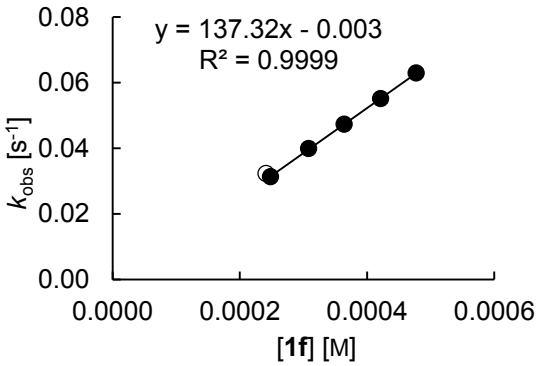

k_2 **(20 °C) = 1.37 × 10^2 M^{-1} s^{-1}**

Rate constants for the reactions of **1f** with (ani)(pop)$CH^+GaCl_4^-$ (**2f–GaCl$_4$**) in CH_2Cl_2 (20 °C, λ = 516 nm).

[**1f**]$_0$ / M	[**2f–Cl**]$_0$ / M	[$GaCl_3$]$_0$ / M	[**1f**]$_0$/[**2f**]$_0$	k_{obs} / s^{-1}
2.18×10^{-4}	2.26×10^{-5}	1.41×10^{-4}	9.6	3.56×10^{-3}
3.10×10^{-4}	2.23×10^{-5}	8.02×10^{-5}	14	4.78×10^{-3}
4.05×10^{-4}	2.22×10^{-5}	7.99×10^{-5}	18	6.15×10^{-3}
4.98×10^{-4}	2.21×10^{-5}	1.09×10^{-4}	23	7.54×10^{-3}
5.98×10^{-3}	2.23×10^{-5}	8.03×10^{-5}	27	9.17×10^{-3}

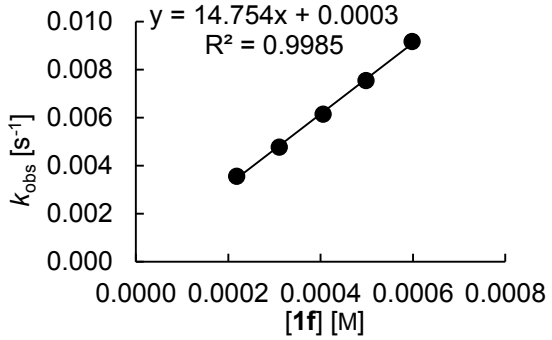

k_2 (20 °C) = 1.48×10^1 M^{-1} s^{-1}

Rate constants for the reactions of **1f** with (ani)$_2CH^+GaCl_4^-$ (**2g–GaCl$_4$**) in CH_2Cl_2 (20 °C, λ = 513 nm).

[**1f**]$_0$ / M	[**2g–Cl**]$_0$ / M	[$GaCl_3$]$_0$ / M	[**1f**]$_0$/[**2g**]$_0$	k_{obs} / s^{-1}
4.78×10^{-4}	1.59×10^{-5}	8.56×10^{-5}	30	2.19×10^{-3}
9.47×10^{-4}	1.55×10^{-5}	7.23×10^{-5}	61	4.59×10^{-3}
1.43×10^{-3}	1.56×10^{-5}	6.54×10^{-5}	92	6.55×10^{-3}
1.88×10^{-3}	1.54×10^{-5}	7.91×10^{-5}	122	8.59×10^{-3}
2.35×10^{-3}	1.54×10^{-5}	7.88×10^{-5}	153	1.07×10^{-2}

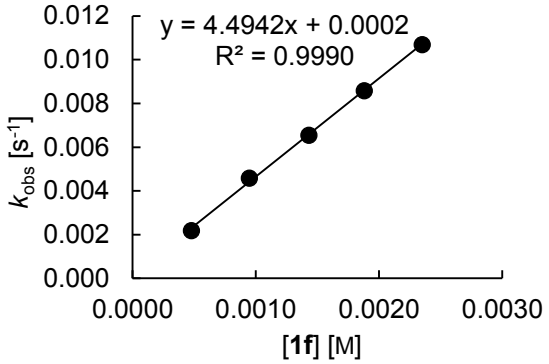

k_2 (20 °C) = 4.49 M^{-1} s^{-1}

Kinetics for the Reactions of (*E*)-(2-Phenylvinyl)trimethylsilane (**1g**) with **2b,d–f**

Rate constants for the reactions of **1g** with (Ph)(pop)CH$^+$GaCl$_4^-$ (**2b–GaCl$_4$**) in CH_2Cl_2 (λ = 478 nm).

T / °C	[**1g**]$_0$ / M	[**2b–Cl**]$_0$ / M	[$GaCl_3$]$_0$ / M	[**1g**]$_0$/[**2b**]$_0$	k_{obs} / s^{-1}	k_2 / M^{-1} s^{-1} [a]
–69.5	1.03×10^{-3}	3.64×10^{-5}	1.25×10^{-3}	28	1.09×10^{-2}	10.8
–60.4	9.10×10^{-4}	3.65×10^{-5}	1.44×10^{-3}	25	1.55×10^{-2}	17.4
–49.9	7.72×10^{-4}	3.58×10^{-5}	1.48×10^{-3}	22	2.32×10^{-2}	30.8
–40.1	6.44×10^{-4}	3.55×10^{-5}	1.26×10^{-3}	18	2.96×10^{-2}	47.3
–29.6	5.20×10^{-4}	3.52×10^{-5}	1.25×10^{-3}	15	3.72×10^{-2}	74.0

[a] Calculated from $k_2 = k_{obs}/([\mathbf{1g}]_0 - 0.5[\mathbf{2b}]_0)$.

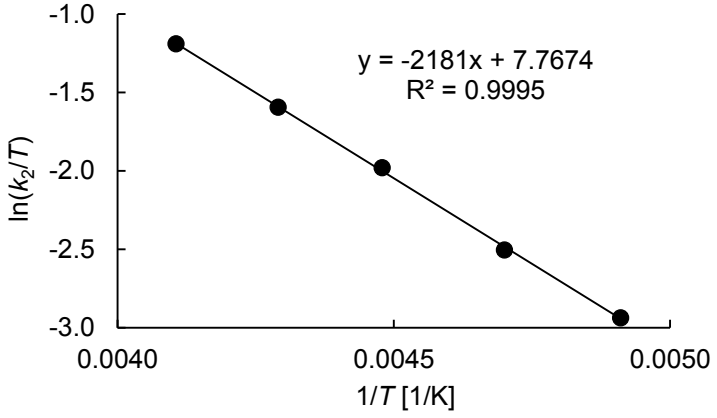

Eyring correlation for the reaction of **2b**–**GaCl$_4$** with **1g**.

Eyring-parameter:

$\Delta H^{\ddagger} = (18.1 \pm 0.2)$ kJ mol^{-1}

$\Delta S^{\ddagger} = (-133.0 \pm 1.0)$ J mol^{-1} K^{-1}

Coefficient of correlation: 0.9995

Arrhenius-parameter:

$E_A = (20.0 \pm 0.2)$ kJ mol^{-1}

$\ln A = 14.2 \pm 0.1$

Coefficient of correlation: 0.9996

k_2 (20 °C) = 4.07 × 10^2 M^{-1} s^{-1}

Rate constants for the reactions of **1g** with (Ph)(ani)CH$^+$GaCl$_4^-$ (**2d–GaCl$_4$**) in CH_2Cl_2 (20 °C, λ = 469 nm).

[**1g**]$_0$ / M	[**2d–Cl**]$_0$ / M	[$GaCl_3$]$_0$ / M	[**1g**]$_0$/[**2d**]$_0$	k_{obs} / s^{-1}
3.72 × 10^{-4}	3.74 × 10^{-5}	2.42 × 10^{-4}	9.9	2.35 × 10^{-2}
4.54 × 10^{-4}	3.75 × 10^{-5}	2.23 × 10^{-4}	12	2.88 × 10^{-2}
5.32 × 10^{-4}	3.74 × 10^{-5}	2.09 × 10^{-4}	14	3.39 × 10^{-2}
6.10 × 10^{-4}	3.73 × 10^{-5}	2.28 × 10^{-4}	16	3.89 × 10^{-2}
6.91 × 10^{-4}	3.74 × 10^{-5}	2.22 × 10^{-4}	18	4.47 × 10^{-2}

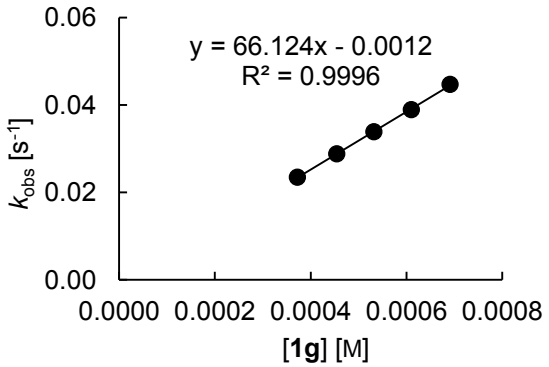

k_2 (20 °C) = 6.61 × 10^1 M^{-1} s^{-1}

Rate constants reported for the reactions of **1g** with (Ph)(ani)$CH^+BCl_4^-$ (**2d–BCl$_4$**) in CH_2Cl_2.[10b]

T / °C	[**1g**]$_0$ / M	[**2d–Cl**]$_0$ / M	[BCl_3]$_0$ / M	[**1g**]$_0$/[**2d**]$_0$	k_2 / M^{-1} s^{-1}
–68.0	3.10×10^{-3}	2.32×10^{-5}	4.44×10^{-2}	134	9.07×10^{-1}
–66.5	1.79×10^{-3}	2.98×10^{-5}	3.43×10^{-2}	60	9.32×10^{-1}
–59.5	1.92×10^{-3}	4.80×10^{-5}	3.68×10^{-2}	40	1.49
–50.5	3.56×10^{-3}	7.11×10^{-5}	4.09×10^{-2}	50	2.90
–38.7	1.67×10^{-3}	6.95×10^{-5}	3.99×10^{-2}	24	5.63
–30.6	7.07×10^{-4}	7.06×10^{-5}	4.21×10^{-2}	10	8.50
–28.8	2.74×10^{-3}	6.84×10^{-5}	4.10×10^{-2}	40	9.05
–27.8	1.45×10^{-3}	7.21×10^{-5}	4.31×10^{-2}	20	9.29

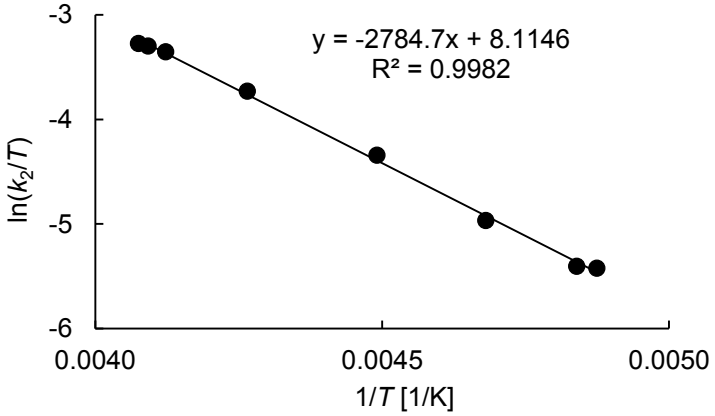

Eyring correlation for the reaction of **2d**–**BCl$_4$** with **1g**.

Eyring-parameter:

$\Delta H^{\ddagger}$ = (23.2 ± 0.4) kJ mol^{-1}

$\Delta S^{\ddagger}$ = (–130.1 ± 1.8) J mol^{-1} K^{-1}

Coefficient of correlation: 0.9982

Arrhenius-parameter:

E_A = (25.0 ± 0.4) kJ mol^{-1}

ln A = 14.5 ± 0.2

Coefficient of correlation: 0.9985

k_2 (20 °C) = 7.34×10^1 M^{-1} s^{-1}

Rate constants for the reactions of **1g** with (tol)(ani)$CH^+GaCl_4^-$ (**2e–GaCl$_4$**) in CH_2Cl_2 (20 °C, λ = 487 nm).

[**1g**]$_0$ / M	[**2e–Cl**]$_0$ / M	[$GaCl_3$]$_0$ / M	[**1g**]$_0$/[**2e**$_0$	k_{obs} / s^{-1}
3.19×10^{-4}	2.72×10^{-5}	1.28×10^{-4}	12	4.03×10^{-3}
4.80×10^{-4}	2.73×10^{-5}	1.01×10^{-4}	18	6.27×10^{-3}
6.38×10^{-4}	2.72×10^{-5}	9.43×10^{-5}	23	8.24×10^{-3}
7.95×10^{-4}	2.71×10^{-5}	1.07×10^{-4}	29	1.06×10^{-2}
9.52×10^{-4}	2.71×10^{-5}	9.37×10^{-5}	35	1.24×10^{-2}

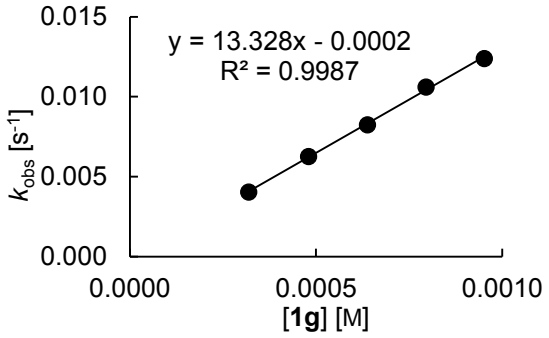

k_2 (20 °C) = 1.33 × 10^1 M^{-1} s^{-1}

Rate constants reported for the reactions of **1g** with (tol)(ani)$CH^+BCl_4^-$ (**2e–BCl$_4$**) in CH_2Cl_2.[10b]

T / °C	[**1g**]$_0$ / M	[**2e–Cl**]$_0$ / M	[BCl_3]$_0$ / M	[**1g**]$_0$/[**2e**]$_0$	k_2 / M^{-1} s^{-1}
–68.0	3.24×10^{-3}	1.54×10^{-4}	4.53×10^{-3}	21	9.10×10^{-2}
–65.5	3.27×10^{-3}	1.56×10^{-4}	2.46×10^{-3}	21	1.16×10^{-1}
–40.0	2.65×10^{-3}	4.26×10^{-5}	2.07×10^{-2}	62	7.99×10^{-1}
–34.2	3.56×10^{-3}	1.35×10^{-4}	1.04×10^{-2}	26	9.76×10^{-1}
–28.8	3.37×10^{-3}	1.60×10^{-4}	3.99×10^{-3}	21	1.42
–20.1	2.77×10^{-3}	3.53×10^{-5}	9.92×10^{-3}	78	2.43
–16.0	6.83×10^{-3}	6.87×10^{-5}	9.27×10^{-3}	99	2.95
–10.8	3.95×10^{-3}	6.35×10^{-5}	1.86×10^{-2}	62	3.54
–10.0	1.15×10^{-3}	3.46×10^{-5}	2.02×10^{-2}	33	3.87
–9.8	2.53×10^{-3}	4.58×10^{-5}	2.23×10^{-2}	55	3.83
0.4	9.12×10^{-4}	4.40×10^{-5}	4.23×10^{-2}	21	5.97

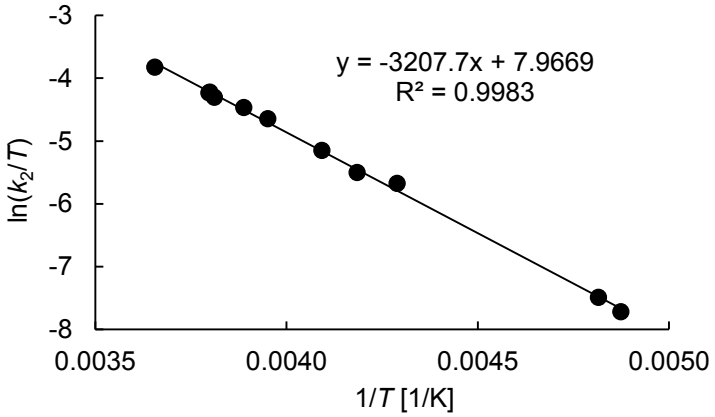

Eyring correlation for the reaction of **2e**–**BCl$_4$** with **1g**.

Eyring-parameter:

$\Delta H^{\ddagger}$ = (26.7 ± 0.4) kJ mol^{-1}

$\Delta S^{\ddagger}$ = (–131.3 ± 1.5) J mol^{-1} K^{-1}

Coefficient of correlation: 0.9983

Arrhenius-parameter:

E_A = (28.6 ± 0.4) kJ mol^{-1}

ln A = 14.4 ± 0.2

Coefficient of correlation: 0.9986

k_2 (20 °C) = 1.50 × 10^1 M^{-1} s^{-1}

Rate constants for the reactions of **1g** with (ani)(pop)CH$^+$GaCl$_4^-$ (**2f–GaCl$_4$**) in CH_2Cl_2 (20 °C, λ = 516 nm).

[**1g**]$_0$ / M	[**2f–Cl**]$_0$ / M	[$GaCl_3$]$_0$ / M	[**1g**]$_0$/[**2f**]$_0$	k_{obs} / s^{-1}
2.22 × 10^{-3}	2.27 × 10^{-5}	1.35 × 10^{-4}	98	3.01 × 10^{-3}
2.77 × 10^{-3}	2.25 × 10^{-5}	1.13 × 10^{-4}	123	3.57 × 10^{-3}
3.33 × 10^{-3}	2.26 × 10^{-5}	1.17 × 10^{-4}	147	4.47 × 10^{-3}
3.84 × 10^{-3}	2.24 × 10^{-5}	1.25 × 10^{-4}	171	5.09 × 10^{-3}
4.38 × 10^{-3}	2.23 × 10^{-5}	1.24 × 10^{-4}	196	5.80 × 10^{-3}

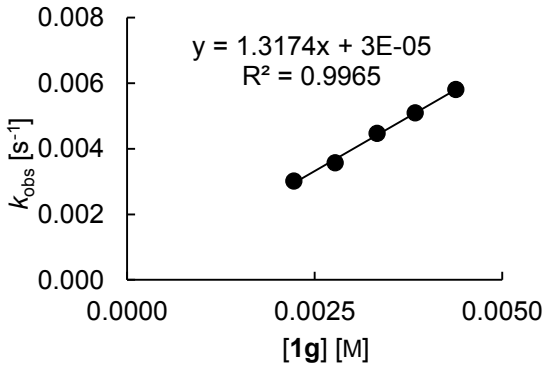

k_2 (20 °C) = 1.32 M^{-1} s^{-1}

Rate constants for the reactions of **1g** with $(ani)_2CH^+GaCl_4^-$ (**2g–GaCl$_4$**) in CH_2Cl_2 (20 °C, λ = 513 nm).

[**1g**]$_0$ / M	[**2g–Cl**]$_0$ / M	[$GaCl_3$]$_0$ / M	[**1g**]$_0$/[**2g**]$_0$	k_{obs} / s^{-1}
2.91×10^{-3}	1.64×10^{-5}	4.01×10^{-5}	177	9.93×10^{-4}
3.85×10^{-3}	1.65×10^{-5}	6.66×10^{-5}	233	1.44×10^{-3}
4.68×10^{-3}	1.61×10^{-5}	4.60×10^{-5}	291	1.65×10^{-3}
5.63×10^{-3}	1.66×10^{-5}	7.52×10^{-5}	339	2.06×10^{-3}
6.44×10^{-3}	1.64×10^{-5}	8.26×10^{-5}	393	2.39×10^{-3}

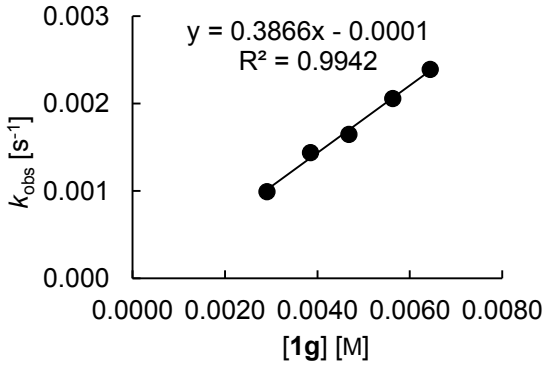

k_2 (20 °C) = 3.87 × 10^{-1} M^{-1} s^{-1}

Rate constants for the reactions of **1g** with $(ani)_2CH^+SnCl_5^-$ (**2g–SnCl$_5$**) in CH_2Cl_2 (20 °C, λ = 513 nm).

[**1g**]$_0$ / M	[**2g–Cl**]$_0$ / M	[$SnCl_4$]$_0$ / M	[**1g**]$_0$/[**2g**]$_0$	k_{obs} / s^{-1}
2.94×10^{-3}	1.70×10^{-5}	1.04×10^{-4}	173	9.53×10^{-4}
3.80×10^{-3}	1.68×10^{-5}	9.08×10^{-5}	226	1.31×10^{-3}
4.75×10^{-3}	1.70×10^{-5}	1.10×10^{-4}	279	1.67×10^{-3}
5.56×10^{-3}	1.66×10^{-5}	1.08×10^{-4}	335	2.10×10^{-3}
6.46×10^{-3}	1.66×10^{-5}	1.56×10^{-4}	389	2.62×10^{-3}

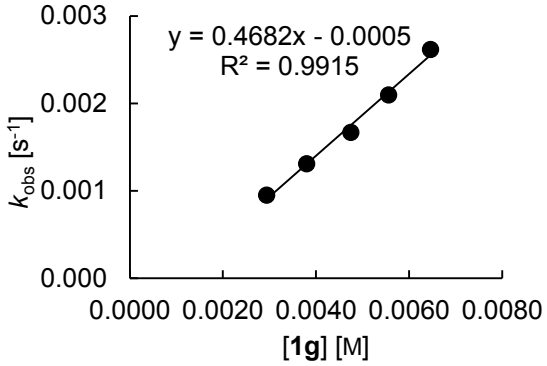

k_2 **(20 °C) = 4.68 × 10^{-1} M^{-1} s^{-1}**

Rate constants for the reactions of **1g** with (ani)$_2$CH$^+$FeCl$_4^-$ (**2g–FeCl$_4$**) in CH_2Cl_2 (20 °C, λ = 513 nm). A saturated solution of $FeCl_3$ in CH_2Cl_2 was used for the ionization of **2g–Cl**.

[**1g**]$_0$ / M	[**2g–Cl**]$_0$ / M	[**1g**]$_0$/[**2g**]$_0$	k_{obs} / s^{-1}
2.85×10^{-3}	1.67×10^{-5}	171	9.45×10^{-4}
3.80×10^{-3}	1.67×10^{-5}	228	1.41×10^{-3}
4.72×10^{-3}	1.66×10^{-5}	284	1.67×10^{-3}
5.60×10^{-3}	1.64×10^{-5}	341	2.13×10^{-3}
6.51×10^{-3}	1.63×10^{-5}	399	2.42×10^{-3}

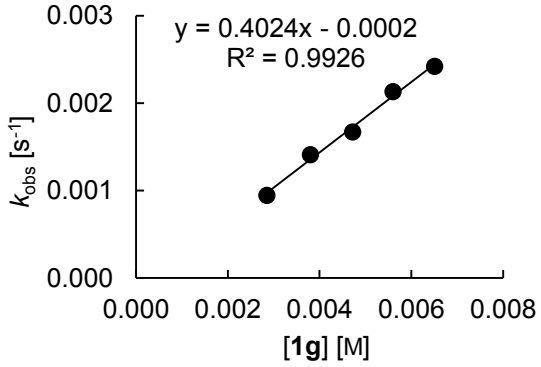

k_2 **(20 °C) = 4.02 × 10^{-1} M^{-1} s^{-1}**

Kinetics for the Reactions of (2-Phenylallyl)trimethylsilane (**1h**) with **2h–j**

Rate constants for the reactions of **1h** with $(pfa)_2CH^+BF_4^-$ (**2h–BF$_4$**) in CH_2Cl_2 (20 °C, λ = 602 nm).

$[\mathbf{1h}]_0$ / M	$[\mathbf{2h}]_0$/M	$[\mathbf{1h}]_0/[\mathbf{2h}]_0$	k_{obs} / s^{-1}
1.47×10^{-4}	1.26×10^{-5}	12	1.45×10^{-2}
1.74×10^{-4}	1.27×10^{-5}	14	1.68×10^{-2}
1.99×10^{-4}	1.26×10^{-5}	16	1.98×10^{-2}
2.25×10^{-4}	1.26×10^{-5}	18	2.23×10^{-2}
2.51×10^{-4}	1.26×10^{-5}	20	2.50×10^{-2}

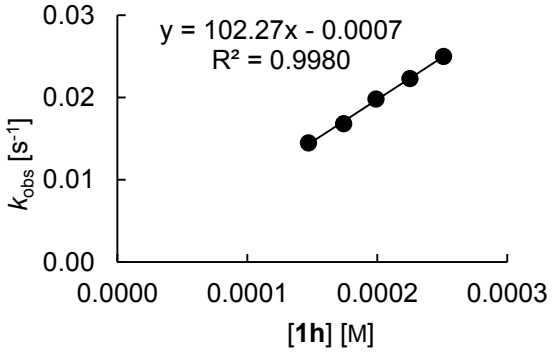

k_2 (20 °C) = 1.02 × 10^2 M^{-1} s^{-1}

Rate constants for the reactions of **1h** with $(mfa)_2CH^+BF_4^-$ (**2i–BF$_4$**) in CH_2Cl_2 (20 °C, λ = 593 nm).

$[\mathbf{1h}]_0$ / M	$[\mathbf{2i}]_0$/M	$[\mathbf{1h}]_0/[\mathbf{2i}]_0$	k_{obs} / s^{-1}
2.17×10^{-4}	9.75×10^{-6}	22	4.49×10^{-3}
4.33×10^{-4}	9.72×10^{-6}	45	9.24×10^{-3}
6.49×10^{-4}	9.71×10^{-6}	67	1.40×10^{-2}
8.58×10^{-4}	9.64×10^{-6}	89	1.87×10^{-2}
1.06×10^{-3}	9.57×10^{-6}	111	2.31×10^{-2}

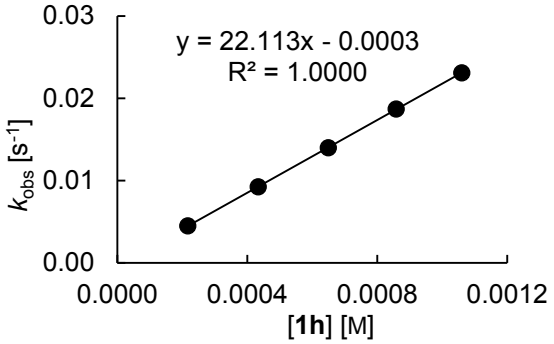

$$k_2\,(20\ °C) = 2.21 \times 10^{1}\ M^{-1}\ s^{-1}$$

Rate constants for the reactions of **1h** with $(dpa)_2CH^+BF_4^-$ (**2j–BF4**) in CH_2Cl_2 (20 °C, λ = 672 nm).

$[\mathbf{1h}]_0$ / M	$[\mathbf{2j}]_0$/M	$[\mathbf{1h}]_0/[\mathbf{2j}]_0$	k_{obs} / s^{-1}
8.46×10^{-4}	2.12×10^{-5}	40	3.53×10^{-3}
1.06×10^{-3}	2.11×10^{-5}	50	4.37×10^{-3}
1.28×10^{-3}	2.11×10^{-5}	61	5.26×10^{-3}
1.50×10^{-3}	2.10×10^{-5}	71	6.12×10^{-3}
1.71×10^{-3}	2.09×10^{-5}	82	6.93×10^{-3}

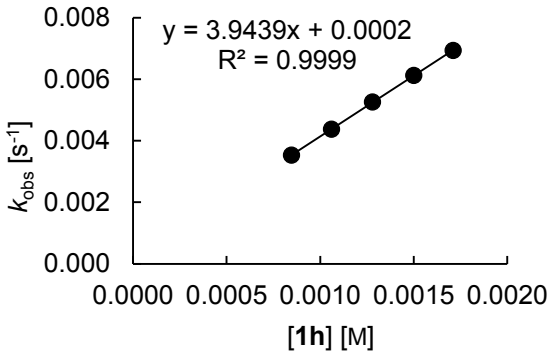

$$k_2\,(20\ °C) = 3.94\ M^{-1}\ s^{-1}$$

4.5 Appendix

4.5.1 Calculations Regarding the Perturbation of the π-Conjugation of α-Substituted Styrenes

According to experimental studies,[14a,b,33] the parent styrene (**6a**) shows a flat torsion potential close to the planar conformation in its ground state, while α-substituted styrene derivatives can possess pronounced local or even global maxima for planarity.[14a,b,33a,34] Theoretical investigations concerning the torsion potentials of styrene derivatives showed good agreement with the experimental data when electron correlation had been considered.[35]

Therefore, the perturbations of the π-conjugation in the ground state of the styrene derivatives discussed in this chapter were determined via quantum chemical calculations at the MP2/6-31G* level with the Gaussian 09 program.[36] Table 4.7 summarizes the data obtained from these calculations (archive entries are given in subsection 4.5.2). In order to illustrate how the introduction of α- or β-substituents influences the torsion potentials of styrene derivatives, the torsion potentials of styrene (**6a**), α-methyl styrene (**6b**), α-(trimethylsilyl)styrene (**1d**), and *trans*-β-(trimethylsilyl)styrene (**1h**) were calculated at the MP2/6-31G* level (Figure 4.7 and Figure 4.8).

In agreement with previous reports,[14a,b,33–35] Figure 4.7 shows a non-planar global minimum for styrene (**6a**) with a flat torsion potential close to the planar conformation which changes to torsion potentials with pronounced local or global maxima for planarity after the introduction of an α-substituent. The parent styrene (**6a**) shows a barrier for planarization of merely 0.24 kcal/mol and a global maximum for $\theta = 90°$ separated from the minimum by 2.7 kcal/mol (Table 4.7). In contrast, the calculated global minimum for α-methyl styrene close to $\theta = 40°$ is stabilized by 1.4 kcal/mol when compared to the coplanar and perpendicular orientations. The most stable structure of α-(trimethylsilyl)styrene (**1d**) has a torsion angle close to $\theta = 60°$, which is separated from the planar conformer by a barrier of 3.7 kcal/mol. Remarkably, the barrier for the perpendicular conformation at $\theta = 90°$ amounts to merely 0.17 kcal/mol in spite of the truncated conjugation.

Table 4.7. Total Electronic Energies ($E_{tot,min}$), Torsion Angles (θ_{min}) and Olefinic Double Bond Lengths ($d(C{=}C)_{min}$) for the Global Minima Together with the Differences to the Respective Molecular Properties of the Coplanar ($\theta = 0°$) and Perpendicular ($\theta = 90°$) Orientation.

	$\theta = 0°$	Global Minimum	$\theta = 90°$
	$\Delta E_{tot,0°}$[a]	$E_{tot,min}$[c] (θ_{min})	$\Delta E_{tot,90°}$[a]
	$\Delta d(C{=}C)_{0°}$[b]	$d(C{=}C)_{min}$ / Å	$\Delta d(C{=}C)_{90°}$[b]
 **6a**	0.24	–308.5934390 (27.2°)	2.73
	0.0004	1.3429	–0.0030
 **8**	0.20	–347.7643959 (25.9°)	2.83
	0.0004	1.3431	–0.0031
 **6b**	1.42	–347.7642979 (40.9°)	1.40
	0.0017	1.3454	–0.0034
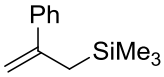 **1h**	2.90	–755.4617080 (47.2°)	2.73
	0.0037	1.3471	–0.0021
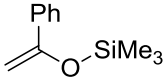 **6d**	1.33	–791.3710578 (34.3°)	2.76
	0.0015	1.3445	–0.0038
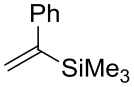 **1d**	3.67	–716.2927300 (61.5°)	0.17
	0.0042	1.3500	–0.0017
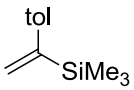 **1e**	3.50	–755.4636325 (59.6°)	0.21
	0.0042	1.3502	–0.0018
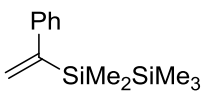 **1f**	3.94	–1084.8093291 (59.1°)	1.02
	0.0037	1.3502	–0.0013
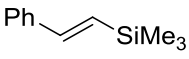 **1g**	0.14	–716.2935203 (23.1°)	3.31
	0.0002	1.3529	–0.0031

[a] In kcal mol^{-1}. [b] In Å; $\Delta d(C{=}C)_{X°} = d(C{=}C)_{X°} - d(C{=}C)_{min}$. [c] In Hartree.

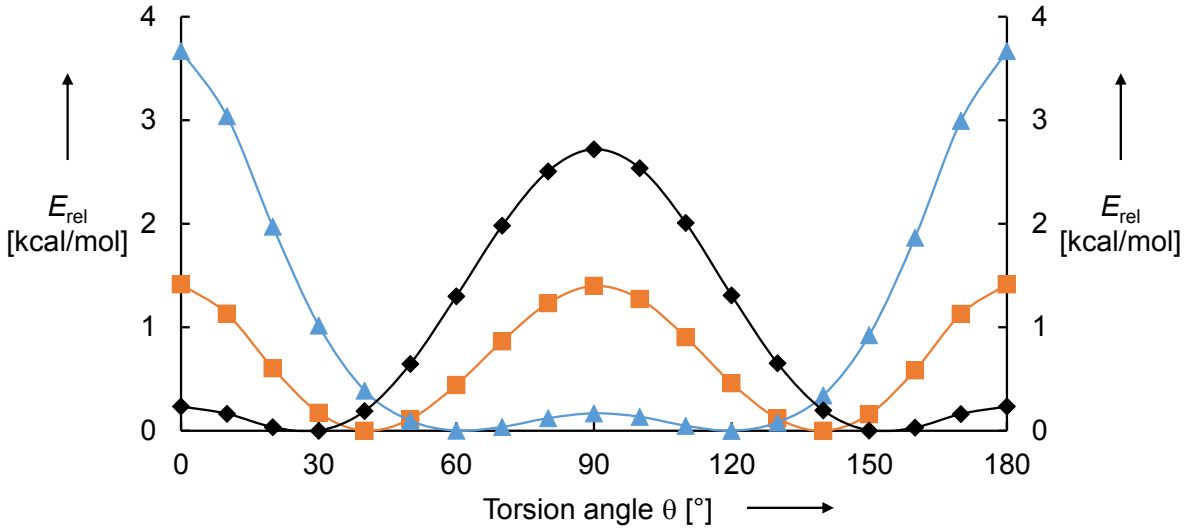

Figure 4.7. Torsion potentials calculated at the MP2/6-31G* level for styrene (**6a**, black diamonds), α-methyl styrene (**6b**, orange squares) and α-(trimethylsilyl)styrene (**1d**, blue triangles).

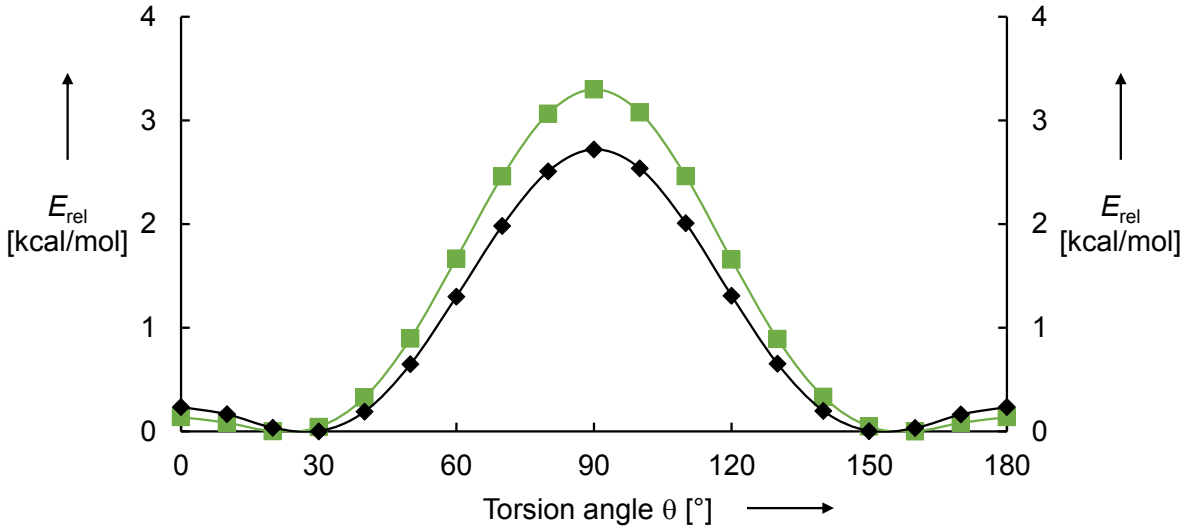

Figure 4.8. Torsion potentials calculated at the MP2/6-31G* level for styrene (**6a**, black diamonds) and *trans*-β-(trimethylsilyl)styrene (**1g**, green squares).

Negligible influences of para-substituents on the orientation of the vinyl to the phenyl group in styrenes (lines 1,2 in Table 4.7) were reported in the literature.[14a,b,33] Similar effects can be observed for α-substituted styrene derivatives when comparing the torsion angles and barriers calculated for α-(trimethylsilyl)styrene (**1d**) and trimethyl(1-(*p*-tolyl)vinyl)silane (**1e**, lines 6,7 in Table 4.7). In contrast, distinct effects can be observed when the steric bulk of the α-substituents is increased: Exchanging one hydrogen of α-methyl styrene (**6b**) against

$SiMe_3$ ($\rightarrow$**1h**) results in a 2-fold increase of both barriers and a further twisted global minimum (lines 3,4 in Table 4.7). Interestingly, the corresponding silyl enol ether **6d** shows a smaller barrier for planarization and a reduced torsion angle even when compared to α-methyl styrene. In the case of α-silylated styrenes, the expansion of the organosilicon moiety in **1d** with $SiMe_3$, leading to pentamethyl(1-phenylvinyl)disilane (**1f**), just results in a slight increase for $\Delta E_{tot,0°}$, while the perpendicular orientation is clearly destabilized (lines 6,8 in Table 4.7).

In contrast to the effects observed for α-substituted styrenes, the introduction of *trans*-β-substituents in styrene does not lead to substantial changes in the torsion potentials of such compounds when compared to styrene (**6a**).[14a,b,33] Therefore, Table 4.7 and Figure 4.8 show that the global minimum calculated for *trans*-β-(trimethylsilyl)styrene (**1h**) has a comparable torsion angle (23.1°) to styrene (27.2°) with a slightly lower barrier of 0.14 kcal/mol for planarization and a higher barrier for the perpendicular orientation (3.3 kcal/mol).

At first glance, torsion angles of 27.2° and 23.1° for the global minima of styrene (**6a**) and *trans*-β-(trimethylsilyl)styrene (**1g**), respectively, might not agree with a low perturbation of π-conjugation in these systems. However, examination of the vinylic bond lengths, which are considered to act as indicators for π-conjugation,[35d] show just slight contractions ($\Delta d(C{=}C)_{0°}$, Table 4.7) for the global minima of **6a** (0.0004 Å) and **1g** (0.0002 Å) when compared to the respective planar conformations. Consequently, strongly shortened vinylic bond lengths are found for the perpendicular conformers of styrene ($\Delta d(C{=}C)_{90°}$ = –0.0030 Å) and *trans*-β-(trimethylsilyl)styrene ($\Delta d(C{=}C)_{90°}$ = –0.0031 Å) due to the truncated conjugation between the π-systems.

According to Table 4.7, the introduction of α-substituents leads to strong contractions of the vinylic bond lengths close to 0.0020 Å found for α-methyl styrene (**6b**) and 1-phenyl-1-(trimethylsiloxy)ethene (**6d**) and even nearby 0.0040 Å found for allylsilane **1h** as well as α-silylated styrenes **1d–f**. Due to this already strong perturbation of π-conjugation present in the global minima of **1d–f,h**, the differences $\Delta d(C{=}C)_{90°}$ in vinylic bond length between these minima and the corresponding non-conjugated (with respect to conjugation between the olefinic double bond and the aromatic ring) conformers are diminished (–0.0013 to –0.0021 Å) when compared to styrene (–0.0030 Å).

In summary, the quantum chemical calculations regarding the ground states of the styrene derivatives discussed in this chapter are in line with the conclusions drawn from the changes in the UV spectra of these compounds (see subsection 4.4.4). Therefore, the introduction of α-substituents leads to a perturbation of the π-conjugation between the vinyl group and the aromatic ring and in consequence to a destabilization of the ground state when compared to the parent styrene (**6a**). To what extent this destabilization is influenced by the degree of π-system perturbation can be deduced from the gas phase basicities of α-methyl and α-trimethylsilyl styrenes reported by Tsuno and co-workers.[38] Although α-methyl groups are known to stabilize carbenium ions much better than α-silyl groups,[39] the corresponding α-substituted styrenes possess almost identical basicities in the gas phase. This can now be explained with the more pronounced ground state destabilization of α-trimethylsilyl styrenes due to the higher degree of π-system perturbation (see lines 3,6 in Table 4.7).

Despite the ground state destabilization of styrene when α-substituents are introduced, the reactivities of α-substituted styrenes (**1d,f,h,6b,d**) relative to styrene (**6a**) are approximately 10^2 times lower than the reactivities of the corresponding 2-substituted propenes (**1a–c** and **5b–d**) relative to propene (**5a**, Table 4.4). One possible explanation might be a remaining π-system perturbation in the transition state and a higher sensitivity of the transition state to this perturbation when compared to the ground state, due to the high electron demand of the developing carbenium center. Another reasoning is given by Frontier Molecular Orbital Theory.[40] A perturbation of π-conjugation in the nucleophile leads to a lowering of its HOMO-energy[14c] and therefore, to a diminished interaction of the Frontier Orbitals. The resulting increase of the activation barrier could account for the diminished activating effects found for the studied substituents when replacing hydrogen in the α-position of styrene compared to the 2-position in propene.

4.5.2 Computational Data

General

All geometry optimizations and torsion potentials for the orientation of the vinyl group to the plane of the aromatic ring were computed at the MP2/6-31G* level with the Gaussian 09 program.[36] Torsion potentials and geometry optimizations were calculated for the global minima of styrene derivatives **1d,h** and **6a,b**. For styrene derivatives **1e** and **8** the geometries

were optimized for the global minimum (full geometry optimization) and for conformers with fixed torsion angles (θ=0° and θ=90°). In the case of styrene derivatives **1f,h** and **6d** the conformational space (in the case of θ=0° and θ=90° with frozen torsion angle) has first been searched using the MMFF force field and the systematic search routine in the MacroModel program.[37] After removal of duplicates, the remaining conformers were taken as starting structures for the geometry optimization of the global minimum (full geometry optimization), the coplanar (torsion angle fixed to θ=0°) and the perpendicular (torsion angle fixed to θ=90°) cases.

Trimethyl(1-phenylvinyl)silane (**1d**)

Relaxed Potential Energy Surface Scan

θ / deg	d(C=C) / Å	E_{tot} / Hartree	ΔE / kcal mol^{-1}
0	1.3542	–716.2868771	3.67
10	1.3540	–716.2878811	3.04
20	1.3535	–716.2895845	1.97
30	1.3529	–716.2911086	1.02
40	1.3521	–716.2921089	0.39
50	1.3512	–716.2925757	0.10
60	1.3501	–716.2927278	0.00
70	1.3492	–716.2926706	0.04
80	1.3486	–716.2925363	0.12
90	1.3483	–716.2924610	0.17
100	1.3485	–716.2925144	0.14
110	1.3491	–716.2926524	0.05
120	1.3500	–716.2927298	0.00
130	1.3511	–716.2926016	0.08
140	1.3521	–716.2921842	0.34
150	1.3529	–716.2912573	0.92
160	1.3536	–716.2897514	1.87
170	1.3540	–716.2879538	3.00
180	1.3542	–716.2868771	3.67

1|1|UNPC-HAFNIUM|Scan|RMP2-FC|6-31G(d)|C11H16Si1|LAUCH|13-Jun-2013|0||
#p opt=(tight,modredundant) nosymm mp2/6-31g(d)||alpha-TMS-sytrene Tor
sion Potential 10deg||0,1|C,-0.0154184933,-0.5698786627,0.0677729128|C
,1.066444619,0.0636165226,-0.5413917168|C,2.3069269741,0.1037234938,0.
0969147654|C,2.5112961765,-0.4834178998,1.3586454744|C,1.4032119994,-1
.1177336321,1.9542607838|C,0.1630281165,-1.1605244888,1.321353615|H,-0
.984209761,-0.6043369717,-0.4246243634|H,0.9494225688,0.5298435648,-1.
5171443797|H,3.1267851923,0.6047771968,-0.4055864842|H,1.4992894126,-1
.5891607928,2.9280448966|H,-0.6702845775,-1.6592189023,1.8114873705|C,
3.8501853344,-0.4216322541,2.0115575207|C,4.0663825684,-0.9808870166,3
.2257992568|H,5.0380521643,-0.9397810409,3.7069067443|H,3.2986536252,-
1.5007144069,3.7949794904|C,6.8439945865,0.3021893328,2.3307009344|H,7
.1316518602,-0.7369544948,2.5154455963|H,7.6971814905,0.7987645439,1.8
561881249|H,6.6798873206,0.7867036675,3.2976611873|C,4.999621151,2.281
0002998,0.9438872153|H,4.1573628469,2.4823492791,0.2777793153|H,4.7791
413428,2.7563440252,1.9052205063|H,5.8828620127,2.775965115,0.52570800
22|C,5.7954486839,-0.4030381942,-0.4340489351|H,5.0010786121,-0.363146
635,-1.1830649696|H,6.6867725137,0.0646946519,-0.8661905092|H,6.028764
0725,-1.4582447758,-0.258472728|Si,5.3410403553,0.4387859847,1.1966059
936||Version=IA32W-G09RevA.02|HF=-714.7937257,-714.7940619,-714.795556
5,-714.7971115,-714.7982386,-714.7989361,-714.7992559,-714.7992696,-71
4.7991599,-714.7990992,-714.7991695,-714.7992878,-714.7992669,-714.798
9439,-714.79824,-714.7971051,-714.7955515,-714.7940631,-714.7937256|MP
2=-716.2868771,-716.2878811,-716.2895845,-716.2911086,-716.2921089,-71
6.2925757,-716.2927278,-716.2926706,-716.2925363,-716.292461,-716.2925
144,-716.2926524,-716.2927298,-716.2926016,-716.2921842,-716.2912573,-
716.2897514,-716.2879538,-716.2868771|RMSD=8.603e-009,4.468e-009,7.880
e-009,8.478e-009,9.973e-009,9.766e-009,6.474e-009,6.540e-009,4.846e-00
9,7.591e-009,5.734e-009,6.237e-009,7.018e-009,9.419e-009,4.443e-009,6.
127e-009,5.812e-009,7.076e-009,5.152e-009|PG=C01 [X(C11H16Si1)]||@

Geometry Optimization

Global minimum at θ = 61.473°

1|1|UNPC-UNUNBIUM|FOpt|RMP2-FC|6-31G(d)|C11H16Si1|LAUCH|14-Jun-2013|0|
|#p opt=(calcfc,tight) freq mp2/6-31g(d)||alpha-TMS-sytrene Opt+freq||
0,1|C,-0.0009949906,0.000273867,0.00305331|C,0.0001925211,-0.006870477
8,1.4000488239|C,1.2065294918,-0.0071542282,2.101701342|C,2.433472944,
-0.0222537566,1.4178075815|C,2.4191790402,-0.0143664061,0.0136081649|C
,1.2123888362,-0.0078739832,-0.6880023444|H,-0.9413935391,0.0066521863
,-0.5427858891|H,-0.94109039,-0.0095553809,1.9452837365|H,1.2003423736
,-0.0367402402,3.1888285282|H,3.365883344,-0.0113587102,-0.523058844|H
,1.220034991,-0.0012554814,-1.7757652769|C,3.7247312017,-0.023006273,2
.1532573184|C,4.5762028991,-1.0565463472,1.9823048101|H,5.5476074155,-
1.0917567497,2.4689822978|H,4.3208770273,-1.911147752,1.3560180858|C,5
.9409214948,1.3074068041,3.8428783566|H,6.6709255254,1.1835689385,3.03
74690642|H,6.2270615578,2.196388432,4.4145959179|H,6.0258109304,0.4450
641482,4.5112227175|C,2.99983596,1.7473134025,4.6198313951|H,1.9841130
497,1.961325678,4.2760355048|H,2.9616847884,0.863531315,5.2643734392|H
,3.3246903956,2.5936817239,5.2348769258|C,4.0893218264,2.9969601588,2.
0288238481|H,3.0862219733,3.0956086802,1.6026199468|H,4.3198027931,3.9
235374806,2.5649974717|H,4.7960745996,2.9045550449,1.1981709453|Si,4.1
883602252,1.5014413851,3.1731618149||Version=IA32W-G09RevA.02|State=1-
A|HF=-714.7992729|MP2=-716.29273|RMSD=5.314e-009|RMSF=1.237e-008|Dipol
e=0.0495435,0.0514759,0.0268284|PG=C01 [X(C11H16Si1)]||@

Trimethyl(1-(*p*-tolyl)vinyl)silane (**1e**)

Geometry Optimization

θ = 0°


```
1\1\GINC-LINUX-IQS7\FOpt\RMP2-FC\6-31G(d)\C12H18Si1\AKM\10-Jul-2013\0\
 \#p opt=(calcfc,tight,modredundant) freq mp2/6-31g(d)\\pMe-alpha-TMS-s
 tyrene Opt+freq 0deg\\0,1\C,-0.0000440071,-0.0000469079,0.0000411787\C
 ,-0.0000356531,0.0001299572,1.4016673544\C,1.1866620062,0.0000462276,2
 .1285648707\C,2.4419645094,0.0135874291,1.4893164178\C,2.430486314,0.0
 120737221,0.0834953678\C,1.2402246357,0.0116629498,-0.6437739392\H,-0.
 9493792632,-0.0128913046,1.9360793334\H,1.1224572291,-0.0022169782,3.2
 131077053\H,3.365368764,0.0147543731,-0.4663456738\H,1.2812460764,0.00
 76906739,-1.7322772932\C,3.7299329751,0.0094825102,2.2378371458\C,3.75
 62005879,-0.0077583701,3.5918584961\H,4.6904151698,-0.0070636384,4.143
 7625142\H,2.8616382692,-0.0268552645,4.2107644647\C,6.7998873984,0.054
 383338,2.6410861368\H,6.7861356959,-0.839007404,3.2722798706\H,7.76690
 70481,0.07744888,2.1272477376\H,6.7545158196,0.9318084963,3.2928239606
 \C,5.6020395881,1.6186279274,0.3250226349\H,4.8571164976,1.7094495839,
 -0.4690068582\H,5.5067919291,2.5001669995,0.9673245826\H,6.5934221583,
 1.6539412726,-0.1396141346\C,5.6567163915,-1.5006492183,0.2933853053\H
 ,4.9217844374,-1.597958917,-0.5091247937\H,6.6524224507,-1.4954566252,
 -0.1633150694\H,5.5839789224,-2.3982416545,0.9161115545\Si,5.416890748
 8,0.0447787556,1.3559561475\C,-1.2892705058,0.0367324722,-0.7770038256
 \H,-1.6617439552,1.0622179845,-0.8779913444\H,-1.1529708446,-0.3679191
 74,-1.7839231397\H,-2.0668336511,-0.5490077356,-0.2777557578\\Version=
 AM64L-G09RevA.02\State=1-A\HF=-753.830911\MP2=-755.4580481\RMSD=5.580e
 -09\RMSF=7.616e-05\Dipole=-0.0999602,0.0149418,-0.0612601\PG=C01 [X(C1
 2H18Si1)]\\@
```


Global minimum at θ = 59.626°


```
1\1\GINC-LINUX-V8CG\FOpt\RMP2-FC\6-31G(d)\C12H18Si1\HANS\05-Jul-2013\0
 \\#p opt=(calcfc,tight) freq mp2/6-31g(d)\\pMe-aTMSst Opt+freq\\0,1\C,
 -0.0013954253,-0.0000704497,0.0011565915\C,-0.0006168823,-0.0059202248
 ,1.401448872\C,1.1941091704,-0.0056348271,2.1214704823\C,2.4327916973,
 -0.0040941415,1.4608281854\C,2.4332068117,0.0101103231,0.0565123745\C,
 1.2352593445,0.0031395008,-0.6573077281\H,-0.9489758682,-0.0099790456,
 1.9375545032\H,1.1759950619,-0.004658547,3.2097809832\H,3.3793459685,-
 0.0183232313,-0.4793025083\H,1.2616070876,-0.0050338241,-1.7463583036\
 C,3.699508989,-0.0005910653,2.2364345026\C,3.9497522143,-1.0169254302,
 3.0893621791\H,4.8431203708,-1.0462097181,3.7080372952\H,3.2698190035,
 -1.8631648726,3.1861383298\C,6.2508304842,1.3355613156,3.3508780118\H,
 6.8722525534,0.4617323713,3.1322262616\H,6.8976560439,2.2181240795,3.3
 089436692\H,5.8858606584,1.2418253029,4.3779718565\C,3.7939206497,3.02
 82169654,2.5321927877\H,2.9449197191,3.1166475593,1.8473902541\H,3.395
 3884029,2.96742262,3.5497797179\H,4.3849124619,3.9470076671,2.45654536
 76\C,5.5499679154,1.7026512057,0.3825463083\H,4.7713042598,1.914201282
 3,-0.3553716103\H,6.2608051229,2.5359538526,0.3592753124\H,6.083829833
 3,0.8015158714,0.064936005\Si,4.8328021367,1.509606044,2.1190531927\C,
 -1.2922569621,0.0437914455,-0.7744463259\H,-1.6000551624,1.076182247,-
 0.9743005684\H,-1.1896089367,-0.4631145088,-1.7383314205\H,-2.10089022
 15,-0.4413696368,-0.2202162554\\Version=AM64L-G09RevA.02\State=1-A\HF=
 -753.83612\MP2=-755.4636325\RMSD=5.582e-09\RMSF=1.807e-08\Dipole=-0.06
 81924,0.0599924,-0.0381222\PG=C01 [X(C12H18Si1)]\\@
```

θ = 90°

1\1\GINC-LINUX-IQS7\FOpt\RMP2-FC\6-31G(d)\C12H18Si1\AKM\15-Jul-2013\0\
\#p opt=(calcfc,tight,modredundant) freq mp2/6-31g(d)\\pMe-alpha-TMS-s
tyrene Opt+freq 90deg\\0,1\C,0.0000338021,0.0000070188,-0.0000311564\C
,0.000000919,-0.0000618052,1.40064803\C,1.1944258438,-0.0000518773,2.1
216788279\C,2.4312891262,-0.0124486935,1.4593418785\C,2.4341996698,-0.
0040434253,0.0562327544\C,1.2361890798,-0.0043782137,-0.6587565662\H,-
0.9487088417,-0.0039392308,1.9361056637\H,1.1737731016,-0.011664681,3.
2100322076\H,3.3848103335,-0.0197436358,-0.4740015156\H,1.2625777383,-
0.0120019778,-1.7478052614\C,3.7067916735,0.0061761315,2.2253187619\C,
4.2835633787,-1.1548720363,2.5959232988\H,5.2147156888,-1.1808351324,3
.1571657017\H,3.8429618695,-2.1205054454,2.3496589151\C,6.0410316216,1
.5000271967,3.6067423011\H,6.7918268954,0.9453034103,3.0358380479\H,6.
4658943647,2.4804466052,3.8459346276\H,5.8772452703,0.9719627617,4.551
0143056\C,3.177268566,2.6631625016,3.6567408773\H,2.2269680048,2.75477
95353,3.1222412598\H,2.9781617914,2.1651422678,4.6109695369\H,3.538307
1633,3.6736812564,3.8755998018\C,4.7695247109,2.618809411,1.0212867315
\H,3.8551224662,2.7129707364,0.4279095483\H,5.1494231323,3.6275843766,
1.214886303\H,5.5117602355,2.093195497,0.4121606977\Si,4.4369506589,1.
6998490822,2.6349576655\C,-1.291205578,0.0445889664,-0.7752622525\H,-1
.6038719692,1.0771823586,-0.9662827083\H,-1.1864004578,-0.4537906912,-
1.7433169447\H,-2.0976670254,-0.44890482,-0.2251960622\\Version=AM64L-
G09RevA.02\State=1-A\HF=-753.8359058\MP2=-755.4633011\RMSD=4.565e-09\R
MSF=9.696e-06\Dipole=-0.0612666,0.0500473,-0.0366406\PG=C01 [X(C12H18S
i1)]\\@

Pentamethyl(1-phenylvinyl)disilane (**1f**)

Geometry Optimization

θ = 0°

1\1\GINC-LINUX-IQS7\FOpt\RMP2-FC\6-31G(d)\C13H22Si2\AKM\11-Jul-2013\0\
\#p opt=(tight,calcfc,modredundant) freq mp2/6-31g(d)\\aSi2st 0deg Opt
+freq conf 3\\0,1\C,0.0293695344,-0.3283781541,-0.0293263806\C,1.43456
47079,-0.2345781227,-0.0578280779\C,1.9840457723,1.0166508086,-0.39084
30918\C,1.1819273032,2.1204282641,-0.6857579707\C,-0.2067517662,2.0023
88717,-0.6538641042\C,-0.7763626211,0.7698014446,-0.3225014681\C,2.331
2204409,-1.3844162197,0.2435345106\C,6.4251336385,-1.5778145892,-2.520
4206173\C,3.507623255,-0.9155801291,-3.2579780861\C,5.3770802433,1.266
347838,-2.1319382256\C,1.8345037592,-2.6018378585,0.5664454809\Si,4.89
83589185,-0.5664930526,-2.0230695833\Si,4.2292533517,-1.2111515428,0.1
508595789\C,5.0074283375,-2.8953111456,0.5407012923\C,4.8438138329,-0.
0152156299,1.4908322\H,-0.4524015736,-1.2692885495,0.2211036298\H,3.06
19888263,1.1396197348,-0.4182910142\H,1.6464032629,3.0711075341,-0.938
7507189\H,-0.8388643619,2.8570861994,-0.8821995141\H,-1.858415667,0.66
20742434,-0.2920087275\H,6.7503140695,-1.3087434806,-3.5313295863\H,7.
2658569388,-1.3975137488,-1.8426249532\H,6.2164136776,-2.6521032194,-2
.5124603035\H,3.817097506,-0.6623854131,-4.2780542018\H,3.2255488249,-
1.9734207746,-3.2464821873\H,2.6136879144,-0.3324107344,-3.0180313678\
H,6.1549673334,1.5234701098,-1.4057615678\H,5.7705893423,1.4885606851,
-3.1303040432\H,4.5256891895,1.9320393298,-1.9623023285\H,0.7700524128
,-2.817827179,0.6348073973\H,2.4849697862,-3.4432226801,0.7820926602\H
,4.7309143992,-3.246240063,1.5401692743\H,4.7205973862,-3.6648524082,-

0.1821703052\H,6.0986464947,-2.8083610032,0.5122900057\H,4.4570861481,
1.0002362658,1.3746009372\H,4.5387410048,-0.3761272347,2.4789464317\H,
5.9379083766,0.039461758,1.4799150257\\Version=AM64L-G09RevA.02\State=
1-A\HF=-1082.9573941\MP2=-1084.8030444\RMSD=9.946e-09\RMSF=2.863e-05\D
ipole=-0.035735,0.0037448,-0.014572\PG=C01 [X(C13H22Si2)]\\@

Global minimum at θ = 59.060°

1\1\GINC-LINUX-IQS7\FOpt\RMP2-FC\6-31G(d)\C13H22Si2\AKM\29-Jun-2013\0\
\#p opt=(tight,calcfc) freq mp2/6-31g(d)\\aSi2st Opt+freq conf 1\\0,1\
C,0.7189986271,0.4185326685,0.7899127987\C,1.6658938224,0.1476777405,-
0.2121706947\C,2.0369675982,1.1861774376,-1.0824044985\C,1.4719484264,
2.4560644632,-0.9582492226\C,0.5403844248,2.716331886,0.0503086585\C,0
.1590464801,1.6912120942,0.9189716084\C,2.2938408535,-1.1945764248,-0.
3035920837\C,6.3608353175,-0.498187492,2.6049877438\C,4.2792912793,1.6
609573148,1.9058188475\C,3.4130435761,-0.8877139494,3.4092581855\C,1.5
149721748,-2.2827166446,-0.4830785014\Si,4.5641036214,-0.2040884517,2.
0681972011\Si,4.1556575187,-1.3196588576,0.0372570726\C,5.1644075497,-
0.5449962074,-1.371240389\C,4.6353958833,-3.148836375,0.1544803879\H,0
.4274484394,-0.3804098524,1.4691312828\H,2.7477200661,0.9854188057,-1.
8805783805\H,1.7630518636,3.2460928829,-1.6470720678\H,0.1080377343,3.
7088231629,0.1522991104\H,-0.5695198733,1.884168357,1.7034681421\H,6.5
683304455,0.0082447349,3.5540262901\H,6.5693811761,-1.563745931,2.7446
022049\H,7.0682733137,-0.1138671002,1.8630454667\H,4.4977952288,2.1636
035699,2.8550206412\H,4.9291322801,2.0995920213,1.1414865755\H,3.24433
28325,1.8845826546,1.6317045625\H,3.6081241172,-0.404915959,4.37323514
66\H,2.3649544085,-0.7094141567,3.1511019545\H,3.547125931,-1.96595936
22,3.5436317569\H,0.4369313386,-2.1984890396,-0.6210213593\H,1.9258723
516,-3.2886812433,-0.5117040375\H,6.2331208496,-0.7152866567,-1.199959
003\H,4.9054891688,-0.9929293169,-2.3363728348\H,5.0110403524,0.535085
3254,-1.4431008509\H,5.705880826,-3.2487111545,0.3620966392\H,4.091792
0024,-3.6595931266,0.9549937949\H,4.430897994,-3.6757878179,-0.7834921
486\\Version=AM64L-G09RevA.02\State=1-A\HF=-1082.9627406\MP2=-1084.809
3291\RMSD=4.580e-09\RMSF=4.247e-08\Dipole=-0.0114692,0.0394214,-0.0018
951\PG=C01 [X(C13H22Si2)]\\@

θ = 90°

1\1\GINC-LINUX-IQS7\FOpt\RMP2-FC\6-31G(d)\C13H22Si2\AKM\05-Jul-2013\0\
\#p opt=(tight,calcfc,modredundant) freq mp2/6-31g(d)\\aSi2st 90deg Op
t+freq conf 2\\0,1\C,0.3536269011,-0.7318278697,-0.562536338\C,1.53398
46671,-0.2007581898,-0.0189593934\C,1.5288500794,1.1291068258,0.430224
7354\C,0.3800019559,1.9144638441,0.3165318757\C,-0.7877390566,1.376732
1138,-0.2296747605\C,-0.7953474326,0.0536795127,-0.6778008684\C,2.7475
847725,-1.0472362171,0.1360676854\C,1.6313382093,-4.4360073466,3.75906
72251\C,-0.4010314474,-2.4132843708,2.6593817462\C,0.8502034247,-4.547
5008382,0.7947698887\C,3.6467000331,-1.1162794791,-0.867090263\Si,1.17
60551523,-3.3774004051,2.2502163406\Si,2.9827966973,-1.9407674945,1.79
00706356\C,3.1102613376,-0.6241223312,3.1485541298\C,4.6005758247,-2.9
254291274,1.7365190761\H,0.3513691392,-1.7583731155,-0.9240161313\H,2.
4399403482,1.5503818798,0.8507164603\H,0.3949894851,2.9461179684,0.661
1924368\H,-1.6828306396,1.9880209934,-0.3157900822\H,-1.6985918721,-0.
3700967379,-1.1115090523\H,1.8410522621,-3.8152967102,4.6362632435\H,0
.8074876498,-5.1094644951,4.0199250817\H,2.5155684514,-5.0519934275,3.
5668310937\H,-1.2226911067,-3.1002153369,2.8917204193\H,-0.250903391,-
1.7692703189,3.532108325\H,-0.7120418467,-1.7769937884,1.8263034746\H,
0.5655563476,-4.0026466165,-0.1099066648\H,1.739529622,-5.1407469873,0

.5582063002\H,0.0399986331,-5.2452274117,1.0338103628\H,3.5048818698,-0.5770123399,-1.8033630887\H,4.5496223246,-1.7171828218,-0.7903247561\H,3.9802764537,0.0211113528,2.9860552173\H,2.2185178205,0.009320714,3.17065577\H,3.216951971,-1.0887951212,4.1347257519\H,5.4564671633,-2.2720133917,1.5377537325\H,4.7781557175,-3.4209495444,2.6966018214\H,4.5788324793,-3.6990433706,0.9626985691\\Version=AM64L-G09RevA.02\State=1-A\HF=-1082.962463\MP2=-1084.8077027\RMSD=5.120e-09\RMSF=2.880e-04\Dipole=-0.001951,0.023079,0.015092\PG=C01 [X(C13H22Si2)]\\@

(*E*)-(2-Phenylvinyl)trimethylsilane (**1g**)

Relaxed Potential Energy Surface Scan

θ / deg	d(C=C) / Å	E_{tot} / Hartree	ΔE / kcal mol^{-1}
0	1.3531	–716.2932930	0.14
10	1.3531	–716.2933780	0.08
20	1.3529	–716.2935083	0.00
30	1.3527	–716.2934448	0.04
40	1.3524	–716.2929899	0.33
50	1.3519	–716.2920825	0.90
60	1.3512	–716.2908528	1.67
70	1.3506	–716.2895877	2.46
80	1.3500	–716.2886249	3.06
90	1.3498	–716.2882500	3.30
100	1.3501	–716.2886029	3.08
110	1.3506	–716.2895835	2.46
120	1.3513	–716.2908690	1.66
130	1.3519	–716.2920888	0.89
140	1.3523	–716.2929801	0.33
150	1.3527	–716.2934377	0.05
160	1.3529	–716.2935102	0.00
170	1.3531	–716.2933797	0.08
180	1.3531	–716.2932930	0.14

1|1|UNPC-CURIUM|Scan|RMP2-FC|6-31G(d)|C11H16Si1|HANS|15-Jun-2013|0||#p
opt=(tight,modredundant) mp2/6-31g(d) nosymm||beta-TMS-styrene Torsio
n Potential 10deg||0,1|C,1.469738719,0.8019818596,-0.0406583114|C,1.30
2695322,0.9056973053,1.3399611126|C,0.8003181571,-0.1678263666,2.09463
42621|C,0.4683109192,-1.355763086,1.4200001371|C,0.6345452556,-1.46098
28756,0.0411413353|C,1.135687333,-0.383904762,-0.6964939127|H,1.860394
7572,1.6464798312,-0.6036888205|H,1.5647404646,1.8330861384,1.84736985
28|H,0.0770903336,-2.2051076474,1.9749785674|H,0.3719510704,-2.3884362
455,-0.4627307757|H,1.2638769149,-0.4703434767,-1.7727859548|C,0.64691
72659,0.0030503269,3.5479416591|H,0.9503647824,0.9865967254,3.91385218
58|C,0.1854283429,-0.9008612201,4.4428590195|H,-0.1174567339,-1.884131
3905,4.073815605|C,0.6154776137,1.1876477428,6.6647369401|H,0.52938585
35,1.3884810988,7.7376636142|H,1.6625722018,1.3386318881,6.3850639463|
H,0.0153098369,1.9377477046,6.1407436926|C,1.0974433959,-1.8061016519,
7.2275975003|H,1.0128380414,-1.653866327,8.3087429953|H,0.7945031029,-
2.8361030606,7.0141305053|H,2.1529357105,-1.7071806542,6.9564665852|C,
-1.7689124025,-0.7635969927,6.8024577924|H,-2.1411851441,-1.7683824662
,6.5787100072|H,-1.8888334676,-0.5985147537,7.8783649979|H,-2.41023656
84,-0.0475382041,6.2796531992|Si,0.0348719371,-0.5653933544,6.28055507
89||Version=IA32W-G09RevA.02|HF=-714.8060816,-714.8060922,-714.8060766
,-714.8058565,-714.8052755,-714.8043197,-714.8031302,-714.8019538,-714
.8010736,-714.8007301,-714.8010318,-714.8018991,-714.8030893,-714.8042
953,-714.8052571,-714.8058436,-714.8060756,-714.8060981,-714.8060817|M
P2=-716.293293,-716.293378,-716.2935083,-716.2934448,-716.2929899,-716
.2920825,-716.2908528,-716.2895877,-716.2886249,-716.28825,-716.288602
9,-716.2895835,-716.290869,-716.2920888,-716.2929801,-716.2934377,-716
.2935102,-716.2933797,-716.293293|RMSD=3.808e-009,3.086e-009,4.360e-00
9,3.446e-009,2.510e-009,4.623e-009,4.886e-009,7.534e-009,5.160e-009,8.
804e-009,3.106e-009,4.060e-009,5.154e-009,4.688e-009,5.303e-009,3.418e
-009,3.507e-009,5.150e-009,6.698e-009|PG=C01 [X(C11H16Si1)]||@

Geometry Optimization

Global minimum at θ = 23.122°

1|1|UNPC-HAFNIUM|FOpt|RMP2-FC|6-31G(d)|C11H16Si1|LAUCH|14-Jun-2013|0||
#p opt=(calcfc,tight) freq mp2/6-31g(d)||beta-TMS-styrene Opt+freq||0,
1|C,0.0043209699,-0.04220469,-0.0021533461|C,-0.0012703331,-0.03360734
16,1.3923088538|C,1.199703684,0.0097574501,2.1195130188|C,2.4100423346
,0.074682866,1.4086968886|C,2.4166435604,0.0673773592,0.0151833555|C,1
.2150038139,0.0057582458,-0.6963630274|H,-0.9359611025,-0.0831038551,-
0.5471552167|H,-0.9472521522,-0.0726517857,1.9305235838|H,3.3488144439
,0.1548728146,1.9521753803|H,3.3622280248,0.1234401268,-0.519356246|H,
1.2229591671,0.0046141218,-1.7836788635|C,1.1505063468,-0.0075275096,3
.5900014095|H,0.198113595,0.3112973271,4.0194445977|C,2.1443701111,-0.
3969494217,4.4211778621|H,3.074119941,-0.7492914594,3.9661792131|C,0.3
024788545,0.2131683506,6.8110497336|H,0.2180837951,0.2186126834,7.9027
138165|H,0.1066060327,1.2312426705,6.4609814013|H,-0.4898058699,-0.434
4820277,6.4233370254|C,3.3316924312,0.7608010525,7.0022079014|H,3.2973
276005,0.7701257481,8.0967211485|H,4.3374229532,0.4463677113,6.7057913
217|H,3.1879677389,1.7879553228,6.6534085082|C,2.2947411723,-2.1383257
243,6.9406244045|H,3.275046021,-2.5221310521,6.6407637574|H,2.24921378
31,-2.1656368116,8.0343949126|H,1.5365881578,-2.8273144377,6.556082057
9|Si,2.0128525192,-0.3883024201,6.290791307||Version=IA32W-G09RevA.02|
State=1-A|HF=-714.8060393|MP2=-716.2935203|RMSD=7.520e-009|RMSF=5.233e
-008|Dipole=-0.0229999,0.0095913,-0.0582698|PG=C01 [X(C11H16Si1)]||@

(2-Phenylallyl)trimethylsilane (**1h**)

Geometry Optimization

$\theta = 0°$

```
1\1\GINC-LINUX-IQS7\FOpt\RMP2-FC\6-31G(d)\C12H18Si1\AKM\27-Jun-2013\0\
 \#p opt=(tight,calcfc,modredundant) freq mp2/6-31g(d)\\2PhallylTMS 0de
 g Opt+freq conf 3\\0,1\C,0.1039781136,0.0852370566,-0.2085838777\C,1.4
 989504036,-0.0263803887,-0.0460882345\C,2.2146890616,1.1640868269,0.17
 77160928\C,1.5768617744,2.405840005,0.2030963161\C,0.1970298378,2.4938
 308526,0.0286572982\C,-0.5341686241,1.3226286846,-0.1851253773\C,2.186
 4596991,-1.3475600094,-0.04335962\C,6.350996884,-0.761925236,-1.391075
 9665\C,4.3678602535,-2.81921708,-2.5704058603\C,3.7146847777,0.1712403
 732,-2.7054448359\C,1.5165689491,-2.5106436562,-0.1957220217\Si,4.5272
 473593,-1.1728057722,-1.6623498545\C,3.6926554226,-1.3759022041,0.0422
 904282\H,-0.4977778345,-0.800913206,-0.3865339295\H,3.2893300607,1.138
 1022307,0.3229356016\H,2.1643508624,3.3052976305,0.3736967605\H,-0.302
 0318805,3.459594481,0.0486032587\H,-1.6122641564,1.3705060222,-0.32133
 46802\H,6.8879127112,-0.6930814757,-2.3427250005\H,6.4688894511,0.1962
 105873,-0.874460097\H,6.8455936827,-1.5284282393,-0.7857846784\H,4.805
 5237324,-2.7613592866,-3.5722104579\H,4.8762169099,-3.6249937376,-2.03
 09110045\H,3.3164373255,-3.1017850161,-2.681169954\H,4.1746612936,0.19
 76556158,-3.699576005\H,2.6457840851,-0.021787185,-2.8358868869\H,3.81
 69993509,1.1655093581,-2.262628454\H,0.4399967801,-2.5749355748,-0.302
 5314658\H,2.0503504651,-3.4564354032,-0.185867089\H,4.0745478707,-0.64
 43513184,0.761827762\H,4.0036653776,-2.3572349352,0.423951833\\Version
 =AM64L-G09RevA.02\State=1-A\HF=-753.828906\MP2=-755.4570824\RMSD=9.327
 e-09\RMSF=3.554e-04\Dipole=0.0635184,0.0860301,-0.0430248\PG=C01 [X(C1
 2H18Si1)]\\@
```

Global minimum at $\theta = 47.224°$

```
1\1\GINC-LINUX-IQS7\FOpt\RMP2-FC\6-31G(d)\C12H18Si1\AKM\28-Jun-2013\0\
 \#p opt=(tight,calcfc) freq mp2/6-31g(d)\\2PhallylTMS Opt+freq conf 1\
 \0,1\C,0.3776186456,-0.3361200646,0.5907773052\C,1.5751894858,-0.09224
 61821,-0.1009964438\C,1.8738508679,1.2264976413,-0.4802966334\C,0.9936
 995882,2.268194452,-0.1877096389\C,-0.1934542382,2.0138080937,0.503922
 6699\C,-0.5004672144,0.7071932672,0.8892666936\C,2.5096100395,-1.20588
 68111,-0.400791596\C,6.0810172592,-1.0854340546,2.18402858\C,3.5320806
 123,0.5798350896,2.6433953798\C,3.3637114032,-2.5022944991,2.603434004
 4\C,2.0427016099,-2.3569925242,-0.9219854125\Si,4.220960983,-0.9941866
 236,1.8646529074\C,3.9537117931,-1.0124918993,-0.0246232709\H,0.149313
 6217,-1.3516271911,0.9079729011\H,2.7887719713,1.4366356565,-1.0301897
 569\H,1.2358608306,3.2824216724,-0.4973986825\H,-0.8741571963,2.828309
 998,0.7396925708\H,-1.4195876102,0.5007796811,1.4331998511\H,6.2980762
 139,-1.0808820081,3.2571370864\H,6.5147251628,-1.9973554163,1.76148056
 72\H,6.6019304084,-0.2319633139,1.7380723335\H,3.7623070934,0.60624464
 74,3.7142972116\H,3.9684817391,1.4746993231,2.1879918308\H,2.447132371
 3,0.6463290517,2.5275012367\H,3.5407570891,-2.5679934419,3.6819304609\
 H,2.2827926543,-2.4556690723,2.441960318\H,3.7260948201,-3.4296803309,
 2.1480753304\H,0.9945454158,-2.4799367724,-1.1774933353\H,2.7025730645
 ,-3.1958678018,-1.1257714028\H,4.5566982756,-1.825057505,-0.4516708743
 \H,4.3474532397,-0.0772630617,-0.4448621913\\Version=AM64L-G09RevA.02\
 State=1-A\HF=-753.832846\MP2=-755.461708\RMSD=4.473e-09\RMSF=6.416e-08
 \Dipole=0.0435922,0.1369616,0.1098958\PG=C01 [X(C12H18Si1)]\\@
```

$\theta = 90°$

1\1\GINC-LINUX-IQS7\FOpt\RMP2-FC\6-31G(d)\C12H18Si1\AKM\03-Jul-2013\0\
\#p opt=(tight,calcfc,modredundant) freq mp2/6-31g(d)\\2PhallylTMS 90d
eg Opt+freq conf 3\\0,1\C,0.0459800617,0.0209581004,0.0697379421\C,1.4
471928809,-0.0374587511,0.0767050967\C,2.1727355128,1.1608487713,0.011
1833169\C,1.5134790365,2.3919350019,-0.018467529\C,0.1179291838,2.4391
2149,-0.0023186951\C,-0.6145119412,1.2502877227,0.039981751\C,2.132560
9386,-1.3605605764,0.0776369058\C,5.2988628863,-1.0239107502,1.3531687
443\C,3.2877619073,0.3151603687,3.3090333357\C,4.2106633598,-2.5692033
157,3.7845674814\C,2.4439698537,-1.948079722,-1.0914484477\Si,3.792794
1251,-1.2906083536,2.4574620114\C,2.3698487223,-2.0156460111,1.4127654
237\H,-0.524177855,-0.906115957,0.0914617343\H,3.2594210462,1.12484220
13,-0.02853935\H,2.0897278871,3.3131876725,-0.0686964633\H,-0.39636967
24,3.3968382653,-0.0273736179\H,-1.7018038523,1.280103666,0.0344021231
\H,6.15508039,-0.6694717499,1.9364127169\H,5.5932424033,-1.9583707753,
0.8641928628\H,5.1030261153,-0.2922341611,0.5645347594\H,4.1067328072,
0.6961258777,3.9287197486\H,3.0110439025,1.0931753161,2.5938014143\H,2
.4271743654,0.1494643589,3.9656724931\H,5.0129296871,-2.2120195346,4.4
384191911\H,3.3418380727,-2.7838692917,4.41523392\H,4.5401807372,-3.51
37676892,3.3401363722\H,2.2550991148,-1.4547811407,-2.0400439504\H,2.9
105342346,-2.9294065546,-1.1270104502\H,1.4485614751,-1.974531875,2.01
14716786\H,2.5984926136,-3.0790126035,1.2551974798\\Version=AM64L-G09R
evA.02\State=1-A\HF=-753.8300807\MP2=-755.4573582\RMSD=3.621e-09\RMSF=
7.526e-04\Dipole=-0.0203673,0.0434811,0.1301914\PG=C01 [X(C12H18Si1)]\
\@

Styrene (**6a**)

Relaxed Potential Energy Surface Scan

θ / deg	d(C=C) / Å	E_{tot} / Hartree	ΔE / kcal mol^{-1}
0	1.3433	–308.5930520	0.23
10	1.3432	–308.5931629	0.16
20	1.3431	–308.5933698	0.03
30	1.3428	–308.5934255	0.00
40	1.3424	–308.5931227	0.19
50	1.3419	–308.5923930	0.65
60	1.3412	–308.5913539	1.30
70	1.3406	–308.5902652	1.98
80	1.3401	–308.5894267	2.51
90	1.3399	–308.5890888	2.72
100	1.3401	–308.5893791	2.54
110	1.3406	–308.5902229	2.01
120	1.3413	–308.5913391	1.31
130	1.3419	–308.5923852	0.65
140	1.3424	–308.5931116	0.20
150	1.3428	–308.5934220	0.00
160	1.3430	–308.5933752	0.03
170	1.3432	–308.5931660	0.16
180	1.3433	–308.5930520	0.23

1|1|UNPC-UNUNBIUM|Scan|RMP2-FC|6-31G(d)|C8H8|LAUCH|13-Jun-2013|0||#p o
pt=(tight,modredundant) mp2/6-31g(d) nosymm||styrene Torsion Potential
10deg||0,1|C,-0.0298384573,1.3232062556,-0.2542753793|C,-0.2853464684
,1.3898254839,1.1153567479|C,0.5564545619,0.7558117617,2.0435633227|C,
1.6690147015,0.048504611,1.5558530292|C,1.9257028762,-0.019068738,0.18
83633525|C,1.0785340397,0.617310968,-0.7237743458|H,-0.6963499055,1.82
249105,-0.9536790473|H,-1.1518423865,1.9421727313,1.4758619099|H,2.341
0637095,-0.4538873581,2.247379151|H,2.7918200436,-0.5714048984,-0.1689
600569|H,1.2823912167,0.5621640178,-1.7903572826|C,0.2358347871,0.8612
320483,3.4756597675|C,0.9209349354,0.3248233348,4.499023143|H,1.820555
6229,-0.266666728,4.3614853079|H,0.5905713214,0.4679106462,5.522278212
7|H,-0.6578877107,1.4416609329,3.7065998939||Version=IA32W-G09RevA.02|
HF=-307.583208,-307.5832305,-307.5832559,-307.5831157,-307.5826529,-30
7.581842,-307.5808039,-307.5797621,-307.5789773,-307.5786724,-307.5789
467,-307.5797216,-307.5807751,-307.5818279,-307.5826437,-307.5831078,-

307.5832544,-307.5832344,-307.5832081|MP2=-308.593052,-308.5931629,-30
8.5933698,-308.5934255,-308.5931227,-308.592393,-308.5913539,-308.5902
652,-308.5894267,-308.5890888,-308.5893791,-308.5902229,-308.5913391,-
308.5923852,-308.5931116,-308.593422,-308.5933752,-308.593166,-308.593
052|RMSD=9.442e-009,5.225e-009,6.137e-009,9.487e-009,7.839e-009,7.235e
-009,4.184e-009,8.592e-009,7.268e-009,6.370e-009,3.071e-009,3.375e-009
,3.756e-009,9.231e-009,4.383e-009,6.575e-009,4.524e-009,6.592e-009,4.5
53e-009|PG=C01 [X(C8H8)]||@

Geometry Optimization

Global minimum at θ = 27.173°

1|1|UNPC-UNUNBIUM|FOpt|RMP2-FC|6-31G(d)|C8H8|LAUCH|13-Jun-2013|0||#p o
pt=(calcfc,tight) freq mp2/6-31g(d)||styrene Opt+freq||0,1|C,-0.001252
7733,0.0130984801,-0.0019843873|C,-0.0010617558,0.0031414744,1.3926048
99|C,1.2036089307,-0.0148463715,2.1134168151|C,2.4123801704,0.00934222
27,1.3984778619|C,2.4132428624,0.0169011501,0.0044404068|C,1.207305614
1,0.0171026753,-0.7015421936|H,-0.9447633024,0.0210213291,-0.542788190
6|H,-0.945745557,-0.0037133216,1.9341516203|H,3.3552493967,0.044710585
3,1.9395822202|H,3.3582156963,0.039409507,-0.5335520537|H,1.210253902,
0.0297240257,-1.7887715803|C,1.1670257825,-0.0506473536,3.5843148381|C
,2.1258785419,-0.5651776041,4.3711906784|H,3.0220289928,-1.0236112858,
3.9639800292|H,2.0321571482,-0.5524120372,5.4519298798|H,0.2703869421,
0.3585784493,4.0504005564||Version=IA32W-G09RevA.02|State=1-A|HF=-307.
5831832|MP2=-308.593439|RMSD=9.049e-009|RMSF=1.550e-008|Dipole=-0.0097
505,0.0068498,-0.0297608|PG=C01 [X(C8H8)]||@

α-Methylstyrene (**6b**)

Relaxed Potential Energy Surface Scan

θ / deg	d(C=C) / Å	E_{tot} / Hartree	ΔE / kcal mol^{-1}
0	1.3471	–347.7620406	1.42
10	1.3470	–347.7624942	1.13
20	1.3466	–347.7633327	0.60
30	1.3462	–347.7640201	0.17
40	1.3455	–347.7642962	0.00
50	1.3446	–347.7641165	0.11
60	1.3437	–347.7635913	0.44
70	1.3429	–347.7629176	0.87
80	1.3423	–347.7623314	1.23
90	1.3420	–347.7620667	1.40
100	1.3422	–347.7622660	1.27
110	1.3428	–347.7628544	0.90
120	1.3437	–347.7635635	0.46
130	1.3446	–347.7641072	0.12
140	1.3455	–347.7642973	0.00
150	1.3462	–347.7640440	0.16
160	1.3466	–347.7633654	0.58
170	1.3470	–347.7624990	1.13
180	1.3471	–347.7620406	1.42

1|1|UNPC-UNUNBIUM|Scan|RMP2-FC|6-31G(d)|C9H10|LAUCH|13-Jun-2013|0||#p
opt=(tight,modredundant) mp2/6-31g(d) nosymm||alpha-Me-sytrene Torsion
Potential 10deg||0,1|C,0.0520732677,2.4399761553,0.1238604211|C,0.106
9844919,2.3559885734,1.5163909089|C,0.389166024,1.1411816152,2.1663728
891|C,0.6144910998,0.0112744275,1.3569431869|C,0.560079937,0.093404704
5,-0.0319190558|C,0.2781734885,1.309615244,-0.6595335203|H,-0.16878215
,3.3953366943,-0.3468464404|H,-0.0741104158,3.2556127952,2.096026035|H
,0.8362975947,-0.9505390819,1.8100652874|H,0.7390807386,-0.7985624697,
-0.628081051|H,0.2359460792,1.3725472249,-1.7441690509|C,0.4424725943,
1.0755519347,3.6503992541|C,0.7078957701,-0.0594205252,4.3256381295|H,
0.9028024644,-1.0105448879,3.8435045885|H,0.7370685162,-0.0624917132,5
.4108202416|C,0.1850454072,2.3477102242,4.4198921801|H,0.2540547749,2.
1607737289,5.4942341964|H,0.912818334,3.1246529256,4.1637205127|H,-0.8
119624702,2.7482375465,4.2090119024||Version=IA32W-G09RevA.02|HF=-346.
6173496,-346.6175376,-346.618197,-346.6188142,-346.619103,-346.6190338

,-346.6186767,-346.6181674,-346.6177154,-346.6175292,-346.6177068,-346
.6181673,-346.618687,-346.6190396,-346.6191059,-346.6188399,-346.61825
96,-346.6176129,-346.6173496|MP2=-347.7620406,-347.7624942,-347.763332
7,-347.7640201,-347.7642962,-347.7641165,-347.7635913,-347.7629176,-34
7.7623314,-347.7620667,-347.762266,-347.7628544,-347.7635635,-347.7641
072,-347.7642973,-347.764044,-347.7633654,-347.762499,-347.7620406|RMS
D=9.790e-009,4.649e-009,8.557e-009,5.394e-009,8.334e-009,4.559e-009,3.
941e-009,6.251e-009,6.036e-009,6.554e-009,5.794e-009,8.547e-009,9.338e
-009,5.991e-009,7.911e-009,4.274e-009,6.241e-009,3.893e-009,4.351e-009
|PG=C01 [X(C9H10)]||@

Geometry Optimization

Global minimum at θ = 40.861°

1|1|UNPC-HAFNIUM|FOpt|RMP2-FC|6-31G(d)|C9H10|LAUCH|13-Jun-2013|0||#p o
pt=(calcfc,tight) freq mp2/6-31g(d)||alpha-Me-sytrene Opt+freq||0,1|C,
-0.0091562043,0.0018829799,0.0059110468|C,-0.0019917155,-0.0177399943,
1.4005615858|C,1.2069751725,-0.0067792694,2.1154734825|C,2.4102273902,
-0.0018796032,1.3910432174|C,2.4035297774,0.0181636883,-0.0038560941|C
,1.1942204975,0.0202366406,-0.7023208381|H,-0.9562162013,-0.0126561039
,-0.5288160125|H,-0.9400279052,-0.0645874591,1.949156463|H,3.361149417
2,0.0083991809,1.9182683662|H,3.3458073028,0.0318916655,-0.5469893903|
H,1.1900621228,0.0303372851,-1.7896037524|C,1.2047744745,-0.0079285486
,3.5982884505|C,0.3217323226,0.7399772017,4.284632645|H,-0.3808298516,
1.3974535612,3.7821191965|H,0.2928990836,0.7273828609,5.3703719309|C,2
.2180837155,-0.876947387,4.2972238603|H,2.0535998232,-0.8698287784,5.3
780867441|H,2.1584907456,-1.9098289975,3.9392073522|H,3.2399411979,-0.
5286063968,4.1129641392||Version=IA32W-G09RevA.02|State=1-A|HF=-346.61
91104|MP2=-347.7642979|RMSD=2.501e-009|RMSF=7.214e-009|Dipole=0.076468
2,-0.0719296,-0.0087354|PG=C01 [X(C9H10)]||@

1-Phenyl-1-(trimethylsiloxy)ethene (**6d**)

Geometry Optimization

θ = 0°

1\1\GINC-LINUX-IQS7\FOpt\RMP2-FC\6-31G(d)\C11H16O1Si1\AKM\25-Jun-2013\
0\\#p opt=(tight,calcfc,modredundant) freq mp2/6-31g(d)\\aOTMSst 0deg
Opt+freq conf 2\\0,1\C,0.0525520134,-0.0197541357,0.0298002211\C,1.457
9920492,-0.0303503778,-0.0009971633\C,2.1355584676,1.1995007287,0.0091
140128\C,1.4307736782,2.4012792085,0.0877106098\C,0.036780598,2.399847
3823,0.1399136455\C,-0.6475203357,1.181556565,0.1132328683\C,2.2321320
793,-1.2907143445,-0.1013636693\C,3.6601226557,-0.7666356609,2.7833873
021\C,4.8710450342,-3.2625707197,1.4480087301\C,6.1457853163,-0.501662
6366,0.9324122337\C,1.711468825,-2.5298709693,-0.1726010731\Si,4.54811
81277,-1.4209997774,1.2645056832\O,3.6050998762,-1.1087712189,-0.11651
22786\H,-0.5045604146,-0.9525846961,0.0172091892\H,3.2180419007,1.2061
939605,-0.0633024411\H,1.9753604408,3.3428019215,0.0965133271\H,-0.512
6583206,3.3360409543,0.2026857661\H,-1.7345459528,1.1668763686,0.14532
57778\H,3.4778728281,0.3091636381,2.7095144682\H,2.6921436766,-1.25953
10526,2.9142283421\H,4.2527466786,-0.9501078516,3.6859834112\H,5.56902
70358,-3.4485139324,2.2715240037\H,3.9507607149,-3.8126740871,1.663768

8319\H,5.3100484355,-3.679648738,0.5367753503\H,5.9689576309,0.5740967
298,0.8428124198\H,6.8681699823,-0.6571720436,1.7401582218\H,6.6054741
755,-0.8435653662,0.0006592122\H,0.6437133168,-2.7040659628,-0.1948122
362\H,2.3635394865,-3.3891638861,-0.2726547661\\Version=AM64L-G09RevA.
02\State=1-A\HF=-789.7005677\MP2=-791.368941\RMSD=2.289e-09\RMSF=5.228
e-04\Dipole=-0.0279235,-0.0149473,0.5033032\PG=C01 [X(C11H16O1Si1)]\\@

Global minimum at θ = 34.317°

1\1\GINC-LINUX-IQS7\FOpt\RMP2-FC\6-31G(d)\C11H16O1Si1\AKM\25-Jun-2013\
0\\#p opt=(tight,calcfc) freq mp2/6-31g(d)\\aOTMSst Opt+freq conf 7\\0
,1\C,4.4457549722,-2.031604094,4.0679310472\C,4.7010861344,-2.46541350
32,2.757839541\C,5.7456307992,-1.8725445972,2.0324279923\C,6.535170934
1,-0.8816352986,2.6157500291\C,6.2830231384,-0.4607475803,3.9237592129
\C,5.2363143177,-1.0390618642,4.6465281897\C,3.8652970992,-3.531766030
6,2.1640494618\C,0.944501904,-3.4121372052,0.1964581001\C,1.9173741828
,-0.8756488252,1.6434988622\C,-0.1097863327,-2.766271522,3.0365595456\
C,4.3183911115,-4.4576285416,1.3008118177\Si,1.3459180621,-2.650413699
,1.8654060862\O,2.5598156033,-3.569178009,2.6255744088\H,3.634944239,-
2.4904384564,4.6272823122\H,5.9228138001,-2.1754594535,1.0027739724\H,
7.3377461791,-0.4241848161,2.0416989477\H,6.8952764303,0.3163673904,4.
3749989221\H,5.0355773426,-0.7155725049,5.6654271206\H,0.1572455448,-2
.8464199726,-0.3129445194\H,1.824081879,-3.4196704505,-0.4541432666\H,
0.5995136575,-4.4444723075,0.3068557697\H,1.127315228,-0.2770796949,1.
1766514547\H,2.1718868431,-0.4149227281,2.602123216\H,2.8034262286,-0.
8150580952,1.0046731917\H,-0.9813679152,-2.237300416,2.6378085741\H,-0
.3960022438,-3.8087383938,3.2022192521\H,0.1347212708,-2.327173855,4.0
079878621\H,5.3629232938,-4.4867067231,1.0154524204\H,3.6554062962,-5.
2221187527,0.9125404758\\Version=AM64L-G09RevA.02\State=1-A\HF=-789.70
19593\MP2=-791.3710578\RMSD=6.982e-09\RMSF=5.241e-08\Dipole=-0.0600589
,0.4706473,-0.258491\PG=C01 [X(C11H16O1Si1)]\\@

θ = 90°

1\1\GINC-LINUX-IQS7\FOpt\RMP2-FC\6-31G(d)\C11H16O1Si1\AKM\27-Jun-2013\
0\\#p opt=(tight,calcfc,modredundant) freq mp2/6-31g(d)\\aOTMSst 90deg
 Opt+freq conf 4\\0,1\C,1.6898421572,-0.3558035568,0.7921684953\C,1.13
52305738,-0.5164923697,-0.4851399751\C,0.6715889682,0.6096146362,-1.18
02088874\C,0.7506677261,1.8757829653,-0.6000405872\C,1.3112235814,2.03
09971273,0.6711580848\C,1.7710190386,0.9127950028,1.3709894223\C,1.130
7883578,-1.8445856204,-1.152264219\C,4.5902754167,-2.2866372203,-0.391
8217073\C,4.5245332943,-2.4166303049,-3.4722357619\C,4.0099469279,0.25
56394078,-2.0402658332\C,0.1340872385,-2.7318358584,-1.022920945\Si,3.
7894713435,-1.6078684486,-1.951152005\O,2.1601156765,-2.0863756956,-2.
0376219689\H,2.0277984995,-1.2329734872,1.3398896892\H,0.2445343244,0.
4820128302,-2.1728360275\H,0.3822556322,2.7440361072,-1.1415833601\H,1
.3756446396,3.0190068105,1.1207693756\H,2.1961340783,1.0289661802,2.36
53484591\H,5.6769230673,-2.1552437039,-0.4387169221\H,4.2348464153,-1.
7752587134,0.5062374441\H,4.3878674023,-3.3558241229,-0.2780816485\H,4
.4036153073,-3.5027872847,-3.4358049504\H,4.0339960478,-2.0560062445,-
4.3807648235\H,5.5938898723,-2.1979985397,-3.5579911566\H,3.6480773251
,0.7633135125,-1.1430301882\H,5.0747699259,0.4890203198,-2.1568681829\
H,3.4819006393,0.6764528931,-2.901158295\H,-0.7051743945,-2.5160609999
,-0.3734705196\H,0.1561309175,-3.675255622,-1.556583006\\Version=AM64L
-G09RevA.02\State=1-A\HF=-789.6948123\MP2=-791.3666622\RMSD=7.250e-09\
RMSF=6.923e-04\Dipole=0.3016198,0.5396883,0.3445493\PG=C01 [X(C11H16O1
Si1)]\\@

p-Methylstyrene (**8**)

Geometry Optimization

θ = 0°


```
1|1|UNPC-HAFNIUM|FOpt|RMP2-FC|6-31G(d)|C9H10|LAUCH|11-Jun-2013|0||#p o
 pt=(calcfc,tight,modredundant) freq mp2/6-31g(d)||pMe-styrene Opt+freq
  0deg||0,1|C,0.0000021704,-0.0003067428,0.0000420791|C,0.0000504367,-0
 .0001659379,1.3917605655|C,1.2074125712,-0.0004222605,2.1112222136|C,2
 .4046812131,-0.0085233784,1.378721962|C,2.3997308388,-0.0087795574,-0.
 0152986426|C,1.1971827913,-0.008998498,-0.7304738203|H,-0.9501024631,-
 0.0037481392,-0.5326931531|H,-0.9504049141,0.00223611,1.9203981999|H,3
 .354313226,-0.013525296,1.9121508643|H,3.3456039163,-0.018730817,-0.55
 4995987|C,1.2721469103,-0.0032772833,3.5801475725|C,0.2356386458,-0.00
 59819417,4.4348472476|H,-0.7990392255,-0.0082894703,4.1068783513|H,0.4
 011580523,-0.0067877791,5.5068912265|H,2.2796388651,-0.0015104848,3.99
 74385408|C,1.1841930999,0.0295980183,-2.2361000007|H,0.3361571837,-0.5
 332094331,-2.6371788654|H,1.1028233772,1.0580224836,-2.6052153224|H,2.
 1018929472,-0.3995005827,-2.6482568947||Version=IA32W-G09RevA.02|State
 =1-A|HF=-346.6203074|MP2=-347.7640695|RMSD=7.971e-009|RMSF=6.487e-006|
 Dipole=0.0027893,0.0146178,-0.188092|PG=C01 [X(C9H10)]||@
```


Global minimum at θ = 25.887°


```
1|1|UNPC-MEITNERIUM|FOpt|RMP2-FC|6-31G(d)|C9H10|LAUCH|05-Jul-2013|0||#
 p opt=(calcfc,tight) freq mp2/6-31g(d)||pMe-styrene Opt+freq||0,1|C,0.
 0022063328,-0.014906417,-0.0010882571|C,0.0022967,-0.0234453316,1.3917
 012729|C,1.2094625214,-0.0118978705,2.1090723852|C,2.4085409638,0.0373
 497336,1.3815662617|C,2.4026966159,0.0477734441,-0.0120844403|C,1.1999
 607423,0.0158336744,-0.728393763|H,-0.9470470556,-0.0240921873,-0.5352
 397294|H,-0.9434291709,-0.0176464547,1.9294122601|H,3.3570060899,0.053
 8168265,1.9167306925|H,3.3479432797,0.0761747406,-0.5523344661|C,1.251
 2026277,-0.0491188466,3.5788769637|C,0.3008142713,-0.5719167211,4.3708
 995066|H,-0.5932427965,-1.0388377938,3.9688448057|H,0.3997311502,-0.55
 70807299,5.4511516291|H,2.1456798767,0.3691030039,4.0413638671|C,1.189
 941665,0.0721578223,-2.2337096312|H,0.3348192707,-0.4741716299,-2.6421
 940216|H,1.124205897,1.1057120809,-2.5914099755|H,2.1022150968,-0.3651
 072522,-2.6494671414||Version=IA32W-G09RevA.02|State=1-A|HF=-346.62023
 77|MP2=-347.7643959|RMSD=8.530e-009|RMSF=2.864e-008|Dipole=0.0092134,0
 .0247309,-0.168531|PG=C01 [X(C9H10)]||@
```


θ = 90°


```
1|1|UNPC-UNUNBIUM|FOpt|RMP2-FC|6-31G(d)|C9H10|LAUCH|05-Jul-2013|0||#p
 opt=(calcfc,tight,modredundant) freq mp2/6-31g(d)||pMe-styrene Opt+fre
 q 90deg||0,1|C,-0.0000257146,-0.0000148314,-0.0000441416|C,-0.00011219
 71,0.0000260676,1.3949888185|C,1.2057450402,0.0000551061,2.1091736553|
 C,2.4083964991,0.0123824673,1.3896494521|C,2.4021312717,0.0123002236,-
 0.005329335|C,1.1994446689,0.0060664706,-0.7229279369|H,-0.9482482326,
 -0.0113168961,-0.5358853635|H,-0.9424634751,-0.0136088765,1.9391991175
 |H,3.353300276,0.00825725,1.929593952|H,3.3480370928,0.0105466504,-0.5
 453673643|C,1.2090734205,0.0042184237,3.593641038|C,1.2088802992,-1.11
 50060605,4.3303873786|H,1.2057288776,-2.0968817241,3.866212037|H,1.211
 6670182,-1.0804993308,5.4154957766|H,1.212885517,0.973772706,4.0934159
```

```
361|C,1.1959570065,0.047587316,-2.22918704|H,0.3118201722,-0.452690123
3,-2.6346610714|H,1.1908478941,1.0796263838,-2.5968769931|H,2.08244936
87,-0.4452938251,-2.6385660137||Version=IA32W-G09RevA.02|State=1-A|HF=
-346.6155798|MP2=-347.7598908|RMSD=9.779e-009|RMSF=2.123e-005|Dipole=0
.0000466,0.0147965,-0.1154965|PG=C01 [X(C9H10)]||@
```

4.6 References

[1] a) C. Eaborn, *Organosilicon Compounds*, Butterworth, London, **1960**; b) E. W. Colvin, *Chem. Soc. Rev.* **1978**, *7*, 15–64; c) T. H. Chan, I. Fleming, *Synthesis* **1979**, 761–786; d) E. W. Colvin, *Silicon in Organic Synthesis*, Butterworth, London, **1981**; e) I. Fleming, *Chem. Soc. Rev.* **1981**, *10*, 83–111; f) L. A. Paquette, *Science* **1982**, *217*, 793–800; g) S. Pawlenko, *Organosilicon Chemistry*, de Gruyter, Berlin, **1986**; h) E. W. Colvin, *Silicon Reagents in Organic Synthesis*, Academic Press, London, **1988**; i) I. Fleming, J. Dunoguès, R. Smithers in *Organic Reactions*, *Vol. 37*, Wiley, Hoboken, NJ, **1989**, pp. 57–575; j) J. S. Panek in *Comprehensive Organic Synthesis, Vol. 1* (Eds.: B. M. Trost, I. Fleming, S. L. Schreiber), Pergamon, Oxford, **1991**, pp. 579–627; k) I. Fleming, A. Barbero, D. Walter, *Chem. Rev.* **1997**, *97*, 2063–2192; l) M. A. Brook, *Silicon in Organic, Organometallic, and Polymer Chemistry*, Wiley, New York, **2000**; m) K. Oshima in *Science of Synthesis*, *Vol. 4* (Eds.: I. Fleming), Thieme Verlag, Stuttgart, **2002**, pp. 713–756; n) T. K. Sarkar in *Science of Synthesis*, *Vol. 4* (Eds.: I. Fleming), Thieme Verlag, Stuttgart, **2002**, pp. 837–925; o) L. Chabaud, P. James, Y. Landais, *Eur. J. Org. Chem.* **2004**, 3173–3199; p) M. J. Curtis-Long, Y. Aye, *Chem. Eur. J.* **2009**, *15*, 5402–5416.

[2] T. A. Blumenkopf, L. E. Overman, *Chem. Rev.* **1986**, *86*, 857–873.

[3] a) J. Cudlin, V. Chvalovsky, *Collect. Czech. Chem. Commun.* **1962**, *27*, 1658–1665; b) J. Cudlin, V. Chvalovsky, *Collect. Czech. Chem. Commun.* **1963**, *28*, 3088–3095; c) I. A. D'Yakonov, G. V. Golodnikov, I. B. Repinskaya, *Zh. Obshch. Khim.* **1965**, *35*, 2181–2189; d) D. Seyferth, H. M. Cohen, *Inorg. Chem.* **1962**, *1*, 913–916; e) D. Seyferth, H. Dertouzos, *J. Organomet. Chem.* **1968**, *11*, 263–270.

[4] a) H. Sakurai, N. Hayashi, M. Kumada, *J. Organomet. Chem.* **1969**, *18*, 351–354; b) G. S. Patil, G. Nagendrappa, *J. Chem. Soc. Perkin Trans. 2* **2001**, 1099–1102.

[5] a) L. H. Sommer, F. J. Evans, *J. Am. Chem. Soc.* **1954**, *76*, 1186–1187; b) L. H. Sommer, D. L. Bailey, G. M. Goldberg, C. E. Buck, T. S. Bye, F. J. Evans, F. C. Whitmore, *J. Am. Chem. Soc.* **1954**, *76*, 1613–1618.

[6] J. A. Soderquist, A. Hassner, *Tetrahedron Lett.* **1988**, *29*, 1899–1902.

[7] a) H. Mayr, T. Bug, M. F. Gotta, N. Hering, B. Irrgang, B. Janker, B. Kempf, R. Loos, A. R. Ofial, G. Remennikov, H. Schimmel, *J. Am. Chem. Soc.* **2001**, *123*, 9500–9512; b) H. Mayr, B. Kempf, A. R. Ofial, *Acc. Chem. Res.* **2003**, *36*, 66–77; c) H. Mayr, A. R. Ofial in *Carbocation Chemistry* (Eds.: G. A. Olah, G. K. S. Prakash), Wiley, Hoboken, NJ, **2004**, pp. 331–358; d) H. Mayr, A. R. Ofial, *Pure Appl. Chem.* **2005**, *77*, 1807–1821; e) H. Mayr, A. R. Ofial, *J. Phys. Org. Chem.* **2008**, *21*, 584–595; f) J. Ammer, C. Nolte, H. Mayr, *J. Am. Chem. Soc.* **2012**, *134*, 13902–13911; g) For a comprehensive database of reactivity parameters see http://www.cup.uni-muenchen.de/oc/mayr/DBintro.html.

[8] a) G. Hagen, H. Mayr, *J. Am. Chem. Soc.* **1991**, *113*, 4954–4961; b) H. A. Laub, H. Yamamoto, H. Mayr, *Org. Lett.* **2010**, *12*, 5206–5209.

[9] J. Burfeindt, M. Patz, M. Müller, H. Mayr, *J. Am. Chem. Soc.* **1998**, *120*, 3629–3634.

[10] a) G. Hagen, PhD thesis, Medizinische Universität zu Lübeck (Germany), **1990**; b) M. Herrlich, PhD thesis, Ludwig-Maximilians-Universität München (Germany), **2001**.

[11] M. D. Paredes, R. Alonso, *J. Org. Chem.* **2000**, *65*, 2292–2304.

[12] a) H. Mayr, R. Pock, *Chem. Ber.* **1986**, *119*, 2473–2496; b) H. Mayr, R. Schneider, B. Irrgang, C. Schade, *J. Am. Chem. Soc.* **1990**, *112*, 4454–4459.

[13] a) H. Mayr, R. Schneider, C. Schade, J. Bartl, R. Bederke, *J. Am. Chem. Soc.* **1990**, *112*, 4446–4454; b) H. Mayr, R. Schneider, U. Grabis, *J. Am. Chem. Soc.* **1990**, *112*, 4460–4467.

[14] a) H. Suzuki, *Bull. Chem. Soc. Jpn.* **1960**, *33*, 619–628; b) H. Suzuki, *Electronic absorption spectra and geometry of organic molecules: An application of molecular orbital theory*, Academic Press, New York, **1967**; c) I. Benito, H. Seidl, H. Bock, *Rev. Fac. Cienc., Univ. Oviedo* **1973**, *14*, 95–110.

[15] a) H. Bock, J. Meuret, K. Ruppert, *Angew. Chem.* **1993**, *105*, 413–415; *Angew. Chem. Int. Ed. Engl.* **1993**, *32*, 414–416; b) M. B. Boxer, H. Yamamoto, *J. Am. Chem. Soc.* **2007**, *129*, 2762–2763.

[16] M. Herrlich, N. Hampel, H. Mayr, *Org. Lett.* **2001**, *3*, 1629–1632.

[17] Similar effects have also been reported for hyperconjugative interactions with C-S vs. S-C bonds: a) I. V. Alabugin, T. A. Zeidan, *J. Am. Chem. Soc.* **2002**, *124*, 3175–3185; b) I. V. Alabugin, K. M. Gilmore, P. W. Peterson, *WIREs Comp. Mol. Sci.* **2011**, *1*, 109–141.

[18] a) H. Bürger, W. Kilian, *J. Organomet. Chem.* **1969**, *18*, 299–306; b) C. Marschner, *Eur. J. Inorg. Chem.* **1998**, *1998*, 221–226.

[19] H. Gilman, R. L. Harrell, *J. Organomet. Chem.* **1966**, *5*, 199–200.

[20] D. C. Anderson, D. W. H. Rankin, H. E. Robertson, C. M. F. Frazão, H. Schmidbaur, *Chem. Ber.* **1989**, *122*, 2213–2218.

[21] M. Kumada, K. Naka, M. Ishikawa, *J. Organomet. Chem.* **1964**, *2*, 136–145.

[22] a) S. Menichetti, C. J. M. Stirling, *J. Chem. Soc. Perkin Trans. 1* **1996**, 1511–1515; b) T. Uchida, Y. Kita, H. Maekawa, I. Nishiguchi, *Tetrahedron* **2006**, *62*, 3103–3111.

[23] H. Sakurai, Y. Kamiya, Y. Nakadaira, *J. Organomet. Chem.* **1980**, *184*, 13–30.

[24] M. Doyle, W. Jackson, P. Perlmutter, *Aust. J. Chem.* **1989**, *42*, 1907–1918.

[25] D. Ferraris, B. Young, C. Cox, T. Dudding, W. J. Drury, L. Ryzhkov, A. E. Taggi, T. Lectka, *J. Am. Chem. Soc.* **2001**, *124*, 67–77.

[26] B. Denegri, A. Streiter, S. Jurić, A. R. Ofial, O. Kronja, H. Mayr, *Chem. Eur. J.* **2006**, *12*, 1648–1656.

[27] W. M. Czaplik, M. Mayer, A. Jacobi von Wangelin, *ChemCatChem* **2011**, *3*, 135–138.

[28] A. M. Caporusso, L. Lardicci, *J. Chem. Soc. Perkin Trans. 1* **1983**, 949–953.

[29] T. Matsuda, S. Shiose, Y. Suda, *Adv. Synth. Catal.* **2011**, *353*, 1923–1926.

[30] H.-L. Yue, W. Wei, M.-M. Li, Y.-R. Yang, J.-X. Ji, *Adv. Synth. Catal.* **2011**, *353*, 3139–3145.

[31] a) H. Bock, H. Seidl, *J. Organomet. Chem.* **1968**, *13*, 87–102; b) C. G. Pitt, *J. Organomet. Chem.* **1973**, *61*, 49–70; c) S. Kyushin, M. Ikarugi, M. Goto, H. Hiratsuka, H. Matsumoto, *Organometallics* **1996**, *15*, 1067–1070.

[32] M. Frenkel, X. Hong, Q. Dong, X. Yan, R. D. Chirico in *Landolt-Börnstein, New Series - Group IV Physical Chemistry*, *Vol. 8J* (Eds.: M. Frenkel, K. N. Marsh), Springer, Berlin, **2003**, pp. 107–130.

[33] (a) J. I. Seeman, V. H. Grassian, E. R. Bernstein, *J. Am. Chem. Soc.* **1988**, *110*, 8542–8543; (b) V. H. Grassian, E. R. Bernstein, H. V. Secor, J. I. Seeman, *J. Phys. Chem.* **1989**, *93*, 3470–3474.

[34] V. H. Grassian, E. R. Bernstein, H. V. Secor, J. I. Seeman, *J. Phys. Chem.* **1990**, *94*, 6691–6695.

[35] (a) S. Tsuzuki, K. Tanabe, E. Osawa, *J. Phys. Chem.* **1990**, *94*, 6175–6179; (b) M. Head-Gordon, J. A. Pople, *J. Phys. Chem.* **1993**, *97*, 1147–1151; (c) A. Karpfen, C. H. Choi, M. Kertesz, *J. Phys. Chem. A* **1997**, *101*, 7426–7433; (d) J. C. Sancho-García, A. J. Pérez-Jiménez, *J. Phys. B: At. Mol. Opt. Phys.* **2002**, *35*, 1509–1523.

[36] Gaussian 09, Revision A.02, Frisch, M. J.; Trucks, G. W.; Schlegel, H. B.; Scuseria, G. E.; Robb, M. A.; Cheeseman, J. R.; Scalmani, G.; Barone, V.; Mennucci, B.; Petersson, G. A.;

Nakatsuji, H.; Caricato, M.; Li, X.; Hratchian, H. P.; Izmaylov, A. F.; Bloino, J.; Zheng, G.; Sonnenberg, J. L.; Hada, M.; Ehara, M.; Toyota, K.; Fukuda, R.; Hasegawa, J.; Ishida, M.; Nakajima, T.; Honda, Y.; Kitao, O.; Nakai, H.; Vreven, T.; Montgomery, Jr., J. A.; Peralta, J. E.; Ogliaro, F.; Bearpark, M.; Heyd, J. J.; Brothers, E.; Kudin, K. N.; Staroverov, V. N.; Kobayashi, R.; Normand, J.; Raghavachari, K.; Rendell, A.; Burant, J. C.; Iyengar, S. S.; Tomasi, J.; Cossi, M.; Rega, N.; Millam, J. M.; Klene, M.; Knox, J. E.; Cross, J. B.; Bakken, V.; Adamo, C.; Jaramillo, J.; Gomperts, R.; Stratmann, R. E.; Yazyev, O.; Austin, A. J.; Cammi, R.; Pomelli, C.; Ochterski, J. W.; Martin, R. L.; Morokuma, K.; Zakrzewski, V. G.; Voth, G. A.; Salvador, P.; Dannenberg, J. J.; Dapprich, S.; Daniels, A. D.; Farkas, Ö.; Foresman, J. B.; Ortiz, J. V.; Cioslowski, J.; Fox, D. J. Gaussian, Inc., Wallingford CT, 2009.

[37] MacroModel, Version 9.7, Schrödinger, LLC, New York, NY, 2009.

[38] M. Mishima, T. Ariga, Y. Tsuno, K. Ikenaga, K. Kikukawa, *Chem. Lett.* **1992**, *21*, 489–492.

[39] S. G. Wierschke, J. Chandrasekhar, W. L. Jorgensen, *J. Am. Chem. Soc.* **1985**, *107*, 1496–1500.

[40] a) K. Fukui, T. Yonezawa, H. Shingu, *J. Chem. Phys.* **1952**, *20*, 722–725; b) I. Fleming, *Frontier Orbitals and Organic Chemical Reactions*; Wiley, Hoboken, NJ, **1977**; c) I. Fleming, *Molecular Orbitals and Organic Chemical Reactions: Reference Edition*; Wiley, Hoboken, NJ, **2010**.

Chapter 5

Hydrocarbation of CC-Triple Bonds: Quantification of the Nucleophilic Reactivity of Ynamides

Reproduced with permission from

H. A. Laub, G. Evano, H. Mayr, *Angew. Chem.*; *Angew. Chem. Int. Ed.* in press.

5.1 Introduction

Hydroborations[1] of CC double and triple bonds belong to the most reliable reactions in organic synthesis (Scheme 5.1a). As carbenium ions are isoelectronic with boranes, one might wonder why analogous reactions of carbenium ions (Scheme 5.1b) have so far not been reported despite the potential of such reactions in organic synthesis. We now show that such reactions occur when ynamides[2] are combined with stabilized benzhydrylium ions and discuss why hydrocarbations of alkenes and alkynes do not usually take place.

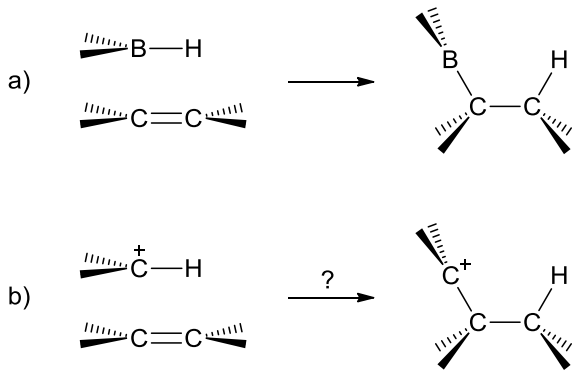

Scheme 5.1. Hydroborations of alkenes (a) compared with analogous hydrocarbations (b).

5.2 Results and Discussion

During our efforts to investigate the nucleophilic reactivity of ynamides **1a–d**[3] (Table 5.1) by the benzhydrylium methodology,[4] we observed the formation of a green species when the blue benzhydrylium tetrafluoroborate **2c–BF$_4$** (Table 5.2) was combined with ynamide **1d** in CH_2Cl_2 (Figure 5.1).

Table 5.1. Absorption Maxima A and B of the Developing α,β-Unsaturated Iminium Ions during the Reactions of Benzhydrylium Ions **2a–c** with Ynamides **1a–d** in Dichloromethane.

Ynamides	Products from **2a**		Products from **2b**		Products from **2c**	
	λ_A / nm	λ_B / nm	λ_A / nm	λ_B / nm	λ_A / nm	λ_B / nm
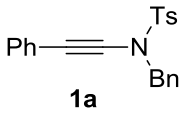 **1a**	520	752	474	670	478	670
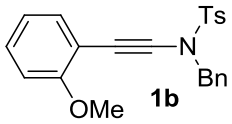 **1b**	510	736	467	652	472	654
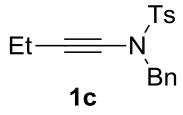 **1c**	513	731	467	650	472	650
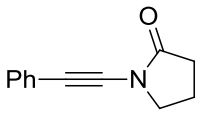 **1d**	–	–	–	–	480	649

Table 5.2. Reference Electrophiles Used for Quantifying the Nucleophilicities of **1a–d**.

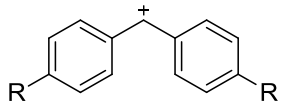

Ar_2CH^+ [a]	R	**2**	λ_{max} [b] / nm	E [c]
$(dpa)_2CH^+$	NPh_2	**2a**	672	–4.72
$(mfa)_2CH^+$	$N(CH_3)CH_2CF_3$	**2b**	593	–3.85
$(pfa)_2CH^+$	$N(Ph)CH_2CF_3$	**2c**	601	–3.14

[a] dpa=4-(*dip*henyl*a*mino)phenyl; mfa=4-(*m*ethyl(tri*f*luoroethyl)*a*mino)phenyl; pfa=4-(*p*henyl(tri*f*luoroethyl)*a*mino)phenyl. [b] In dichloromethane. [c] Empirical electrophilicities E from ref [4a].

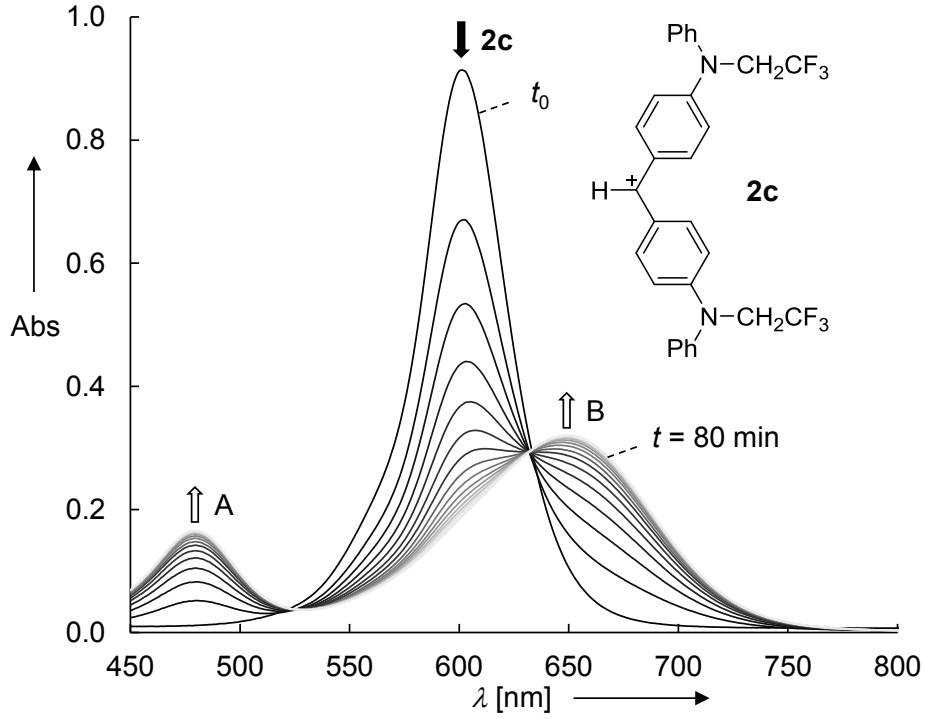

Figure 5.1. Time-dependent UV-Vis spectra during the reaction of ynamide **1d** ($c = 1.02 \times 10^{-3}$ M) with benzhydrylium salt **2c–BF4** ($c = 1.13 \times 10^{-5}$ M) in dichloromethane at 20 °C.

UV-Vis spectroscopic monitoring of this reaction showed that the green species was formed with the same rate as the blue carbenium ion disappeared. The assumption that the green species is the result of a hydrocarbation reaction was confirmed by the isolation of the allylic sulfonamide **4**, which was obtained by treatment of the reaction product **3ac** with DIBAL-H (Scheme 5.2).

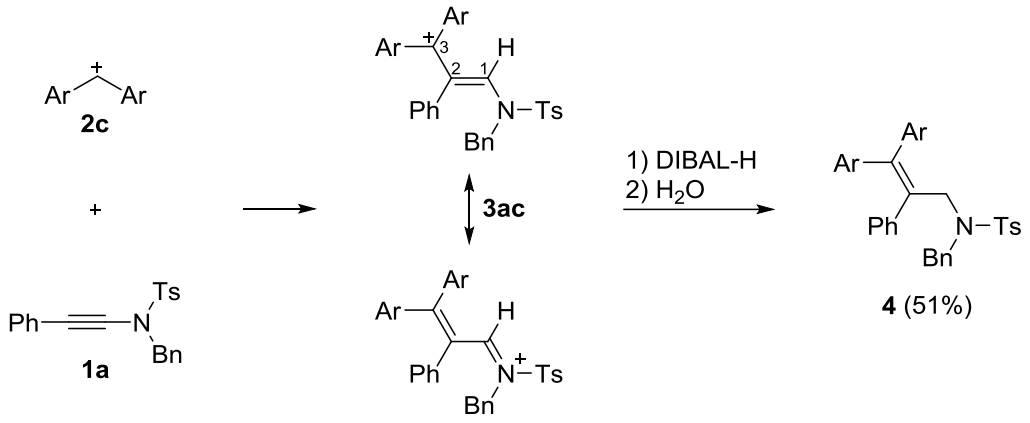

Scheme 5.2. Formation of the allylic sulfonamide **4** by treatment of the colored intermediate **3ac** with DIBAL-H (Ar see Table 5.2).

As shown in Table 5.1, the UV-Vis absorption maxima of the 1-amido-3,3-diarylallyl cations (↔ α,β-unsaturated iminium ions) **3** depend only slightly on the nature of the substituents at nitrogen and at C-2, but are strongly affected by the nature of the aryl groups at C-3. The considerably longer wavelength of the absorption maximum of **2a** (compared to **2b** and **2c**, Table 5.2) is in line with the bathochromic shifts of both bands of the allyl cations derived from **2a** compared to those obtained from **2b** and **2c** (Table 5.1). The analogous conjugation of the aryl rings with a carbenium center in the products **3**, as in the benzhydrylium ions **2**, is thus indicated.

When the kinetics of the reactions of the ynamides **1a–d** with the benzhydrylium ions **2a–c** were studied under pseudo-first order conditions ([**1a–d**] >> [**2a–c**]), mono-exponential decays of the absorbances of the benzhydrylium ions **2** (Figure 5.2, left) and mono-exponential

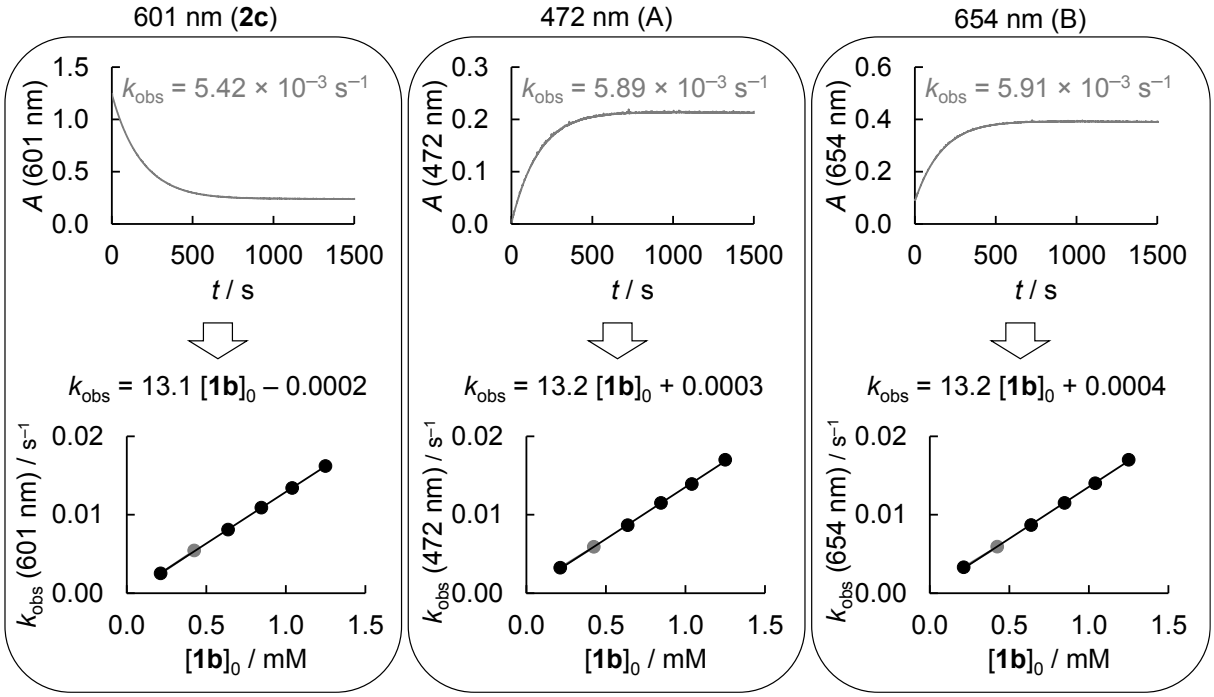

Figure 5.2. Upper part: From the exponential decay of the absorbance of **2c** (left) and the exponential increases of the absorbances at 472 nm (middle) and 654 nm (right) during the reaction of **1b** (c = 4.25 × 10^{-4} M) with **2c** (c = 2.17 × 10^{-5} M) at 20 °C in CH_2Cl_2 the corresponding first-order rate constants k_{obs} (**2c**), k_{obs} (472 nm) and k_{obs} (654 nm) are derived. Lower part: The respective second-order rate constants k_2 (**2c**), k_2 (472 nm) and k_2 (654 nm) are obtained as the slopes of the linear correlations of the corresponding first-order rate constants k_{obs} against [**1b**]$_0$.

increases of both absorbances of the unsaturated iminium ions **3** (Figure 5.2, middle and right) were observed, as depicted for the reaction of **2c** with **1b**.

Since some of the iminium ions **3** undergo subsequent reactions, which are only slightly slower than their formations, the second-order rate constants derived from the consumption of the benzhydrylium ions **2** and from the formation of the iminium ions **3** sometimes differ slightly, while Figure 5.2 shows the coincidence of the different values, Table 5.4 of the Experimental Section also includes examples for slight deviations. As the rate constants derived from the decay of the benzhydrylium absorbances are directly related to the rates of the bimolecular reactions, only these rate constants are given in Table 5.3.

Table 5.3. Second-Order Rate Constants k_2 (in M^{-1} s^{-1}) for the Reactions of the Ynamides **1a–d** with the Benzhydrylium Ions **2a–c** in Dichloromethane at 20 °C.

Ynamide	k_2 (**2a**)	k_2 (**2b**)	k_2 (**2c**)
1a	0.181	1.07	3.75
1b	0.574	2.51	13.1
1c	2.48	12.1	55.5
1d	–	–	0.963

As depicted in Scheme 5.3, the formation of **3** may either be concerted or stepwise with reversible or irreversible formation of a keteniminium ion **5**, which undergoes a subsequent 1,3-hydride shift to give the observed amido allyl cation **3**. This 1,3-hydride shift is not a 1,3-sigmatropic process which is subject to the orbital symmetry rules. Unlike in a 1,3-sigmatropic shift, the involved σ_{CH}-bond is in the plane of the three carbon atoms, and the Ar_2C^+-fragment must rotate to achieve conjugation between the developing carbenium center and the enamide fragment of **3**.

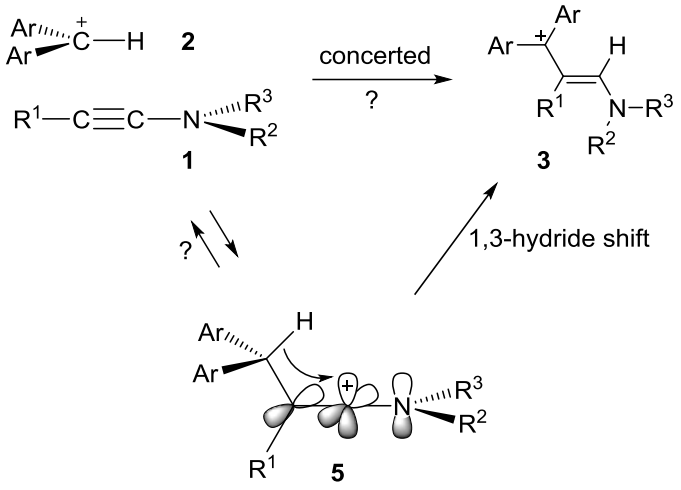

Scheme 5.3. Mechanistic alternatives for the reactions of the ynamides **1** with the benzhydrylium ions **2** can occur concerted or stepwise, which involves a 1,3-hydride shift in keteniminium ion **5**.

In order to differentiate these mechanistic alternatives, we have also studied the rate of the reaction of the C-1-deuterated benzhydrylium ion D-**2b** ($Ar_2C\text{-}D^+$) with the ynamide **1a**. As shown in Figure 5.3, the deuterated benzhydrylium ion D-**2b** reacts even faster than its ^1H-isotopomer **2b**, which excludes breaking of the C-H bond in the rate-determining step.

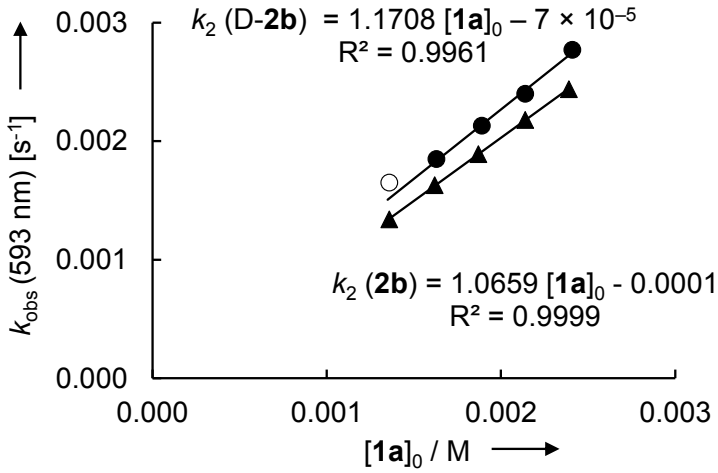

Figure 5.3. Comparison of the first-order rate constants k_{obs} obtained for the reactions of benzhydrylium ions $(mfa)_2CH^+$ (**2b**, triangles) and $(mfa)_2CD^+$ (D-**2b**, circles) with different amounts of ynamide **1a** (data point shown as an open circle was not used for determining k_2 (D-**2b**)).

The ratio k_2 (**2b**) / k_2 (D-**2b**) = 0.91 rather corresponds to an inverse α-secondary kinetic isoptope effect, which is typical for reactions involving rehybridization $C_{sp2} \rightarrow C_{sp3}$ in the rate-determining step.[5] We, thus, conclude that the rate constants listed in Table 5.3 reflect the attack of the benzhydrylium ions **2a–c** at the ynamides **1a–d** with irreversible formation of the keteniminium ions **5**.

As this step corresponds to the type of reactions, for which Equation (5.1) was derived, it is now possible to determine the nucleophile-specific parameters N and s_N by plotting log k_2 of the rate constants in Table 5.3 against the electrophilicity parameters E of the benzhydrylium ions **2a–c** (Figure 5.4).

$$\lg k\ (20\ ^\circ\mathrm{C}) = s_N(N + E) \qquad (5.1)$$

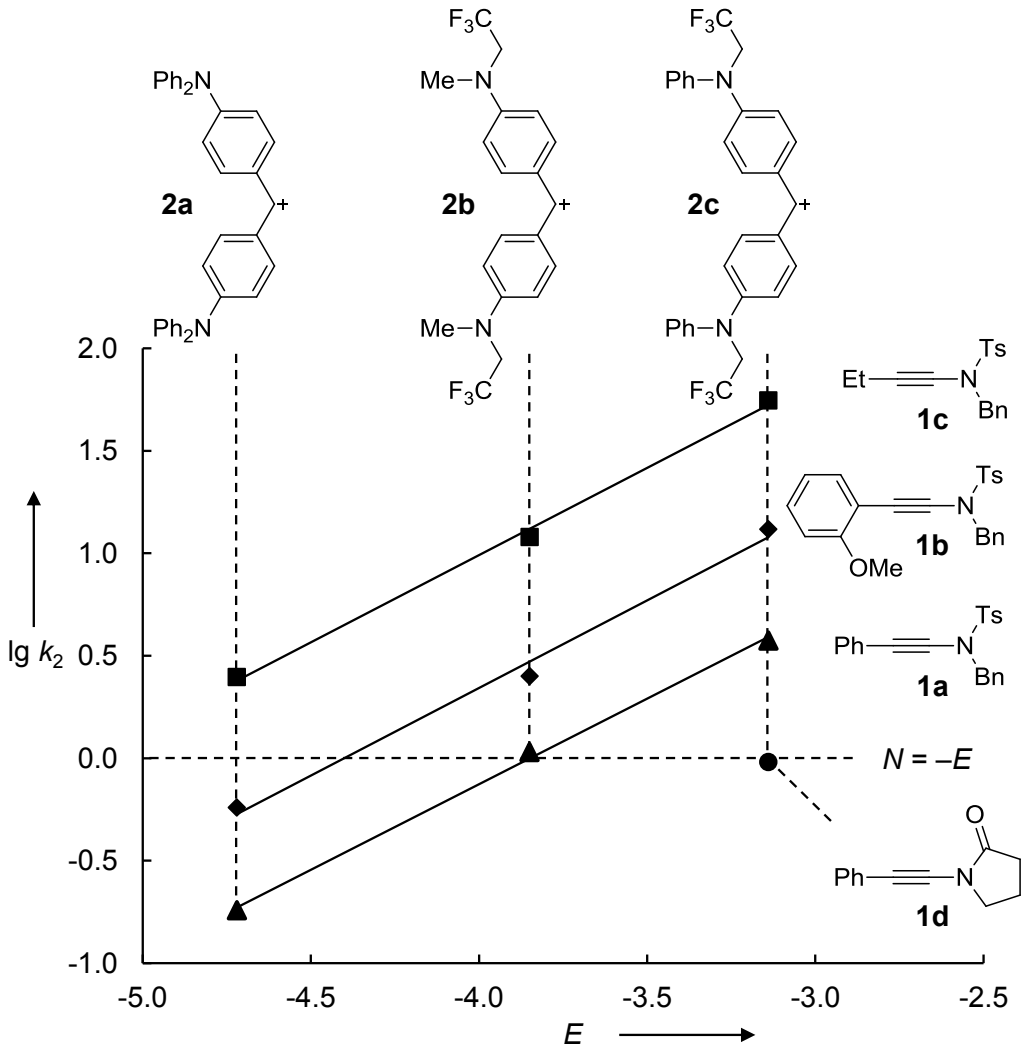

Figure 5.4. Plots of lg k_2 for the reactions of benzhydrylium ions **2a–c** with ynamides **1a–d** in CH_2Cl_2 at 20 °C versus the electrophilicity parameters E of the reference electrophiles.

The linear correlations shown in Figure 4 indicate that all investigated reactions follow analogous mechanisms. As the sensitivities s_N (slopes of the correlation lines) are similar to those of related π-nucleophiles,[4g] the nucleophilicity parameters N (negative intercepts on the abscissa) can directly be employed to discuss structure-reactivity relationships.

Figure 5.5 shows that ynamides **1a–d** possess nucleophilicities which are comparable to those of (2-methylallyl)trimethylsilane (**6**)[4a] and butyl vinyl ether (**7**).[4f] They are significantly less reactive than enamines,[6] as shown by the comparison of the structurally related compounds **8b** and **1c**. Replacement of the alkyl substituents at the position of electrophilic attack by a phenyl group decreases the nucleophilicities of enamines (**8b→8a**) as well as of ynamides (**1c→1a**) by approximately one order of magnitude.

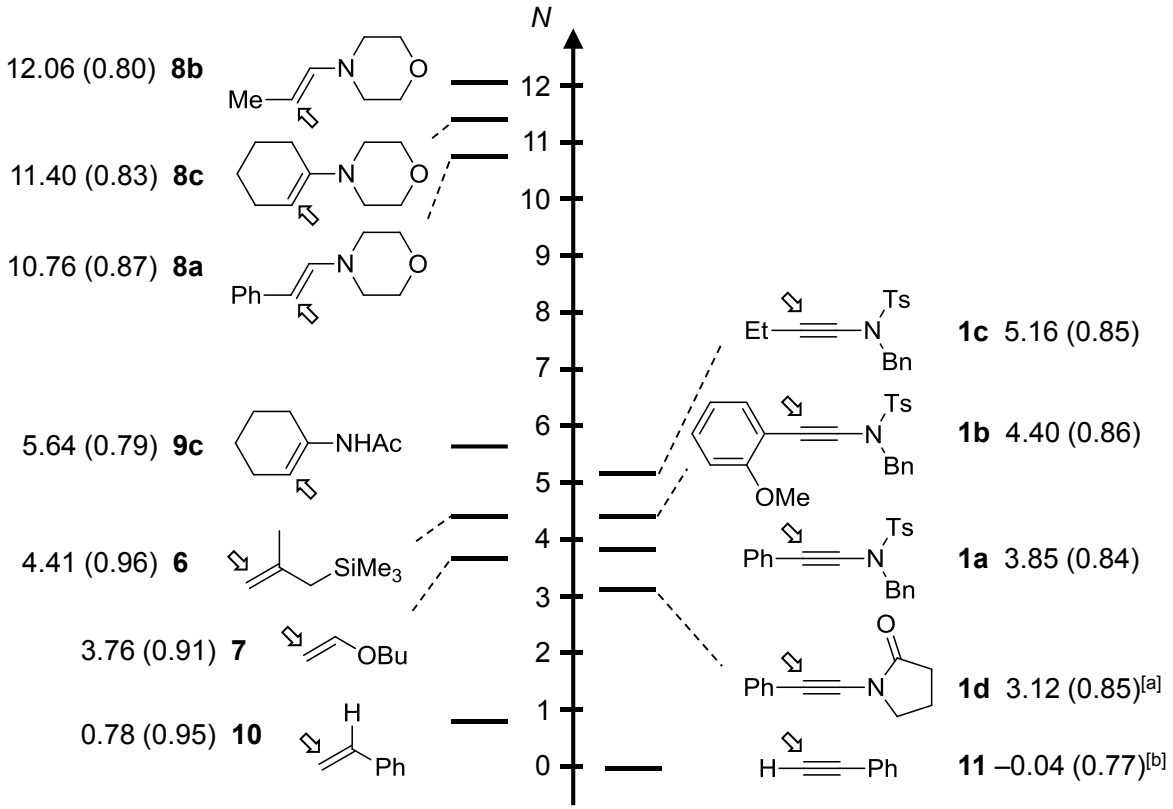

Figure 5.5. Comparison of the nucleophilicity N of ynamides **1a–d** (s_N in parentheses) with those of other π-nucleophiles[4g] in CH_2Cl_2 (CH_3CN for enamides; [a] estimated value of s_N; [b] nucleophilicity parameter adjusted to the revised electrophilicity parameters E of the reference electrophiles given in ref [4f]).

Structurally related enamides,[7] as **9c**, were reported to possess nucleophilicities $4.6 < N < 7.1$, *i.e.*, somewhat higher than those found for the ynamides **1a–d** in this work. As

open-chain β-substituted enamides have not been characterized, the direct comparison with the studied ynamides is difficult. From the reactivity difference **8b**/**8c** one can derive, however, that **9c** should also be slightly less reactive than **9b** (Figure 5.6), and one can estimate N(**9b**) ≈ 6.3. Similarly, the reactivity difference **8a**/**8c** leads to an estimated value of N(**9a**) ≈ 5. The difference in reactivity of approximately one order of magnitude when comparing the estimated nucleophilicities of **9a** and **9b** with those determined for the corresponding ynamides **1a** and **1c**, respectively, nearly reflects the reactivity difference between styrene (**10**) and phenylacetylene (**11**, Figure 5.5). Therefore, the influence of the secondary acetamido group on the nucleophilic reactivity of CC double bonds is comparable with the effect of the tertiary sulfonamido substituent on the nucleophilicity of CC triple bonds.

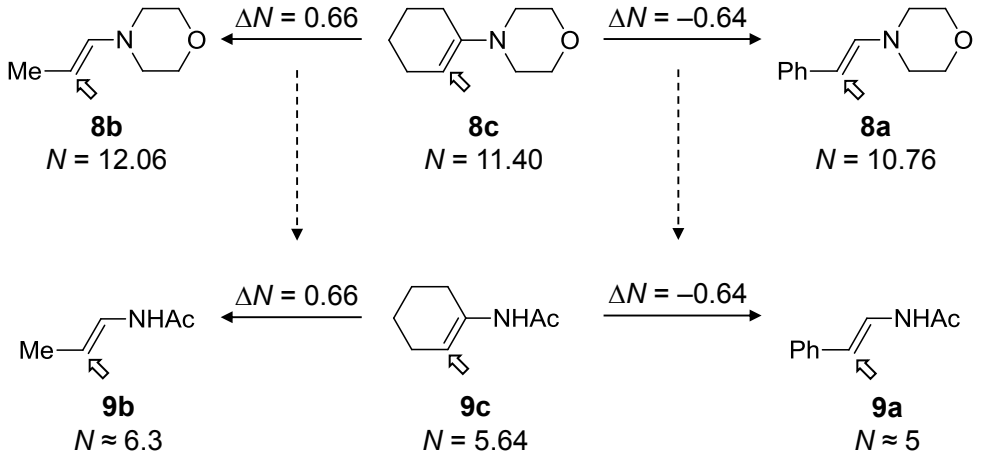

Figure 5.6. Estimation of nucleophilicity parameters for β-methyl and β-phenyl substituted enamides **9a,b** from the reactivity differences ΔN found for the corresponding enamines **8a,b** to **8c**.

Why do hydrocarbations, as described in Scheme 5.1b, in contrast to hydroborations generally not take place? As B-H bonds in borohydride anions are far better hydride donors than C-H bonds,[8] the zwitterion **12** shown in Scheme 5.4 is not formed as an intermediate in hydroboration reactions as it would undergo activation-less collapse to the hydroboration product (Jencks' criterion[9]). In contrast, C-H bonds are much poorer hydride donors, and 1,3-hydride migrations in carbocations are generally slow, even when the hydride transfer is exothermic.[10] As a consequence, carbocations **13**, which are formed by the addition of a carbocation to an olefin (Scheme 5.1b and 5.4), are usually trapped by external nucleophiles.[11]

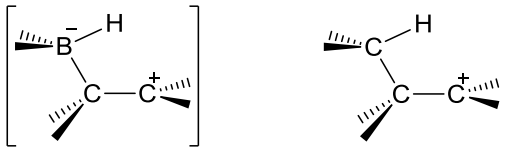

12 **13**

Scheme 5.4. Comparison of the hypothetical intermediate **12** of a stepwise hydroboration with the intermediate **13** obtained after the addition of a carbocation to an alkene.

For the same reason, Lewis acid catalyzed reactions of alkyl halides to alkynes give vinyl halides in good yields (Scheme 5.5), indicating that a hydride transfer in the intermediate vinyl cation **14** cannot be a major process.[12]

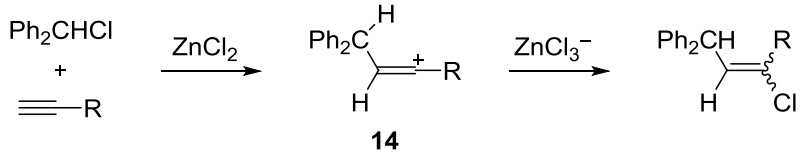

14

Scheme 5.5. Lewis acid catalyzed additions of alkyl halides to alkynes.[12]

A recent report[13] on the formation of benzofurans **15** by Lewis acid catalyzed reactions of methoxy- and methyl-substituted or unsubstituted benzhydrols with ynamide **1b** (Scheme 5.6, pathway a) shows that hydrocarbations through hydride transfer in the intermediate keteniminium ions **5** (Scheme 5.6, pathway b), as observed in this work only occur when the carbocation generated by hydride transfer is stabilized by strong electron-donating groups.

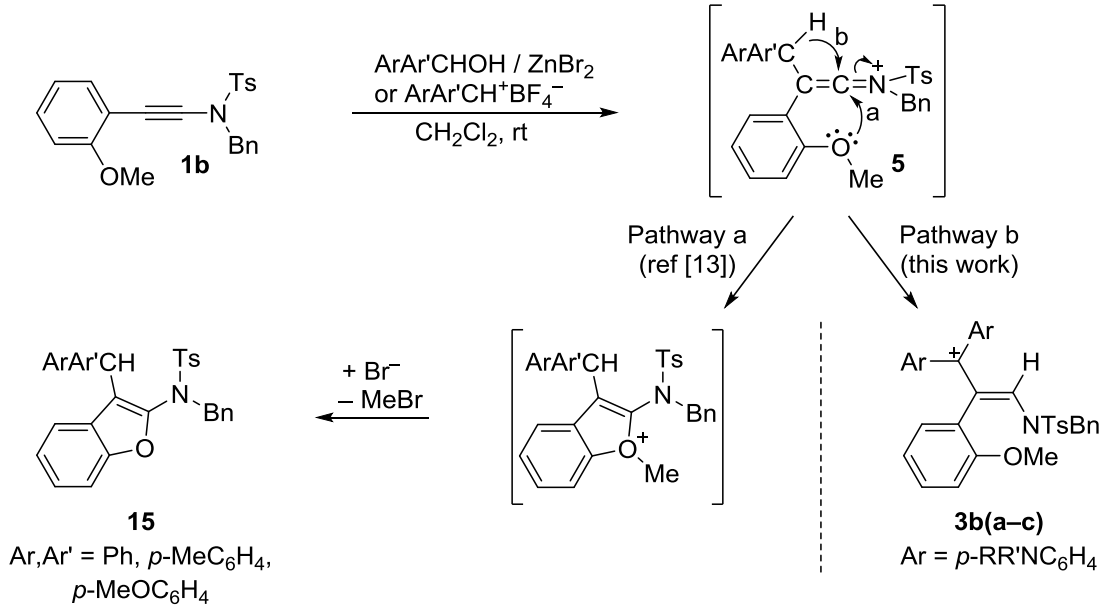

1b **5**

15
Ar,Ar' = Ph, *p*-MeC_6H_4, *p*-$MeOC_6H_4$

3b(a–c)
Ar = *p*-RR'NC_6H_4

Scheme 5.6. The substitution pattern in the benzhydrylium moiety determines the subsequent reaction pathway of the keteniminium ion **5**.

5.3 Conclusion

In summary, we have shown that hydrocarbations of alkynes with carbenium ions are possible when electron-donating substituents are present in the alkynes as well as in the carbenium ions. The observation of an inverse α-secondary kinetic isotope effect when replacing the C-1 hydrogen of a carbenium ion with deuterium showed that an irreversible electrophilic attack of benzhydrylium ions at the ynamides is the rate-determining step of the studied reactions.

5.4 Experimental Section

5.4.1 General Methods

All reactions were performed in carefully dried Schlenk glassware in an atmosphere of dry nitrogen. The reactions were not optimized for high yields.

NMR spectra were recorded on Varian NMR instruments (300, 400 and 600 MHz). Chemical shifts are expressed in ppm and refer to $CDCl_3$ (δ_H: 7.26, δ_C: 77.16), CD_3CN (δ_H: 1.94, δ_C: 1.32) and TMS (δ_H: 0.00, δ_C: 0.00) as internal standard. MS and HRMS were performed on a Finnigan MAT 95 (EI) or a Finnigan LTQ FT (ESI) instrument.

Solvents. CH_2Cl_2 (*p.a.* grade) used for kinetic experiments was purchased from Merck and successively treated with concentrated sulfuric acid, water, 10% $NaHCO_3$ solution, and water. After drying with $CaCl_2$, it was freshly distilled over CaH_2 under exclusion of moisture (N_2 atmosphere).

Reference Electrophiles. Procedures for the syntheses of benzhydrylium tetrafluoroborates **2a–c**[4a] were reported previously.

Nucleophiles. Ynamides **1a–d** were synthesized according to previously reported procedures.[3]

5.4.2 Synthesis of Deuterated Benzhydrylium Tetrafluoroborate D-2b–BF_4

bis(4-(methyl(2,2,2-trifluoroethyl)amino)phenyl)deuteromethanol ($(mfa)_2CDOH$)

Sodium borodeuteride (0.20 g, 4.8 mmol) was added to a suspension of $(mfa)_2CO$ (2.4 g, 5.9 mmol) and potassium hydroxide (67 mg, 1.2 mmol) in ethanol (15 mL) and the resulting mixture was heated to reflux for 3 h. Further sodium borodeuteride (0.20 g, 4.8 mmol) was added before the mixture was heated to reflux for additional 3 h. Sodium borodeuteride (0.10 g, 2.4 mmol) was added and the mixture was heated to reflux for 3 h. A GC-MS analysis showed remaining $(mfa)_2CO$ and therefore, more sodium borodeuteride (0.25 g, 6.0 mmol) was added and the resulting mixture heated to reflux for additional 65 h. After cooling the reaction mixture was poured in ice-water (0.15 L) resulting in precipitation of a white solid. After filtration and washing with water the solid was dried under high vacuum to give a colorless solid containing $(mfa)_2CDOH$ and $(mfa)_2CHOH$ in a ratio of 5:1 (2.0 g, 84%).

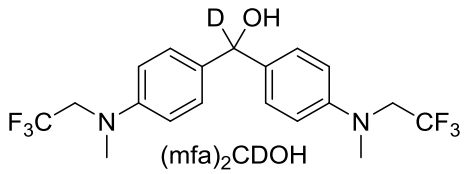

^{1}H NMR (599 MHz, $CDCl_3$): δ = 1.55 (s, 1 H, OH), 3.02 (s, 6 H, 2×NCH_3), 3.82 (q, $^3J_{H\text{-}F}$ = 9.0 Hz, 4 H, 2×NCH_2CF_3), 6.73 (d, ^3J = 8.7 Hz, 4 H, 4×ArH), 7.22 (d, ^3J = 8.7 Hz, 4 H, 4×ArH) ppm.

^{13}C NMR (151 MHz, $CDCl_3$): δ = 39.2 (q, 2×NCH_3), 54.5 (tq, $^2J_{C\text{-}F}$ = 33 Hz, 2×N<u>C</u>H_2CF_3), 78.3 (t, $^1J_{C\text{-}D}$ = 20 Hz, Ar_2<u>C</u>DOH), 112.5 (d, 4×ArH), 125.6 (q, $^1J_{C\text{-}F}$ = 283 Hz, 2×NCH_2<u>C</u>F_3), 128.3 (d, 4×ArH), 132.6 (s, 2×C_q), 147.8 (s, 2×C_q) ppm.

^{19}F NMR (282 MHz, $CDCl_3$): δ = –70.6 (t, $^3J_{F\text{-}H}$ = 9.0 Hz) ppm.

HR-MS (EI, pos.) *m*/*z* calcd. for $C_{19}H_{19}DF_6N_2O$ $[M]^+$ 407.1537, found 407.1538.

(mfa)$_2$CD$^+$BF$_4^-$ (D-**2b–BF$_4$**)

$HBF_4 \cdot Et_2O$ complex (7.3 M, 0.34 mL, 2.5 mmol) dissolved in dry Et_2O (20 mL) was slowly added to a solution of (mfa)$_2$CDOH (1.0 g, 2.5 mmol) in dry Et_2O (60 mL) at ambient temperature. The resulting mixture was stirred for 1 h before the precipitate was separated from the solution via filtration under nitrogen. The solid was washed with Et_2O and dried under high vacuum. The obtained blue solid contained (mfa)$_2$CD$^+$BF$_4^-$ and (mfa)$_2$CH$^+$BF$_4^-$ in a ratio of 90:10 (1.1 g, 92%).

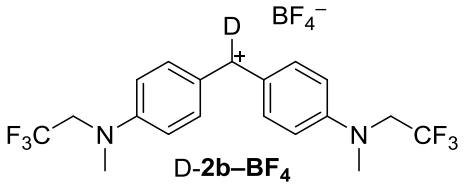

D-**2b–BF$_4$**

^{1}H NMR (400 MHz, CD_3CN): δ = 3.38 (s, 6 H, 2×NCH_3), 4.42 (q, $^3J_{H\text{-}F}$ = 8.8 Hz, 4 H, 2×NCH_2CF_3), 7.16 (d, ^3J = 9.4 Hz, 4 H, 4×ArH), 8.04 (d, ^3J = 9.4 Hz, 4 H, 4×ArH) ppm.

^{13}C NMR (101 MHz, CD_3CN): δ = 41.5 (q, 2×NCH_3), 53.7 (tq, $^2J_{C\text{-}F}$ = 33 Hz, 2×N<u>C</u>H_2CF_3), 116.3 (d, 4×ArH), 125.8 (q, $^1J_{C\text{-}F}$ = 283 Hz, 2×NCH_2<u>C</u>F_3), 127.0 (s, 2×C_q), 142.0 (d, 4×ArH), 159.3 (s, 2×C_q), 166.7 (t, $^1J_{C\text{-}D}$ = 24 Hz, Ar_2<u>C</u>D^+) ppm.

^{19}F NMR (376 MHz, CD_3CN): δ = –151.8 (s, $^{11}BF_4^-$), –151.7 (s, $^{10}BF_4^-$), –70.3 (t, $^3J_{F\text{-}H}$ = 8.8 Hz, 2×NCH_2CF_3) ppm.

HR-MS (ESI, pos.) *m*/*z* calcd. for $C_{19}H_{18}DF_6N_2^+$ [**2bD**] 390.1510, found 390.1508.

5.4.3 Products from the Reactions of Ynamide 1a with Benzhydrylium Ion 2b

Reaction of **1a** with $(mfa)_2CH^+BF_4^-$

A solution of **1a** (0.18 g, 0.50 mmol) in dichloromethane (5 mL) was added to a solution of benzhydryl tetrafluoroborate **2b–BF4** (0.24 g, 0.50 mmol) in dichloromethane (15 mL) at room temperature. The resulting mixture was stirred for 30 min during which the color changed from blue to green. A 1 M solution of DIBAL-H (1.2 mL, 1.2 mmol) in *n*-hexane was added before the reaction mixture was treated with water (20 mL) and saturated aqueous NH_4Cl solution (40 mL). The layers were separated and the aqueous layer was extracted with Et_2O (3 × 0.10 L). The combined organic layers were dried over $MgSO_4$ and the solvent removed under reduced pressure. Crystallization from dichloromethane/pentane and recrystallization from ethanol gave **4** as a pale yellow solid (0.19 g, 51%); mp 167.7–168.5 °C) with minor impurities. Signal assignments are based on additional gCOSY (^{1}H), DEPT, gHSQC (^{1}H/^{13}C) and gHMBCAD (^{1}H/^{13}C) experiments.

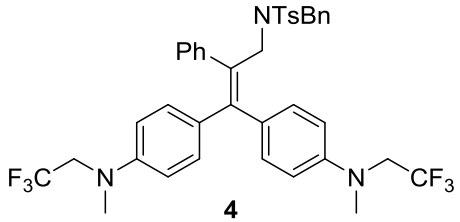

4

^{1}H NMR (599 MHz, $CDCl_3$): δ = 2.34 (s, 3 H, $ArCH_3$), 2.97 (s, 3 H, NCH_3), 3.06 (s, 3 H, NCH_3), 3.66 (s, 2 H, $NCH_2C(Ph)=CAr_2$), 3.76 (q, $^3J_{H\text{-}F}$ = 9.0 Hz, 2 H, NCH_2CF_3), 3.87 (q, $^3J_{H\text{-}F}$ = 8.9 Hz, 2 H, NCH_2CF_3), 3.94 (s, 1 H, NCHHPh), 4.05 (s, 1 H, NCHHPh), 6.61 (d, ^3J = 8.7 Hz, 2 H, 2×ArH), 6.64–6.71 (m, 4 H, 4×ArH), 6.83 (d, ^3J = 8.3 Hz, 2 H, 2×ArH), 6.90 (d, ^3J = 8.7 Hz, 2 H, 2×ArH), 6.97 (d, ^3J = 8.3 Hz, 2 H, 2×ArH), 6.98–7.00 (m, 2H, 2×ArH), 7.13–7.17 (m, 2 H, 2×ArH), 7.17–7.23 (m, 5 H, 5×ArH), 7.26–7.30 (m, 1 H, ArH) ppm.

^{13}C NMR (151 MHz, $CDCl_3$): δ = 21.4 (q, $C\underline{C}H_3$), 39.2 (q, 2×NCH_3), 40.5 (t, $N\underline{C}H_2C(Ph)=CAr_2$), 51.4 (t, NCH_2Ph), 54.0 (tq, $^2J_{C\text{-}F}$ = 33 Hz, $N\underline{C}H_2CF_3$), 54.7 (tq, $^2J_{C\text{-}F}$ = 33 Hz, $N\underline{C}H_2CF_3$), 112.0 (d, 2×ArH), 112.7 (d, 2×ArH), 125.5 (q, $^1J_{C\text{-}F}$ = 283 Hz, CF_3), 125.6 (q, $^1J_{C\text{-}F}$ = 283 Hz, CF_3),126.4 (s, C_q), 126.8 (d, ArH), 127.9–128.2 (m, 7×ArH), 128.86 (d, 2×ArH), 128.90 (s, C_q), 129.1 (d, 2×ArH), 129.6 (d, 2×ArH), 130.1 (d, 2×ArH), 131.4 (d, 2×ArH), 133.9 (s, C_q), 136.0 (s, C_q), 137.6 (s, $\underline{C}SO_2$), 140.4 (s, C_q), 140.6 (s, C_q), 142.8 (s, $\underline{C}CH_3$), 146.9 (s, $\underline{C}N(Me)CH_2CF_3$), 148.1 (s, $\underline{C}N(Me)CH_2CF_3$) ppm.

^{19}F NMR (282 MHz, $CDCl_3$): δ = –70.6 (t, $^3J_{F-H}$ = 9.0 Hz), –70.3 (t, $^3J_{F-H}$ = 8.9 Hz) ppm.

HR-MS (EI, pos.) *m*/*z* calcd. for $C_{41}H_{39}F_6N_3O_2S$ $[M]^+$ 751.2662, found 751.2656.

5.4.4 Kinetic Experiments

The kinetics of the reactions of ynamides **1a–d** with benzhydrylium ions **2a–c** were determined by using a J&M TIDAS diode array spectrophotometer controlled by Labcontrol Spectacle Software and connected to a Hellma 661.502-QX quartz Suprasil immersion probe (5 mm light path) via fibre optic cables and standard SMA connectors. Stock solutions of the ynamides **1a–d** and benzhydryl tetrafluoroborates **2(a–c)–BF$_4$** were prepared by dissolving the compounds in dichloromethane. The flame-dried Schlenk flasks with nitrogen atmosphere were filled with approximately 25 mL of solvent. The exact solvent quantity was determined by weighing. Then, this flask was submerged into a circulating water bath with a constant temperature, followed by the equipment with the Hellma probe. When a constant temperature was reached a well-defined amount of the benzhydryl tetrafluoroborate stock solution was added via a gas-tight syringe. After addition of a well-defined amount of the nucleophile stock solution, the change in the absorption spectrum of the reaction mixture in dependence of the recording time was monitored.

Table 5.4. Second-Order Rate Constants k_2 (**2**), k_2 (A) and k_2 (B) Derived from the Consumption of the Benzhydrylium Ions **2** and from the Formation of Bands A and B of the Iminium Ions **3** during the Reactions of Ynamides **1a–d** with Benzhydrylium Salts **2–BF$_4$** in Dichloromethane at 20 °C.

Nucleophile	**2**	k_{rel} (**2c**)	k_2 (**2**, 20 °C) / M^{-1} s^{-1}	k_2 (A, 20 °C) / M^{-1} s^{-1}	k_2 (B, 20 °C) / M^{-1} s^{-1}
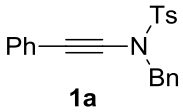 **1a**	**2a**	–	0.181	0.116	[a]
	2b	–	1.07	0.827	0.961
	2c	1	3.75	3.15	3.13
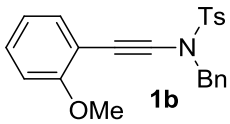 **1b**	**2a**	–	0.574	0.550	0.512
	2b	–	2.51	2.57	2.56
	2c	3.49	13.1	13.2	13.2
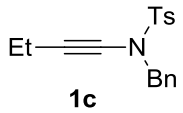 **1c**	**2a**	–	2.48	2.77	2.86
	2b	–	12.1	12.9	13.0
	2c	14.8	55.5	58.0	58.4
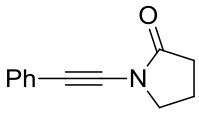 **1d**	**2c**	0.256	0.963	1.00	0.989

[a] The slope of the correlation of k_{obs} (B) against the corresponding concentrations [**1a**]$_0$ has a negative value, which is prohibited for second-order rate constants.

Kinetics for the Reactions of **1a** with **2a–c**

Rate constants for the reactions of **1a** with $(dpa)_2CH^+BF_4^-$ (**2a–BF$_4$**, λ_{max} = 672 nm) in CH_2Cl_2 (20 °C).

$[\mathbf{1a}]_0$ / M	$[\mathbf{2a}]_0$ / M	$[\mathbf{1a}]_0/[\mathbf{2a}]_0$	k_{obs} (**2a**) / s^{-1}	k_{obs} (520 nm) / s^{-1}	k_{obs} (752 nm) / s^{-1}
8.83×10^{-4}	2.17×10^{-5}	41	1.98×10^{-4}	3.21×10^{-4}	5.42×10^{-4}
1.29×10^{-3}	2.13×10^{-5}	61	2.69×10^{-4}	3.77×10^{-4}	4.83×10^{-4}
1.69×10^{-3}	2.11×10^{-5}	80	2.97×10^{-4}	4.19×10^{-4}	4.62×10^{-4}
2.09×10^{-3}	2.09×10^{-5}	100	4.31×10^{-4}	4.62×10^{-4}	4.27×10^{-4}
	k_2 (20 °C) / M^{-1} s^{-1}		**1.81×10^{-1}**	**1.16×10^{-1}**	**(-9.11×10^{-2})**

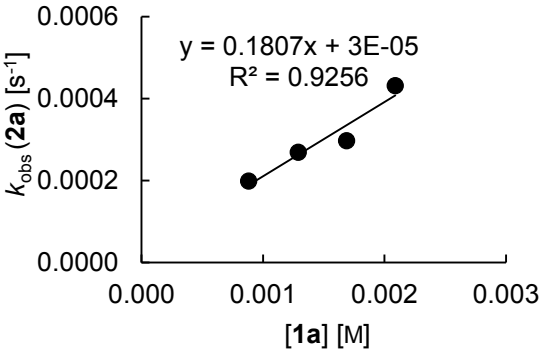

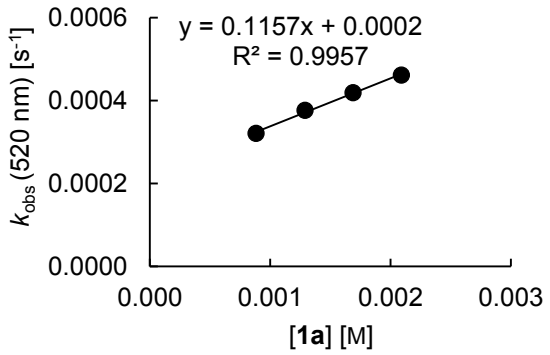

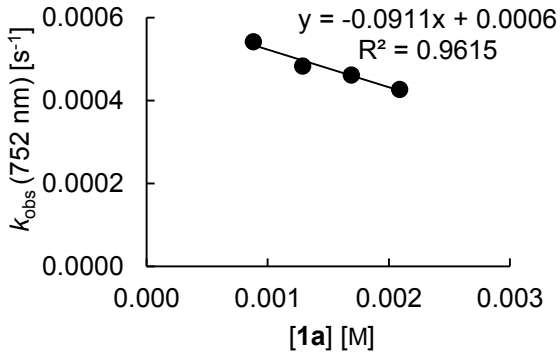

Rate constants for the reactions of **1a** with $(mfa)_2CH^+BF_4^-$ (**2b–BF$_4$**, λ_{max} = 593 nm) in CH_2Cl_2 (20 °C).

[**1a**]$_0$ / M	[**2b**]$_0$/M	[**1a**]$_0$/[**2b**]$_0$	k_{obs} (**2b**) / s^{-1}	k_{obs} (474 nm) / s^{-1}	k_{obs} (670 nm) / s^{-1}
1.36×10^{-3}	1.31×10^{-5}	104	1.34×10^{-3}	1.43×10^{-3}	1.42×10^{-3}
1.62×10^{-3}	1.30×10^{-5}	125	1.63×10^{-3}	1.94×10^{-3}	1.78×10^{-3}
1.87×10^{-3}	1.29×10^{-5}	145	1.89×10^{-3}	1.99×10^{-3}	2.02×10^{-3}
2.14×10^{-3}	1.29×10^{-5}	166	2.18×10^{-3}	2.29×10^{-3}	2.22×10^{-3}
2.39×10^{-3}	1.28×10^{-5}	187	2.44×10^{-3}	2.32×10^{-3}	2.44×10^{-3}
	$k_{2,H}$ (20 °C) / M^{-1} s^{-1}		**1.07**	**8.27×10^{-1}**	**9.61×10^{-1}**

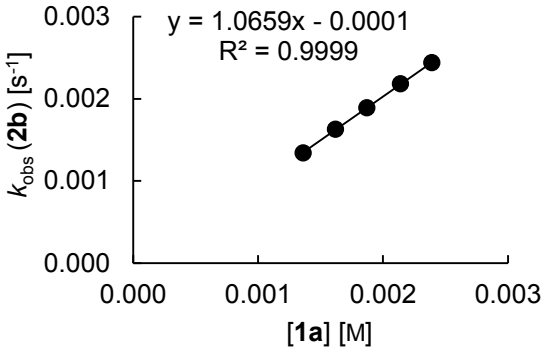

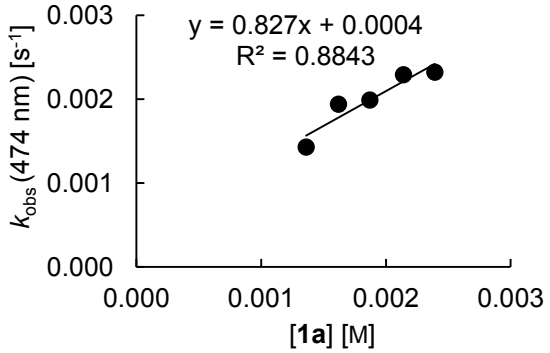

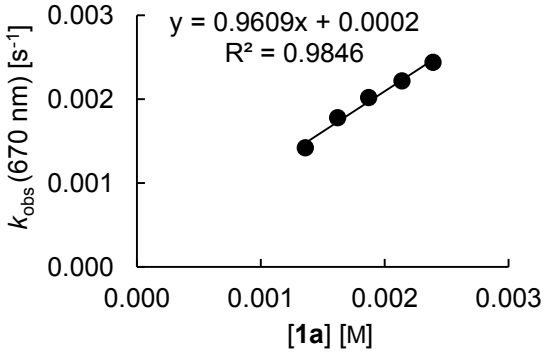

Rate constants for the reactions of **1a** with a 90:10 mixture of $(mfa)_2CD^+BF_4^-$ (D-**2b–BF$_4$**, λ_{max} = 593 nm**)** and $(mfa)_2CH^+BF_4^-$ (**2b–BF$_4$**, λ_{max} = 593 nm) in CH_2Cl_2 (20 °C).

$[\mathbf{1a}]_0$ / M	$[\mathbf{2b}_{mix}]_0$/M	$[\mathbf{1a}]_0/[\mathbf{2b}_{mix}]_0$	$k_{obs,mix}$ (593 nm) / s^{-1}	$k_{obs,mix}$ (473 nm) / s^{-1}	$k_{obs,mix}$ (670 nm) / s^{-1}
1.36×10^{-3}	1.60×10^{-5}	85	1.63×10^{-3}	1.55×10^{-3}	1.65×10^{-3}
1.63×10^{-3}	1.60×10^{-5}	102	1.84×10^{-3}	1.77×10^{-3}	1.89×10^{-3}
1.89×10^{-3}	1.59×10^{-5}	119	2.12×10^{-3}	2.19×10^{-3}	2.18×10^{-3}
2.14×10^{-3}	1.58×10^{-5}	135	2.39×10^{-3}	2.36×10^{-3}	2.45×10^{-3}
2.41×10^{-3}	1.58×10^{-5}	153	2.75×10^{-3}	2.78×10^{-3}	2.77×10^{-3}
	k_2 (20 °C) / M^{-1} s^{-1}		**1.16**	**1.24**	**1.12**

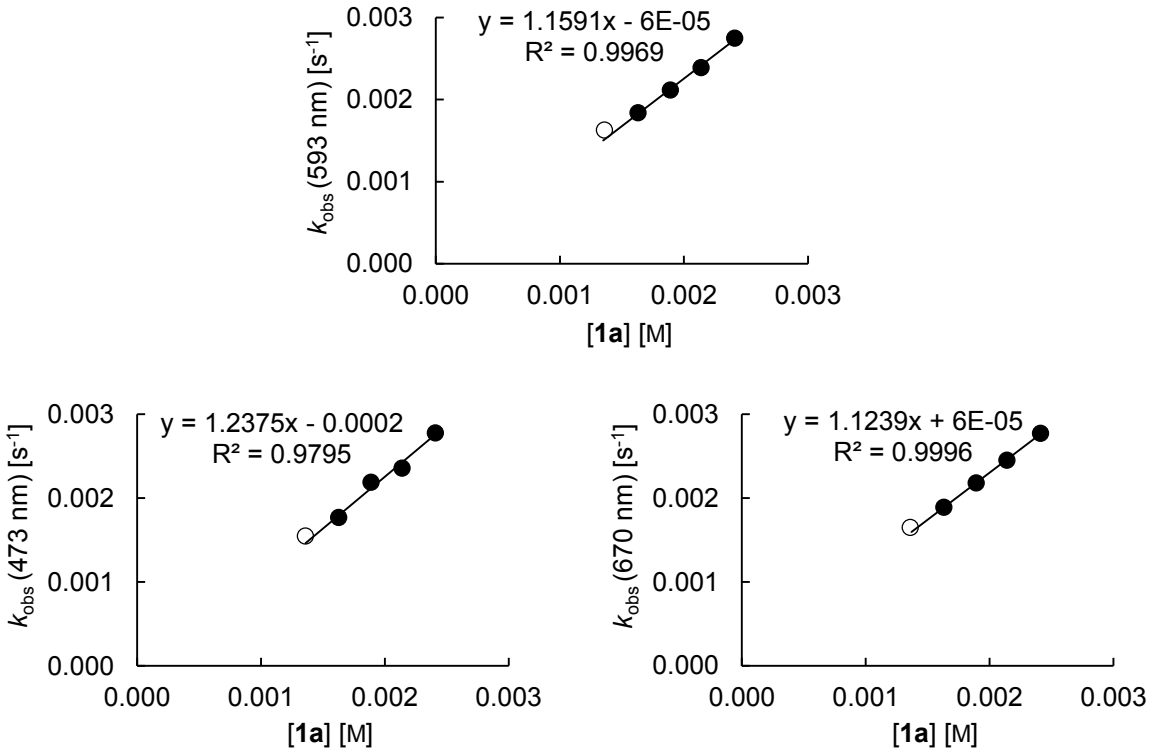

From the second-order rate constants $k_{2,H}$ for the reaction of **1a** with **2b–BF$_4$** monitored at the specified wavelengths and the pseudo-first order rate constants $k_{obs,mix}$ for the reaction of the 90:10 mixture of $(mfa)_2CD^+BF_4^-$ (D-**2b–BF$_4$**) and $(mfa)_2CH^+BF_4^-$ (**2b–BF$_4$**) monitored at

similar wavelenghts, the corresponding pseudo-first order rate constants $k_{obs,D}$ for the reaction of pure D-**2b–BF4** with **1a** can be derived by the following equation (5.2):

$$k_{\mathrm{obs},D} = \frac{10}{9}\left(k_{\mathrm{obs,mix}} - \frac{1}{10}\,k_{2,\mathrm{H}}\,[\mathbf{1a}]_0\right) \qquad (5.2)$$

Calculated rate constants via equation (5.2) for the reactions of **1a** with pure $(mfa)_2CD^+BF_4^-$ (D-**2b–BF4**) in CH_2Cl_2 (20 °C).

$[\mathbf{1a}]_0$ / M	$k_{obs,D}$ (593 nm) / s^{-1}	$k_{obs,D}$ (473 nm) / s^{-1}	$k_{obs,D}$ (670 nm) / s^{-1}
1.36×10^{-3}	1.65×10^{-3}	1.60×10^{-3}	1.69×10^{-3}
1.63×10^{-3}	1.85×10^{-3}	1.82×10^{-3}	1.93×10^{-3}
1.89×10^{-3}	2.13×10^{-3}	2.26×10^{-3}	2.22×10^{-3}
2.14×10^{-3}	2.40×10^{-3}	2.43×10^{-3}	2.49×10^{-3}
2.41×10^{-3}	2.77×10^{-3}	2.87×10^{-3}	2.82×10^{-3}
k_2 (20 °C) / M^{-1} s^{-1}	**1.17**	**1.28**	**1.14**

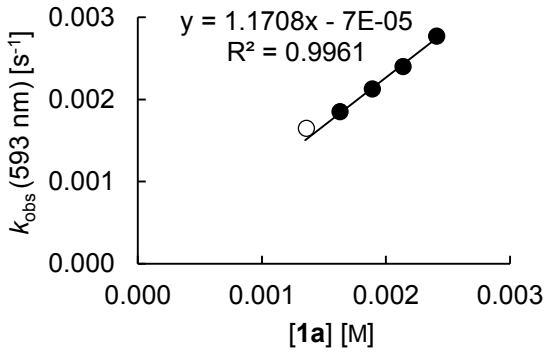

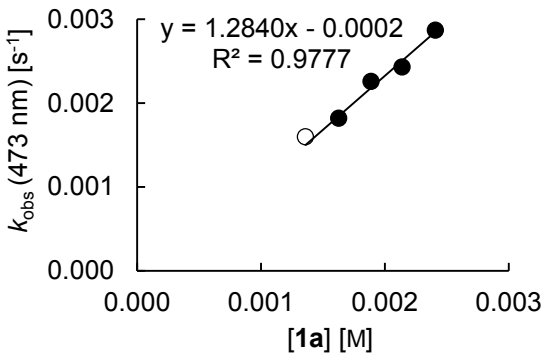

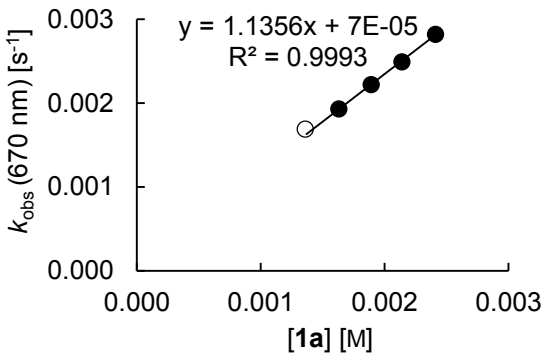

Rate constants for the reactions of **1a** with $(pfa)_2CH^+BF_4^-$ (**2c–BF$_4$**, λ_{max} = 601 nm) in CH_2Cl_2 (20 °C).

[**1a**]$_0$ / M	[**2c**]$_0$/M	[**1a**]$_0$/[**2c**]$_0$	k_{obs} (**2c**) / s^{-1}	k_{obs} (478 nm) / s^{-1}	k_{obs} (670 nm) / s^{-1}
9.28×10^{-5}	1.13×10^{-5}	8.2	6.59×10^{-4}	1.12×10^{-3}	1.12×10^{-3}
4.72×10^{-4}	1.15×10^{-5}	41	1.99×10^{-3}	2.09×10^{-3}	2.09×10^{-3}
6.85×10^{-4}	1.13×10^{-5}	61	2.85×10^{-3}	2.95×10^{-3}	2.93×10^{-3}
8.95×10^{-4}	1.12×10^{-5}	80	3.66×10^{-3}	3.62×10^{-3}	3.61×10^{-3}
	k_2 (20 °C) / M^{-1} s^{-1}		**3.75**	**3.15**	**3.13**

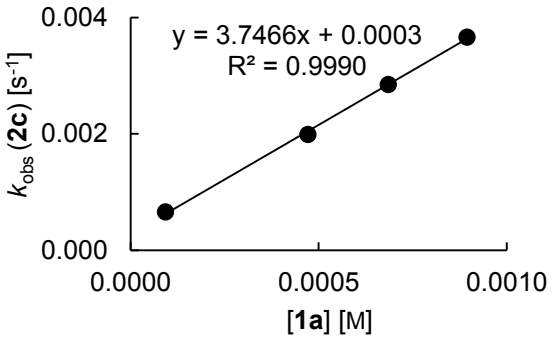

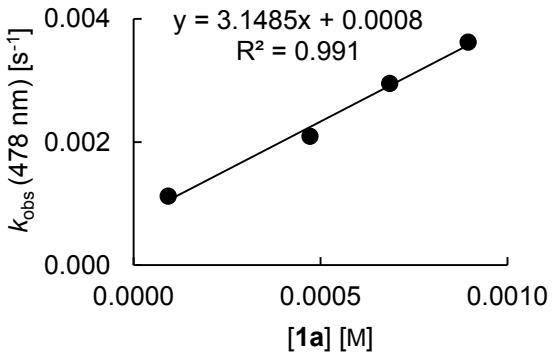

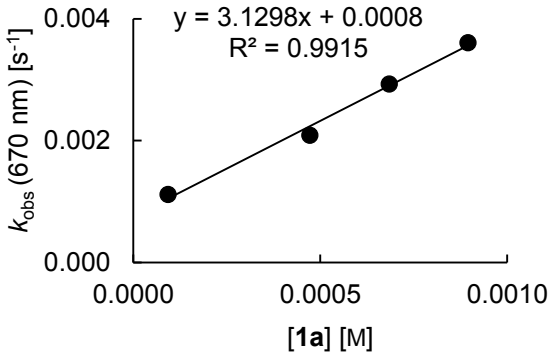

Kinetics for the Reactions of **1b** with **2a–c**

Rate constants for the reactions of **1b** with $(dpa)_2CH^+BF_4^-$ (**2a–BF$_4$**, λ_{max} = 672 nm) in CH_2Cl_2 (20 °C).

$[\mathbf{1b}]_0$ / M	$[\mathbf{2a}]_0$/M	$[\mathbf{1b}]_0/[\mathbf{2a}]_0$	k_{obs} (**2a**) / s^{-1}	k_{obs} (510 nm) / s^{-1}	k_{obs} (736 nm) / s^{-1}
8.80×10^{-4}	2.09×10^{-5}	42	5.10×10^{-4}	5.33×10^{-4}	5.74×10^{-4}
1.27×10^{-3}	2.05×10^{-5}	62	7.02×10^{-4}	7.27×10^{-4}	7.19×10^{-4}
2.08×10^{-3}	2.02×10^{-5}	103	1.12×10^{-3}	1.12×10^{-3}	1.10×10^{-3}
2.54×10^{-3}	2.03×10^{-5}	125	1.49×10^{-3}	1.47×10^{-3}	1.43×10^{-3}
3.00×10^{-3}	2.04×10^{-5}	147	1.70×10^{-3}	1.68×10^{-3}	1.63×10^{-3}
	k_2 (20 °C) / M^{-1} s^{-1}		**5.74×10^{-1}**	**5.50×10^{-1}**	**5.12×10^{-1}**

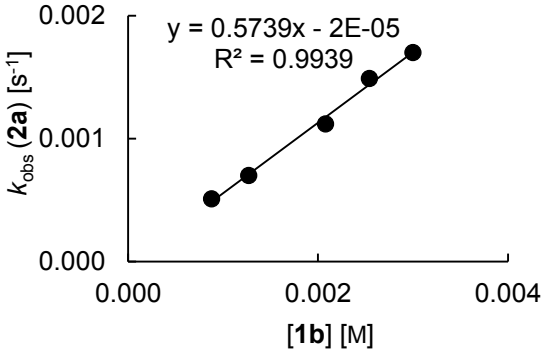

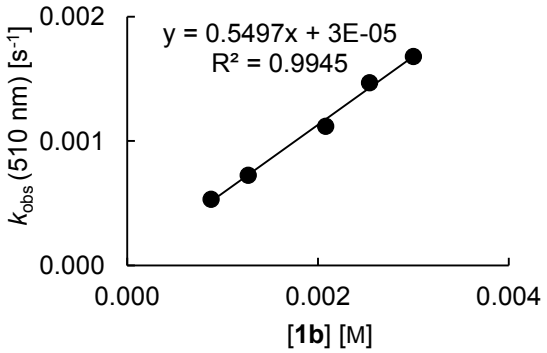

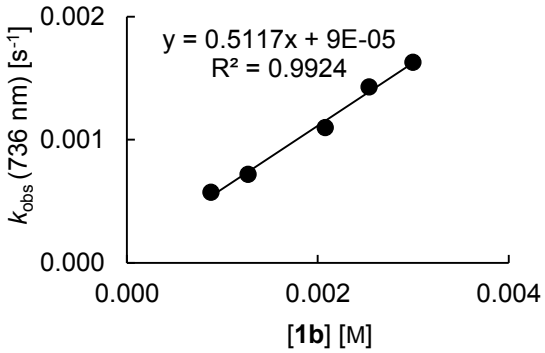

Rate constants for the reactions of **1b** with $(mfa)_2CH^+BF_4^-$ (**2b–BF$_4$**, λ_{max} = 593 nm) in CH_2Cl_2 (20 °C).

$[\mathbf{1b}]_0$ / M	$[\mathbf{2b}]_0$/M	$[\mathbf{1b}]_0/[\mathbf{2b}]_0$	k_{obs} (**2b**) / s^{-1}	k_{obs} (467 nm) / s^{-1}	k_{obs} (652 nm) / s^{-1}
6.60×10^{-4}	9.86×10^{-6}	67	1.61×10^{-3}	1.66×10^{-3}	1.65×10^{-3}
9.90×10^{-4}	9.86×10^{-6}	100	2.40×10^{-3}	2.47×10^{-3}	2.44×10^{-3}
1.31×10^{-3}	9.77×10^{-6}	134	3.23×10^{-3}	3.32×10^{-3}	3.29×10^{-3}
1.64×10^{-3}	1.20×10^{-5}	137	3.96×10^{-3}	4.10×10^{-3}	4.08×10^{-3}
1.95×10^{-3}	9.70×10^{-6}	201	4.89×10^{-3}	5.00×10^{-3}	4.97×10^{-3}
	k_2 (20 °C) / M^{-1} s^{-1}		**2.51**	**2.57**	**2.56**

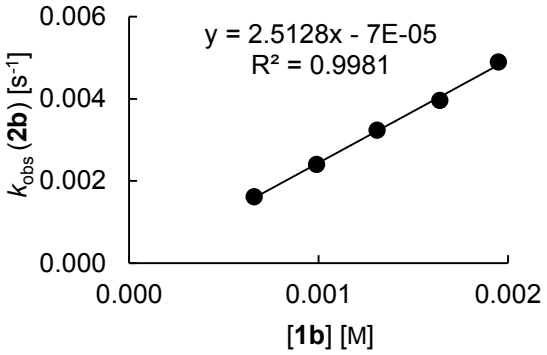

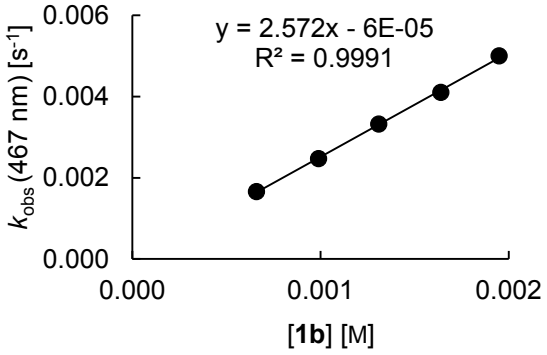

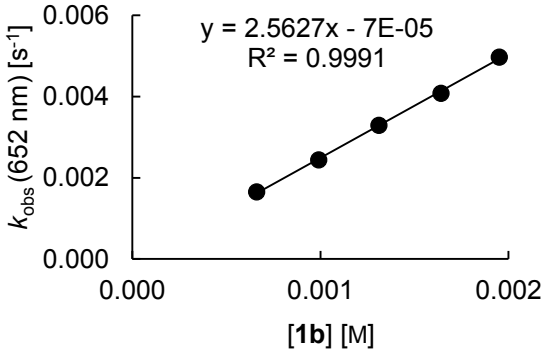

Rate constants for the reactions of **1b** with $(pfa)_2CH^+BF_4^-$ (**2c–BF4**, λ_{max} = 601 nm) in CH_2Cl_2 (20 °C).

$[\mathbf{1b}]_0$ / M	$[\mathbf{2c}]_0$/M	$[\mathbf{1b}]_0/[\mathbf{2c}]_0$	k_{obs} (**2c**) / s^{-1}	k_{obs} (472 nm) / s^{-1}	k_{obs} (654 nm) / s^{-1}
2.13×10^{-4}	2.18×10^{-5}	9.8	2.51×10^{-3}	3.24×10^{-3}	3.30×10^{-3}
4.25×10^{-4}	2.17×10^{-5}	20	5.42×10^{-3}	5.89×10^{-3}	5.91×10^{-3}
6.37×10^{-4}	2.16×10^{-5}	29	8.10×10^{-3}	8.66×10^{-3}	8.68×10^{-3}
8.47×10^{-4}	2.16×10^{-5}	39	1.09×10^{-2}	1.15×10^{-2}	1.15×10^{-2}
1.04×10^{-3}	2.13×10^{-5}	49	1.34×10^{-2}	1.39×10^{-2}	1.40×10^{-2}
1.25×10^{-3}	2.12×10^{-5}	59	1.62×10^{-2}	1.70×10^{-2}	1.70×10^{-2}
	k_2 (20 °C) / M^{-1} s^{-1}		**1.31×10^1**	**1.32×10^1**	**1.32×10^1**

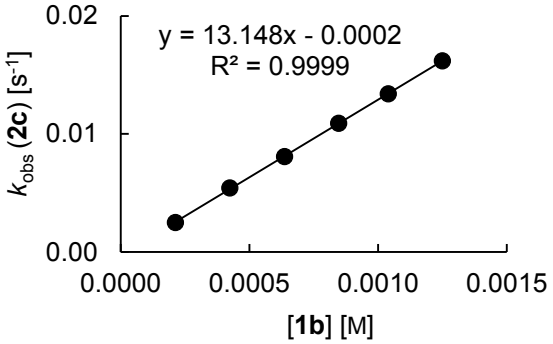

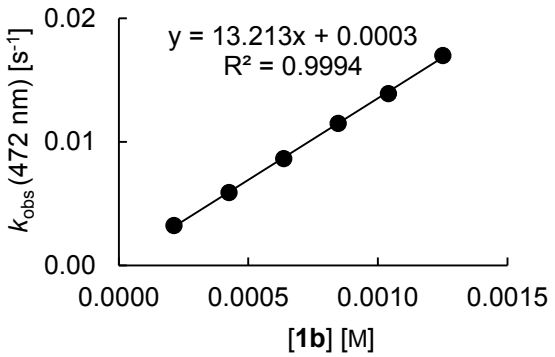

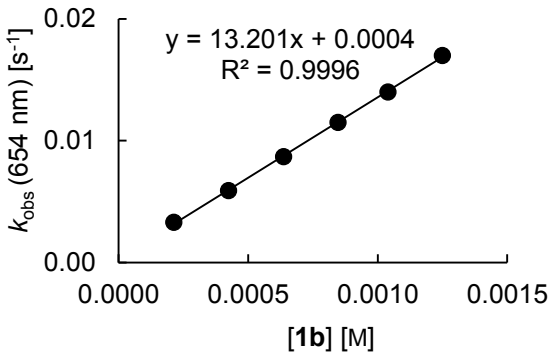

Kinetics for the Reactions of **1c** with **2a–c**

Rate constants for the reactions of **1c** with $(dpa)_2CH^+BF_4^-$ (**2a–BF$_4$**, λ_{max} = 672 nm) in CH_2Cl_2 (20 °C).

$[\mathbf{1c}]_0$ / M	$[\mathbf{2a}]_0$/M	$[\mathbf{1c}]_0/[\mathbf{2a}]_0$	k_{obs} (**2a**) / s^{-1}	k_{obs} (513 nm) / s^{-1}	k_{obs} (731 nm) / s^{-1}
9.71×10^{-4}	1.92×10^{-5}	51	2.69×10^{-3}	3.26×10^{-3}	4.21×10^{-3}
1.16×10^{-3}	1.92×10^{-5}	60	3.24×10^{-3}	3.93×10^{-3}	5.22×10^{-3}
1.35×10^{-3}	1.92×10^{-5}	70	3.81×10^{-3}	4.41×10^{-3}	5.43×10^{-3}
1.53×10^{-3}	1.90×10^{-5}	81	4.10×10^{-3}	4.92×10^{-3}	6.16×10^{-3}
1.71×10^{-3}	1.89×10^{-5}	90	4.55×10^{-3}	5.32×10^{-3}	6.38×10^{-3}
	k_2 (20 °C) / M^{-1} s^{-1}		**2.48**	**2.77**	**2.86**

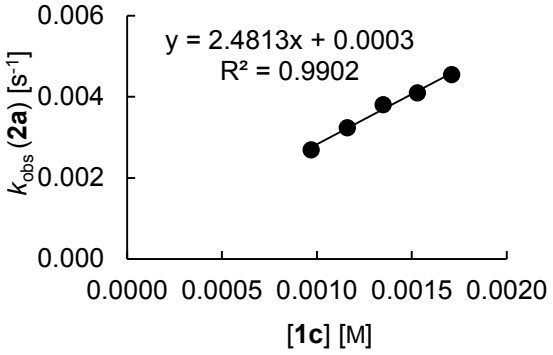

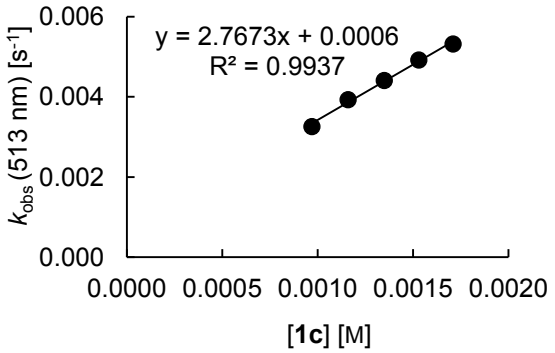

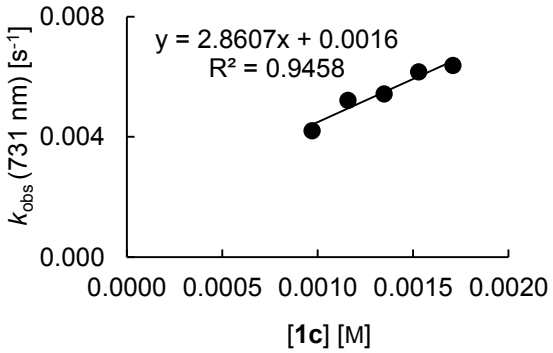

Rate constants for the reactions of **1c** with $(mfa)_2CH^+BF_4^-$ (**2b–BF$_4$**, λ_{max} = 593 nm) in CH_2Cl_2 (20 °C).

$[\mathbf{1c}]_0$ / M	$[\mathbf{2b}]_0$/M	$[\mathbf{1c}]_0/[\mathbf{2b}]_0$	k_{obs} (**2b**) / s^{-1}	k_{obs} (467 nm) / s^{-1}	k_{obs} (650 nm) / s^{-1}
6.10×10^{-4}	1.02×10^{-5}	60	7.92×10^{-3}	8.21×10^{-3}	8.20×10^{-3}
7.23×10^{-4}	1.03×10^{-5}	70	9.16×10^{-3}	9.65×10^{-3}	9.70×10^{-3}
8.27×10^{-4}	1.02×10^{-5}	81	1.04×10^{-2}	1.10×10^{-2}	1.10×10^{-2}
9.26×10^{-4}	1.02×10^{-5}	91	1.16×10^{-2}	1.21×10^{-2}	1.21×10^{-2}
1.03×10^{-3}	1.02×10^{-5}	101	1.30×10^{-2}	1.37×10^{-2}	1.38×10^{-2}
	k_2 (20 °C) / M^{-1} s^{-1}		**1.21×10^1**	**1.29×10^1**	**1.30×10^1**

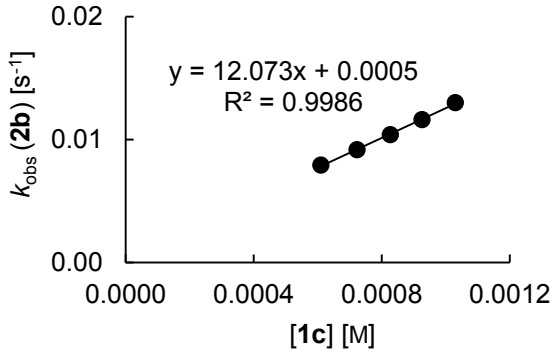

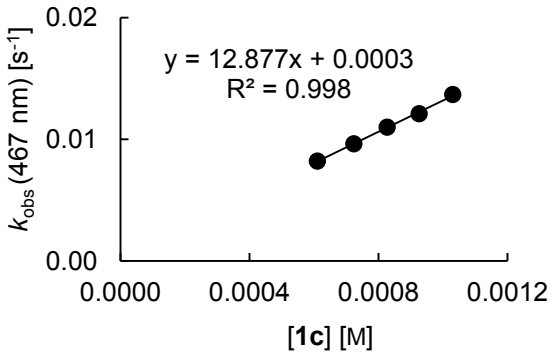

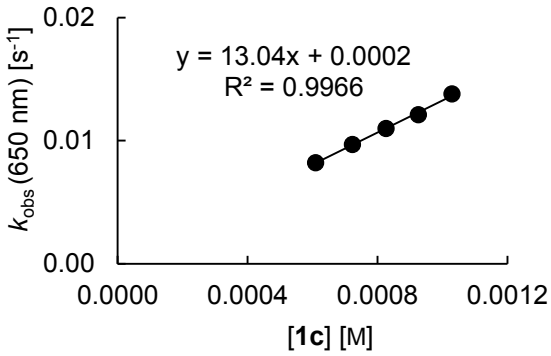

Rate constants for the reactions of **1c** with $(pfa)_2CH^+BF_4^-$ (**2c–BF$_4$**, λ_{max} = 601 nm) in CH_2Cl_2 (20 °C).

$[\mathbf{1c}]_0$ / M	$[\mathbf{2c}]_0$/M	$[\mathbf{1c}]_0/[\mathbf{2c}]_0$	k_{obs} (**2c**) / s^{-1}	k_{obs} (472 nm) / s^{-1}	k_{obs} (650 nm) / s^{-1}
1.10×10^{-4}	1.11×10^{-5}	10	5.78×10^{-3}	7.29×10^{-3}	7.51×10^{-3}
1.67×10^{-4}	1.11×10^{-5}	15	8.66×10^{-3}	1.01×10^{-2}	1.03×10^{-2}
2.26×10^{-4}	1.11×10^{-5}	20	1.24×10^{-2}	1.39×10^{-2}	1.41×10^{-2}
2.80×10^{-4}	1.11×10^{-5}	25	1.62×10^{-2}	1.78×10^{-2}	1.80×10^{-2}
3.46×10^{-4}	1.15×10^{-5}	30	1.98×10^{-2}	2.18×10^{-2}	2.19×10^{-2}
4.66×10^{-4}	1.15×10^{-5}	41	2.50×10^{-2}	2.73×10^{-2}	2.77×10^{-2}
	k_2 (20 °C) / M^{-1} s^{-1}		**5.55×10^1**	**5.80×10^1**	**5.84×10^1**

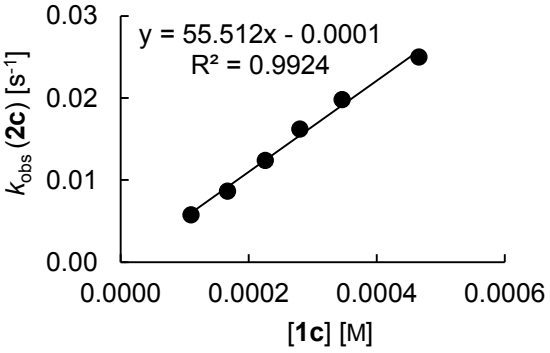

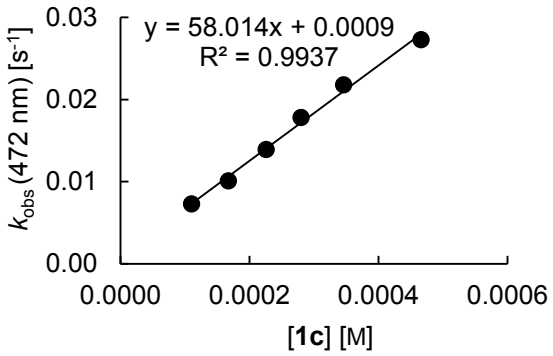

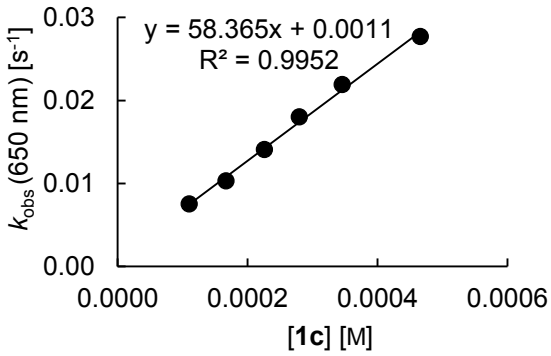

Kinetics for the Reactions of **1d** with **2c**

Rate constants for the reactions of **1d** with $(pfa)_2CH^+BF_4^-$ (**2c–BF4**, λ_{max} = 601 nm) in CH_2Cl_2 (20 °C).

$[\mathbf{1d}]_0$ / M	$[\mathbf{2c}]_0$/M	$[\mathbf{1d}]_0/[\mathbf{2c}]_0$	k_{obs} (**2c**) / s^{-1}	k_{obs} (480 nm) / s^{-1}	k_{obs} (649 nm) / s^{-1}
9.30×10^{-4}	1.13×10^{-5}	82	1.08×10^{-3}	1.01×10^{-3}	9.75×10^{-4}
1.02×10^{-3}	1.13×10^{-5}	91	1.14×10^{-3}	1.09×10^{-3}	1.05×10^{-3}
1.12×10^{-3}	1.13×10^{-5}	99	1.26×10^{-3}	1.19×10^{-3}	1.15×10^{-3}
1.24×10^{-3}	1.13×10^{-5}	110	1.37×10^{-3}	1.32×10^{-3}	1.28×10^{-3}
k_2 (20 °C) / M^{-1} s^{-1}			**9.63×10^{-1}**	**1.00**	**9.89×10^{-1}**

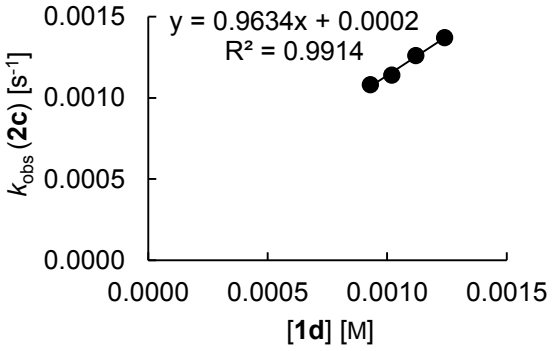

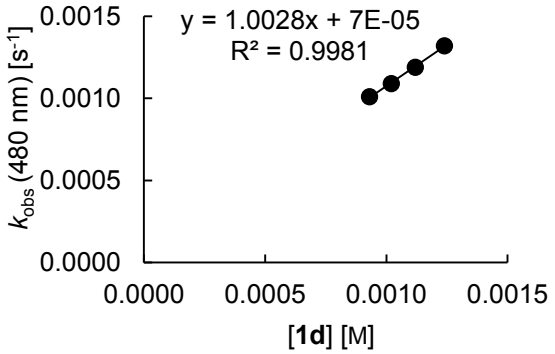

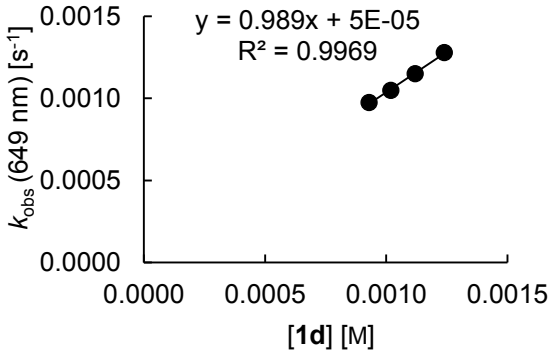

5.5 References

[1] a) H. C. Brown, *Pure Appl. Chem.* **1976**, *47*, 49–60; b) H. C. Brown, B. Singaram, *Pure Appl. Chem.* **1987**, *59*, 879–894; c) H. C. Brown, B. Singaram, *Acc. Chem. Res.* **1988**, *21*, 287–293; d) I. Beletskaya, A. Pelter, *Tetrahedron* **1997**, *53*, 4957–5026; e) Cathleen M. Crudden, D. Edwards, *Eur. J. Org. Chem.* **2003**, 4695–4712.

[2] a) C. A. Zificsak, J. A. Mulder, R. P. Hsung, C. Rameshkumar, L.-L. Wei, *Tetrahedron* **2001**, *57*, 7575–7606; b) K. A. DeKorver, H. Li, A. G. Lohse, R. Hayashi, Z. Lu, Y. Zhang, R. P. Hsung, *Chem. Rev.* **2010**, *110*, 5064–5106; c) G. Evano, A. Coste, K. Jouvin, *Angew. Chem.* **2010**, *122*, 2902–2921; *Angew. Chem. Int. Ed.* **2010**, *49*, 2840–2859. d) X.-N. Wang, H.-S. Yeom, L.-C. Fang, S. He, Z.-X. Ma, B. L. Kedrowski, R. P. Hsung, *Acc. Chem. Res.* **2014**, *47*, 560-578.

[3] Ynamides **1a–d** were synthesized using our previously reported procedures: a) A. Coste, G. Karthikeyan, F. Couty, G. Evano, *Angew. Chem.* **2009**, *121*, 4445–4449; *Angew. Chem. Int. Ed.* **2009**, *48*, 4381-4385; b) K. Jouvin, F. Couty, G. Evano, *Org. Lett.* **2010**, *12*, 3272-3275; c) K. Jouvin, A. Coste, A. Bayle, F. Legrand, G. Karthikeyan, K. Tadiparthi, G. Evano, *Organometallics*, **2012**, *31*, 7933-7947.

[4] a) H. Mayr, T. Bug, M. F. Gotta, N. Hering, B. Irrgang, B. Janker, B. Kempf, R. Loos, A. R. Ofial, G. Remennikov, H. Schimmel, *J. Am. Chem. Soc.* **2001**, *123*, 9500–9512; b) H. Mayr, B. Kempf, A. R. Ofial, *Acc. Chem. Res.* **2003**, *36*, 66–77; c) H. Mayr, A. R. Ofial in *Carbocation Chemistry* (Eds.: G. A. Olah, G. K. S. Prakash), Wiley, Hoboken, NJ, **2004**, pp. 331–358; d) H. Mayr, A. R. Ofial, *Pure Appl. Chem.* **2005**, *77*, 1807–1821; e) H. Mayr, A. R. Ofial, *J. Phys. Org. Chem.* **2008**, *21*, 584–595; f) J. Ammer, C. Nolte, H. Mayr, *J. Am. Chem. Soc.* **2012**, *134*, 13902–13911; g) For a comprehensive database of reactivity parameters see http://www.cup.uni-muenchen.de/oc/mayr/DBintro.html.

[5] a) A. Streitwieser, R. H. Jagow, R. C. Fahey, S. Suzuki, *J. Am. Chem. Soc.* **1958**, *80*, 2326-2332; b) E. V. Anslyn, D. A. Dougherty, *Modern Physical Organic Chemistry*; University Science Books, Sausalito, CA, **2006**, p. 429.

[6] B. Kempf, N. Hampel, A. R. Ofial, H. Mayr, *Chem. Eur. J.* **2003**, *9*, 2209–2218.

[7] B. Maji, S. Lakhdar, H. Mayr, *Chem. Eur. J.* **2012**, *18*, 5732–5740.

[8] M. Horn, L. H. Schappele, G. Lang-Wittkowski, H. Mayr, A. R. Ofial, *Chem. Eur. J.* **2013**, *19*, 249–263.

[9] W. P. Jencks, *Acc. Chem. Res.* **1980**, *13*, 161-169.

[10] a) M. Saunders, J. J. Stofko, *J. Am. Chem. Soc.* **1973**, *95*, 252–253; b) M. Saunders, J. Chandrasekhar, P. v. R. Schleyer in *Rearrangements in Ground and Excited State*, *Vol. 1* (Eds.: P. de Mayo), Academic Press, New York, **1980**, pp. 1–53; c) I. V. Vrček, V. Vrček, H.-U. Siehl, *J. Phys. Chem. A* **2002**, *106*, 1604–1611.

[11] H. Mayr, R. Schneider, C. Schade, J. Bartl, R. Bederke, *J. Am. Chem. Soc.* **1990**, *112*, 4446–4454.

[12] a) R. Maroni, G. Melloni, G. Modena, *J. Chem. Soc., Perkin Trans. 1* **1973**, 2491–2496; b) F. Marcuzzi, G. Melloni, *J. Am. Chem. Soc.* **1976**, *98*, 3295–3300; c) F. Marcuzzi, G. Melloni, *J. Chem. Soc., Perkin Trans. 2* **1976**, 1517–1522; d) H. Mayr, J. L. Gonzalez, K. Lüdtke, *Chem. Ber.* **1994**, *127*, 525–531.

[12] Y. Kong, K. Jiang, J. Cao, L. Fu, L. Yu, G. Lai, Y. Cui, Z. Hu, G. Wang, *Org. Lett.* **2013**, *15*, 422–425.